

NASA Contractor Report 181944

**NEAR ZONE - BASIC SCATTERING CODE
USER'S MANUAL WITH SPACE STATION APPLICATIONS**

R. J. Marhefka and J. W. Silvestro

**THE OHIO STATE UNIVERSITY
ElectroScience Laboratory
Columbus, Ohio**

**Grant NSG-1498
December 1989**

[REDACTED]
Date for general release December 31, 1991



National Aeronautics and
Space Administration

Langley Research Center
Hampton, Virginia 23665-5225

(NASA-CR-181944) NEAR ZONE: BASIC
SCATTERING CODE USER'S MANUAL WITH SPACE
STATION APPLICATIONS (Ohio State Univ.)
378 p

CSCL 20N

N92-22638

Unclas
G3/32 0085736

Preface

This code has been developed at the Ohio State University, ElectroScience Laboratory, Columbus, Ohio under the sponsorship of many organizations throughout the years. The following organizations have contributed significantly to its development.

- NASA - Langley Research Center - Hampton, Virginia
- Naval Air Development Center - Westminister, Pennsylvania
- Naval Ocean System Center - San Diego, California
- Naval Weapons Center - Chiana Lake, California
- Pacific Missile Test Center - Pt. Mugu, California
- U. S. Army CEEIA - Ft. Huachuca, Arizona
- Wright Patterson Air Force Base - Dayton, Ohio

In addition, many individuals have contributed to the code through their support and suggestions throughout the the engineering community as well as at the ElectroScience Laboratory. Not all of them can be recognized, but the following individuals should receive special considerations for their involvement in the development of the code in past and the present:

N. Akhter, W. D. Burnside, J. H. Choi, E. Constantinides, E. D. Greer, C. McCleese, P. H. Pathak, R. C. Rudduck, F. W. Schmidt, J. W. Silvestro, L. A. Takacs, C. L. Yu.

This document was prepared with \LaTeX .

Contents

Preface	i
List of Tables	vii
List of Figures	ix
1 Introduction	1
2 Definition Of The Model	9
2.1 Modeling The Structure	10
2.2 Modeling The Antennas	12
2.3 Receivers And Coupling	18
3 Principle Of Operation	23
3.1 Overview	23
3.2 Input Section	25
3.3 Geometry Fixed Bounds	29
3.4 Field Computations	29
3.5 Output Section	33
3.6 Installation Hints	41
4 Description Of Commands	45
4.1 Command BF: Scattered Fields	47
4.2 Command BP: Antenna Movement	48
4.3 Command CC: Cone Frustum	50
4.4 Command CF: Composite Ellipsoid Geometry	54
4.5 Command CG: Cylinder Geometry	58
4.6 Command CM: and CE: Comments	62

4.7	Command EN: End Program	62
4.8	Command FM: Swept Frequencies	63
4.9	Command FR: Frequency	64
4.10	Command GP: Ground Plane	65
4.11	Command GR: Range Gate	67
4.12	Command LP: Printer Output	69
4.13	Command NC: Next Set of Cylinders	70
4.14	Command NG: No Ground Plane	70
4.15	Command NM: No Antenna Movement	70
4.16	Command NP: Next Set of Plates	70
4.17	Command NR: Next Set of Receivers	70
4.18	Command NS: Next Set of Sources	71
4.19	Command NX: Next Problem	71
4.20	Command OB: Obscuration Option	72
4.21	Command PD: Far Zone Pattern	73
4.22	Command PF: Far Zone Cut	77
4.23	Command PG: Plate Geometry	79
4.24	Command PN: Near Zone Pattern	83
4.25	Command PP: Plot Data	88
4.26	Command PR: Normalization Factors	91
4.27	Command RA: Receiver Array	95
4.28	Command RD: Far Zone Range	101
4.29	Command RG: Receiver Geometry	102
4.30	Command RI: Interpolated Receiver	106
4.31	Command RM: MOM Receiver Input	110
4.32	Command RT: Rotate-Translate Geometry	112
4.33	Command SA: Source Array	115
4.34	Command SG: Source Geometry	120
4.35	Command SI: Interpolated Source	126
4.36	Command SM: MOM Source Input	131
4.37	Command TC: Test Cylinder	134
4.38	Command TO: Test Output	135
4.39	Command TP: Test Plate	138
4.40	Command UF: Scale Factor	139
4.41	Command UN: Units of Geometry	140
4.42	Command US: Units of Source	141
4.43	Command VD: Volumetric Far Zone	142

4.44	Command VF: Far Zone Volumetric Pattern	144
4.45	Command VN: Volumetric Near Zone	147
4.46	Command VP: Volumetric Plot Data	151
4.47	Command XQ: Execute Code	154
4.48	Command XT: Execute Terms	154
5	Interpretation Of Input Data	157
5.1	Moving Antennas	157
5.2	Plates	158
5.3	Plate Mounted Antennas	163
5.4	Curved Surfaces	164
5.5	Geometry Warning Messages	164
5.6	Term Interpreter Input	165
6	Interpretation Of Output Data	167
6.1	Far Zone Case	167
6.1.1	Far Zone Electric Field Theta And Phi Components	168
6.1.2	Far Zone Total Field Components	169
6.2	Near Zone Case	170
6.2.1	Near Zone Electric Field Components	171
6.2.2	Near Zone Magnetic Field Components	172
6.2.3	Near Zone Power Density Components	174
6.3	Coupling Case	175
6.3.1	Near Zone Coupling	175
7	Applications	179
7.1	Example 1A: Plate - Dipole	181
7.2	Example 1B: Plate - Dipole	188
7.3	Example 1C: Plate - Dipole	190
7.4	Example 2: Plate - Slot	196
7.5	Example 3: Near Zone Plate	200
7.6	Example 4: Frequency Sweep	208
7.7	Example 5: Corner Reflector	211
7.8	Example 6: Eight Sided Box	214
7.9	Example 7: Dielectric Plate	218
7.10	Example 8: Dielectric Plate	222
7.11	Example 9: Lossy Dielectric	225

7.12	Example 10: Radome and Horn	228
7.13	Example 11A: Antenna Coupling	237
7.14	Example 11B: Antenna Coupling	247
7.15	Example 11C: Antenna Coupling	250
7.16	Example 12: NEC - MM Input	252
7.17	Example 13: Cylinder - Dipole	259
7.18	Example 14: Elliptic Cylinder	267
7.19	Example 15: Near Zone Cylinder	271
7.20	Example 16: Ship Masts	279
7.21	Example 17: Plate - Cylinder	286
7.22	Example 18: Ship Yardarm	292
7.23	Example 19: Aircraft	298
7.24	Example 20A: Near Zone Scatter	302
7.25	Example 20B: Near Zone Scatter, Using an Ellipsoid	308
7.26	Example 20C: Near Zone Scatter, Using a Cone Frustum .	312
8	Space Station Applications	319
8.1	Description of Problem	319
8.2	Sighting of Antennas	321
8.3	Volumetric Pattern Study	323
8.4	Modeling Validation	324
8.5	Overall Considerations	336
A	Array Dimensions	337
B	Logical Unit Numbers	341
C	Installation and Operation (VAX)	343
D	Plottable Output	347
E	Plottable Geometry	351
	Bibliography	361
	Index	365

List of Tables

3.1	Block Diagram of Main Program.	24
3.2	Table of command words (also see Table 3.3).	27
3.3	Table of command words continued from Table 3.2.	28
4.1	Individual Plate Field Types Printed when LOUT is set true.	136
4.2	Individual Curved Surface Field Types Printed when LOUT is set true.	137

List of Figures

3.1	Illustration of source and scattering objects.	33
3.2	Source field ray paths.	34
3.3	Source field.	34
3.4	Illustration of first order plate ray paths.	34
3.5	Fields due to single order plate reflection.	35
3.6	Fields due to plate diffraction.	35
3.7	First order ray paths for the cylinder's curved surface. . . .	35
3.8	First order uniformly reflected field from the cylinder curved surface.	36
3.9	First order uniformly diffracted fields from the cylinder curved surface.	36
3.10	Ray paths for end cap diffracted fields.	36
3.11	Fields due to end cap diffraction.	36
3.12	Illustration of ray paths for end cap reflected fields.	37
3.13	Ray path for plate double reflected fields.	37
3.14	Fields due to double reflected plate rays.	37
3.15	Ray paths for plate reflection - diffraction.	38
3.16	Fields resulting from plate reflection - diffraction.	38
3.17	Illustration of plate diffracted - reflected ray paths.	38
3.18	Fields due to plate diffraction - reflection mechanism. . . .	38
3.19	Total field of UTD terms used to calculate the source in the presence of the scattering bodies.	39
4.1	Definition of finite cylinder geometry composed of cone frustum segments with elliptic cross section.	53
4.2	Definition of the finite composite ellipsoid geometry.	57
4.3	Definition of finite elliptic cylinder geometry.	61
4.4	Definition of pattern coordinate system.	74

4.5	Conic pattern cut, LCNPAT=.TRUE., TPPD=THP	75
4.6	Great circle pattern cut, LCNPAT=.FALSE., TPPD=PHP. . . .	75
4.7	Definition of flat plate geometry.	81
4.8	Definition of pattern coordinate system.	85
4.9	Spherical pattern cuts, LRECT=.FALSE.	86
4.10	Linear pattern cuts, LRECT=.TRUE.	86
4.11	Definition of rotate-translate coordinate system geometry. . .	113
4.12	Definition of source geometry for dipole antennas.	123
4.13	Definition of source geometry for rectangular aperture antennas.	124
4.14	Definition of source geometry for circular aperture antennas. .	125
4.15	Polarization angle of fields, Tau	129
4.16	Definition of NEC geometry.	133
5.1	Definition of antenna coordinate system for a linearly moving antenna.	159
5.2	Definition of antenna coordinate system for a circularly moving antenna.	160
5.3	Data format used to define a flat plate intersecting another flat plate.	161
5.4	Data format used to define a box structure.	162
5.5	Illustration of geometry for plate-mounted antennas.	163
7.1	Dipole in presence of a square ground plane.	182
7.2	Line printer output for the code's interpretation of the input data set of Example 1A. The figure is continued on the following pages.	183
7.3	Figure 7.2 continued.	184
7.4	Figure 7.2 continued.	185
7.5	Figure 7.2 continued.	186
7.6	Comparison of measured and calculated H -plane pattern (E_{θ_p}) for a half-wave dipole located above a square plate. (VAX 8550 run time is 0.106 min and VAX 11/750 run time is 1.2 min.)	187
7.7	Comparison of measured and calculated E -plane pattern (E_{θ_p}) for a half-wave dipole located above a square plate. (VAX 11/750 run time is 1.15 min.)	189

7.8	Dipole in presence of a square ground plane with a pattern cut corresponding to Example 1C.	191
7.9	Comparison of measured and calculated E_{θ_p} pattern taken over the corner of a square plate with a half-wave dipole mounted above it. (VAX 11/750 run time is 1.7 min.) . . .	192
7.10	Comparison of measured and calculated E_{ϕ_p} pattern taken over the corner of a square plate with a half-wave dipole mounted above it.	193
7.11	Line printer output of the electric fields of Example 1C. . .	194
7.12	Line printer output of the total radiation intensity of Example 1C.	195
7.13	A half-wavelength cavity backed slot mounted on top of a perfectly conducting square ground plane.	197
7.14	Comparison of E_{θ_p} pattern with and without corner diffracted fields for a half-wave slot antenna mounted on a square plate. (VAX 11/750 run time for case with corner diffracted fields is 1.3 min and the peak value of the E_{θ} is -11.45 dB.) . . .	198
7.15	Comparison of E_{ϕ_p} pattern with and without corner diffracted fields for a half-wave slot antenna mounted on a square plate.	199
7.16	Comparison of the measured and calculated E_{ϕ_p} radiation pattern of a dipole.	202
7.17	Comparison of the measured and calculated E_{ϕ_p} radiation pattern in the $x - y$ plane 37" from a dipole in the presence of a square plate.	203
7.18	Comparison of the measured and calculated E_{ϕ_p} radiation pattern in the $x - y$ plane 37" from a square plate in the presence of a dipole.	203
7.19	Comparison of the measured and calculated E_{ϕ_p} radiation pattern in the $x - y$ plane 26.125" from a square plate in the presence of a dipole.	204
7.20	Line printer output of the near zone electric fields of Example 3.	205
7.21	Line printer output of the near zone magnetic fields of Example 3.	206
7.22	Line printer output of the near zone power density of Example 3.	207
7.23	The E_{ϕ_p} component of the field for a pattern location directly in front of the plate. (VAX 11/750 run time is 0.8 min.) . .	210

7.24	The E_{ϕ_p} component of the field for a pattern location directly behind the plate.	210
7.25	Geometry of a corner reflector antenna.	213
7.26	Comparison of the E_{θ_p} radiation pattern in the $x - y$ plane 36.75" from the junction of two plates forming a corner reflector antenna (the maximum value of the E_{θ} is 45.28 dB).	213
7.27	Electric dipole in the presence of an eight sided box.	216
7.28	Comparison of measured (Bach) and calculated radiation E_{θ_p} pattern for an electric dipole in the presence of an eight sided box. (VAX 11/750 run time is 11.5 min and the maximum value of E_{θ} is 42.5 dB.)	217
7.29	Geometry for a dielectric cover metallic square ground plane.	219
7.30	E -plane patterns ($\phi = 0^\circ$) for a dipole over a polystyrene covered ground plate at 8 GHz.	220
7.31	H -plane patterns ($\phi = 90^\circ$) for a dipole over a polystyrene covered ground plate at 8 GHz.	220
7.32	E_ϕ component for a diagonal pattern ($\phi = 45^\circ$) for a dipole over a polystyrene covered ground plate at 8 GHz.	221
7.33	E_θ component for a diagonal patterns ($\phi = 45^\circ$) for a dipole over a polystyrene covered ground plate at 8 GHz.	221
7.34	Comparison of the E -plane patterns of a bare metallic ground plane with a polystyrene covered metallic ground plane.	224
7.35	Comparison of the E -plane pattern of a polystyrene covered ground plane with and without the diffraction terms included. (VAX 11/750 run time is 0.8 min for the case without diffractions)	224
7.36	Comparison of E_{θ_p} measured and calculated patterns for a perfectly conducting metallic plate.	227
7.37	Comparison of E_{θ_p} measured and calculated patterns for a thin ferrite absorber covered metallic plate. (VAX 11/750 run time is 2.4 min and the maximum value of E_θ is -14.9 dB.)	227
7.38	Geometry of radome and horn over aircraft belly model.	230
7.39	The E_{θ_p} radiation pattern of the simulated horn in free space.	231
7.40	The E_{ϕ_p} radiation pattern of the simulated horn in free space.	232
7.41	The E_{θ_p} radiation pattern of the horn over the plate model of the belly of the aircraft.	233

7.42	The E_{ϕ_p} radiation pattern of the horn over the plate model of the belly of the aircraft.	234
7.43	The E_{θ_p} radiation pattern of the radome covered horn over the belly of the aircraft. (VAX 11/750 run time is 11 min.)	235
7.44	The E_{ϕ_p} radiation pattern of the radome covered horn over the belly of the aircraft.	236
7.45	Illustration of the geometry used to find the coupling between two dipole antennas.	241
7.46	The coupling between two half wavelength dipoles in free space as they move apart along the x -axis. The NEC - Method of Moments results are shown as dots.	242
7.47	The coupling between two half wavelength dipoles in free space as they move apart along the z -axis. The NEC - Method of Moments results are shown as dots.	243
7.48	The coupling between two half wavelength dipoles over a infinite ground plane as they move apart along the x -axis. The NEC - Method of Moments results are shown as dots.	244
7.49	The coupling between two half wavelength dipoles over a infinite ground plane as they move apart along the z -axis. The NEC - Method of Moments results are shown as dots.	245
7.50	Line printer output for the coupling between two dipoles in free space as they move apart in the x direction. The dipoles are represented by a numerical integration of seven segments apiece and the modified Frii's transmission formula is used to represented the coupling.	246
7.51	Geometry for the problems of dipoles over a square plate and infinite ground plane showing the side and top view.	256
7.52	Comparison of the directive gain of four dipoles over an infinite ground with four dipoles over a square plate over an infinite ground and four dipoles over a square plate alone ($\phi = 0$ degrees, vertical polarization).	257
7.53	Comparison of the directive gain of four dipoles over an infinite ground with four dipoles over a square plate over an infinite ground and four dipoles over a square plate alone ($\phi = 90$ degrees, horizontal polarization).	258
7.54	An electric dipole parallel to the x -axis on the side of a finite circular cylinder for Example 13A and 13B.	261

7.55	An electric dipole parallel to the x -axis on the top of a finite circular cylinder for Example 13C.	261
7.56	Line printer output of the electric fields of Example 13A.	262
7.57	Line printer output of the total radiation intensity of Example 13A.	263
7.58	Comparison of measured (Bach) and calculated E_{ϕ_p} radiation pattern of an electric dipole on the y -axis parallel to the x -axis in the presence of a finite circular cylinder (pattern taken in the $x - y$ plane).	264
7.59	Comparison of measured (Bach) and calculated E_{ϕ_r} radiation pattern of an electric dipole on the y -axis parallel to the x -axis in the presence of a finite circular cylinder (pattern taken in the $y - z$ plane).	265
7.60	Comparison of measured (Bach) and calculated E_{ϕ_p} radiation pattern of an electric dipole parallel to the x -axis mounted above the end cap of a finite circular cylinder (pattern taken in the $y - z$ plane). (VAX 11/750 run time is 2.1 min.) . . .	266
7.61	Elliptic cylinder configuration excited by a magnetic source parallel to the z -axis.	268
7.62	Line printer output of the individual fields diffracted by the elliptic cylinder of Example 14 with LOUT=TRUE.	269
7.63	Comparison of UTD and moment method results for E_{ϕ_p} pattern. (VAX 8550 run time is 0.23 min and VAX 11/750 run time is 2.7 min.)	270
7.64	Comparison of the measured and calculated E_{ϕ} radiation pattern in the $x - y$ plane 36.75" from a dipole in the presence of a circular cylinder.	274
7.65	Comparison of the measured and calculated E_{ϕ} radiation pattern in the $x - y$ plane 26.25" from a dipole in the presence of a circular cylinder.	274
7.66	Comparison of the measured and calculated E_{ϕ} radiation pattern in the $x - y$ plane 36.75" from a circular cylinder in the presence of a dipole.	275
7.67	Comparison of the measured and calculated E_{ϕ} radiation pattern in the $x - y$ plane 26.25" from a circular cylinder in the presence of a dipole.	275

7.68	Line printer output of the near zone electric fields of Example 15.	276
7.69	Line printer output of the near zone magnetic fields of Example 15.	277
7.70	Line printer output of the near zone power density of Example 15.	278
7.71	The geometry used to study the pattern of four antennas in the presence of two masts.	282
7.72	Comparison of the exact modal solution and the uniform asymptotic solution of the E_θ pattern in the azimuth plane for one dipole on one mast.	283
7.73	Calculated azimuth plane pattern at a range of 250 meters for four dipoles located around a mast in the presence of a second mast without higher order cylinder interactions terms (frequency = 0.3125 GHz) (VAX 11/750 run time is 47.3 min).	284
7.74	Calculated azimuth plane pattern at a range of 250 meters for four dipoles located around a mast in the presence of a second mast with higher order cylinder interactions terms (frequency = 0.3125 GHz).	285
7.75	Comparison of the measured and calculated E_ϕ far zone radiation pattern of a dipole in the presence of a square plate and a finite circular cylinder (without plate - cylinder interactions).	289
7.76	Comparison of the measured and calculated E_ϕ far zone radiation pattern of a dipole in the presence of a square plate and a finite circular cylinder (with plate - cylinder interactions).	289
7.77	Comparison of the measured and calculated E_ϕ near zone radiation pattern 36.875" from a dipole in the presence of a square plate and a circular cylinder (without plate - cylinder interactions).	290
7.78	Comparison of the measured and calculated E_ϕ near zone radiation pattern 26.25" from a dipole in the presence of a square plate and a circular cylinder (without plate - cylinder interactions).	290
7.79	Comparison of the measured and calculated E_ϕ near zone radiation pattern 36.875" from a circular cylinder in the presence of a dipole and a square plate (without plate - cylinder interactions).	291

7.80	Geometry of an antenna in a mast and yardarm environment.	294
7.81	Top and side view of computer model corresponding to the mast and yardarm example.	295
7.82	Comparison of the measured and calculated azimuth pattern for the mast and yardarm example. The calculated result includes the mast only. The measurements were made on a 1/10 scale model including the yardarms at NOSC [23] . . .	296
7.83	Comparison of the measured and calculated azimuth pattern for the mast and yardarm example. The calculated result includes both the mast and one yardarm. The measurements were made on a 1/10 scale model including the yardarms at NOSC [23].	297
7.84	Illustration of geometry of Boeing 737 aircraft model used in finite elliptic cylinder model. The larger radius is used for an antenna mounted on the top of the wings and the smaller radius is used for an antenna mounted on the bottom. . . .	300
7.85	Comparison of measured and calculated E_{ϕ_p} results. (VAX 11/750 run time is 3 min and maximum E_{θ} value is -32.2 dB.)	301
7.86	Simplified aircraft shape used in RCS example.	305
7.87	Calculated RCS result for horizontal polarization in the azimuth plane. The computer model does not include the nose cone. The results are normalized with respect to a square meter. (VAX 11/750 run time is 24.7 min. and VAX 8550 is 2.16 min.)	306
7.88	Measured RCS result made at Pacific Missile Test Center for horizontal polarization in the azimuth plane. The results are normalized with respect to a square meter.	307
7.89	Calculated RCS result for horizontal polarization in the azimuth plane. The computer model does not include a nose cone and uses a truncated ellipsoid for the fuselage. (VAX 8550 run time is 2.20 min.)	311
7.90	Calculated result for horizontal polarization in the azimuth plane of the fuselage only composed of multiple cone frustum sections. (VAX 8550 run time is 0.25 min.)	315
7.91	Measured RCS made at Pacific Missile Test Center for horizontal polarization in the azimuth plane of the fuselage only.	316

7.92	Calculated result for horizontal polarization in the azimuth plane of the complete model using a multiple cone frustum fuselage. (VAX 8550 run time is 2.83 min.)	317
8.1	Illustration of the Space Station with some of its many antenna systems.	320
8.2	Space Station configuration showing antenna location used for shadowing example.	322
8.3	Calculated obscuration of the target antenna showing shadow of the Space Station.	323
8.4	Contour and 3-D plot of volumetric E_θ pattern of target antenna mounted vertically without the Space Station. . . .	325
8.5	Contour and 3-D plot of volumetric E_θ pattern of target antenna mounted vertically on the Space Station.	326
8.6	Contour and 3-D plot of volumetric E_θ pattern of target antenna mounted at a 45° angle without the Space Station. . . .	327
8.7	Contour and 3-D plot of volumetric E_θ pattern of target antenna mounted at a 45° angle on the Space Station. . . .	328
8.8	NEC-BSC model of portion of Space Station used to model GPS antenna environment.	329
8.9	Comparison of E -plane cut ($\phi = 0^\circ$) measured and calculated patterns for the GPS antenna without the Space Station. . . .	330
8.10	Comparison of H -plane cut ($\phi = 90^\circ$) measured and calculated patterns for the GPS antenna without the Space Station. . . .	330
8.11	Comparison of E -plane cut ($\phi = 0^\circ$) measured and calculated patterns for the GPS antenna with the Space Station model.	331
8.12	Comparison of H -plane cut ($\phi = 90^\circ$) measured and calculated patterns for the GPS antenna with the Space Station model.	331
8.13	Comparison of elevation cut ($\phi = -60^\circ$) measured and calculated patterns for the GPS antenna with the Space Station model.	332
8.14	Comparison of elevation cut ($\phi = -45^\circ$) measured and calculated patterns for the GPS antenna with the Space Station model.	332

8.15	Comparison of elevation cut ($\phi = -30^\circ$) measured and calculated patterns for the GPS antenna with the Space Station model.	333
8.16	Comparison of elevation cut ($\phi = -15^\circ$) measured and calculated patterns for the GPS antenna with the Space Station model.	333
8.17	Comparison of elevation cut ($\phi = 15^\circ$) measured and calculated patterns for the GPS antenna with the Space Station model.	334
8.18	Comparison of elevation cut ($\phi = 30^\circ$) measured and calculated patterns for the GPS antenna with the Space Station model.	334
8.19	Comparison of elevation cut ($\phi = 45^\circ$) measured and calculated patterns for the GPS antenna with the Space Station model.	335
8.20	Comparison of elevation cut ($\phi = 60^\circ$) measured and calculated patterns for the GPS antenna with the Space Station model.	335
E.1	Output of a DRAW REPORT_SIZE command after a SET VIEW 45.,45.is given.	355
E.2	Output of a DRAW ALL command.	356
E.3	Output of a DRAW command after a NOTEXT, NOBOX, and SET VIEW 45.,315. is executed.	359

Chapter 1

Introduction

The Numerical Electromagnetic Code - Basic Scattering Code (NEC-BSC) is a user-oriented computer code for the electromagnetic analysis of the radiation from antennas in the presence of complex structures at high frequency. For many practical sized structures this corresponds to UHF and above. The code can be used to predict far zone patterns of antennas in the presence of scattering structures, to provide the EMC or coupling between antennas in a complex environment, and to determine potential radiation hazards. Simulation of the scattering structures is accomplished by using combinations of perfectly conducting multiple flat plates, finite elliptic cylinders, composite cone frustums, and finite composite ellipsoids. The code, also, has a limited finite thin dielectric slab capability. This version of the NEC-BSC is an update to previous versions, the latest being version 2 [1,2].

This is version 3, and it has been specifically designed to help place antennas on structures such as the space station which has a large number of plate and cylinder type structures. There can be a very large number of systems requiring antennas on such a structure. The various systems can not all have the same prime locations, therefore, some tough choices must be made. The number of antennas needed to avoid blockage effects of the structure and the complexity of the antenna systems chosen can greatly impact on the cost. Prediction codes give the antenna designer a chance to optimize these choices even when the actual structure is not flying yet. The first step in the design process for a structure is to site the antennas based on blockage effects. An obscuration code has been developed for this

purpose that is quick and interactive [3]. The next step is to use a code such as this to determine the best type and orientation of the antenna to reduce multipath and antenna to antenna interference. The last step is to test the predicted locations with measured results on scale models of the structure or portions of the structure.

The type of analysis used in this code has been very successfully in the past in modeling aircraft [4,5,6,7]. The aircraft code restricts that the antennas be mounted on the curved surface of the structures. The present solution as described in this manual has been used to model a wide range of practical problems where the antennas are not mounted on curved surfaces. For example, the Basic Scattering Code (BSC) has been used to simulate the scattering from the superstructure of a ship, the body of a truck or tank, or the fuselage, wings, and stores of an aircraft or the living quarters of a space station using perfectly conducting plates and cylinders. The dielectric capability [8] can be used as an isolated thin slab which can simulate a radome or windshield, or it can be mounted on a perfectly conducting plate in order to simulate composite material or an absorber-coated ground plane, or as an semi-infinite half space to simulate the earth. The thin dielectric slab modification is not complete but is meant to be applied to practical problems in order to ascertain its usefulness as well as its limitations. In this way the next generation BSC can incorporate and extend the useful features of the thin dielectric slab analysis.

The analysis is based on uniform asymptotic techniques formulated in terms of the Uniform Geometrical Theory of Diffraction (UTD) [9,10,11,12] or sometimes referred to as the modern Geometrical Theory of Diffraction (GTD). The UTD approach is ideal for a general high frequency study of antennas in a complex environment in that only the most basic structural features of an otherwise very complicated structure need to be modeled. This is because ray optical techniques are used to determine components of the field incident on and diffracted by the various structures. Components of the diffracted fields are found using the UTD solutions in terms of the individual rays which are summed with the geometrical optics terms in the far zone of the scattering centers but they can be in the near zone of the entire structure. The rays from a given scatterer tend to interact with other structures causing various higher-order terms. One can trace out the various possible combinations of rays that interact between scatterers and determine and include only the dominant terms. Thus, one need only be

concerned with the important scattering components and neglect all other higher-order terms. This method normally leads to accurate and efficient computer codes that can be systematically written and tested. Complex problems can be built up from simpler problems in manageable pieces.

The limitations associated with the computer code result mainly from the basic nature of the analysis. The solution is derived using the UTD which is a high frequency approach. In terms of the scattering from plate structures this means that each plate should have edges at least a wavelength long. If a dielectric slab is used the source must be at least a wavelength from the surface, and the incident field should not strike the slab too close to grazing. In addition, each antenna element should be at least a wavelength from all edges. In many cases, the wavelength limit can be reduced to a quarter wavelength for engineering purposes.

Modeling small structures, antennas, and coupling between elements in an array can be accomplished using an integral equation solution [13,14,15]. For example, the moment method can be used to analyze the currents and impedances of an antenna. Also, a synthesis technique [16,17] could be used to determine the array aperture distribution based on its radiation pattern. The NEC - General Reflector Code can be used to analyze a general reflector antenna [18,19]. This scattering code can be interfaced with these and other methods by including the magnitude and phase of the current weights found by these techniques. The scattering code, then predicts the effects of the scattering environment on the performance of the antennas for arbitrary situations.

It should be noted that the NEC-BSC is meant to complement other design techniques such as scale model measurements. It is a fast and cost effective means of anticipating problems at the early design stages of a system and to optimize design parameters such as antenna placement. In addition, it can be used at the measurement stage of development to confirm the experimental results or to project near zone measurements into far zone patterns when it is very difficult to obtain the necessary range to be in the far zone of a whole structure.

A summary of the basic capabilities of the code are listed here:

- User oriented command word based input structure.
- Pattern calculations.

- Near zone source fixed or moving.
 - Far zone observer.
 - Near zone observer.
- Single or multiple frequencies.
- Antenna to antenna spacial coupling calculations.
 - Near zone receiver fixed or moving.
- Efficient representation of antennas.
 - Infinitesimal Green's function representation.
 - Six built in antenna types.
 - Linear interpolation of table look up data.
 - Method of Moments code or Reflector Code interface.
- Multiple sided flat plates.
 - Separate or joined.
 - Infinite ground plane.
 - Limited dielectric plate capability.
- Multiple elliptic cylinders.
- UTD single and multiple interactions included.
 - Second order plate terms not including double diffraction.
 - First order cylinder terms only.
 - Presently no plate - cylinder interactions.

The differences between version 2 of this code and the version designated version 3.0 are listed here:

- Code has been rewritten in FORTRAN 77
 - While rewriting the code the main program section was re-structured, making future code modifications easier.

- Dimension sizes are now changed using “PARAMETER” statements.
- The **US**’s default value is now meters.
- The **TO** command has been split into 3 commands.
 - Some of the flags from the old **TO** have been removed (since their terms can now be controlled by the **XT** command) and the remaining ones are now set in the **TO**, **TC**, or **TP** commands.
- The **XT** command, allowing the execution of specified terms, has been added.
 - This replaces the **XQ** command when used. It reads from an external file the field terms to use or not to use in the solution.
- The number of pattern commands have been expanded.
 - A non-integer far zone increment command, **PF**, has been added.
 - Volumetric pattern commands (**VF**, **VN**) have been added.
- A range gate and weight command (**GR**) has been added.
- The source and receivers can now be moved independently of each other.
 - The motion of the sources and receivers can be input separately, allowing for moving sources and stationary receivers. This is accomplished using the **BP** command and a normal pattern command.
 - The coordinate system for the moving antennas has been changed.
 - All source types (**SA**, **SG**, **SI**, **SM**) are now allowed to move.
- New antennas have been added.
 - An interpolated antenna (in the **RI** and **SI** commands).
 - An annular ring of current.

- A circular distribution of constant current.
- A circular TE_{11} current.
- A revised **SA** and **RA** that allows for arrays of different element types and orientations and can partially correct for the defocusing that occurs when scatterers are not quite in the far zone of the antenna.

In addition to the above changes, the present version designated 3.1 has the following added features.

- New curved surfaces have been added.
 - An multiple sectioned elliptic cone frustum uses the **CC** command.
 - A composite ellipsoid uses the **CF** command.
- The command **BF** provides the scattered field which is the total field minus the incident field.
- The command **OB** provides the obscuration pattern only, that is, just an indicator of the lit and shadow regions with no field information.

This document is designed to give an overall view of the operation of the computer code, to instruct a user in how to use it to simulate the scattering from various complex structures, and to show the validity of the code by comparing various computed results against measured data whenever available. Chapter 2 describes an overall view of the modeling problem as it pertains to the structure and efficient antenna models. A brief description of the organization of the code is given in Chapter 3. It gives an overview of the input commands, how the UTD works in a qualitative way, and hints on implementing the code on a new machine. The input command words and their associated input parameters are given in detail in Chapter 4. How to apply the capabilities of this input data to a practical structure is briefly discussed in Chapter 5. This includes a clarification of the subtle points of interpreting the input data. The representation of the output is discussed in Chapter 6. Various sample problems are presented in Chapter 7 to illustrate the operation, versatility, and validity of the code. Chapter 8 details the use of the code for a practical design problem. In this

case, it is the placement of antennas on a space station configuration. The procedure is validated by comparing with measurements.

The appendices provided give some specific information pertaining to the computer code. Appendix A shows how to change the number of structural elements that can be used in the code. The logical unit numbers used for input and output are given in Appendix B. Hints on VAX computer installation and operation are in Appendix C. A discussion of a plotting code for the results is given in Appendix D. The geometry plotting code that reads and plots the information in the input sets is discussed in Appendix E.

Chapter 2

Definition Of The Model

The modern Geometrical Theory of Diffraction is a very powerful tool for the analysis of problems concerning pattern distorting effects, coupling between antennas, and radiation hazard predictions. Its power lies in the ability to systematically construct practical models to simulate complex geometrical situations. The construction of the models are based on piecing together the canonical solutions for such problems as diffraction from a straight or curved wedge, vertex, and/or curved surface. The mathematical formulations are very amenable to numerical calculations and follow an intuitively satisfying geometrical interpretation. Specific problems can be modeled in detail if methods can be found to calculate all of the various ray paths and other geometrical parameters. In addition, other types of solutions, such as moment methods, can be interfaced with the UTD when these solutions present a more efficient or accurate means of obtaining a result.

The construction of a general purpose user - oriented solution, that can quickly and efficiently provide answers for a practicing antenna designer, relies on the ability of UTD to model complex shapes by simpler shapes. This discussion is intended to give insight into how to use arbitrarily oriented multiple sided flat plates, finite dielectric slabs, and analytically defined curved surfaces to model quite general problems. It also discusses how to model practical antennas as efficiently as possible in terms of this UTD solution. This type of user - oriented code allows an antenna designer, who has a minimum working knowledge of the UTD, to piece together a practical model to a problem in a short amount of time.

2.1 Modeling The Structure

In many practical UTD modeling situations, two basic types structures can be used to form an approximation to a real scattering shape, that is, multi-sided flat plates and finite elliptic curved surfaces such as cylinders, cone frustums, and ellipsoids. A set of flat plates each having an arbitrary number of edges can be used to model most shapes that have a slowly varying radius of curvature. For example, flat structures such as a ship's deck structures and yard arms, or satellite shapes, buildings or vehicle bodies can be modeled using multiple flat plates. In addition, an aircraft wing can be effectively approximated by such a flat plate for antenna pattern distortion problems as verified by numerous aircraft modeling comparisons. Even the fuselage of some high speed aircraft can be modeled by flat plates, since they are often very flat in nature.

The arbitrary sided plate is defined by specifying its corner points in a cartesian coordinate system. It is assumed that the points can be defined accurately enough in a three dimensional coordinate system so that all of the corners lie in the same plane. If this is difficult to accomplish for a given geometry, it is always possible to define the corners of the plate in two dimensions and then rotate and translate the plate into its proper position in the three dimensional configuration. The plates can be attached together in two ways. A pair of corners of one plate can be defined identically the same as a pair of corners of another plate. This union between the two plates forms a wedge with a wedge angle defined by the angle between the two plates based on the direction of incoming illumination. In the case of a box shape the wedge angle should be defined as the angle formed on the interior side of the box, since the outside of the wedge must be illuminated. Another convenient means of joining two plates, is by attaching one plate into the middle of another plate. This can be accomplished by defining the corners of one plate slightly within the plane of another plate. The wedge angle is defined in a similar way as discussed above. By defining a series of these isolated plates, a quite general structure can be formed.

A limited dielectric plate capability can be used to approximately model such structures as glass windows, absorbing panels, dielectric coated plates, or an earth model. In the case of finite flat plates, multiple layered dielectric plates can be defined by giving the number of layers along with their thickness, relative permittivity, permeability and their loss tangents. They

can be all dielectric or be backed by a metal plate. The infinite ground plane is only a single homogeneous half space. The dielectric layers must be thin, that is, they can only support one mode of the fields. The solution does not at present contain the surface waves, so the antennas can not be placed close to the surface. In addition, it assumed that any given ray path will only be allowed to propagate through one opaque plate. This restricts the complexity of the structures that can be modeled using the opaque dielectric plates.

If the structure to be modeled has a substantial radius of curvature, the flat plate model is inadequate. A finite elliptic cylinder, multiple sectioned elliptic cone frustum and composite ellipsoid are include in the code for these cases. For example, they can be used to model the masts, smoke stacks or hull of a ship; or a portion of a fuselage of some types of aircraft and their engines and stores. These curved surfaces are defined by the location of their origin in the general model coordinate system, along with their orientation and the direction of their major and minor axes. Within this coordinate system, the major and minor radii are defined. For the elliptic cylinder, the positions of the end caps are defined by their location along the cylinder axis. The tilt of each end cap is defined by the angle the surface of the end cap makes with the cylinder axis. This cylinder model breaks down for general doubly curved surfaces. The cone frustum structure is defined by the location of its rim junctions. The ellipticity of each section must remain the same for now. The ellipsoid can have a different radii of curvature along the positive and negative z -axis. It can be truncated like the cylinder except no tilt is allowed at the present time.

The general rule for defining the plates and curved surfaces is based on how the antenna illuminates the structure. The model should be defined most accurately in the area which is illuminated the strongest by the antenna. In the case of narrow beam antennas, this means that the model needs to be defined most accurately in the direction of the main beam. In the case of broader beamed antennas, the part of the model closest to the antenna should be emphasized. Also, as stated above, the parts of the model in the direction of the pattern cut desired should be given entire consideration when the model is defined. This means that more than one model may be needed to completely define the actual structure when more than one pattern cut is desired.

The limitations associated with this solution results from the basic na-

ture of the analysis. The solution is derived using the UTD which is a high frequency approach. In terms of the scattering from plate structures this means that each plate should have edges at least a wavelength long. In terms of the curved surfaces their major and minor radii and length should be at least a wavelength in extent. In addition, each antenna element should be at least a wavelength from all edges. The antenna elements, however, can be on the surface of the perfectly conducting flat plates. In many cases, the wavelength limit can be reduced to a quarter wavelength for engineering purposes. Modeling small structures can be better accomplished using an integral equation solution and interfacing the result with the UTD solution. The upper limit on the frequency is dictated by the fine structural details that can be modeled by the basic scattering shapes available.

The antenna can not be mounted on the curved surface using this particular code. If an antenna mounted on a curved surface is desired, then the UTD curved surface radiation solution must be used. If a far zone backscatter or bistatic scattering result is desired, this code is also inadequate. The higher order terms that are necessary to accurately compute the RCS of even a simple structure such as a flat plate are not included in the present code. In addition, the curved surface models and knife edged plate structures are not good enough for modeling shapes such as an actual aircraft when a plane wave is washing across the entire structure. With this in mind the user can expect the result to be reasonably accurate for the first 30(?) dB of the pattern using this code. The modern GTD is applicable for modeling general shapes with a greater degree of accuracy over the pattern, however, alternative coding is necessary.

The number of edges, plates, and antennas in a given model is only limited by the size of the area reserved to store the information. In practice, however, the number of plates used in the model is limited by the number of UTD interactions that are included in the solution. This will be discussed in more detail in a following chapter.

2.2 Modeling The Antennas

The general purpose solution discussed here can be used with a wide range of antennas. It is basically a Green's function type solution; that is, the

solution has been developed for infinitely small current elements. If the current distribution of the antenna is known, such as from a moment method analysis [14,15], a synthesis scheme [16,17], or other means, the field from the various weighted current segments can be summed to give the total field [20]. If the scattering centers are in the far zone of the antenna as a whole, the antenna can be represented by its pattern factor or in the case of an array of antennas by its array factor [21]. This can save a large amount of computation time by eliminating multiple calculations for each infinitesimal current element. It is also possible to interface the NEC - General Reflector Code's aperture patches to the source elements used here [18,19].

The source type is specified by a non zero integer corresponding to the type of pattern factor desired. A negative integer corresponds to an electric source type and a positive integer corresponds to a magnetic source type through duality. There are six different types of sources presently implemented. Three are rectangular distributions of current and three are circular distributions. For the first three source types, the general form of the transmitted electric field is given by

$$\vec{E} = j Z_o I_m k \vec{h} \frac{e^{-jkr}}{4\pi r}$$

where

$$I_m \vec{h} = \hat{\theta} l w J_m \sin \theta F_x(\theta, \phi) F_z(\theta) F_a(\theta, \phi)$$

for an electric source type. The electric source weights are assumed to be in peak values of amperes (I_m) for $w = 0$ and amperes/meter (J_m) for $w \neq 0$. From duality a magnetic type source is given by

$$\vec{E} = -j K_m k \vec{h} \frac{e^{-jkr}}{4\pi r}$$

where

$$K_m \vec{h} = \hat{\phi} l w M_m \sin \theta F_x(\theta, \phi) F_z(\theta) F_a(\theta, \phi).$$

The magnetic source weights are assumed to be in peak values of volts (K_m) for $w = 0$ and volts/meter (M_m) for $w \neq 0$. Note that the relationship $K_m = Z_o I_m$ is a useful one when trying to use both types of sources in the code and the amplitudes need to be matched. The electric source type will be emphasized here, but the details apply equally for a magnetic source

type. For a line source $w \rightarrow 0$; therefore, $wJ_m \rightarrow I_m$ and $F_x(\theta, \phi) = 1$. For an aperture source, with the aperture in the $x - z$ plane

$$F_x(\theta, \phi) = \frac{\sin\left(\frac{1}{2}kw \cos \phi \sin \theta\right)}{\frac{1}{2}kw \cos \phi \sin \theta}.$$

The equation for $F_z(\theta)$ depends on the source type chosen. If the current distribution is given by

$$I_z(z') = I_m, -l/2 \leq z' \leq l/2$$

then

$$F_z(\theta) = \frac{\sin\left(\frac{1}{2}kl \cos \theta\right)}{\frac{1}{2}kl \cos \theta}$$

If the current distribution is of the standard piecewise sinusoid type, that is,

$$I_z(z') = I_m \frac{\sin\left[k\left(\frac{1}{2}l - |z'|\right)\right]}{\sin\left(\frac{1}{2}kl\right)}, -l/2 \leq z' \leq l/2,$$

then

$$F_z(\theta) = \frac{\cos\left(\frac{1}{2}kl \cos \theta\right) - \cos\left(\frac{1}{2}kl\right)}{\frac{1}{2}kl \sin\left(\frac{1}{2}kl\right) \sin^2 \theta}.$$

If the current distribution is of the standard TE_{01} mode type (cavity backed slot) given by

$$I_z(z') = I_m \cos(z'/l), -l/2 \leq z' \leq l/2$$

then

$$F_z(\theta) = \frac{2\pi \cos\left(\frac{1}{2}kl \cos \theta\right)}{\pi^2 - (kl \cos \theta)^2}.$$

The last three element types are for circular distributions of current. For these types the currents are assumed to lie in the $x - y$ plane. The equations for \vec{E} are of the same form as before but with new definitions for the $I_m \vec{h}$ (electric currents) and $K_m \vec{h}$ (magnetic currents), where

$$I_m \vec{h} = \pi a^2 J_m \left[F_l(\theta, \phi) \hat{\theta} - F_r(\theta, \phi) \hat{\phi} \right] F_a(\theta, \phi)$$

and

$$K_m \vec{h} = \pi a^2 M_m \left[F_r(\theta, \phi) \hat{\theta} + F_l(\theta, \phi) \hat{\phi} \right] F_a(\theta, \phi)$$

The first element is an annular ring of $\hat{\phi}$ directed current, with a being the inner radius and b the outer. The form of the current is:

$$\vec{J} = \frac{I_m \hat{\phi}}{\rho \ln(b/a)}$$

where ρ is the radial position in the $x - y$ plane. The resulting factor is then

$$F_r(\theta) = \frac{2j}{a^2 \ln(b/a)} \frac{J_0(ka \sin \theta) - J_0(kb \sin \theta)}{k \sin \theta}$$

and

$$F_l(\theta, \phi) = 0$$

where J_i signifies the Bessel Function of order i . The second type is a constant \hat{x} directed current over a circle of radius a . The current is of the form:

$$\vec{J} = J_m \hat{x}$$

with the resulting pattern factors:

$$F_l(\theta, \phi) = -2 \cos \theta \cos \phi \frac{J_1(ka \sin \theta)}{ka \sin \theta}$$

and

$$F_r(\theta, \phi) = -2 \sin \phi \frac{J_1(ka \sin \theta)}{ka \sin \theta}$$

The last element type is a TE_{11} type of distribution over a circle of radius a . The currents are defined by:

$$\vec{J} = J_m [J_0(\rho'_{11}\rho) - \cos 2\phi J_2(\rho'_{11}\rho)\hat{x} - \sin 2\phi J_2(\rho'_{11}\rho)\hat{y}]$$

The resulting pattern factors are:

$$F_l(\theta, \phi) = -4 \cos \phi \cos \theta \frac{\rho'_{11} J_1(\rho'_{11}) J'_1(ka \sin \theta)}{\rho'^2_{11} - (ka \sin \theta)^2}$$

and

$$F_r(\theta, \phi) = -4 \sin \phi \frac{J_1(\rho'_{11}) J_1(ka \sin \theta)}{\rho'_{11} ka \sin \theta}$$

where ρ'_{11} is the first root of J'_1 .

Any other type of pattern factor can be added but these represent a very useful set for many applications.

The array pattern factor, $F_a(\theta, \phi)$, is particularly useful for simulating the pattern of a large number of closely spaced array elements or antenna segments. If a group of N elements are arrayed together the array pattern factor is given by

$$F_a(\theta, \phi) = \sum_{n=1}^N I_n e^{jk\hat{r} \cdot \vec{x}_n}$$

where \vec{x}_n is the relative position of the n th array element, I_n is its relative current weight, and r is the direction of propagation.

There are three options that can be used to customize this array factor term. The first is the choice of adding the next order phase term to the exponential in the F_a sum. The resulting factor would be:

$$F_a(\theta, \phi) = \sum_{n=1}^N I_n e^{jk(\hat{r} \cdot \vec{x}_n + \frac{1}{2r}((\hat{r} \cdot \vec{x}_n)^2 - r^2))}$$

where r is the distance to the scattering center or field point. This added term allows the array factor term to be used for arrays that have scattering centers that are far away but aren't quite in the far zone. This is an approximation and may not be completely accurate (the shadowing may be incorrect), so it should be used with caution. In cases where this can be used though, the savings in run time are immense. The other two options allow the user the choice of selecting the element types and sizes and element orientations individually or setting them once for the entire array. This allows complex antennas to be modeled using the more efficient array factor. It is especially useful for arrays of circularly polarized elements. The grouping of the elements in an array factor greatly increases the efficiency of the code since the summing of the elements is done in a very tight loop and should be used where ever possible.

The code is able to define a range of frequencies to be calculated for a given pattern location. It is assumed that the current distribution for the antenna is correctly defined over the frequency range. Also, the code does not add the effect of the change in antenna impedance over the frequencies considered. These effects must be added external to the code.

In the NEC-BSC there must always be a source defined. The code can be used to provide the pattern distortion effects of the source in the presence of

a scattering structure. Often times in antenna design, absolute magnitude of the fields are not important. It is only necessary to see how the pattern is perturbed from the ideal pattern or from the free space pattern of the source. The NEC-BSC can also be used to obtain absolute magnitudes, however. In the far zone the code provides the radiation intensity of the total fields. The radiation intensity is defined by

$$U = R^2 |\vec{E}|^2 / (2Z_o)$$

where R is the far zone distance, \vec{E} is the total electric field, and Z_o is the impedance of free space. If directive gain or power gain is desired, it is necessary to normalize the radiation intensity by the power radiated of the antenna. The NEC-BSC does not know this value by itself. This value must be supplied by the user to the code. The power radiated can be obtained by integrating the radiation intensity over the far zone radiation sphere. This can be a costly computation in terms of computer time but it has the advantage that the fields in the presence of the accompanying structures can be used. This value can also be obtained from a moment method code, where in practice its often only necessary to obtain the power radiated for the antenna in free space or over a ground plane not in situ. The gain is given by

$$G = 4\pi U / P_t$$

where if P_t is the power radiated the directive gain is obtained, and if P_i is the power input the power gain is obtained. In the near zone, the directive or power gain of the antenna does not have a clear meaning. In this case the power density found from the Poynting vector is of some interest. The power density is given by

$$\vec{P} = 1/2 \vec{E} \times \vec{H}^*$$

where the \vec{H}^* is the conjugate value of the total magnetic field. The total magnetic field is obtained by summing the individual UTD magnetic fields by using

$$\vec{H}_n = \hat{R}_n \times \vec{E}_n / Z_o$$

where the subscript "n" refers to the nth term, that is the field associated with a single ray path. The real part of the Poynting vector can be interpreted as the average power flow per square meter. The imaginary part of

the Poynting vector can be interpreted as the average reactive power per square meter. In general, this interpretation is correct. These values may be useful in radiation hazard estimates. Also, they can be used in analyzing quasi far zone patterns, where the antenna is in the far zone of the observer but the scattering structure may not be.

2.3 Receivers And Coupling

The receiving elements are represented by the same pattern factors described above for the source elements, that is, by their vector effective heights, \vec{h} . The expressions for the various models of receiving antennas are given in the previous section. It is not necessary to define an antenna in the NEC-BSC unless the coupling between two antennas is desired. If more than one receiver is present the code will sum the effects of the antennas based on their weights. This means that the effects of the transmission lines connecting the antennas to the load must be determined external to the code and transformed into weighting effects. A further restriction, at present, is that the receiving elements can not be placed on a plate.

The receiving antennas' locations are slaved to its near zone pattern trace location. The various receivers can be specified in relation to one another in their coordinate system. This has been done to allow the code to represent measurement situations where the transmitter and receiver can both be modeled. It, also, allows the antenna designer to place the antennas at various locations along a line of candidate sites to find an optimum location. Either a spherical pattern trace or a linear trace can be defined. When a spherical pattern trace is defined the orientation of the receiver is changed in such a way as to follow the spherical coordinate vector directions (θ and ϕ) as would be the case in an experimental situation. In a similar way the source antennas can be moved independently as is described later.

The coupling between two systems of antennas is found by superimposing all of the individual terms given by

$$C_{np} = I_n \vec{h}_n \cdot \vec{E}_p$$

where I_n is the weight of the nth receiver element, \vec{h}_n is the effective height of that element and \vec{E}_p is the electric field from the pth ray path between

antennas. Note that for a magnetic source

$$C_{np} = K_n \vec{h}_n \cdot \vec{E}_p / Z_o$$

because K_n is the input and $K_n = Z_o I_n$. The total coupling can be given by

$$C_t = I_m V_{oc}$$

where this represents the reaction between a receiving system with weight I_m which has a open circuit voltage V_{oc} produced at its terminals from the source antenna system.

The reaction between the two antenna systems can be normalized to give results in more meaningful terms to the antenna designer. The NEC-BSC has three possible normalization options. The first option represents the coupling in terms of the mutual impedance between the two antennas. The mutual impedance is given by

$$Z_{12} = \frac{I_m V_{oc}}{I_{11} I_{22}}$$

where values I_{11} and I_{22} are the transmitter and receiver terminal currents. The next option will represent the results in terms of a modified Frii's transmission method, which gives the power out over power in between the two antennas. The modified Frii's transmission result is given by

$$\frac{P_o}{P_i} = \frac{\left| \frac{1}{2} I_m V_{oc} \right|^2}{P_{rt} P_{rr}} \left[\frac{R_r R_L}{|Z_r + Z_L|^2} \right]$$

where P_{rt} is the power radiated by the transmitter and P_{rr} is the power radiated by the receiver as if it were acting as a transmitter. The radiation impedance and the load impedances are assumed to be conjugately matched so that the quantity in the large bracket above goes to a factor of one fourth. The last coupling option is to define the coupling in terms of the Linville method, which is the maximum coupling gain between the two antennas. The Linville coupling is found by first finding the mutual impedance between the antennas as given above and then use it to find the maximum coupling gain where

$$L = \frac{|Z_{12}^2|}{2\text{Re}(Z_{11})\text{Re}(Z_{22}) - \text{Re}(Z_{12}^2)}$$

so

$$G_{max} = \frac{1 - \sqrt{1 - L^2}}{L}.$$

The terminal current is I_{11} and I_{22} and terminal impedance is Z_{11} and Z_{22} .

In the case of the NEC-BSC, the modified Frii's Transmission formula and the Linville method of defining the coupling give essentially the same results as the distance between the two antennas is increased. The results are slightly different if the two antennas are within about a wavelength. It should be noted that if the transmitting and receiving antenna is approaching a half a wavelength from one another it is not anticipated that the NEC-BSC will give very accurate answers for the coupling between the two antennas. This is because the NEC-BSC assumes that the current from one antenna does not modified the other one. This will not be the case if they are very close together. Further details of the representation of the fields and coupling are given in the output discussion in Chapter 6 and examples are given in Chapter 7.

As mentioned, it is possible to do RCS type calculations using the NEC-BSC. This is accomplished by defining a source and receiver that are enslaved to the pattern cut coordinate system. The results will be output then as a coupling type answer between the transmitting and receiving antennas. In most cases, it is desirable to have the RCS results normalized with respect to a square meter. This can be accomplished by replacing the scattering object with a sphere, redoing the calculations, than normalizing the desired result relative to the know geometrical optics result for the sphere. An alternative method is to use the following approximation derived by using the using the sphere result in the coupling equations. The modified Frii's formula is set equal to the radar cross section equation given by

$$A_e = 4\pi R^2 \frac{|\vec{E}^s|^2}{|\vec{E}^i|^2}.$$

An equivalent power radiated can be defined for the transmitter and receiver given by

$$P'_r = \frac{Z_o |I_w J F_{max}|^2}{16\sqrt{\pi}\lambda R^2}.$$

for a electric antenna type and

$$P'_r = \frac{|lwMF_{max}|^2}{Z_o 16 \sqrt{\pi} \lambda R^2}$$

for a magnetic antenna type, where F_{max} refers to the maximum value of the antenna's pattern factor in the direction to the scattering object and R is the distance from the antenna to the center of rotation. Assuming that the antennas are directed with their maximum pattern factor at the center of the object F_{max} can be given as follows:

$$F_{max} = \begin{cases} 1, & \text{for type 1} \\ \frac{1 - \cos(kl/2)}{(kl/2) \sin(kl/2)}, & \text{for type 2} \\ 2/\pi, & \text{for type 3} \end{cases}$$

When using these equations, it is necessary that the units of all the length parameters be in meters. It should, also, be noted that these expressions do not give the proper dimensionality of power, but it is merely a convenience so that the final result is scaled properly.

Chapter 3

Principle Of Operation

3.1 Overview

The NEC - Basic Scattering Code is designed to be a user oriented computer code. The necessary data to describe a problem can be input and the resulting answers can be obtained with a minimum amount of knowledge by the user on how the code operates. As with most codes, however, it is necessary to have at least a basic knowledge of the key points in order to be able to intelligently use it and interpret its results. This section is designed to give just a brief description of the code for this purpose.

The NEC - BSC is constructed in a systematic way, such that the various operations of the code are set up in modular sections. The block diagram shown below, in Table 3.1, illustrates the major divisions of the main program. The first part of the main program is the input section where the geometry of the problem is defined. The next part makes any necessary conversions to the geometry, and defines the geometry fixed parameters that are needed later. The third part computes the fields associated with the individual mechanisms and superimposes the results. The last part of the main program outputs the resulting data either by numerical values on a printing device or in a form suitable for plotting the results.

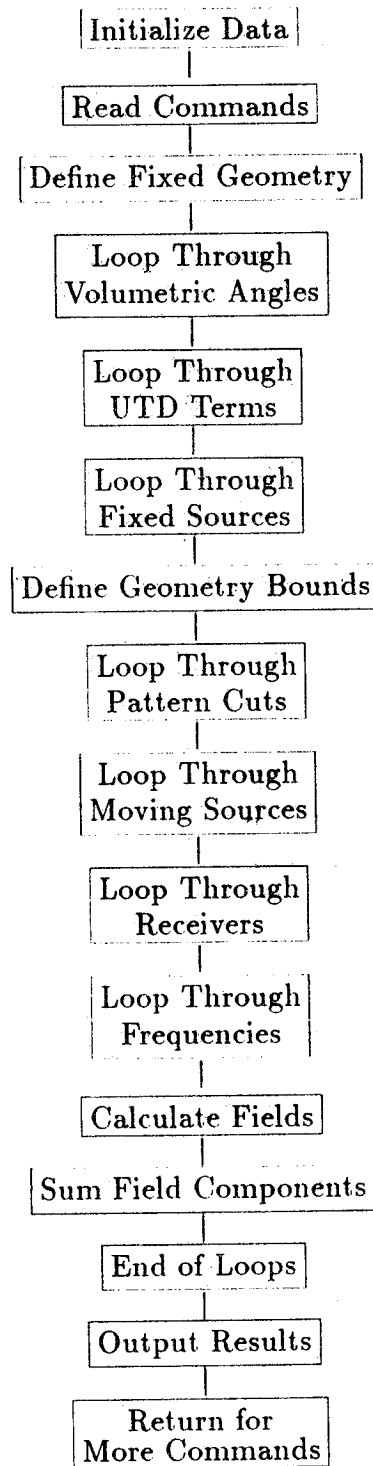


Table 3.1: Block Diagram of Main Program.

3.2 Input Section

The definition of the input data and the interpretation of the resulting output is of most importance to the user. The input section of the code is based on a command word system. The specific details of each command is given in Chapter 4. This description is intended to give an overview of the various commands and how they fit together. Hints and kinks on interpreting the input data for particular situations are given in Chapter 5.

The command word system used in this code is designed to make the definition of a given problem as easy as possible. Only the information necessary for the particular problem under consideration needs to be input in a given data set. The main program first initializes the input set using a list of default data defined at the beginning of the code. This list can be changed to fit the specific needs of the user. If input information that is frequently used is properly defined in the default list it need not be repeated in the input data set. The input data sets are read from a disk file or card device on logical unit IUI which is normally #5. (See Appendix B.) It is recommended that the information be written into a file using an editor and then that file can be assigned to the logical unit IUI. The data is read in free format to make it convenient to create the input sets on computer terminals, that is, the data need not be spaced in a specific way, it need only be separated by commas. To illustrate this, example data sets with their corresponding results are given in Chapter 7. The code, also, echoes back information concerning how the code has interpreted the individual commands as they are being processed. This is convenient when debugging input set syntax errors, since the code flags the errors right at the time that command is working on the specific input. This and all other numerical data is output on logical unit IUO which is normally #6.

The commands themselves can be grouped into four broad classifications. These are the geometry definition commands, the pattern control commands, the program control commands, and the output commands. The geometry definition commands form the largest group, with subgroups that define the units **UN**, **US**, and **UF**; definition coordinate systems **RT**; structure definitions for plates **PG**, infinite ground planes **GP**, and cylinders **CG**, elliptic cone frustums **CC**, and composite ellipsoids **CF**. Antenna information for single sources is accomplished using **SG**, for arrayed sources using **SA**, for method of moments files using **SM**, and for interpolated pat-

tern sources using **SI**. Similarly receivers have the corresponding commands **RG**, **RA**, **RM**, and **RI**. Resetting of and individual structure information can be accomplished using **NP**, **NG**, **NC**, **NS**, and **NR**.

The pattern control commands allow the user to chose the frequency either fixed **FR** or swept **FM**. Single pattern cuts can be defined in the far zone **PF** or **PD**; or near zone **PN**. Volumetric pattern cuts can also be defined in the far zone **VF** or **VD**; or near zone **VN**. A command that allows movement of the source as well as receiver with the pattern cut is **BP** with a reset command of **NM**.

The program control commands tell the code when to execute the given data set **XQ**, initialize a new problem set **NX**, or end the code **EN**. Definition of any special considerations such as limiting the number of mechanisms used **XT**, listing the value of the individual terms **TO**, specifying a particular type of theory **TP** for a plate or **TC** for a curved surface can be accomplished. In addition, a shadow only command can be specified for shadow maps on the volumetric far zone sphere using **OB**. Also, the **BF** command will provide the scattered field, which are the total field minus the incident field everywhere, instead of the total field.

The output commands allow the input echo print out to include comments **CM** and/or **CE**; determine whether a line printer listing is given **LP** or a plotter data set is written **PP** or **VP**. The data can be normalized for far zone distances **RD**; or normalized so that it represents directive gain, power gain, absolute antenna coupling numbers, or radar cross section **PR**. A listing of the commands are given in Tables 3.2 and 3.3.

As the geometry is being defined the input values are being converted from the given definition coordinate systems and units to a fixed reference coordinate system expressed in meters. These new values are echoed back with the original input values in the command output. This allows the code to compute all the fields in a consistent frame of reference. The default unit is meters for all lengths. In addition, the default frequency is 2.9979 GHz so that if the frequency and units commands are left out of the input set, the default for all the dimensions in the data set is wavelengths. All angles are assumed to be given in degrees.

There is no preferred order for the commands. The plates, curved surfaces, sources and receivers can be placed at the most convenient location in the input set. The code automatically counts up and keeps tracks of the number of these structures. If the number of structures specified exceeds

COMMAND	DEFINITION	LOCATION
BP	pattern movement control	pg 48
BF	scattered field option	pg 47
CC	cone frustum geometry	pg 50
CE	last or only comment	pg 62
CF	ellipsoid geometry	pg 54
CG	cylinder geometry	pg 58
CM	comment card	pg 62
EN	end execution	pg 62
FM	swept frequencies	pg 63
FR	frequency	pg 64
GP	infinite ground plane	pg 65
GR	range gate and weight	pg 67
LP	line printer output	pg 69
NC	next set of cylinders	pg 70
NG	no ground plane	pg 70
NM	no pattern movement	pg 70
NP	next set of plates	pg 70
NR	next set of receivers	pg 70
NS	next set of sources	pg 71
NX	next problem	pg 71
OB	shadowing only option	pg 72
PD	far zone pattern cut	pg 73
PF	far zone cut (non integer)	pg 77
PG	plate geometry	pg 79
PN	near zone pattern cut	pg 83
PP	plotter output	pg 88
PR	gain or coupling factors	pg 91

Table 3.2: Table of command words (also see Table 3.3).

COMMAND	DEFINITION	LOCATION
RA	receiver array geometry	pg 95
RD	far zone range	pg 101
RG	receiver geometry	pg 102
RI	interpolated receiver	pg 106
RM	NEC-MOM receiver input	pg 110
RT	rotate-translate geometry	pg 112
SA	source array geometry	pg 115
SG	source geometry	pg 120
SI	interpolated source	pg 126
SM	NEC-MOM source input	pg 131
TC	cylinder test options	pg 134
TO	output test options	pg 135
TP	plate test options	pg 138
UF	model scale factor	pg 139
UN	units of geometry	pg 140
US	units of source size	pg 141
VD	volumetric cut (integer)	pg 142
VF	volumetric far zone cut	pg 144
VN	volumetric near zone cut	pg 147
VP	volumetric plotter output	pg 151
XQ	execute code	pg 154
XT	execute with term file	pg 154

Table 3.3: Table of command words continued from Table 3.2.

the dimensions set aside for the storage of the information for that type of structure the code will flag the error and stop. The user can increase the dimensions as needed. (See Appendix A.) As the structures are being defined, it should be noted that once a rotated and/or translated input coordinate system is defined the input data will be referred to that system for all subsequent inputs until it is changed.

The pattern coordinate systems are not affected by the rotate - translate command. It has been assumed that the pattern coordinate system corresponds to the act of placing a model on a measurement pedestal or similar thought experiment. This means it will be used in a manner independent to the way the model was originally defined. The default is for the source to remain fixed and the observer to move. A source has to always be specified, however, a receiver does not. The movement of source or receiver is changed by using the **BP** command number of interest and then specifying one of the pattern movement commands. Whichever type of movement that is in effect will stay that way until it is change using **BP** or it is reset using **NM**.

3.3 Geometry Fixed Bounds

Once the necessary information to describe a problem is input into the code, the program analyzes the data and puts it into the correct form so that the electric and magnetic fields, or coupling information can be calculated. This includes reorganizing some of the data, and defining the fixed geometry bounds where applicable. The fixed geometry bounds are stored in arrays for later use. By calculating many of these parameters at the onset the algorithms are speeded up later on when the individual fields are being computed as a function of the observation point. Of course, all of these operations and the ones that follow are done opaque to the user.

3.4 Field Computations

The scattering code computes the fields for each individual source in succession. Each UTD scattered field type is broken up into a separate subroutine. The code is structured so that all of one type of scattered field is computed at one time for the complete pattern cut so that the amount

of core swapping is minimized thereby reducing overlaying and increasing efficiency. This also is an important feature that allows the code to be used on small computers that are not large enough to accept the entire code at one time. The code can be broken into smaller overlay segments which will individually fit in the machine. The results are, then, superimposed in the main program as the various segments are executed.

The field computation can be viewed as comprised of different classes of UTD terms. The first class contains the incident field, that is the direct field from the source to the observation point. The second class contains the major scattered fields associated with the individual flat plates and the interactions between the different plates. These include the singly reflected fields, doubly reflected fields, the singly diffracted fields, the reflected - diffracted fields, and the diffracted - reflected fields. The diffracted fields include the normal diffracted fields as well as slope diffraction, a heuristic corner diffracted field and a slope - corner diffracted field. The double diffracted fields are not included at present, but a warning is provided wherever this field component might be important. This is usually only a small angular section of space. This field may be included later whenever time and effort permit.

The third class contains the major scattered fields associated with the curved surfaces. This includes the uniformly reflected field, the uniformly diffracted fields, the reflected fields from the end caps, and the diffracted fields from the end cap rims. Only the creeping waves for the elliptic cylinders are present in this version of the code. Also, the diffracted field from the end cap rim is not at present corrected in the pseudo caustic regions. This is only important in small angular regions in space and is not deemed appropriate to be included at the present time. An equivalent current method could be used for this small region but it is rather time consuming to use for the benefits derived from it for such a general code as this.

Other classes of terms can be important in various situations. For instance, the interaction terms between the curved surfaces or the terms between curved surfaces and plates can be important in many instances. The terms that are presently included have been chosen because of application consideration along with time and budget constraints. Others will be added in the future.

The subroutines for each of the scattered field components are all struc-

tured in the same basic way. First, the ray path is traced backward from the chosen observation direction to a particular scatterer and subsequently to the source using either the laws of reflection or diffraction. Each ray path, assuming one is possible, is then checked to see if it is shadowed by any structure along the complete ray path. If it is shadowed the field is not computed and the code proceeds to the next scatterer or observation direction. If the path is not interrupted the scattered field is computed using the appropriate UTD solutions. The fields are then superimposed in the main program. This shadowing process is often speeded up by making various decisions based on bounds associated with the geometry of the structure. This type of knowledge is used wherever possible.

The shadowing of rays is a very important part of the scattering code. It is obvious that this approach should lead to various discontinuities in the resulting pattern. However, the UTD diffraction coefficients are designed to smooth out the discontinuities in the fields such that a continuous field is obtained. When a scattered field is not included in the result a so-called glitch or jump will appear in the pattern; therefore, the absence of a shadowed field is apparent. This can be used to advantage in analyzing complicated problems. Obviously in a complex problem not all the possible scattered fields can be included. In the UTD scattering code the importance of the neglected terms are determined by the size of these glitches or jumps in the pattern trace. If the glitches are small no additional terms are needed for a good engineering solution. In any case the user has a gauge with which he can examine the accuracy of the results and is not falsely led into believing a result is correct when in fact there could be an error. The examples in Chapter 7 illustrate these points and confirm the validity of the solution.

In order to illustrate the above points, the fields due to individual mechanisms can be plotted out separately. The geometry used for this example is shown in Figure 3.1. It is composed of a corner reflector type shape and a finite circular cylinder. The pattern cut is taken in a plane normal to the cylinder axis. The radiation patterns are shown plotted from 20 to -20 dB which represent the radiation intensity for fields produced by the source used. The patterns can be compared directly with one another.

The direct source field's ray paths are illustrated in Figure 3.2 and the resulting field plot is shown in Figure 3.3. Note in these figures that the scattering objects shadow the fields when they get in between the ray path

from the scattering center to the observation point. In this case, the direct field, which normally has an omnidirectional pattern, has two holes created by the plates and the cylinder blocking the path from the source to the observer. Figure 3.4 illustrates the first order plate terms, that is, the fields that reflect once off of the plate surfaces and then diffract once off of the plate edges. The sum of the reflected fields from the two plates is shown in Figure 3.5. The sum of all the diffracted fields from all the edges is shown in Figure 3.6. Note that the shadowing effects of the cylinder are somewhat hidden here, because when one edge is being shadowed another edge is not. All of the above terms are first order terms since they only react at most once with a scattering body.

The first order terms associated with the cylinder are shown next. The fields reflected and diffracted by the curved surface of the cylinder is illustrated in Figure 3.7. The resultant field uniformly reflected is shown in Figure 3.8 and the field uniformly diffracted is shown in Figure 3.9. Some of the ray paths associated with the diffractions from the rim of the end caps are illustrated in Figure 3.10. The sum of the end cap diffracted fields are shown in Figure 3.11. The fields in this case are small because the pattern cut does not cross any shadow boundaries due to the end cap rims. Note also, that the reflected field from the end cap are not present for this particular situation. Figure 3.12 illustrates a case where end cap reflections would exist.

Second order mechanisms occur for a plate when a ray interacts twice with the scattering objects. Figure 3.13 illustrates this for the double reflected field between two plates. The resulting pattern for all the double reflected fields for this configuration is shown in Figure 3.14. The field reflected by one plate then diffracted by another is illustrated in Figure 3.15, with the resulting field plot shown in Figure 3.16. The field diffracted by an edge of a plate then reflected by another plate is illustrated in Figure 3.17. The fields due to this mechanism are shown in Figure 3.18.

Second order terms can also occur between the plates and cylinders. They are not included in this version at the present time. Version 1 of the code had some preliminary results for these mechanisms. It is obvious from the configuration that some of these fields will play a role in this pattern. Some of the discontinuities in the total pattern are due to the fact that these terms are missing.

Note that the fields for the second order mechanism, in general, tend

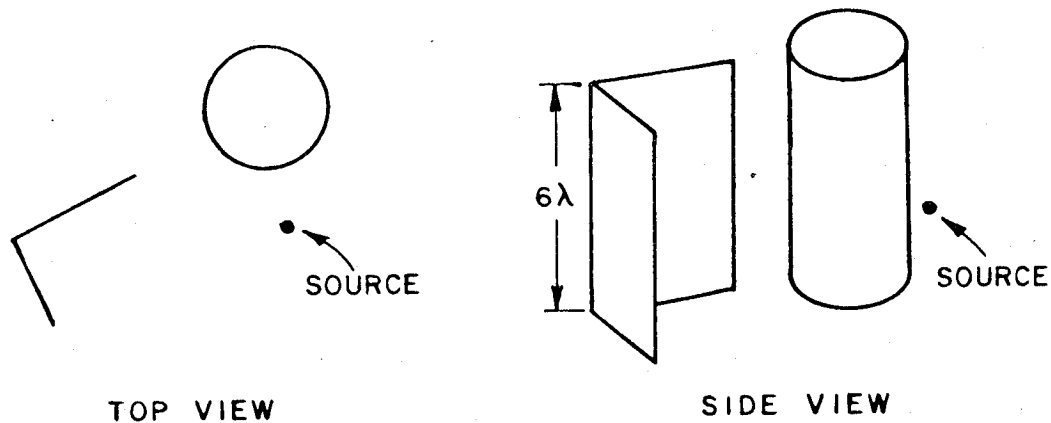


Figure 3.1: Illustration of source and scattering objects.

to become smaller in amplitude than the first order fields. When they do become somewhat large, they tend to only do so for small angular regions of the patterns. It is reasonable to expect that the third order mechanisms will be even smaller and more narrow in extent. For this reason, it would seem that second order mechanisms are sufficient in most cases.

The total pattern is obtained by summing the field components for the mechanisms mentioned. The total field pattern is shown in Figure 3.19. The resulting plot does have some discontinuities, however, they are rather small. This would tend to indicate the premise mentioned above is valid, that is, in general second order terms are sufficient to obtain a good engineering answer. Higher order terms can also be computed, which will in some cases improve the accuracy of the field computations. Generally, it is found that such terms are more difficult and costly to compute and therefore should only be done when absolutely necessary for a particular problem.

3.5 Output Section

The results of the code can be output on a printer or plotter device. The numerical results are output on logical unit IUO which is normally #6 when the LP command is set true or the default list automatically sets

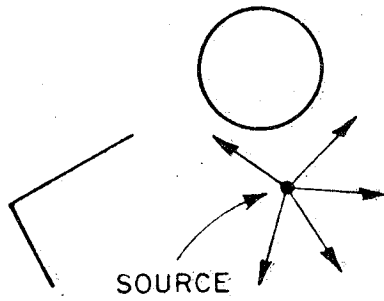


Figure 3.2: Source field ray paths.

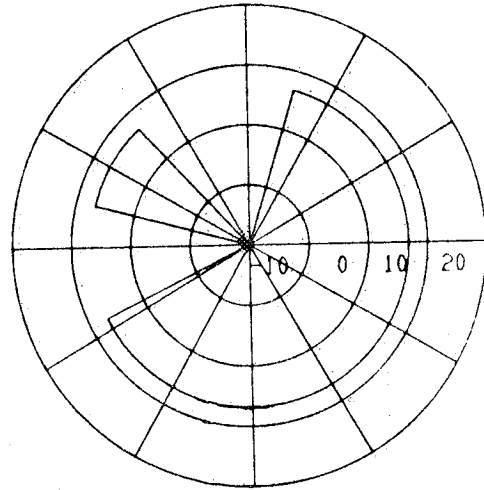


Figure 3.3: Source field.

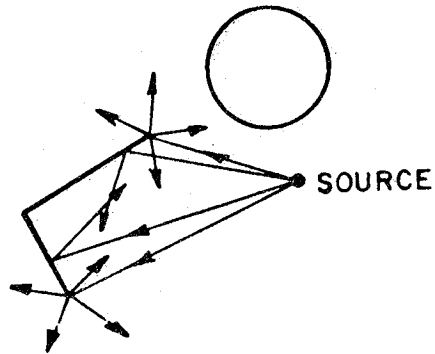


Figure 3.4: Illustration of first order plate ray paths.

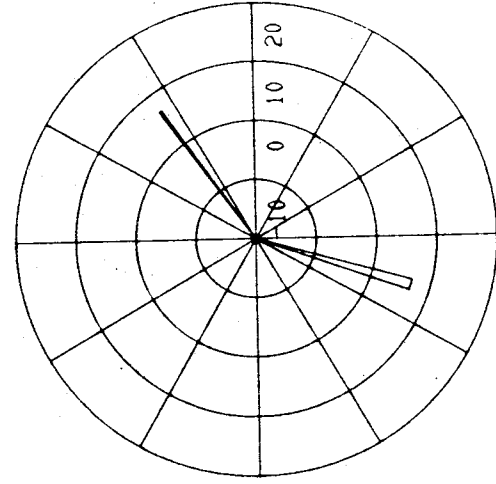


Figure 3.5: Fields due to single order plate reflection.

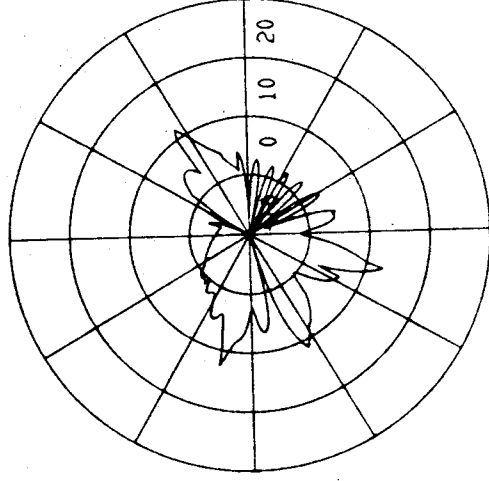


Figure 3.6: Fields due to plate diffraction.

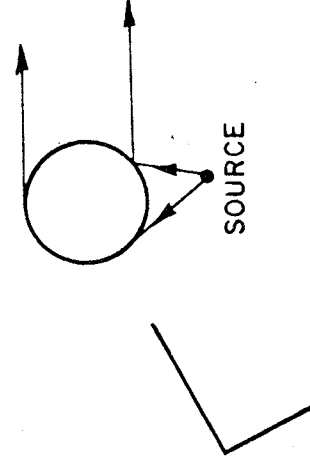


Figure 3.7: First order ray paths for the cylinder's curved surface.

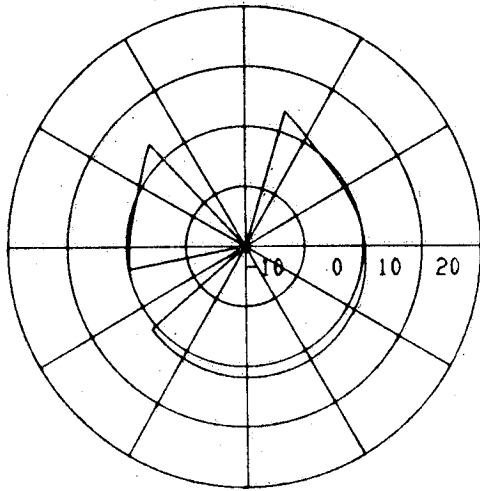


Figure 3.8: First order uniformly reflected field from the cylinder curved surface.

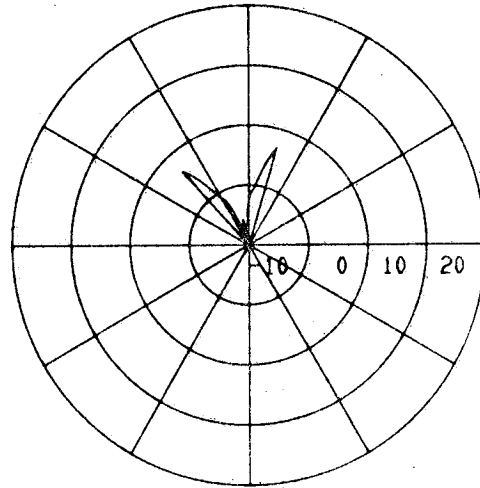


Figure 3.9: First order uniformly diffracted fields from the cylinder curved surface.

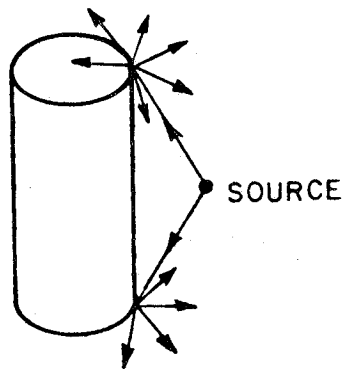


Figure 3.10: Ray paths for end cap diffracted fields.

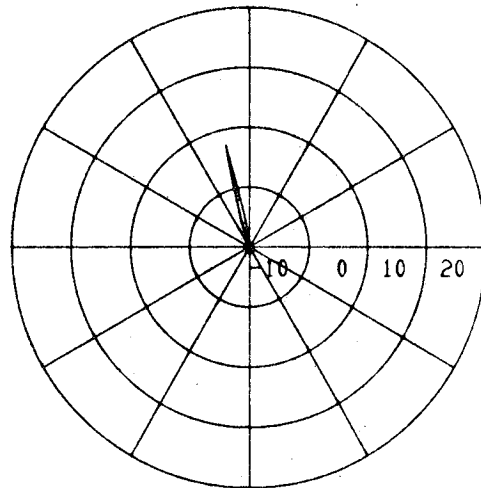


Figure 3.11: Fields due to end cap diffraction.

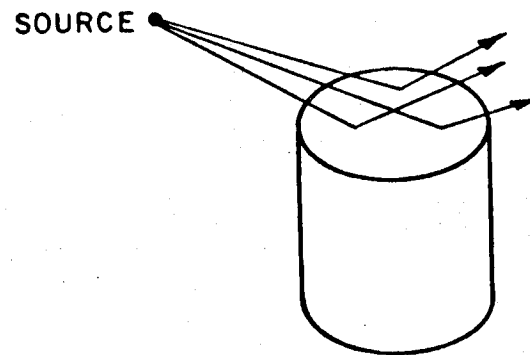


Figure 3.12: Illustration of ray paths for end cap reflected fields.

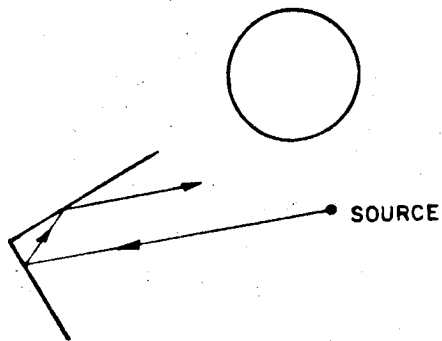


Figure 3.13: Ray path for plate double reflected fields.

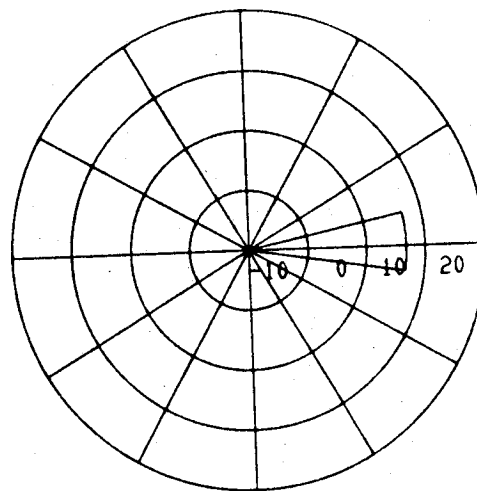


Figure 3.14: Fields due to double reflected plate rays.

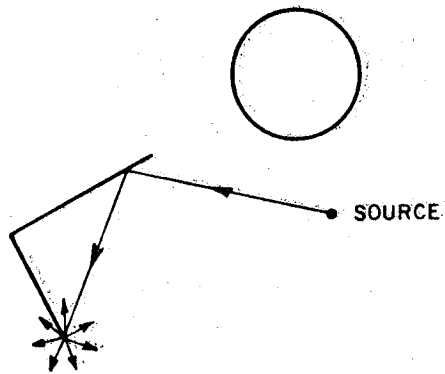


Figure 3.15: Ray paths for plate reflection - diffraction.

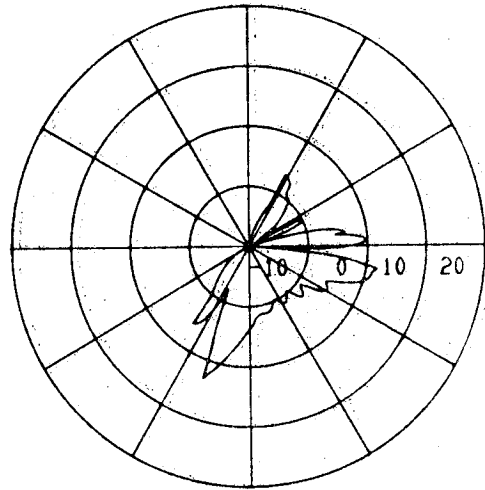


Figure 3.16: Fields resulting from plate reflection - diffraction.

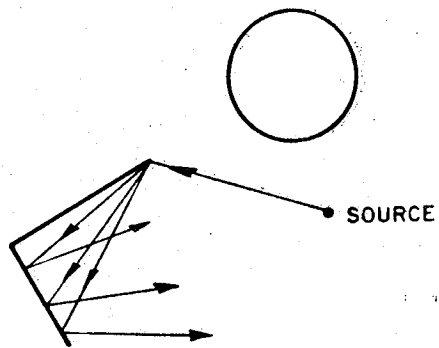


Figure 3.17: Illustration of plate diffracted - reflected ray paths.

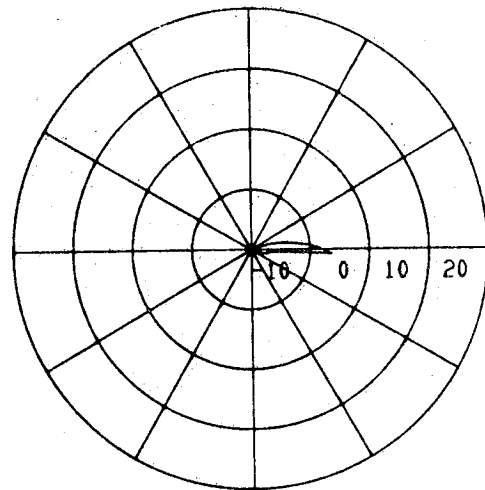


Figure 3.18: Fields due to plate diffraction - reflection mechanism.

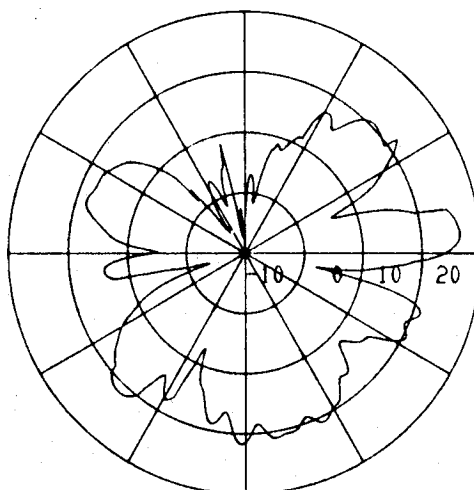


Figure 3.19: Total field of UTD terms used to calculate the source in the presence of the scattering bodies.

it true. The results are output in a form corresponding to the way the problem is defined. A complete break down of the output forms for the different possibilities is detailed in Chapter 6. Sample listing of some of these cases are shown in various examples in Chapter 7. For example, if a far zone pattern problem is being studied where the **PF** command has been used, the resulting output given will be the magnitude, phase, and dB values of the theta and phi components of the electric field given in the pattern coordinate reference frame as a function of the angles theta and phi or the frequency if the **FM** command is used. The electric field is given in volts/unit unless the far zone range is defined using the **RD** command in which case the result is given in volts/meter. The dB value of the field is given in terms of the radiation intensity unless option one of the **PR** command is used to normalize this value to directivity or power gain. Also, the dB value of the field is output in terms of the major, minor and total values of radiation intensity, directivity, or gain; along with the axial ratio, tilt angle, and sense of the polarization ellipse. An example of this type of print out is given in Example 1C of Chapter 7.

If the near zone pattern is specified using the **PN** command, the resulting output will be the magnitude, phase, and dB value of the electric and magnetic radial, theta and phi components, if the spherical pattern

coordinate option is chosen, or the x, y, and z components, if the rectangular pattern coordinate option is chosen. Again, the fields are referenced to the pattern coordinate system and will be displayed versus position unless the **FM** command is used in which case it will be versus frequency. The distances are given in meters and the angles in degrees. The electric field values are given in volts/meter and the magnetic field values are given in amperes/meter. The dB values are just the logarithmic representation of the fields in the first part of the print out. The second part gives the dB value of the Poynting vector. The real part of the Poynting vector corresponds to the radiated power density of the fields. The imaginary part, in general, can be correctly interpreted as the reactive power density of the fields in the near zone. These values can be of use for radiation hazard (RADHAZ) considerations. Directivity or gain does not have a reasonable interpretation in the near zone so this type of normalization option is not available in this case. An example print out of a near zone problem is given in Example 3 of Chapter 7.

If antenna to antenna coupling is desired, the **PN** command and one of the receiver commands must be used. The coupling results are displayed as the magnitude, phase, magnitude squared, and dB values of the reaction between the two antennas versus the spherical or linear position, or frequency as specified. The **PR** command has three options (options two through four) for normalizing this coupling data. If option two is used, the last two columns actually represent the magnitude and phase of the mutual impedance between the two antennas. If option three is used, the dB value is the coupling given as the ratio of the power out over power in using a modified Frii's transmission formula for conjugate matched loads. If option four is used, the dB value is the coupling given as the maximum gain between the antennas using the Linville method. An example output for a coupling problem is given in Example 11A of Chapter 7. In all of these sample print outs, the user should be cautioned that different types of computers have different architectures which results in different levels of accuracy. This manifests itself most often in the lower level fields. Specifically this means that if the results from the user's computer compares with the given example print out in some of the columns but not all of them, it usually indicates that the code is functioning properly on the user's system within the accuracy of that machine. The higher level results, which are of most importance, are the ones that should compare fairly closely; whereas,

the lower level cross polarized results could disagree. The physical interpretation, if this were a real measured result, is that the cross polarized results are down in the noise level of the experimental set up.

These results can also be output in a form suitable for plotting. The NEC-BSC does not support a particular plotting subroutine, because of the lack of standardization between computer facilities. The code will output the fields, normalization, and graph presentation information on logical unit IUP which is normally #7 in binary form, however, if the **PP** command is used. This is done so separate plotting programs can be used to obtain graphs of the output. Plots of the data are the most efficient method for representing the results, since a large amount of information can be shown in a small area. This manual displays most of its results in graphical form. The user can interface his own plotting packages using these files or a plotting package specifically for this code and written in the ANSI standard called the Graphical Kernel System (GKS) can be used as detailed in Appendix D. A binary format is chosen to conserve disk storage space. Other formats may be chosen depending on the needs of the user's facilities.

It should be noted here that an extended output of the individual fields can be obtained by specifying the LOUT variable in the **TO** command. These values can be used to debug the code or input set, or to use as a design tool since all the individual type fields are broken down to their particular ray paths. The form of this output is given in Tables 4.1 and 4.2. This information can come in handy when it is desirable to locate scattering centers that may be causing undesirable pattern distortion effects. This could lead to solutions such as the proper placement of absorber to reduce undesirable scattering mechanisms. For this case only the electric fields are output in x, y, z components referred to the reference coordinate system. A sample print out is given in Example 14 of Chapter 7.

3.6 Installation Hints

The NEC-BSC has been developed on a VAX 11/780 and 8550 computer system. It is written in FORTRAN 77 so that it will be as transportable as possible. Specific suggestions for running the code cannot be made for all computers, however, some suggestions for VAXes are given in Appendix C.

This section is intended to give some hints on what to look for when first running the code on a general computer.

The code is provided as a single file. It needs to be run through a FORTRAN compiler and then linked. It is self contained except for standard functions in the FORTRAN library and a few handy but unessential functions discussed in Appendix C. If a particular computer's compiler does not like the syntax used it may be necessary to make a few changes. For example, CHARACTER variables have been used in a few places such as in the storage of the command names. If the user's computer does not accept this variable type, they can be converted to INTEGER variables taking care to dimension the arrays so that the right number of characters fit within the user's computer word size. It is not anticipated that many of these types of problems will arise, since this version of the code and its predecessor have been compiled on many different types of computers.

The present version of the code takes up approximately 515 kilobytes of computer memory to run on a VAX. The size of the code is not a problem on the VAX since it is a virtual memory operating system. The code has been programed in such a way, however, that the amount of paging and swapping has been reduced to a minimum. The code generally runs within a 150 page working set size. On other machines, this modular construction feature can be used to advantage for various overlay schemes. The size of the code can also be reduced some what by decreasing the dimension of the variable used to store plate, cylinder, source or receiver information.

When the code has been compiled on a computer and any system specific compiler corrections have been made, the best way to test the operation of the code is to run the examples in Chapter 7 and compare the results against the given print out and plots. This will insure that there are no scrambled lines or other errors that might occur. The most common problem that can be anticipated is associated with the differing accuracies between different types of computers. As already explained in the previous section, this usually manifests itself in the cross polarized fields, that are many dB down from the co-polarized maximum values, not comparing with another computers results. If the large numbers compare well, but the lower levels do not the code is probably functioning properly within the accuracy of the machine. A VAX has approximately 7 digits of accuracy.

Another possible source of accuracy problems on different machines involves the fact that there are many small delta test numbers that are used

in the logical IF statements of the code. These can often present accuracy problems on different machines. An attempt has been made to localize these numbers in a common statement called LIMITS defined in the BLOCK DATA area. It is possible to vary the numbers in this statement corresponding to the accuracy of the machine being used to attempt to correct any errors. In addition, a set of warning flags have been placed in the code to detect and indicate to the user any problems that may crop up usually in the ray tracing algorithms. This option can be set in the **TO** command with the **LWARN** variable. If warning messages do occur, it does not necessarily indicate that the code is giving incorrect results within the its level of accuracy. The code is by the nature of the problem geometry sensitive. Every effort has been made to anticipate a wide range of geometrical situations. Not all situations can be predetermined, however. When a new class of geometries are tried by the user and a problem occurs, the user can use the **XT** command to eliminate the offending terms and evaluate the resulting pattern as has been illustrated in the discussions above. If the pattern does not change much, it is quite possible that the ray tracing algorithms are trying to find ray paths for field terms that will not contribute significantly to the final results.

If a real difficult code related problem is believed to exist, a large dump of information can be obtained by using the **LDEBUG** and **LTEST** variables in the **TO** command. A vary large amount of data will be printed out. As a consequence, the code will print out the data for only the first pattern location given for any one run. This data can be used to trace the internal workings of many of the individual subroutines.

Chapter 4

Description Of Commands

The commands discussed in this chapter are an updated set of the commands used in previous versions of the NEC-BSC. The following sections define in detail each command word and the variables that are read in association with them. This chapter is organized in alphabetical order of the commands. It is intended to be used as a reference for the user. Chapter 7 will give specific examples using this input method.

The method used to input data into the computer is presently based on a command word system. This is especially convenient when more than one problem is to be analyzed during a single computer run. The code stores the previous input data such that one need only input that data which has to be changed from the previous execution in those cases. Also, there is a default list of data so for any given problem the amount of data that needs to be input has been shortened. The command word options presently available are listed in Tables 3.2 and 3.3 on pages 27 and 28. The colon after the command word is not necessary and is sometimes used just to illustrate the separation between the command word and the space where comments can be inserted.

In this system, all linear dimensions may be specified in either meters, inches, or feet and all angular dimensions are in degrees. All the dimensions are eventually referred to a fixed cartesian coordinate system used as a common reference for the source and scattering structures. There is, however, a geometry definition coordinate system that may be defined using the **RT** command. This command enables the user to rotate and translate the coordinate system to be used to input any selected data set into the best

coordinate system for that particular geometry. Once the **RT** command is used all the input following the command will be in that rotated and translated coordinate system until the **RT** command is called again. See below for more details. There is also a separate coordinate system that can be used to define a pattern coordinate system. This is discussed in more detail in terms of the **PF**, **VF**, **PN**, and **VN** commands.

It is felt that the maximum usefulness of the computer code can be achieved using it on an interactive computer system. As a consequence, all input data are defined in free format such that the operator need only put commas between the various inputs. This allows the user on an interactive terminal to avoid the problems associated with typing in the field length associated with a fixed format. This method also is useful on batch processing computers. Note that all read statements are made on unit IUI which is usually #5, i.e., `READ(IUI,*)`, where the "*" symbol refers to free format. Other machines, however, may have different symbols representing free format. In any case, it is assumed that the user will use an interactive editor such as EDT, EVE, or LSE on a VAX, for example, to create the input sets. Typing them in real time is not recommended.

In all the following discussions associated with logical variables a "T" will imply true, and an "F" will imply false. The complete words true and false need not be input since most compilers just consider the first character in determining the state of the logical variable.

4.1 Command BF: Scattered Fields

This command enables the user to calculate the backscatter or bistatic near zone scattered fields. The scattered field is defined to be the total field minus the incident field everywhere (without the scatter present). For backscatter and some bistatic scattering cases this is similar to not including the incident field using the **XT** command. In the case of the general bistatic case, however, this would not subtract the incident field in the shadow regions as this command will. It has the added convenience that the **XQ** command can be used if other field tailoring is not required.

READ: LSCATF

_____ where _____

LSCATF This is a logical variable. It specifies whether the scatter field option is used. If false, the total field is calculated. If true, the free space incident field is subtracted from the total field.

EXAMPLE:

BF
T

This enables the scattered field option.

4.2 Command BP: Antenna Movement

This command enables the user to slave both the source and/or the receiver to their respective pattern coordinate systems. This means that pattern distortion plots can be obtained where both the source and receiver are moving in different orbits. In addition, the code can be used to obtain near zone type radar cross section results. Either backscatter or bistatic simulations are possible. The idea is to simulate as near as possible the actual physical set up of the actual measurement situation as far as source type, receiver type and distance is concerned.

READ: ISCAT

_____ where _____

ISCAT This is an integer variable. It specifies whether the pattern commands that follow specify the source or receiver movement or both simultaneously.

- 1= Pattern commands specify movement of the receiver or field point when **PD**, **PF**, **PN**, **VD**, **VF**, or **VN** are given. This is the default.
- 2= Pattern commands specify movement of the source when the **PN** or **VN** commands are given.
- 3= Pattern commands specify movement of the source and receiver simultaneously when the **PN** or **VN** commands are given.

Once the **BP** command is given, it stays in effect with that option until it is changed. It is set for a default of moving the receiver only, that is the pattern commands do not effect the source. Notice that it is presently assumed that the source can not be placed in the far zone. Once a source or receiver movement is specified, than all of the antennas of that type will move together based on their type's pattern command, respectively.

Note for radar cross section type results, the **SG**, **RG**, and **PN** commands must be used. Specifying both the source and receiver in the far

BP

49

zone will not work. In addition, the direct field from the source to receiver should be suppressed using the **BF** or **XT** commands, unless the user is specifically trying to simulate this type of effect in some way. Also, it should be noted that the results will not be normalized to the usual radar cross-sectional area unless the proper weights are used. This can be accomplished in more than one way by using the weights in the **SG** or **RG** commands, by the normalization constants provided in the **PR** command, or by simply comparing the desired results with that of a sphere run in the code. This is discussed in more detail in another part of the manual. Also, it should be cautioned that the plates and cylinders available in this general purpose code can only very crudely model a practical shape for a radar cross section type problem. Furthermore, the second order solution provided in this code can only be expected to provide a solution with approximately a 30(?) dB dynamic range, that is provide accurate answers for fields that are no more than 30(?) dB down from the peak result.

EXAMPLE:BP
3

The source and receiver will move together defined by the next pattern command called.

EXAMPLE:NM
BP
2

The source motion will be defined by the next pattern command, with the receiver held stationary.

4.3 Command CC: Cone Frustum

This command enables the user to define the geometry of the finite multiple sectioned elliptic cone frustum structures to be considered. The geometry is illustrated in Figure 4.1. One call to this command defines one structure. The number of curved surface units in the structure are automatically counted by the number of calls to this command. See Appendix A on how to adjust the number of curved surface units (NCX) and the number of cone rims (NNX) available.

READ: (XCL(N,MC),N=1,3)

_____ where _____

XCL(N,MC) This is a doubly dimensioned real variable. It is used to specify the location of the origin of the MCth curved surface unit relative to the definition coordinate system. It is input on a single line with the real numbers being the x, y, z coordinates of the origin which correspond to $N=1,2,3$, respectively.

READ: TCLZ, PCLZ, TCLX, PCLX

_____ where _____

TCLZ,PCLZ These are real variables. They are input in degrees as spherical angles that define the z_c -axis of the cylinder coordinate system as if it was a radial vector in the definition coordinate system.

TCLX,PCLX These are real variables. They are input in degrees as spherical angles that define the x_c -axis of the cylinder coordinate system as if it was a radial vector in the definition coordinate system.

CC

51

Note that the new x_c -axis and z_c -axis must be defined orthogonal to each other. The new y_c -axis is found from the cross product of the x_c - and z_c -axes.

READ: NEC(MC)

_____ where _____

NEC(MC) This is a dimensioned integer variable which defines the number of rims for the cone frustum cylinder.

**READ: (AC(NC,MC), BC(NC,MC), ZC(NC,MC),
NC=1,NEC(MC))**

_____ where _____

AC(NC,MC) This is a double dimensioned real variable which defines the radius of the NCth rim of the cone frustum on the x_c -axis of the MCth curved surface unit.

BC(NC,MC) This is a double dimensioned real variable which defines the radius of the NCth rim of the cone frustum on the y_c -axis of the MCth curved surface unit.

ZC(NC,MC) This is a double dimensioned real variable which defines the z position of the NCth rim of the cone frustum along the z_c -axis of the MCth curved surface unit.

Note that the program will keep increasing the number of curved surface units in the solution by the number of calls to this command unless the **NC** or **NX** commands are called to reinitialize the curved surface geometry. Also, the ellipticity of a conical structure must remain the same for the entire length of that structure (that is $AC(i,MC)/BC(i,MC) = AC(j,MC)/BC(j,MC)$ for all i and j). The most positive rim should be defined first until all NC rims are defined in descending order.

EXAMPLE:

CC

0.,0.,0.

0.,0.,90.,0.

3

2.,3.,5.

1.,1.5,0.

.75,1.125,-2.

This defines a cone frustum centered at the origin and z directed. It has three rim sections at $z = 5, 0$ and -2 with a different a and b for each. Note that a/b is the same for all three.

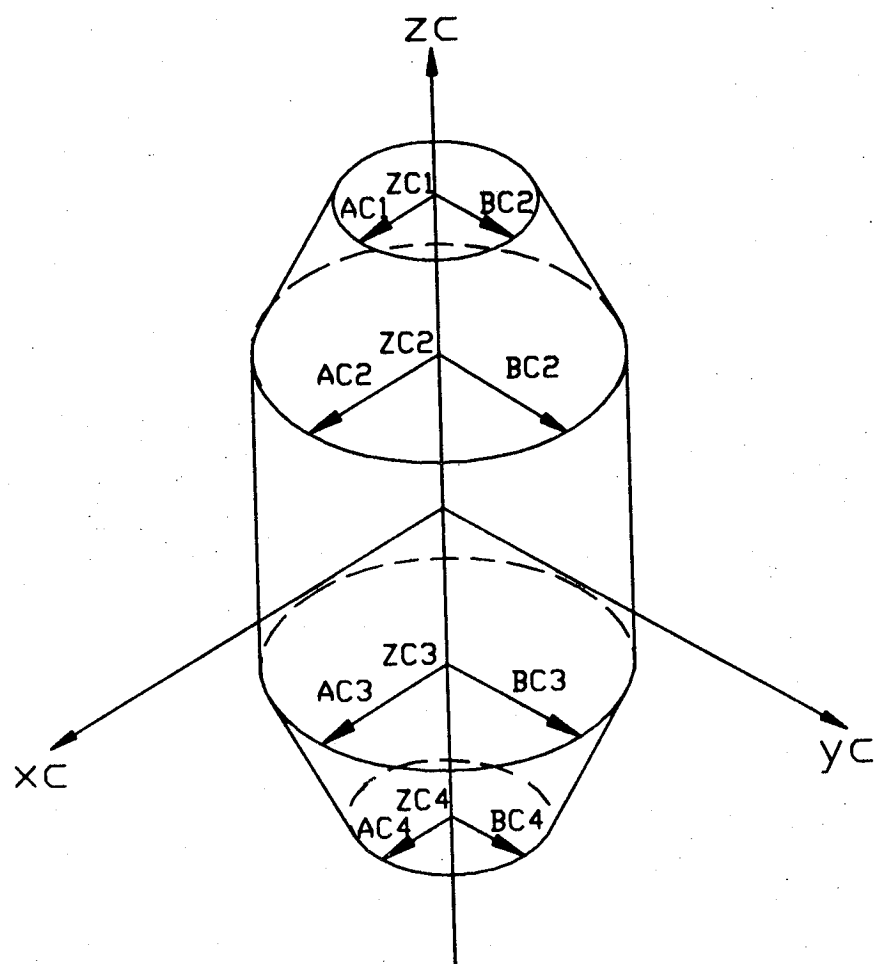


Figure 4.1: Definition of finite cylinder geometry composed of cone frustum segments with elliptic cross section.

4.4 Command CF: Composite Ellipsoid Geometry

This command enables the user to define the geometry of a composite ellipsoid which can be truncated in front and/or in back. The geometry is illustrated in Figure 4.2. The ellipsoid is counted as another curved surface unit by the code and is numbered accordingly. See Appendix A on how to adjust the number of curved surface units (NCX) available.

READ: (XCL(N,MC),N=1,3)

_____ where _____

XCL(N,MC) This is a doubly dimensioned real variable. It is used to specify the location of the origin of the MCth curved surface unit relative to the definition coordinate system. It is input on a single line with the real numbers being the x, y, z coordinates of the origin which correspond to $N=1,2,3$, respectively.

READ: TCLZ, PCLZ, TCLX, PCLX

_____ where _____

TCLZ,PCLZ These are real variables. They are input in degrees as spherical angles that define the z_c -axis of the sphere coordinate system as if it was a radial vector in the definition coordinate system.

TCLX,PCLX These are real variables. They are input in degrees as spherical angles that define the x_c -axis of the sphere coordinate system as if it was a radial vector in the definition coordinate system.

Note that the new x_c -axis and z_c -axis must be defined orthogonal to each other. The new y_c -axis is found from the cross product of the x_c - and z_c -axes.

READ: AC(1,MC), BC(1,MC), CCN, CCP

_____ where _____

AC(1,MC) This is a real variable that defines the radius of the MCth curved surface unit along the x_c axis of the composite ellipsoid.

BC(1,MC) This is a real variable that defines the radius of the MCth curved surface unit along the y_c axis of the composite ellipsoid.

CCN This is a real variable that defines the radius of the MCth curved surface unit along the negative z_c axis of the composite ellipsoid.

CCP This is a real variable that defines the radius of the MCth curved surface unit along the positive z_c axis of the composite ellipsoid.

READ: LELLIC

_____ where _____

LELLIC This is a logical variable that tells the code whether the composite ellipsoid is truncated.

If this is false skip the next read.

READ: ZCN, THTN, ZCP, THTP

_____ where _____

ZCN This is a real variable that defines the position the center of the most negative end cap on the z_c -axis of the truncated ellipsoid.

THTN This is a real variable. It is input in degrees and defines the angle the surface of the most negative end cap makes with the positive z_c -axis in the x_c - z_c plane. Must be 90° for now.

ZCP This is a real variable that defines the position of the center of the most positive end cap on the z_c -axis of the truncated ellipsoid.

THTP This is a real variable. It is input in degrees and defines the angle the surface of the most positive end cap makes with the positive z_c -axis in the x_c - z_c plane. Must be 90° for now.

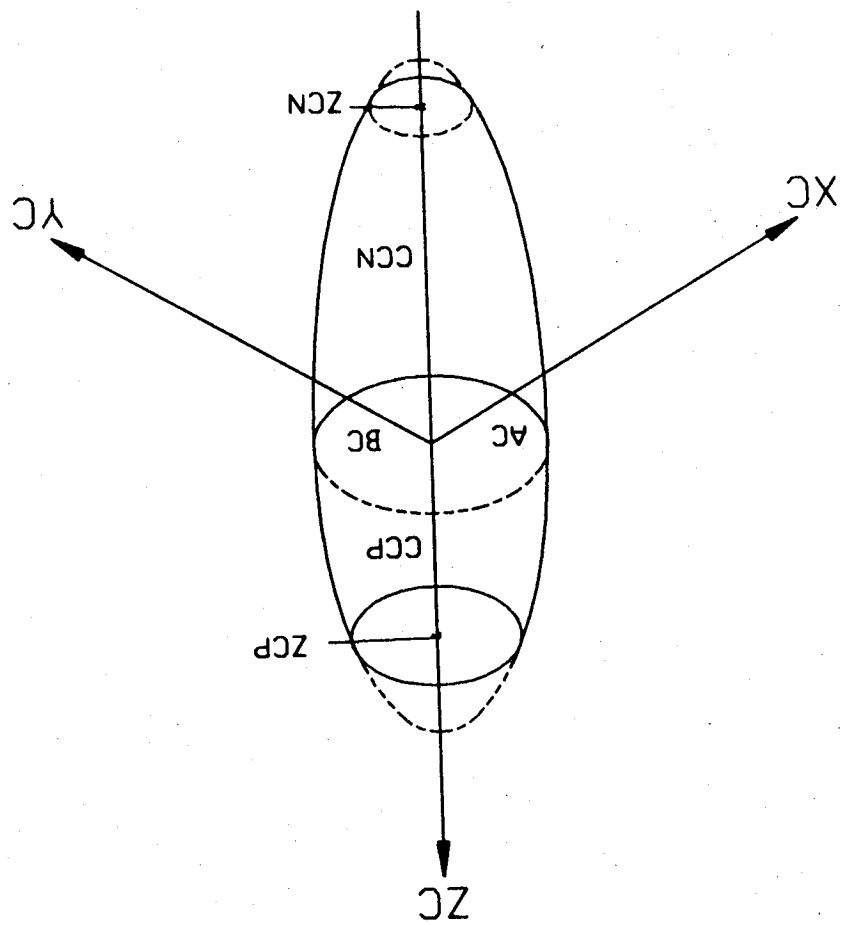
Note that the program will keep increasing the number of curved surface units in the solution by the number of calls to this command unless the **NC** or **NX** commands are called to reinitialize the curved surface geometry.

EXAMPLE:

CF
0.,0.,0.,
0.,0.,90.,0.
2.,3.,5.,10.
T
-3.,90.,5.,90.

This defines a composite ellipsoid located at the origin. Where for $z > 0$, $c = 10$ and for $z < 0$, $c = 5$ with $a = 2$ and $b = 3$ for both. The ellipsoid is truncated at $z = -3$ and 5 with 90° end caps.

Figure 4.2: Definition of the finite composite ellipsoid geometry.



4.5 Command CG: Cylinder Geometry

This command enables the user to define the geometry of the finite elliptic cylinder structures to be considered. The geometry is illustrated in Figure 4.3. One call to this command defines one curved surface unit. The number of curved surface units in the structure are automatically counted by the number of calls to this command. See Appendix A on how to adjust the number of curved surface units (NCX) available.

READ: (XCL(N,MC),N=1,3)

_____ where _____

XCL(N,MC) This is a doubly dimensioned real variable. It is used to specify the location of the origin of the MCth curved surface unit relative to the definition coordinate system. It is input on a single line with the real numbers being the x, y, z coordinates of the origin which correspond to $N=1,2,3$, respectively.

READ: TCLZ, PCLZ, TCLX, PCLX

_____ where _____

TCLZ,PCLZ These are real variables. They are input in degrees as spherical angles that define the z_c -axis of the cylinder coordinate system as if it was a radial vector in the definition coordinate system.

TCLX,PCLX These are real variables. They are input in degrees as spherical angles that define the x_c -axis of the cylinder coordinate system as if it was a radial vector in the definition coordinate system.

Note that the new x_c -axis and z_c -axis must be defined orthogonal to each other. The new y_c -axis is found from the cross product of the x_c - and z_c -axes.

READ: AC(1,MC), BC(1,MC)

_____ where _____

AC(1,MC) This is a double dimensioned real variable which defines the radius of the MCth curved surface unit on the x_c -axis of the elliptic cylinder.

BC(1,MC) This is a double dimensioned real variable which defines the radius of the MCth curved surface unit on the y_c -axis of the elliptic cylinder.

READ: ZCN, THTN, ZCP, THTP

_____ where _____

ZCN This is a real variable that defines the position the center of the most negative end cap on the z_c -axis of the cylinder.

THTN This is a real variable. It is input in degrees and defines the angle the surface of the most negative end cap makes with the positive z_c -axis in the x_c - z_c plane.

ZCP This is a real variable that defines the position of the center of the most positive end cap on the z_c -axis of the cylinder.

THTP This is a real variable. It is input in degrees and defines the angle the surface of the most positive end cap makes with the positive z_c -axis in the x_c - z_c plane.

Note that the program will keep increasing the number of curved surface units in the solution by the number of calls to this command unless the **NC** or **NX** commands are called to reinitialize the curved surface geometry.

EXAMPLE:

CG

0.,0.,0.

90.,90.,90.,0.

1.,1.

-5.,90.,5.,90.

Defines a circular cylinder with it's
axis in the *y* direction, centered at the
origin with a length of 10.

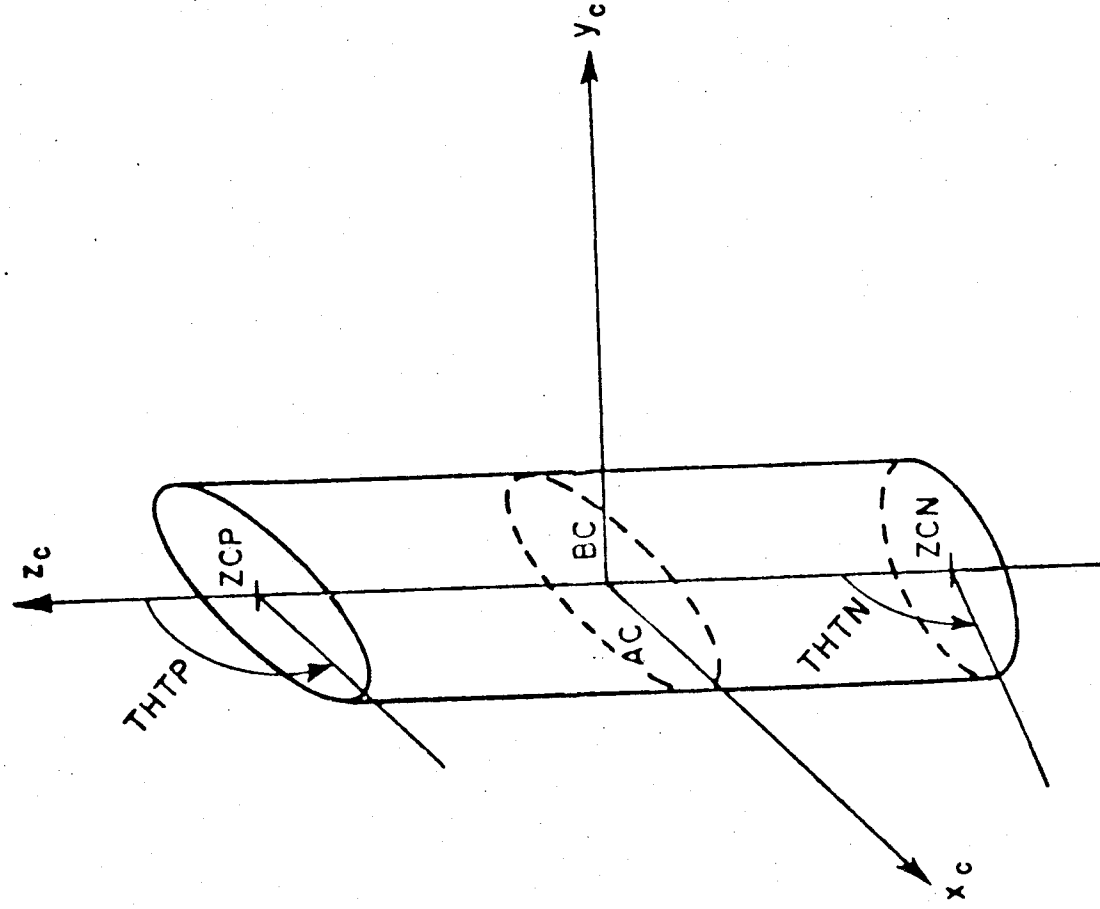


Figure 4.3: Definition of finite elliptic cylinder geometry.

4.6 Command CM: and CE: Comments

These commands enable the user to place comment cards in the input and output data in order to help identify the computer runs for present and future reference.

READ: (IR(I), I=1,36)

_____ where _____

IR(I) This is a CHARACTER*2 dimensioned array used to store the command word and comments. Each card should have **CM** or **CE** on them followed by an alphanumeric string of characters. The **CM** command implies that there will be another comment card following it. The last comment card must have the **CE** command on it. If there is only one comment card the **CE** command must be used.

Note that it is possible to place comments to the right of all the command words, if desired.

EXAMPLE:

CM: TEST CASE

CE: NEAR ZONE SCATTERING FROM A PLATE

4.7 Command EN: End Program

This command enables the user to terminate the execution of the scattering code.

4.8 Command FM: Swept Frequencies

This command enables the user to define a set of frequencies to be analyzed.

READ: NFQG, FQGS, FQGI

_____ where _____

NFQG This is an integer variable that defines the number of frequencies desired.

FQGS This is a real variable that defines the starting frequency in gigahertz.

FQGI This is a real variable that defines the incremental frequency change in gigahertz.

Note that the source length and width must not be specified in wavelengths. It is assumed that the analytic definition of the currents on the antenna are a correct variation of frequency. Also, only one pattern location can be specified for a given execution.

EXAMPLE:

FM
51,5.0,0.02

Sweep the frequency from 5 to 6 GHz
in 0.02 GHz steps.

4.9 Command FR: Frequency

This command enables the user to define the frequency in gigahertz.

READ: FRQG

_____ where _____

FRQG This is a real variable which is used to define the frequency in gigahertz.

Note that the default frequency is 0.2997925 GHz. This means that if the frequency and units are not specified, all calculations are assumed to be in wavelengths.

EXAMPLE:

FR
9.0

The frequency of operation is 9 GHz.

4.10 Command GP: Ground Plane

This command enables the user to specify an infinite ground plane in the x_t - y_t plane.

READ: LSLAB(MPDX)

_____ where _____

LSLAB(MPDX) This is a dimensioned integer variable. It is used to define the type of plate desired as follows:

0 = Perfectly conducting metallic plate

-3 = Dielectric half space

Note that if **LSLAB(MPDX)=0** the code will skip around the **READ** statement for the dielectric information, therefore, the next line defining the dielectric properties should not be placed in the input data set.

**READ: ERSLAB(1,MPDX), TESLAB(1,MPDX),
URSLAB(1,MPDX), TMSLAB(1,MPDX)**

_____ where _____

ERSLAB(1,MPDX) This is a doubly dimensioned variable. It is used to specify the relative dielectric constant of the half space.

TESLAB(1,MPDX) This is a doubly dimensioned variable. It is used to specify the dielectric loss tangent if the number is positive or the conductivity if the number is negative of the half space.

URSLAB(1,MPDX) This is a doubly dimensioned variable. It is used to specify the relative permeability constant of the half space.

TMSLAB(1,MPDX) This is a doubly dimensioned variable.
It is used to specify the permeability loss tangent of the half space.

EXAMPLE:

GP Defines a perfectly conducting ground
0 plane in the $x - y$ plane.

EXAMPLE:

GP Defines a half space of polystyrene.
-3
2.55,0.,1.,0.

4.11 Command GR: Range Gate

This command enables the range gate and weight subroutine. This subroutine can be user defined. Predefined options are presented for convenience. This command should only be used for a near zone problem. That is, the PN or VN command must be used to specify the source and receiver movement if they are moving.

READ: LGATE

_____ where _____

LGATE This is a logical variable. If true, it enables the range gate and weight options.

READ: IGATE

_____ where _____

IGATE This is an integer variable. It is used to indicate the range gate and weight option desired.

1= No range weight, that is, a range weight of unity.

2= Linear range weight with RCUT specified.

3= Quadratic range weight with RCUT specified.

READ: RMIN, RMAX

_____ where _____

RMIN This is a real variable. It specifies the minimum distance from the transmitter to scatterer (if present) and back to the receiver that fits within the range gate.

RMAX This is a real variable. It specifies the maximum distance from the transmitter to scatter (if present) and back to the receiver that fits within the range gate.

If IGATE is 2 or 3, then the next line is read.

READ: RCUT

_____ where _____

RCUT This is a real variable. It specifies the cut off range for a range gate weight. If IGATE is 2, it is used in the linear weight. If IGATE is 3, it is used in a quadratic weight.

EXAMPLE:

GR
T
2
100.,200.
1.5

The received signal is range gated.
Only fields that travel a distance of
between 100 and 200 will be "seen".
Also a linear range weight of 1.5 is
defined.

4.12 Command LP: Printer Output

This command enables the user to specify whether a line printer listing of the results is desired.

READ: LWRITE

_____ where _____

LWRITE This is a logical variable defined by T or F. It is used to indicate if a line printer listing of the results is desired. (normally set true)

4.13 Command NC: Next Set of Cylinders

This command enables the user to initialize the cylinder data. All of the cylinders are removed from the problem unless they are respecified following this command.

4.14 Command NG: No Ground Plane

This command enables the user to initialize the infinite ground plane. The ground plane is removed from the problem unless it is respecified following this command.

4.15 Command NM: No Antenna Movement

This command enables the user to specify initial antenna movement such as a stationary receiver. The default condition of the receivers always moving is cancelled by this command.

For an example of it's use see the **BP** command on page 48.

4.16 Command NP: Next Set of Plates

This command enables the user to initialize the plate data. All of the plates are removed from the problem unless they are respecified following this command.

4.17 Command NR: Next Set of Receivers

This command enable the user to initialize the receiver data. All of the receivers are removed from the problem unless they are respecified following the command.

4.18 Command NS: Next Set of Sources

This command enables the user to initialize the source data. All of the sources are removed from the problem unless they are respecified following the command.

4.19 Command NX: Next Problem

This command enables the user to initialize the commands to their default conditions specified in the list at the beginning of the main program.

4.20 Command OB: Obscuration Option

This command enables the user to obtain the projected shadow of the incident fields only.

READ: LSHDW

_____ where _____

LSHDW This is a logical variable. If set true, it provides only the shadow of the incident field due to the defined structure present. In other words it turns off all field calculations, except the shadowing algorithms for the direct rays. It can be used in combination with the volumetric pattern commands like **VF**, to produce the projected shadow on the far zone sphere.

4.21 Command PD: Far Zone Pattern

This command enables the user to define the far zone pattern coordinate system, the pattern cut, and the angular range that is desired using integer angle increments. The **PF** command provides more versatility with non-integer angle increments. The geometry is illustrated in Figures 4.4, 4.5, and 4.6. See Appendix A on how to adjust the number of observation points (NOX) available.

READ: THCZ, PHCZ, THCX, PHCX

_____ where _____

THCZ,PHCZ These are real variables. They are input in degrees as spherical angles that define the z_p -axis of the pattern coordinate system as if it was a radial vector in the reference coordinate system.

THCX,PHCX These are real variables. They are input in degrees as spherical angles that define the x_p -axis of the pattern coordinate system as if it was a radial vector in the reference coordinate system.

Note that the new x_p -axis and z_p -axis must be defined orthogonal to each other. The new y_p -axis is found from the cross product of the x_p - and z_p -axes.

READ: LCNPAT, TPPD

_____ where _____

LCNPAT This is a logical variable that defines the pattern cut desired, such that

T= THETA CUT (conical cut)

F= PHI CUT (great-circle cut)

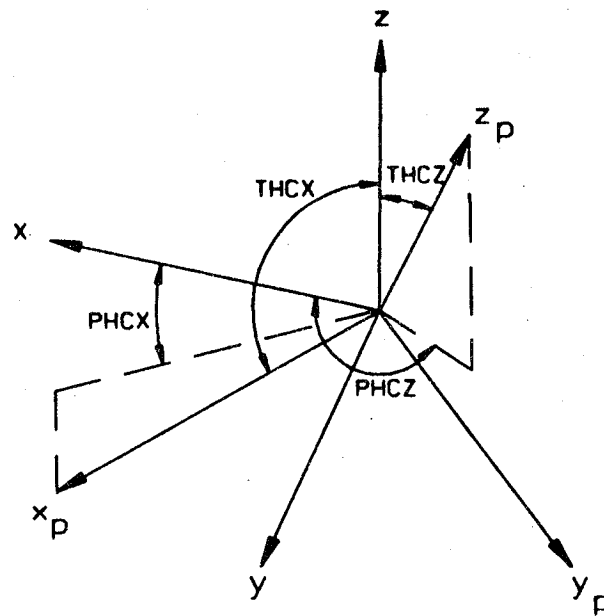


Figure 4.4: Definition of pattern coordinate system.

TPPD This is a real variable that defines the pattern angle that is to be held constant, such that

TPPD=THP constant, if LCNPAT=T

TPPD=PHP constant, if LCNPAT=F

READ: IB, IE, IS

_____ where _____

IB,IE,IS These are integer variables used to define angles in degrees. They are, respectively, the beginning, ending, and incremental values of the pattern angle.

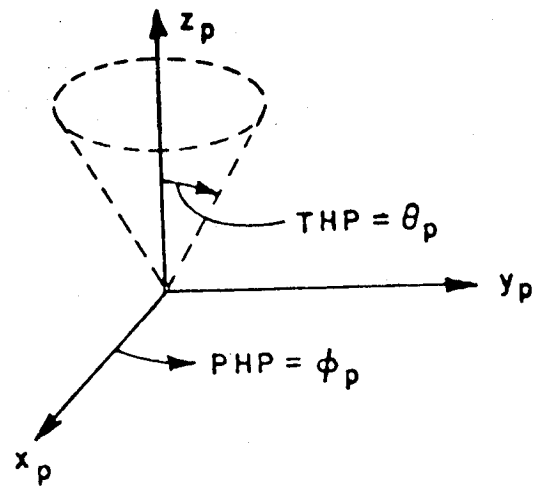


Figure 4.5: Conic pattern cut, $LCNPAT=.TRUE.$, $TPPD=THP$

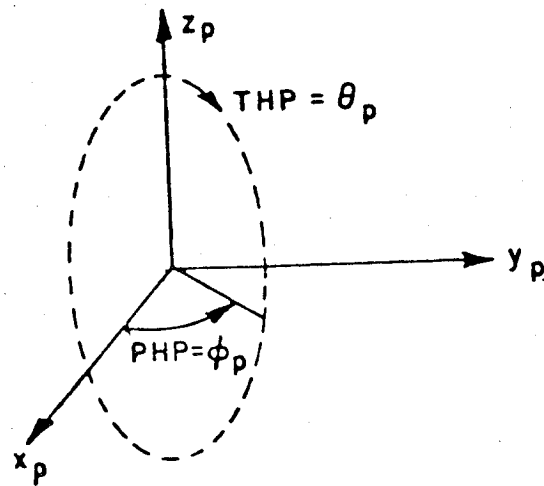


Figure 4.6: Great circle pattern cut, $LCNPAT=.FALSE.$, $TPPD=PHP$.

EXAMPLE:

PD
 0.,0.,90.,0.
 F,0.
 0,360,1

Same axes as definition coordinate system with a $\phi = 0^\circ$ cut and with θ from 0° to 360° in 1° steps.

EXAMPLE:

PD
 0.,0.,90.,0.
 T,25.
 0,180,1

Same axes as above, but cut is a cone at $\theta = 25^\circ$ for ϕ from 0° to 180° in 1° steps.

4.22 Command PF: Far Zone Cut

This command enables the user to specify a far zone pattern cut with non - integer pattern points. It supersedes the **PD** command which does the same thing but with only integer values for the angles. The geometry is illustrated in Figure 4.4, 4.5, and 4.6. See Appendix A on how to adjust the number of observation points (NOX) available.

READ: THCZ, PHCZ, THCX, PHCX

_____ where _____

THCZ,PHCZ These are real variables. They are input in degrees as spherical angles that define the z_p -axis of the pattern coordinate system as if it was a radial vector in the reference coordinate system.

THCX,PHCX These are real variables. They are input in degrees as spherical angles that define the x_p -axis of the pattern coordinate system as if it was a radial vector in the reference coordinate system.

Note that the new x_p -axis and z_p -axis must be defined orthogonal to each other. The new y_p -axis is found from the cross product of the x_p - and z_p -axes.

READ: LCNPAT, TPPD

_____ where _____

LCNPAT This is a logical variable that defines the pattern cut desired, such that

T= THETA CUT (conical cut)

F= PHI CUT (great-circle cut)

TPPD This is a real variable that defines the pattern angle that is to be held constant, such that

TPPD=THP constant, if LCNPAT=T

TPPD=PHP constant, if LCNPAT=F

READ: TPPS, TPPI, NPN

_____ where _____

TPPS This is a real variable used to define the starting angle in degrees.

TPPI This is a real variable used to define the incremental angle in degrees for each step of the pattern.

NPN This is an integer variable used to define the total number of steps of the pattern desired.

EXAMPLE:

PF
0.,0.,90.,0.
F,0.
0.,0.5,721

Same axes as definition coordinate system with a $\phi = 0^\circ$ cut and with θ from 0° to 360° in half of a degree steps.

4.23 Command PG: Plate Geometry

This command enables the user to define the geometry of the flat plate structures to be considered. The geometry is illustrated in Figure 4.7. One call to this command defines one plate. The number of plates in the structure are automatically counted by the number of calls to this command. See Appendix A on how to adjust the number of plates (NPX), edges (NEX), and layers (NLX) available.

READ: MEP(MP), LSLAB(MP)

_____ where _____

MEP(MP) This is a dimensioned integer variable. It is used to define the number of corners (or edges) on the MPth plate.

LSLAB(MP) This is a dimensioned integer variable. It is used to define the type of plate desired as follows:

- 1 = Transparent thin dielectric slab
- 0 = Perfectly conducting metallic plate
- 2 = Double-sided coated dielectric plate
- 4 = One-sided coated dielectric plate

Note that if LSLAB(MP)=0 the code will skip to the read statements associated with the corners XX(N,ME,MP). Therefore, the information for the different slab layers should not be included in the data list for the perfectly conducting plate.

READ: NSLAB(MP)

_____ where _____

NSLAB(MP) This is a dimensioned integer variable. It is used to define the number of dielectric layers on the MPth plate.

**READ: DSLAB(NS,MP), ERLAB(NS,MP), TESLAB(NS,MP),
URSLAB(NS,MP), TMSLAB(NS,MP)**

_____ where _____

DSLAB(NS,MP) This is a doubly dimensioned variable. It is used to specify the thickness of the NSt^h layer.

ERLAB(NS,MP) This is a doubly dimensioned variable. It is used to specify the relative dielectric constant of the NSt^h layer.

TESLAB(NS,MP) This is a doubly dimensioned variable. It is used to specify the dielectric loss tangent if the number is positive or the conductivity if the number is negative of the NSt^h layer.

URSLAB(NS,MP) This is a doubly dimensioned variable. It is used to specify the relative permeability constant of the NSt^h layer.

TMSLAB(NS,MP) This is a doubly dimensioned variable. It is used to specify the permeability loss tangent of the NSt^h layer.

Note there will be NSLAB(MP) number of lines of the above data. The first layer specified is closest to the metal plate. One sided coating is on side of positive normal (right hand rule).

READ: (XX(N,ME,MP),N=1,3)

_____ where _____

XX(N,ME,MP) This is a triply dimensioned real variable. It is used to specify the location of the MEth corner of the MPth plate. It is input on a single line with the real numbers being

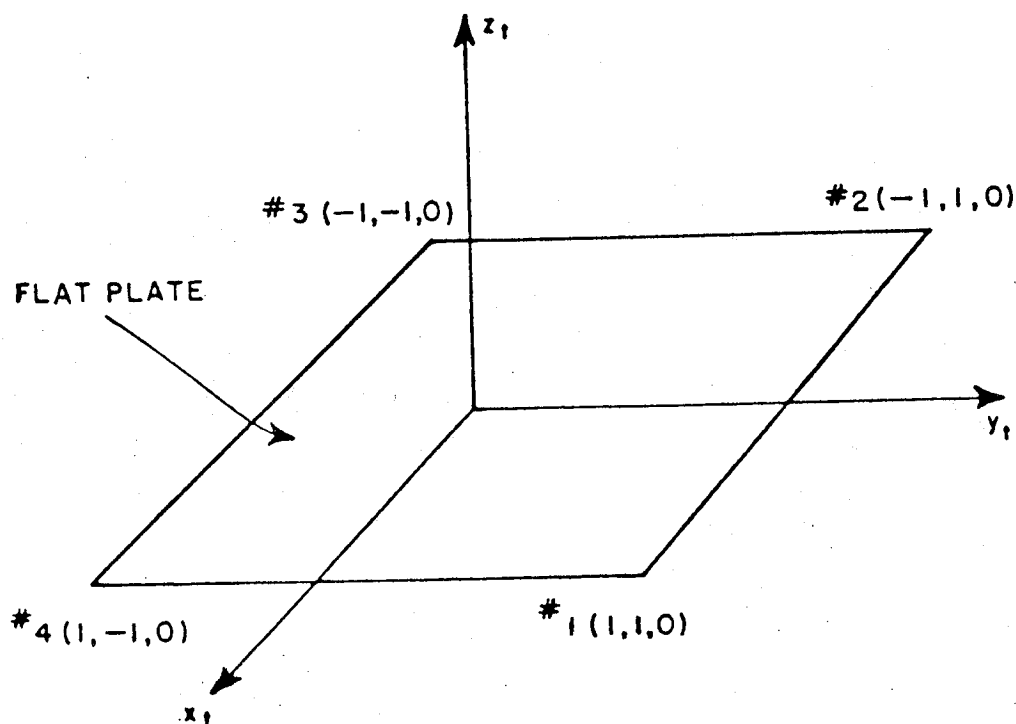


Figure 4.7: Definition of flat plate geometry.

the x, y, z coordinates of the corner, in the specified coordinate system, which corresponds to $N=1,2,3$, respectively, in the array. This is illustrate in the examples that follow.

This read statement will be called MEP(MP) times so that all the corners are defined.

See elsewhere for further details on how to number the corners. Note that the program will keep increasing the number of plates in the solution by the number of calls to this command unless the NP or NX commands are called to reinitialize the plate geometry.

82

PG

EXAMPLE:

PG

4,0

1.,1.,0.

-1.,1.,0.

-1.,-1.,0.

1.,-1.,0.

Defines a square perfectly conducting plate with a length of 2. (See the figure below.)

EXAMPLE:

PG

4,-2

1

.275,2.55,0,1.,0

1.,1.,0.

-1.,1.,0.

-1.,-1.,0.

1.,-1.,0.

Same plate but with a single polystyrene layer of .275 thickness on it. (See Example 9 for more details.)



4.24 Command PN: Near Zone Pattern

This command enables the user to define the near zone pattern coordinate system, the pattern cut, and the spacial range that is desired. The geometry is illustrated in Figures 4.8, 4.9 and 4.10. See Appendix A on how to adjust the number of observation points (NOX) available.

READ: (XPC(N),N=1,3)

_____ where _____

XPC(N) This is a dimensioned real variable. It is used to specify the origin of the near zone pattern coordinate system relative to the reference coordinate system. It is input on a single line with the real numbers being the x, y, z coordinates of the origin which corresponds to $N=1,2,3$, respectively.

READ: THCZ, PHCZ, THCX, PHCX

_____ where _____

THCZ,PHCZ These are real variables. They are input in degrees as spherical angles that define the z_p -axis of the pattern coordinate system as if it was a radial vector in the reference coordinate system.

THCX,PHCX These are real variables. They are input in degrees as spherical angles that define the x_p -axis of the pattern coordinate system as if it was a radial vector in the reference coordinate system.

Note that the new x_p -axis and z_p -axis must be defined orthogonal to each other. The new y_p -axis is found from the cross product of the x_p - and z_p -axes.

READ: LRECT

_____ where _____

LRECT This is a logical variable that defines whether a spherical or linear pattern cut is desired. It is designated as follows:

T= linear pattern cut

F= spherical pattern cut

READ: RXS, TYS, PZS

_____ where _____

RXS,TYS,PZS These are real variables. They define the starting position of the pattern trace. If **LRECT=F**, they are the radial, theta, and phi coordinates of the start location, respectively. If **LRECT=T**, they are the *x*, *y*, and *z* coordinates of the starting location, respectively.

READ: RXI, TYI, PZI

_____ where _____

RXI,TYI,PZI These are real variables. They define the size of the incremental steps for the pattern trace. If **LRECT=F**, they are the radial, theta, and phi step sizes, respectively. If **LRECT=T**, they are the *x*, *y*, and *z* step sizes, respectively.

READ: NPN

_____ where _____

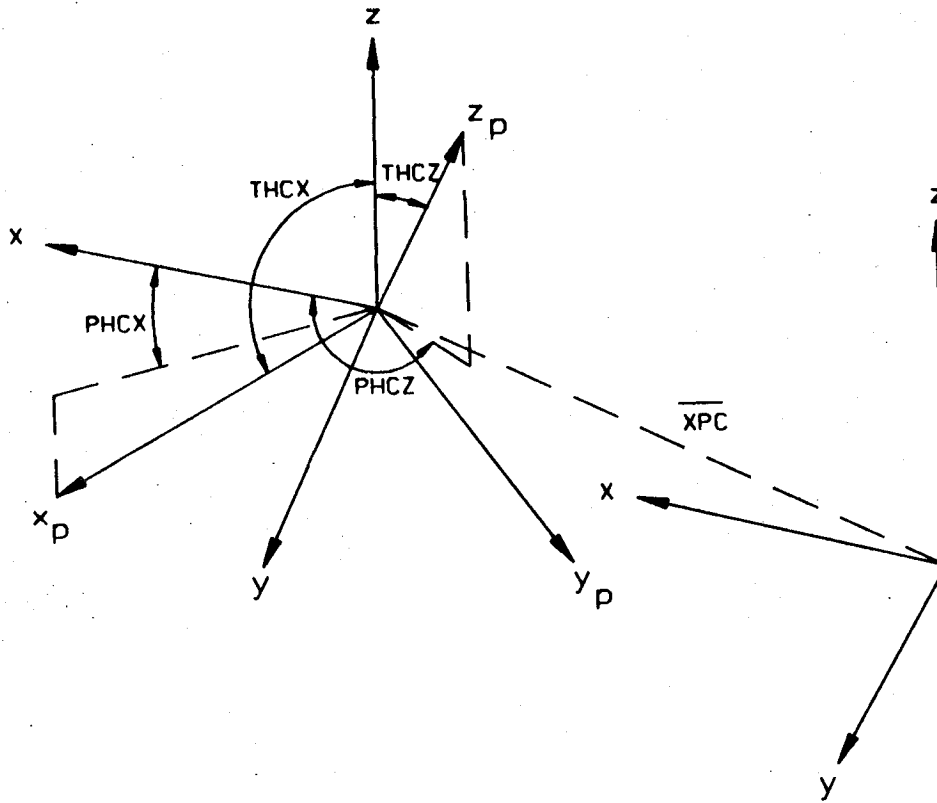


Figure 4.8: Definition of pattern coordinate system.

NPN This is an integer variable used to define the number of pattern points that are desired.

Note that only one pattern cut can be made for each call to **PN**, that is, the step size of **RXI**, **TYI**, and **PZI** is added to the pattern trace for each incremental step.

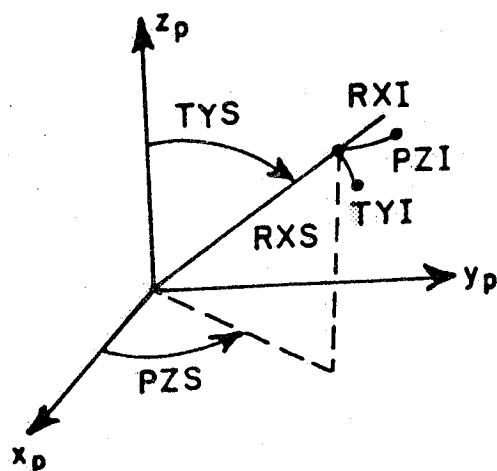


Figure 4.9: Spherical pattern cuts, LRECT=.FALSE.

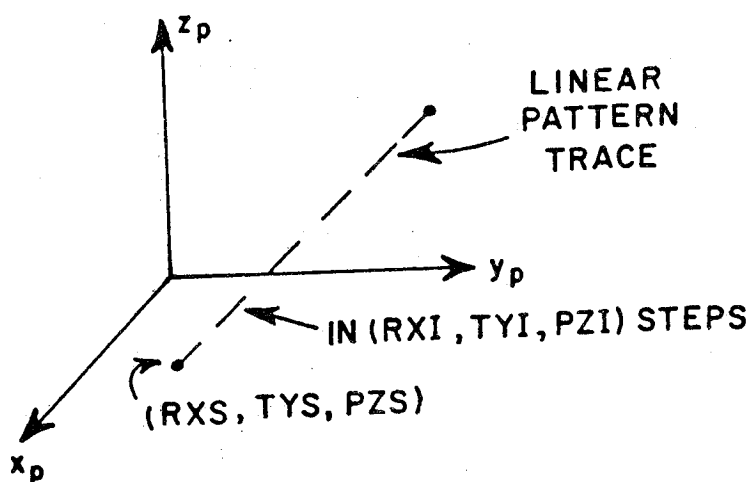


Figure 4.10: Linear pattern cuts, LRECT=.TRUE.

PN

87

EXAMPLE:

PN
0.,0.,0.
0.,0.,90.,0.
T
0.,0.,0.
1.,1.,1.
101

In the definition coordinate system the pattern cut starts at the origin and traces a linear path to $x = y = z = 100$ in steps of 1.

EXAMPLE:

PN
0.,0.,0.
0.,0.,90.,0.
F
0.,45.,45.
1.732,0.,0.
101

This is the same pattern as above but defined using the spherical pattern variables.

4.25 Command PP: Plot Data

This command enables the user to specify whether a rectangular or polar plot of the results is desired.

READ: LPLT

_____ where _____

LPLT This is a logical variable defined by T or F. It is used to indicate if a plot of the results is desired.

READ: LPPREC, PPXL, PPYL

_____ where _____

LPPREC This is a logical variable defined by T or F that is used to specify whether a rectangular or polar plot is desired. If LPPREC is TRUE, a rectangular plot is specified. If LPPREC is FALSE, a polar plot is specified.

PPXL This is a real variable. If LPPREC is TRUE, this is the length of the x -axis. The x -axis is the angle definition axis. If LPPREC is FALSE, this is the angular position of the zero angle axis.

PPYL This is a real variable. If LPPREC is TRUE, this is the length of the y -axis. The y -axis is the dB definition axis. If LPPREC is FALSE, this is the radius of the polar plot.

READ: PPXB, PPXE, PPXS

_____ where _____

PPXB This is a real variable that defines the beginning value of the grid's x -axis.

PPXE This is a real variable that defines the end value of the grid's x -axis.

PPXS This is a real variable that defines the step size of the grid's x -axis.

READ: PPYB, PPYE, PPYS

_____ where _____

PPYB This is a real variable that defines the beginning value of the grid's y -axis.

PPYE This is a real variable that defines the end value of the grid's y -axis.

PPYS This is a real variable that defines the step size of the grid's y -axis.

EXAMPLE:

PP
T
T,8.,4.
0.,360.,30.
-50.,0.,10

This defines the plot data for a rectangular plot of 8×4 inches. The x axis is defined over 0° to 360° with steps of 30° and y over -50 dB to 0 dB in step of 10 dB.

EXAMPLE:

PP

T

F,0.,3.

0.,360.,30.

-50.,0.,10.

This defines the same plot as above
but in a polar form with a 3 inch ra-
dius.

4.26 Command PR: Normalization Factors

This command enables the user to specify the total power radiated by the antenna, the input power of the antenna, or the terminal currents and impedances of the antennas. These variables are used to normalize the calculations so that the results are output in directive gain, power gain, mutual impedance coupling, modified Frii's coupling, or Linville coupling.

READ: IPRAD

_____ where _____

IPRAD=1 This is an integer variable. When it is one, it signifies the far zone pattern is to be normalized by the number of PRAD.

READ: PRAD

_____ where _____

PRAD This is a real variable. It is input in watts and defines the total power radiated by the antenna or the input power to the antennas.

Note that if PRAD is less than or equal to 1.E-30, it will be assumed that the power radiated or the input power, as the case may be, is not specified so the results will not be normalized.

***** OR *****

READ: IPRAD

_____ where _____

IPRAD=2 This is an integer variable. When it is equal to two, it signifies that the coupling is found by the reaction method, such that it gives the mutual impedance (Z_{12}) between two antennas.

READ: CI11, CI22

_____ where _____

CI11, CI22 These are complex variables. They are each input in amperes and define the source terminal current (CI11) and the receiver terminal current (CI22).

***** OR *****

READ: IPRAD

_____ where _____

IPRAD=3 This is an integer variable. When it is equal to three, it signifies that the coupling is found by the reaction method, such that it gives a modified Frii's transmission type result.

READ: PRAD, PRADR

_____ where _____

PRAD, PRADR These are real variables. They are each input in watts and define the power radiated by the source (PRAD) and the power radiated by the receiver as if it were a source (PRADR).

***** OR *****

READ: IPRAD

_____ where _____

IPRAD=4 This is an integer variable. When it is equal to four, it signifies that the coupling is found by the reaction method, such that it gives a result by means of the Linville method.

READ: CI11, CI22

_____ where _____

CI11, CI22 These are complex variables. They are each input in amperes and define the source terminal current (CI11) and the receiver terminal current (CI22).

READ: Z11, Z22

_____ where _____

Z11, Z22 These are complex variables. They are each input in ohms and define the source terminal impedance (Z11) and the receiver terminal impedance (Z22).

Note that for this method the values are read in two steps. With one line used for current values and a second line used for impedance values.

EXAMPLE:

PR
1
.01

This specifies that the far zone pattern is to be normalized by 0.01 watts.

EXAMPLE:

PR
2
(.1,0.),(.1,0.)

This specifies that the coupling is found so as to give the mutual impedance. The two terminal currents are 0.1 amps.

EXAMPLE:

PR
3
.001,.001

This specifies that coupling is found using the Frii's method with the source and receiver having input power of 0.001 watts.

EXAMPLE:

PR
4
(1.,0.), (0.,1.)
(1.,-1.), (1.,1.)

This specifies that the coupling using the Linville method is to be found. The input currents are defined as 1.0 and $1.0j$ with terminal impedances of $1 + j$ and $1 - j$.

4.27 Command RA: Receiver Array

This command enables a group of receivers to be arrayed together in order to reduce computation time. The antenna type, size and orientation can be input individually for each element or by setting the proper flag any of these characteristics can be set once for the entire array. This ability to input the orientation of each element allows the user to specify arrays of circularly polarized elements. The geometry is illustrated in Figures 4.12, 4.13, and 4.14. The entire group of elements defined by this command is treated as one equivalent receiver with an array pattern factor for computation purposes. The equivalent receiver position of the array is found by a weighted average of the individual element positions, and its location is specified the same as for a receiver defined by the **RG** command. The position weighting factor is proportional to the magnitude of the individual receiver's excitation weight. An added phase term can be included in the array factor for cases where a scatterer may not be quite far enough away from the receiver to be in the far zone of the array (see Section 2.2 for more details).

The **RA** command can be used by itself or in conjunction with other **RG** commands. One call to this command defines one equivalent receiver. The number of receivers in the problem is automatically counted by the number of calls to this command and the **RG** command. See Appendix A on how to adjust the number of receivers (NRX) available.

As a reminder, the current elements lie in the $x - z$ plane and are z directed for $|IMR| \leq 3$ and lie in the $x - y$ plane and are x directed for $|IMR| \geq 4$ (see Figures 4.13 and 4.14).

Warnings: Using the near zone phase factor (LDRO=T) may incorrectly shadow the array elements and may give incorrect results if a nearby source is also using the added term (LDSO=T). In addition, the receivers may not be defined on the surface of the plates.

READ: LDRO(MR),LMO,LMT

_____ where _____

LDRO(MR) This is a logical array defined by T or F. If set true, the added near zone phase term will be included in the array factor calculation.

LMO This is a logical variable defined by T or F. If set true, the orientation (THRZ, PHRZ, etc.) is to be input individually for each element. If false, the orientation is input once for the entire array.

LMT This is a logical variable defined by T or F. If set true, the type (IMR) and size (HR and HAWR) are to be input individually for each element. If false, they are input once for the entire array.

READ: MRAX

_____ where _____

MRAX This is an integer that defines the number of elements in this array grouping.

READ: (XRR(N,MA),N=1,3)

_____ where _____

XRR(N,MA) This is a doubly dimensioned real array which is used to define the x, y, z location of the MATH element relative to the pattern location for each pattern point if the receiver is moving or relative to the definition coordinate system if it is stationary. If the receiver is moving in a spherical pattern, then these represent linear displacements in the \hat{r} , $\hat{\theta}$ and $\hat{\phi}$ directions respectively. A single line of data contains the x, y, z ($N=1,2,3$) locations. There needs to be MRAX lines of receiver locations input.

The equivalent receiver location is given by

$$XRR(N, MR) = \frac{\sum_{MA} |WR(MA)| XRR(N, MA)}{\sum_{MA} |WR(MA)|},$$

where $N=1$ to 3.

READ: THRZ, PHRZ, THRX, PHRX

_____ where _____

THRZ,PHRZ These are real variables which are used to define the orientation of the MATH element in the definition coordinate system. They are input in degrees as spherical angles that define the z -axis of the antenna coordinate system.

THRX,PHRX These are real variables which are used to define the orientation of the MATH element in the definition coordinate system. They are input in degrees as spherical angles that define the x -axis of the antenna coordinate system.

For a dipole antenna, these angles can be made in a convenient direction. The x -axis and z -axis specified by these angles must be defined orthogonal to each other. The y -axis is found by the cross product of the x - and z -axes.

If the receiver is moving in a spherical pattern, then these angles are defined relative to the spherical coordinate axes of the pattern system at the pattern point. The receiver coordinate axes are still \hat{x} , \hat{y} and \hat{z} , but they are defined relative to the \hat{r} , $\hat{\theta}$ and $\hat{\phi}$ directions. The THRZ and THRX are angles relative to the $\hat{\phi}$ axis and the PHRZ and PHRX are angles relative to the \hat{r} axis. For example: if you want the receiver coordinate \hat{z} in the \hat{r} direction of the pattern system and \hat{x} in the $\hat{\theta}$, then input THRZ, PHRZ, THRX, PHRX = 90,0,90,90.

If LMO=T, then this is entered MRAX times.

READ: IMR(MA), HR(MA), HAWR(MA)

_____ where _____

IMR(MA) This is an integer array which is used to define the Math element's receiver type. The details of the different types of receivers are given elsewhere. The designations are defined as follows:

IMR(MA) < 0 for an electric element

IMR(MA) > 0 for a magnetic element

|IMR(MA)| = 1 for a uniform current distribution

|IMR(MA)| = 2 for a piece-wise sinusoidal distribution

|IMR(MA)| = 3 for a TE_{01} cosine current distribution

|IMS(MA)| = 4 for an annular ring current distribution

|IMR(MA)| = 5 for a constant circular current distribution

|IMR(MA)| = 6 for a TE_{11} circular current distribution

HR(MA) This is a real array which is used to input the length of the Math element. If $|IMR| = 4, 5$ or 6 this is the aperture radius.

HAWR(MA) This is a real array which is used to input the width of the Math element in the case of an aperture antenna. If $HAWR(MA) = 0$, then it is assumed to be a dipole. If $|IMR| = 4$, this is the outer radius of the ring, b. If $|IMR| = 5$ or 6 , set this to 0.

Note that the units of the variable **HR(MA)** and **HAWR(MA)** can be specified by the **US** command. If wavelengths are chosen, it uses λ at the time of definition. It does not change as the frequency changes. If $LMT = T$, this is entered **MRAX** times.

READ: WMR, WPR

_____ where _____

WMR, WPR These are real variables used to define the excitation associated with the Math element of the group. The magnitude is given by **WMR** and the phase in degrees by **WPR**. There needs to be **MRAX** lines of these two numbers

RA

99

corresponding to the weights of each of the elements of the group.

Note that the program will keep increasing the number of receivers or groups of receivers in the solution by the number of calls to this command unless the **NR** or **NX** commands are called to reinitialize the receiver geometry. Presently, the total number of receivers and elements in the receiver groups can not be more than 30. This is set by the **PARAMETER** statements and can be changed if desired.

EXAMPLE:

```
RA
F,F,F
3
-1.,0.,0.
0.,0.,0.
1.,0.,0.
0.,0.,90.,0.
-1.,.5,.5
1.,0.
1.,90.
1.,180.
```

This specifies an array of 3 identical square patches of uniform z directed electric current that are driven with unit amplitude and a 90° phase shift from element to element.

EXAMPLE:

```

RA
F,T,F
6
-1.,0.,0.
-1.,0.,0.
0.,0.,0.
0.,0.,0.
1.,0.,0.
1.,0.,0.
90.,90.,90.,0.
90.,0.,90.,90.
90.,90.,90.,0.
90.,0.,90.,90.
90.,90.,90.,0.
90.,0.,90.,90.
-1.,.5,0.
1.,0.
1.,90.
1.,0.
1.,90.
1.,0.
1.,90.

```

This specifies an array of 3 circularly polarized elements. Each element is composed of 2 half-wave dipoles of uniform electric current, where one is y directed and the second is x directed and driven 90° out of phase.

4.28 Command RD: Far Zone Range

This command enables the user to specify a far zone distance, R , to the observer. The fields are then normalized by the factor $\frac{e^{-jkR}}{R}$.

READ: RANGS

_____ where _____

RANGS This is a real variable which is used to specify the far zone range, R .

Note that R should be in the far zone of the scattering structure, that is, $R > \frac{2D^2}{\lambda}$, where D is the maximum dimension of the structure, and λ is the wavelength. However, if $R \geq 10^{30}$, then the factor $\frac{e^{-jkR}}{R}$ is suppressed.

EXAMPLE:

RD
1000.

Defines a far zone range of 1000.

4.29 Command RG: Receiver Geometry

This command enables the user to specify the location and type of receiver used. The geometry is illustrated in Figures 4.12, 4.13, and 4.14. One call to this command defines one receiver. The number of receivers in the problem are automatically counted by the number of calls to this command. See Appendix A on how to adjust the number of receivers (NRX) available.

The receiver location is specified by the XRR which give the linear displacement from the pattern point for a moving receiver or from the definition origin for a stationary receiver. The receiver can be specified stationary by calling the NM command. In addition, the receivers may not be defined on the surface of the plates.

As a reminder, the current elements lie in the $x - z$ plane and are z directed for $|IMR| \leq 3$ and lie in the $x - y$ plane and are x directed for $|IMR| \geq 4$ (see Figures 4.13 and 4.14).

READ: (XRR(N,MR),N=1,3)

_____ where _____

XRR(N,MR) This is a doubly dimensioned real array which is used to define the x, y, z location of the MRth element relative to the pattern location for each pattern point if the receiver is moving or relative to the definition coordinate system if it is stationary. If the receiver is moving in a spherical pattern, then these represent linear displacements in the \hat{r} , $\hat{\theta}$ and $\hat{\phi}$ directions respectively. Again, a single line of data contains the x, y, z ($N=1,2,3$) locations.

READ: THRZ, PHRZ, THRX ,PHRX

_____ where _____

THRZ,PHRZ These are real variables which are used to define the orientation of the MRth element in the definition coordinate system. They are input in degrees as spherical angles that define the z-axis of the antenna coordinate system.

THRX,PHRX These are real variables which are used to define the orientation of the MRth element in the definition coordinate system. They are input in degrees as spherical angles that define the x-axis of the antenna coordinate system.

For a dipole antenna, these angles can be made in a convenient direction.

The x-axis and z-axis specified by these angles must be defined orthogonal to each other. The y-axis is found by the cross product of the x- and z-axes.

If the receiver is moving in a spherical pattern, then these angles are defined relative to the spherical coordinate axes of the pattern system at the pattern point. The receiver coordinate axes are still \hat{x} , \hat{y} and \hat{z} , but they are defined relative to the \hat{r} , $\hat{\theta}$ and $\hat{\phi}$ directions. The THRZ and THRX are angles relative to the $\hat{\phi}$ axis and the PHRZ and PHRX are angles relative to the \hat{r} axis. For example: if you want the receiver coordinate \hat{z} in the \hat{r} direction of the pattern system and \hat{x} in the $\hat{\theta}$ then input THRZ, PHRZ, THRX, PHRX = 90,0,90,90.

READ: IMR(MR), HR(MR), HAWR(MR)

_____ where _____

IMR(MR) This is an integer array which is used to define the MRth element's receiver type. The details of the different types of receivers are elsewhere. The designations are defined as follows:

IMR(MR) < 0 for an electric element

IMR(MR) > 0 for a magnetic element

|IMR(MR)| = 1 for a uniform current distribution

$|IMR(MR)|=2$ for a piece-wise sinusoidal distribution

$|IMR(MR)|=3$ for a TE_{01} cosine current distribution

$|IMS(MS)|=4$ for a annular ring current distribution

$|IMR(MR)|=5$ for a constant circular current distribution

$|IMR(MR)|=6$ for a TE_{11} circular current distribution

HR(MR) This is a real array which is used to input the length of the MRth element. If $|IMR|=4, 5$ or 6 this is the aperture radius.

HAWR(MR) This is a real array which is used to input the width of the MRth element in the case of an aperture antenna. If $HAWR(MR)=0$, then it is assumed to be a dipole. If $|IMR|=4$, then this is the outer radius, b . If $|IMR|=5$ or 6 , set this to 0 .

Note that the units of the variable $HR(MR)$ and $HAWR(MR)$ can be specified by the **US** command. If wavelengths are chosen, it uses λ at time of definition. It does not change as the frequency changes.

READ: WMR, WPR

_____ where _____

WMR, WPR These are real variables used to define the excitation associated with the MRth element. The magnitude is given by **WMR** and the phase in degrees by **WPR**.

Note that the program will keep increasing the number of receivers in the solution by the number of calls to this command unless the **NR** or **NX** commands are called to reinitialize the receiver geometry.

EXAMPLE:

RG

0.,0.,0.

0.,0.,90.,90.

-2.,.5,0.

1.,0.

This defines a half-wave dipole that is a z directed electric current with a piece-wise sinusoidal distribution.

EXAMPLE:

RG

0.,0.,0.

90.,90.,90.,0.

3.,.6,.6

1.,0.

This specifies a TE_{10} magnetic current over a square patch that lies in the $x - y$ plane and is y directed.

4.30 Command RI: Interpolated Receiver

This command enables the user to approximate a complex antenna using linear interpolation to determine field values from a finite set of measured or calculated points. The entire antenna will be treated as a point receiver with a complex pattern. The field values are assumed to be from surface currents that lie in $x - y$ plane of the antenna coordinate system. These currents must be linear of a known polarization, or circularly polarized. The data is entered as magnitude and phase of the radiated electric or magnetic field at various θ and ϕ values. To ease the data entry process a symmetry option is included. If the pattern is symmetric about the y -axis, then patterns for $-90 \leq \phi \leq 90$ are entered. If it's symmetric about the x -axis, then $0 \leq \phi \leq 180$ is used and if it's symmetric about both axes, then $0 \leq \phi \leq 90$ is used. The data is entered in NPHIR pattern cuts, where each cut is a constant ϕ cut over $0 \leq \theta \leq 180$. The phi and theta values must be entered in increasing order. See Appendix A on how to adjust the number of interpolation points (NIX) available.

Warnings: This command can only be called once and will increment the total number of receivers by one. The accuracy of this routine is dependent on the number of points entered and their measured accuracy.

READ: (XRR(N,MR),N=1,3)

_____ where _____

XRR(N,MR) This is a doubly dimensioned real array which is used to define the x, y, z location of the MRth element in the definition coordinate system for a stationary receiver or the linear displacement relative to the pattern location for a moving receiver. If the receiver is moving in a spherical pattern then these represent linear displacements in the \hat{r} , $\hat{\theta}$ and $\hat{\phi}$ directions respectively. Again, a single line of data contains the x, y, z ($N=1,2,3$) locations.

READ: THRZ, PHRZ, THRX ,PHRX

_____ where _____

THRZ,PHRZ These are real variables which are used to define the orientation of the MRth element in the definition coordinate system. They are input in degrees as spherical angles that define the z-axis of the antenna coordinate system.

THRX,PHRX These are real variables which are used to define the orientation of the MRth element in the definition coordinate system. They are input in degrees as spherical angles that define the x-axis of the antenna coordinate system.

The x-axis and z-axis specified by these angles must be defined orthogonal to each other. The y-axis is found by the cross product of the x- and z-axes.

If the receiver is moving in a spherical pattern, then these angles are defined relative to the spherical coordinate axes of the pattern system at the pattern point. The receiver coordinate axes are still \hat{x} , \hat{y} and \hat{z} , but they are defined relative to the \hat{r} , $\hat{\theta}$ and $\hat{\phi}$ directions. The THRZ and THRX are angles relative to the $\hat{\phi}$ axis and the PHRZ and PHRX are angles relative to the \hat{r} axis. For example: if you want the receiver coordinate \hat{z} in the \hat{r} direction of the pattern system and \hat{x} in the $\hat{\theta}$ then input THRZ, PHRZ, THRX, PHRX = 90,0,90,90.

The following data is input on logical unit IURI:

READ: ISYMR,NPHIR,NPTR,TAUR

_____ where _____

ISYMR This is an integer variable that defines the type of symmetry the feed pattern has; where:

ISYMR=0 for no symmetry

ISYMR=1 even symmetry about the x and y axes

ISYMR=2 even symmetry about the x axis only

ISYMR=3 even symmetry about the y axis only

NPHIR This integer variable is the number of pattern cuts to be entered. The number of ϕ values.

NPTR This integer is the number of θ points per pattern cut. This number is the same for each cut.

TAUR This real variable is the angle (in degrees) relative to the x -axis of the antenna polarization for linearly polarized fields (see Figure 4.15). If a circularly polarized field is chosen, then this should be set to 0.

READ: LDBR,LCPR,LEHR

_____ where _____

LDBR This is a logical variable used to tell the code how the magnitudes of the input field values are to be entered. If true, then these values are input in dB.

LCPR This is a logical variable that is set true if a circularly polarized field is wanted.

LEHR This is a logical variable that tells the code if the data to be entered is the electric field values (LEHR=T) or magnetic field values (LEHR=F).

READ: (PHINR(I), I=1,NPHIR)

_____ where _____

PHINR(I) This is real array which holds the NPHIR ϕ values, in degrees, of the pattern cuts to be entered next. They must be entered in increasing order.

READ: THPTR, MG1, PH1

_____ where _____

These real variables are the θ value (in degrees) and the magnitude and phase (in degrees) of the field at that value. This is entered NPTR times for each PHINR value entered above. So the NPTR values for the $\phi = \text{PHINR}(1)$ cut are entered first, then the next NPTR values for the $\phi = \text{PNINR}(2)$ cut, etc. Remember if LDBR=T, the MG1 are entered in dB.

EXAMPLE:

```
RI
0.,0.,0.
0.,0.,90.,0.
1,2,15,90.
F,F,T
0.,90.
0.,.15,0.
.
.
.
```

This specifies a receiver that is at the origin. The symmetry (1) indicates only cuts over $\phi = 0^\circ$ to 90° are needed, so here only $\phi = 0^\circ, 90^\circ$ are input. The 15 values input per cut are the field amplitudes of a y directed linearly polarized electric field.

4.31 Command RM: MOM Receiver Input

This command enables the user to interface the Numerical Electromagnetics Code (NEC) - Moment Method Code with the Basic Scattering Code in order to use the antenna modeling capabilities of NEC to specify the needed receiver data such as location and current weights of the elements. The geometry is illustrated in Figure 4.16. See Appendix A on how to adjust the number of receivers (NRX) available.

READ: PRAD

_____ where _____

PRAD This is a real variable which is used to define the total power radiated in watts from the NEC modeled antenna (as if it were a source). This allows the coupling to be computed. If Pin is substituted for Prad, the power gain will be computed.

READ: MRX

_____ where _____

MRX This is an integer variable which defines the maximum number of elemental wire radiators that have been used in the NEC code to model the antenna.

READ: (XRR(N,MR),N=1,3), HR(MR), THRZ, PHRZ

_____ where _____

XRR(N,MR) This is a doubly dimensioned real array which is used to define the x, y, z location of the MRth elemental radiator in the definition coordinate system.

RM

111

HR(MR) This is a real array which is used to input the length of the MRth element in the units specified by IUNIT from the UN command or the default option.

THRZ,PHRZ These are real variables which are used to define the orientation of the MRth element in the definition coordinate system. The angles are in degrees and define a radial direction which is parallel to the MRth element current flow. The angle THRZ is the angle of the element measured up from the $x - y$ plane. The angle PHRZ is the phi angle in a normal spherical coordinate system.

READ: WMR, WPR

_____ where _____

WMR,WPR These are real variables used to define the excitation associated with the MRth element. The real part is given by WMR and the imaginary part by WPR.

Note that for the NEC code input all the elements are assumed to be electric current elements.

4.32 Command RT: Rotate-Translate Geometry

This command enables the user to translate and/or rotate the coordinate system used to define the input data in order to simplify the specification of the plate, curved surface, source, and receiver geometries. The geometry is illustrated in Figure 4.11.

READ: (TR(N),N=1,3)

_____ where _____

TR(N) This is a dimensioned real variable. It is used to specify the origin of the new coordinate system to be used to input the data for the source or the scattering structures. It is input on a single line with the real numbers being the x, y, z coordinates of the new origin which corresponds to $N=1,2,3$, respectively.

READ: THZP, PHZP, THXP, PHXP

_____ where _____

THZP,PHZP These are real variables. They are input in degrees as spherical angles that define the z -axis of the new coordinate system as if it was a radial vector in the reference coordinate system.

THXP,PHXP These are real variables. They are input in degrees as spherical angles that define the x -axis of the new coordinate system as if it was a radial vector in the reference coordinate system.

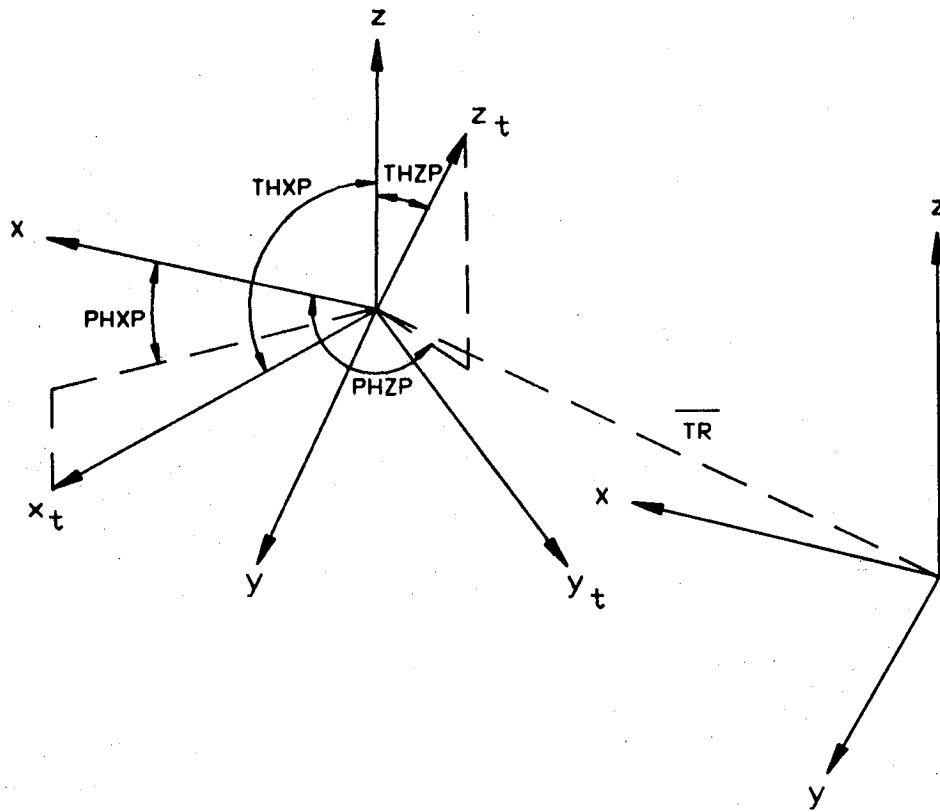


Figure 4.11: Definition of rotate-translate coordinate system geometry.

The new x -axis and z -axis must be defined orthogonal to each other. The new y -axis is found from the cross product of the x - and z -axis. All the subsequent inputs will be made relative to this new coordinate system, which is shown as x_t, y_t, z_t , unless command **RT** is called again and redefined.

EXAMPLE:

RT
0.,0.,10.
90.,90.,90.,0.

Moves the origin to $x, y, z = 0, 0, 10$
and new z axis is in the definition y
axis direction. New x axis is same.

EXAMPLE:

RT
0.,0.,0.
0.,0.,90.,0.

Redefines the origin and axes to their
default condition.

4.33 Command SA: Source Array

This command enables a group of sources to be arrayed together in order to reduce computation time. The antenna type, size and orientation can be input individually for each element or by setting the proper flag any of these characteristics can be set once for the entire array. The ability to input the orientation of each element allows the user to specify arrays of circularly polarized elements. The geometry is illustrated in Figures 4.12, 4.13, and 4.14. They are, also, assumed to be all mounted on a given plate or removed from all plates. The entire group of elements defined by this command is treated as one equivalent source with an array pattern factor for computation purposes. The equivalent source position of the array is found by a weighted average of the individual element positions, and this location is specified the same as for a source defined by the **SG** command. The position weighting factor is proportional to the magnitude of the individual source's excitation weight. An added phase term can also be included in the array factor for cases where a scatterer may not be quite far enough away from the source to be in the far zone of the array (see Section 2.2 for more details).

The **SA** command can be used by itself or in conjunction with other **SG** commands. One call to this command defines one equivalent source. The number of sources in the problem is automatically counted by the number of calls to this command and the **SG** command. See Appendix A on how to adjust the number of sources (NSX) available.

As a reminder, the current elements lie in the $x - z$ plane and are z directed for $|IMS| \leq 3$ and lie in the $x - y$ plane and are x directed for $|IMS| \geq 4$ (see Figures 4.13 and 4.14).

Warnings: Using the near zone phase factor (LDSO=T) may incorrectly shadow the array elements and may give incorrect results if a nearby receiver is using the added term (LDRO=T).

READ: LDSO(MS),LMO,LMT

_____ where _____

LDSO(MS) This is a logical array defined by T or F. If set true, the added near zone phase term will be included in the array factor calculation.

LMO This is a logical variable defined by T or F. If set true, the orientation (THSZ, PHSZ etc.) is to be input individually for each element. If false, the orientation is input once for the entire array.

LMT This is a logical variable defined by T or F. If set true, the type (IMS) and size (HS and HAWS) are to be input individually for each element. If false, they are input once for the entire array.

READ: MSAX

_____ where _____

MSAX This is an integer that defines the number of elements in this array grouping.

READ: (XSS(N,MA),N=1,3)

_____ where _____

XSS(N,MA) This is a doubly dimensioned real array which is used to define the x, y, z location of the MATH element relative to the pattern location for each pattern point if the source is moving or relative to the definition coordinate system if it is stationary. If the source is moving in a spherical pattern, then these represent linear displacements in the \hat{r} , $\hat{\theta}$ and $\hat{\phi}$ directions respectively. A single line of data contains the x, y, z ($N=1,2,3$) locations. There needs to be MSAX lines of source locations input.

The equivalent source location is given by

$$XSS(N, MS) = \frac{\sum_{MA} |WS(MA)| XSS(N, MA)}{\sum_{MA} |WS(MA)|},$$

where N=1 to 3.

READ: THSZ, PHSZ, THSX, PHSX

_____ where _____

THSZ,PHSZ These are real variables which are used to define the orientation of the MATH element in the definition coordinate system. They are input in degrees as spherical angles that define the z-axis of the antenna coordinate system.

THSX,PHSX These are real variables which are used to define the orientation of the MATH element in the definition coordinate system. They are input in degrees as spherical angles that define the x-axis of the antenna coordinate system.

For a dipole antenna, these angles can be made in a convenient direction. The x-axis and z-axis specified by these angles must be defined orthogonal to each other. The y-axis is found by the cross product of the x- and z-axes.

If the source is moving in a spherical pattern, then these angles are defined relative to the spherical coordinate axes of the pattern system at the pattern point. The source coordinate axes are still \hat{x} , \hat{y} and \hat{z} , but they are defined relative to the \hat{r} , $\hat{\theta}$ and $\hat{\phi}$ directions. The THSZ and THSX are angles relative to the $\hat{\phi}$ axis and the PHSZ and PHSX are angles relative to the \hat{r} axis. For example: if you want the source coordinate \hat{z} in the \hat{r} direction of the pattern system and \hat{x} in the $\hat{\theta}$ then input THSZ, PHSZ, THSX, PHSX = 90,0,90,90.

If LMO=T, then this is entered MSAX times.

READ: IMS(MA), HS(MA), HAWS(MA)

_____ where _____

IMS(MA) This is an integer array which is used to define the MATH element's source type. The details of the different types of sources are given elsewhere. The designations are defined as follows:

IMS(MA) < 0 for an electric element

IMS(MA) > 0 for a magnetic element

|IMS(MA)| = 1 for a uniform current distribution

|IMS(MA)| = 2 for a piece-wise sinusoidal distribution

|IMS(MA)| = 3 for a TE_{01} cosine current distribution

|IMS(MA)| = 4 for an annular ring current distribution

|IMS(MA)| = 5 for a constant circular current distribution

|IMS(MA)| = 6 for a TE_{11} circular current distribution

HS(MA) This is a real array which is used to input the length of the MATH element. If $|IMS| = 4, 5$ or 6 this is the aperture radius.

HAWS(MA) This is a real array which is used to input the width of the MATH element in the case of an aperture antenna. If **HAWS(MS) = 0** then it is assumed to be a dipole. If $|IMS| = 4$, this is the outer radius of the ring, b. If $|IMS| = 5$ or 6 , set this to 0.

Note that the units of the variable **HS(MA)** and **HAWS(MA)** can be specified by the **US** command. If wavelengths are chosen, it uses λ at the time of definition. It does not change as the frequency changes. If **LMT = T** this is entered **MSAX** times.

READ: WMS, WPS

_____ where _____

WMS,WPS These are real variables used to define the excitation associated with the MATH element of the group. The magnitude is given by WMS and the phase in degrees by WPS. There needs to be MSAX lines of these two numbers corresponding to the weights of each of the elements of the group.

Note that the program will keep increasing the number of sources or groups of sources in the solution by the number of calls to this command unless the NS or NX commands are called to reinitialize the source geometry. Presently, the total number of sources and elements in the source groups can not be more than 30. This is set by the PARAMETER statements and can be changed if desired.

EXAMPLE:

```
SA
T,F,F
5
0.,-2.,0.
0.,-1.,0.
0.,0.,0.
0.,1.,0.
0.,2.,0.
0.,0.,90.,0.
-1.,.8,.8
10.,0.
10.,0.
10.,0.
10.,0.
10.,0.
```

This specifies an array of 5 uniform square (0.8×0.8) patches of electric current. The LDSO has been set true so the code will use the second order array factor when computing the fields.

4.34 Command SG: Source Geometry

This command enables the user to specify the location and type of source to used. The geometry is illustrated in Figures 4.12, 4.13 and 4.14. One call to this command defines one source. The number of sources in the problem are automatically counted by the number of calls to this command and the SA command. See Appendix A on how to adjust the number of sources (NSX) available.

The source location is specified by the XSS which give the linear displacement from the pattern point for a moving source or from the definition origin for a stationary one.

As a reminder, the current elements lie in the $x - z$ plane and are z directed for $|IMS| \leq 3$ and lie in the $x - y$ plane and are x directed for $|IMS| \geq 4$.

READ: (XSS(N,MS),N=1,3)

_____ where _____

XSS(N,MS) This is a doubly dimensioned real array which is used to define the x, y, z location of the MSt^h element relative to the pattern location for each pattern point if the source is moving or relative to the definition coordinate system if it is stationary. If the source is moving in a spherical pattern, then these represent linear displacements in the \hat{r} , $\hat{\theta}$ and $\hat{\phi}$ directions respectively. Again, a single line of data contains the x, y, z ($N=1,2,3$) locations.

READ: THSZ, PHSZ, THSX, PHSX

_____ where _____

THSZ,PHSZ These are real variables which are used to define the orientation of the MSt^h element in the definition coordinate system. They are input in degrees as spherical angles that define the z -axis of the antenna coordinate system.

THSX,PHSX These are real variables which are used to define the orientation of the MSt^h element in the definition coordinate system. They are input in degrees as spherical angles that define the x -axis of the antenna coordinate system. For a dipole antenna, these angles can be made in a convenient direction.

The x -axis and z -axis specified by these angles must be defined orthogonal to each other. The y -axis is found by the cross product of the x - and z -axes.

The source coordinate axes are still \hat{x} , \hat{y} and \hat{z} , but they are defined relative to the \hat{r} , $\hat{\theta}$ and $\hat{\phi}$ directions. The THSZ and THSX are angles relative to the $\hat{\phi}$ axis and the PHSZ and PHSX are angles relative to the \hat{r} axis. For example: if you want the source coordinate \hat{z} in the \hat{r} direction of the pattern system and \hat{x} in the $\hat{\theta}$ then input THSZ, PHSZ, THSX, PHSX = 90,0,90,90.

READ: IMS(MS), HS(MS), HAWS(MS)

_____ where _____

IMS(MS) This is an integer array which is used to define the MSt^h element's source type. The details of the different types of sources are given elsewhere. The designations are defined as follows:

IMS(MS)<0 for an electric element

IMS(MS)>0 for a magnetic element

|IMS(MS)|=1 for a uniform current distribution

|IMS(MS)|=2 for a piece-wise sinusoidal distribution

|IMS(MS)|=3 for a TE₀₁ cosine current distribution

|IMS(MS)|=4 for an annular ring current distribution

|IMS(MS)|=5 for a constant circular current distribution

|IMS(MS)|=6 for a TE₁₁ circular current distribution

HS(MS) This is a real array which is used to input the length of the MSt^h element. If $|IMS|=4, 5$ or 6 this is the aperture radius.

HAWS(MS) This is a real array which is used to input the width of the MSt^h element in the case of an aperture antenna. If $HAWS(MS)=0$, then it is assumed to be a dipole. If $|IMS|=4$, then this is the outer radius of the ring, b . If $|IMS|=5$ or 6 set this to 0 .

Note that the units of the variable **HS(MS)** and **HAWS(MS)** can be specified by the **US** command. If wavelengths are chosen, it uses λ at the time of definition. It does not change as frequency changes.

READ: WMS, WPS

_____ where _____

WMS, WPS These are real variables used to define the excitation associated with the MSt^h element. The magnitude is given by **WMS** and the phase in degrees by **WPS**.

Note that the program will keep increasing the number of sources in the solution by the number of calls to this command unless the **NS** or **NX** commands are called to reinitialize the source geometry.

EXAMPLE:

```
SG
0.,10.,0.
90.,0.,0.,0.
-1.,.5,0.
15.,90.
```

This specifies an electric half-wave dipole directed in the x direction. The antenna is driven with an amplitude of 15 and phase of 90° .

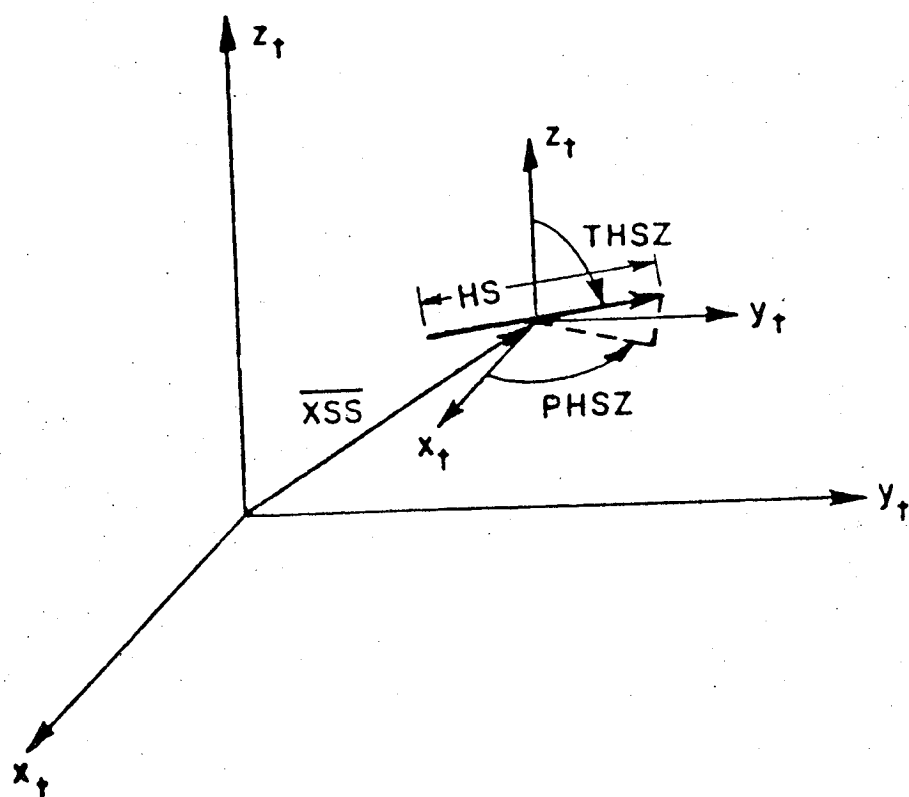


Figure 4.12: Definition of source geometry for dipole antennas.

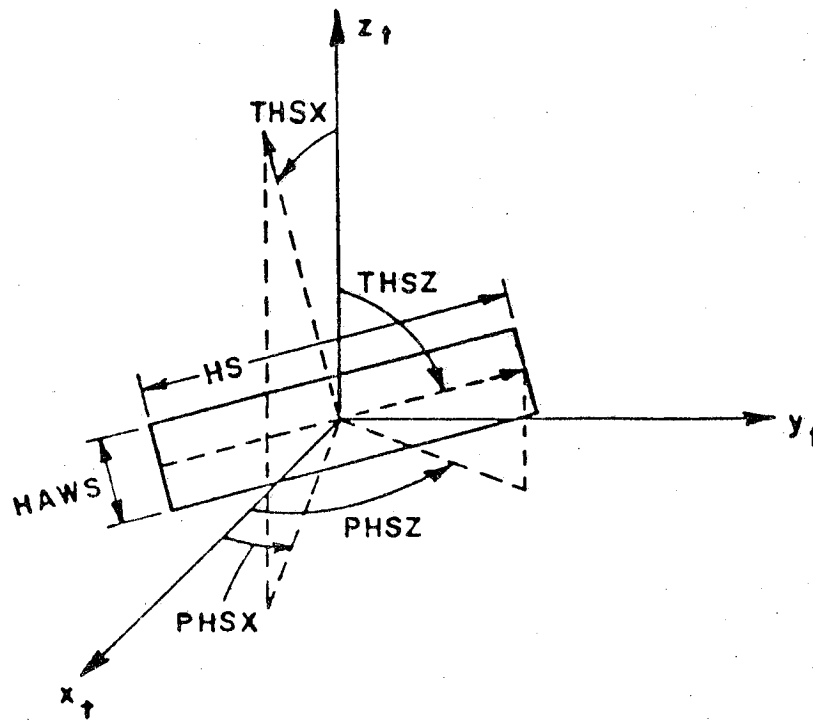


Figure 4.13: Definition of source geometry for rectangular aperture antennas.

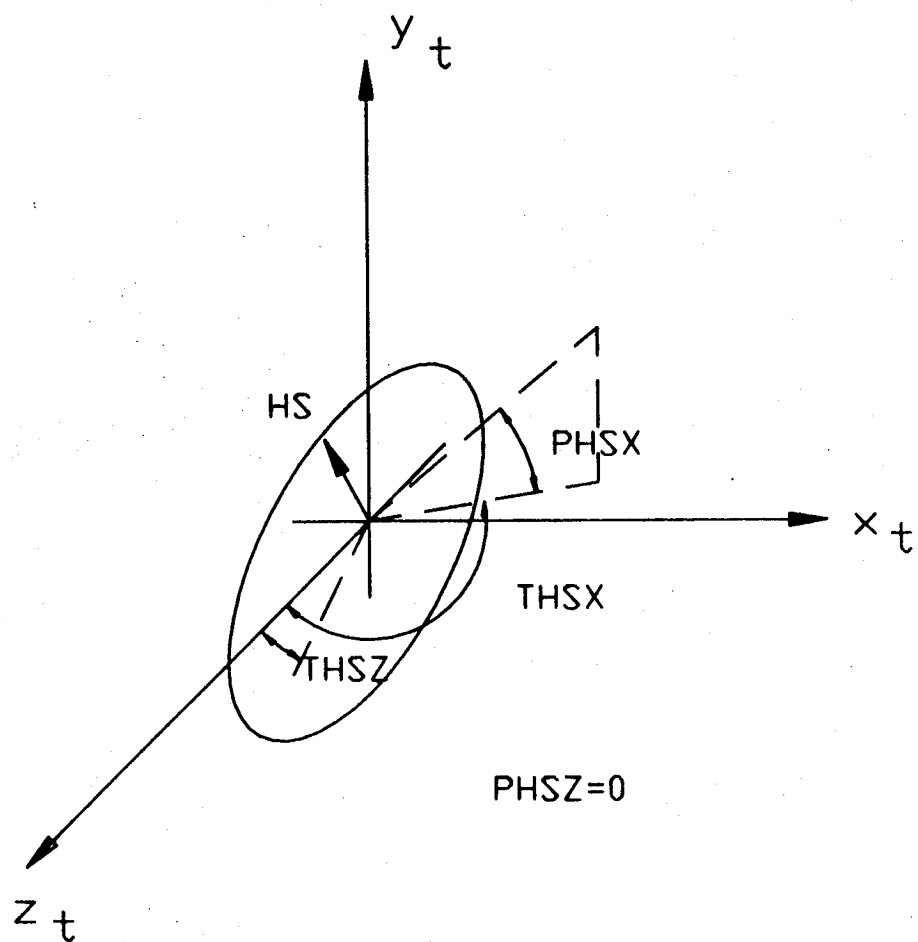


Figure 4.14: Definition of source geometry for circular aperture antennas.

4.35 Command SI: Interpolated Source

This command enables the user to approximate a complex antenna using linear interpolation to determine field values from a finite set of measured or calculated points. The entire antenna will be treated as a point source with a complex pattern. The field values are assumed to be from surface currents that lie in $x - y$ plane of the antenna coordinate system. These currents must be linear of a known polarization, or circularly polarized. The data is entered as magnitude and phase of the radiated electric or magnetic field at various θ and ϕ values. To ease the data entry process a symmetry option is included. If the pattern is symmetric about the y -axis, then patterns for $-90 \leq \phi \leq 90$ are entered. If it's symmetric about the x -axis, then $0 \leq \phi \leq 180$ is used and if it's symmetric about both axes, then $0 \leq \phi \leq 90$ is used. The data is entered in NPHI pattern cuts, where each cut is a constant ϕ cut over $0 \leq \theta \leq 180$. The phi and theta values must be entered in increasing order. See Appendix A on how to adjust the number of interpolation points (NIX) available.

Warnings: This command can only be called once and will increment the total number of sources by one. The accuracy of this routine is dependent on the number of points entered and their measured accuracy. Do not mount this on a plate since the imaging may be incorrect.

READ: (XSS(N,MS),N=1,3)

_____ where _____

XSS(N,MS) This is a doubly dimensioned real array which is used to define the x, y, z location of the MSt^h element in the definition coordinate system for a stationary source or the location relative to the pattern point for a moving source. If the source is moving in a spherical pattern then these represent linear displacements in the \hat{r} , $\hat{\theta}$ and $\hat{\phi}$ directions respectively. Again, a single line of data contains the x, y, z (N=1,2,3) locations.

READ: THSZ, PHSZ, THSX ,PHSX

_____ where _____

THSZ,PHSZ These are real variables which are used to define the orientation of the MStH element in the definition coordinate system. They are input in degrees as spherical angles that define the z-axis of the antenna coordinate system.

THSX,PHSX These are real variables which are used to define the orientation of the MStH element in the definition coordinate system. They are input in degrees as spherical angles that define the x-axis of the antenna coordinate system.

The x-axis and z-axis specified by these angles must be defined orthogonal to each other. The y-axis is found by the cross product of the x- and z-axes.

If the source is moving in a spherical pattern, then these angles are defined relative to the spherical coordinate axes of the pattern system at the pattern point. The source coordinate axes are still \hat{x} , \hat{y} and \hat{z} , but they are defined relative to the \hat{r} , $\hat{\theta}$ and $\hat{\phi}$ directions. The THSZ and THSX are angles relative to the $\hat{\phi}$ axis and the PHSZ and PHSX are angles relative to the \hat{r} axis. For example: if you want the source coordinate \hat{z} in the \hat{r} direction of the pattern system and \hat{x} in the $\hat{\theta}$ then input THSZ, PHSZ, THSX, PHSX = 90,0,90,90.

The following data is input on logical unit IUSI:

READ: ISYM,NPHI,NPTS,TAU

_____ where _____

ISYM This is an integer variable that defines the type of symmetry the feed pattern has; where:

ISYM=0 for no symmetry

ISYM=1 even symmetry about the x and y axes

ISYM=2 even symmetry about the x axis only

ISYM=3 even symmetry about the y axis only

NPHI This integer variable is the number of pattern cuts to be entered. The number of ϕ values.

NPTS This integer is the number of θ points per pattern cut. This number is the same for each cut.

TAU This real variable is the angle (in degrees) relative to the x -axis of the antenna polarization for linearly polarized fields (see Figure 4.15). If a circularly polarized field is chosen, then this should be set to 0.

READ: LDB,LCP,LEH

_____ where _____

LDB This is a logical variable used to tell the code how the magnitudes of the input field values are to be entered. If true then, these values are input in dB.

LCP This is a logical variable that is set true if a circularly polarized field is wanted.

LEH This is a logical variable that tells the code if the data to be entered is the electric field values ($LEH=T$) or magnetic field values ($LEH=F$).

READ: (PHIN(I), I=1,NPHI)

_____ where _____

PHIN(I) This is real array which holds the $NPHI$ ϕ values, in degrees, of the pattern cuts to be entered next. They must be entered in increasing order.

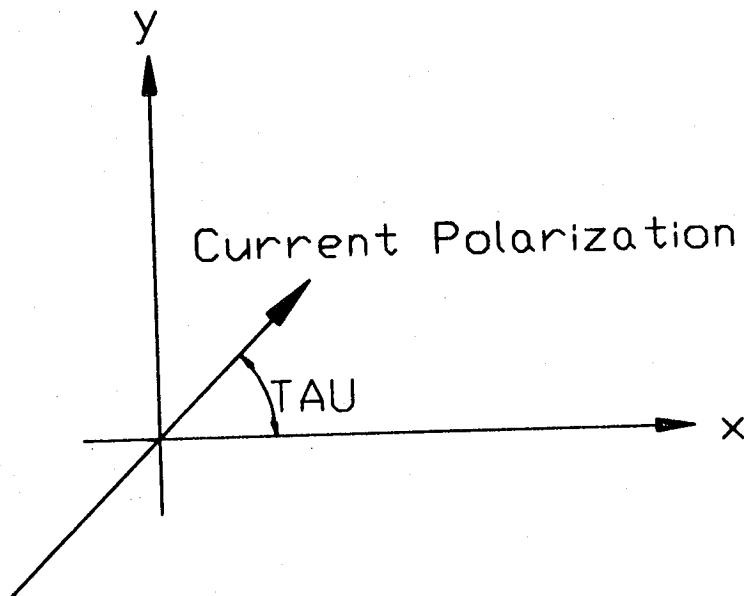


Figure 4.15: Polarization angle of fields, Tau

READ: THPTS, MG1, PH1

_____ where _____

These real variables are the θ value (in degrees) and the magnitude and phase (in degrees) of the field at that value. This is entered NPTS times for each PHIN value entered above. So the NPTS values for the $\phi = \text{PHIN}(1)$ cut are entered first, then the next NPTS values for the $\phi = \text{PNIN}(2)$ cut, etc. Remember if $\text{LDB} = \text{T}$, the MG1 are entered in dB.

EXAMPLE:

SI
 0.,0.,0.
 0.,0.,90.,0.
 0,4,9,0.
 T,T,F
 0.,90.,180.,270.
 0.,-22.,35.
 .
 .
 .

This specifies an interpolated antenna where there is no symmetry, so ϕ over 0° to 360° are used (0° to 270° to be specific). The values input are magnetic field amplitudes of a circularly polarized antenna in dB. Nine points (θ 's) are input for each cut.

4.36 Command SM: MOM Source Input

This command enables the user to interface the Numerical Electromagnetics Code (NEC) - Moment Method Code with the Basic Scattering Code in order to use the antenna modeling capabilities of NEC to specify the needed source data such as location and current weights of the elements. The geometry is illustrated in Figure 4.16. See Appendix A on how to adjust the number of sources (NSX) available.

READ: PRAD

_____ where _____

PRAD This is a real variable which is used to define the total power radiated in watts from the NEC modeled antenna. This allows the directive gain to be computed in the far zone. If Pin is substituted for Prad, the power gain will be computed.

READ: MSX

_____ where _____

MSX This is an integer variable which defines the maximum number of elemental wire radiators that have been used in the NEC code to model the antenna.

READ: (XSS(N,MS),N=1,3), HS(MS), THSZ, PHSZ

_____ where _____

XSS(N,MS) This is a doubly dimensioned real array which is used to define the x, y, z location of the MSt^h elemental radiator in the definition coordinate system.

HS(MS) This is a real array which is used to input the length of the MSt^h element in the units specified by IUNIT from the UN command or the default option.

THSZ,PHSZ These are real variables which are used to define the orientation of the MSt^h element in the definition coordinate system. The angles are in degrees and define a radial direction which is parallel to the MSt^h element current flow. The angle THSZ is the angle of the element measured up from the $x - y$ plane. The angle PHSZ is the phi angle in a normal spherical coordinate system.

READ: WMS, WPS

_____ where _____

WMS,WPS These are real variables used to define the excitation associated with the MSt^h element. The real part is given by WMS and the imaginary part by WPS.

Note that for the NEC code input all the elements are assumed to be electric current elements.

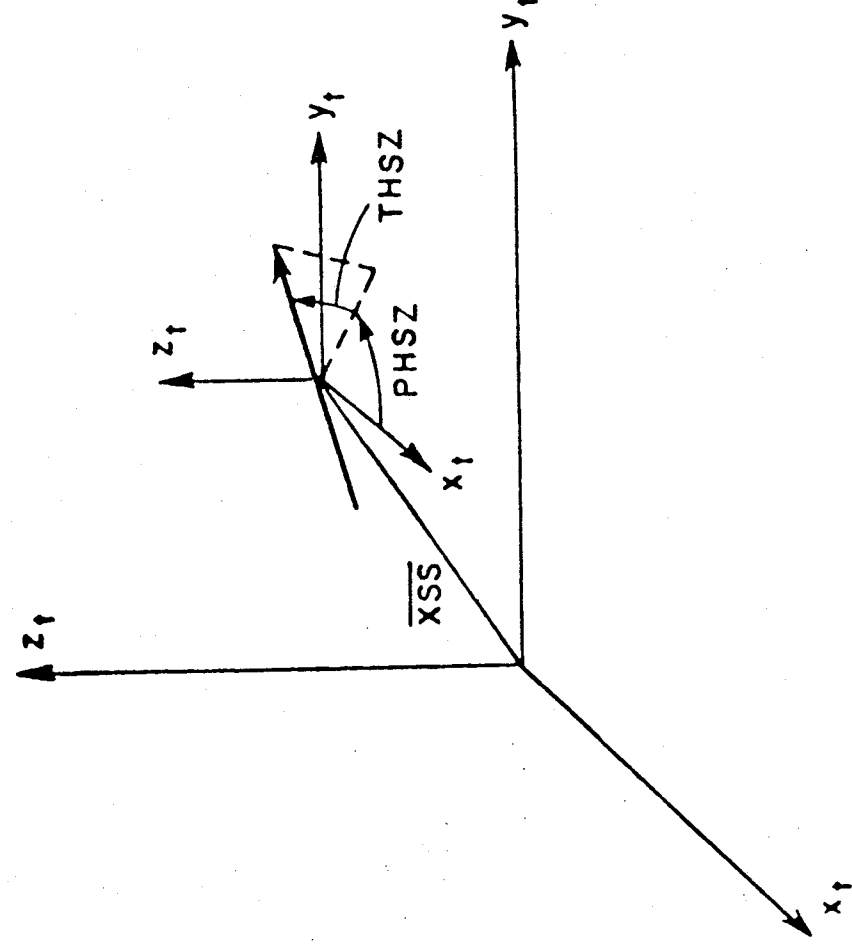


Figure 4.16: Definition of NEC geometry.

4.37 Command TC: Test Cylinder

This command enables the user to set options to be used to test the cylinder fields.

READ: LNUCF

_____ where _____

LNUCF This is a logical variable. If true, it uses the classical non-uniform diffraction coefficients for the reflection and creeping wave fields for a curved surface.

4.38 Command TO: Test Output

This command enables the user to obtain an extended output of various intermediate quantities in the computer code. This is useful in testing the program or in analyzing the contributions from various scattering mechanisms in terms of the total solution.

READ: LDEBUG, LTEST, LOUT, LWARN

_____ where _____

LDEBUG This is a logical variable defined by T or F. It is used to debug the program if errors are suspected within the program. If set true, the program prints out data on unit IUO, which is usually #6, associated with each of its internal operations. These data can, then be compared with previous data which are known to be correct. It is, also, used to insure initial operation of the code. Only one pattern angle is considered. (normally set false)

LTEST This is a logical variable defined by T or F. It is used to test the input/output associated with each subroutine. The data written out on unit IUO are associated with the data in the window of the subroutine. They are written out each time the subroutine is called. It is, also, used to insure initial operation of the code. Only one pattern angle is considered. (normally set false)

LOUT This is a logical variable defined by T or F. It is used to output data on unit IUO associated with the main program. It too is used to initially insure proper operation. It can, also be used to examine the various components of the pattern. This is especially useful to someone interested in analyzing which scattering center contributes in a particular direction. The field subroutine name is output along with the plate, edge, cylinder, and end cap numbers when applicable. See Tables 4.1 and 4.2 for the format of the printed information. (normally set false)

LWARN This is a logical variable defined by T or F. It is used to give warning messages programed internally into the code indicating when the code may have numerical difficulties. It outputs the messages on unit IUW, which is usually #6. These messages are intended to help correctly identify a problem if it exist, they do not necessarily indicate that there is an error.

Table 4.1: Individual Plate Field Types Printed when LOUT is set true.

TYPE	IDENTIFIERS				DESCRIPTION
INCFLD	0	0	0	0	Direct field
RP	MP	0	0	0	Field reflected by plate MP
RPRP	MP	MPP	0	0	Field reflected by plate MP then reflected by plate MPP
DP	MP	ME	0	0	Field diffracted by edge ME of plate MP
CORNER	MP	ME	0	0	Field diffracted by corners of edge ME of plate MP
RPDP	MPR	MP	ME	0	Field reflected by plate MPR then diffracted by edge ME of plate MP
CORNER	MPR	MP	ME	0	Field reflected by plate MPR then diffracted by the corners of edge ME of plate MP
DPRP	MP	ME	MPR	0	Field diffracted by edge ME of plate MP then reflected by plate MPR
CORNER	MP	ME	MPR	0	Field diffracted by the corners of edge ME of plate MP then reflected by plate MPR

Table 4.2: Individual Curved Surface Field Types Printed when LOUT is set true.

TYPE	IDENTIFIERS				DESCRIPTION
RC	MC	MN	0	0	Field uniformly reflected by section MN of the curved surface cylinder MC
GO	MC	MN	0	0	Geometrical optics field reflected by section MN of the curved surface cylinder MC (for comparison purposes)
DC	MC	MN	0	0	Field uniformly diffracted by section MN of the curved surface cylinder MC
RN	MC	MN	0	0	Field reflected by end cap MN of curved surface cylinder MC
DN	MC	MN	0	0	Field diffracted by end cap rim MN of cylinder MC
SUBTOTAL	ITERM	IK	0	0	Sum of fields of given type number ITERM and location or frequency number IK
TOTAL	II	II	II	II	Total field for a given position or frequency number II

4.39 Command TP: Test Plate

This command is used to test the plate diffraction options.

READ: LSLOPE, LCORNR

_____ where _____

LSLOPE This is a logical variable defined by T or F. It is used to tell the code whether or not slope diffraction is desired during the computation. (normally set true)

LCORNR This is a logical variable defined by T or F. It is used to tell the code whether or not corner diffraction is desired during the computation. (normally set true)

4.40 Command UF: Scale Factor

This command enables the user to scale the linear dimensions that follow the command by the factor specified.

READ: UNITF

_____ where _____

UNITF This is a real variable that is used as a scale factor for all the linear dimensions that follow the command.

Note the default value for this factor is 1.

EXAMPLE:

UF
1.5

This scales all linear dimensions to follow by a factor of 1.5.

4.41 Command UN: Units of Geometry

This command enables the user to specify the units of all the linear dimensions to be input after the command is called. (The exceptions are the source length HS and width HAWS, and receiver length HR and width HAWR, see command US.)

READ: IUNIT

_____ where _____

IUNIT This is an integer variable that indicates the units for the input data that follows, such that

1= meters

2= feet

3= inches

Note the default value is meters. If this command and the frequency command **FR** are not specified then the geometry is assumed to be specified in wavelengths.

EXAMPLE:

UN
3

The linear dimensions to follow are to be in inches.

4.42 Command US: Units of Source

This command enables the user to specify the units of the source length HS and width HAWS or receiver length HR and width HAWR to be input after the command is called. These variables are in the commands SG, SA, RG, and RA.

READ: IUNST

_____ where _____

IUNST This is an integer variable that indicates the units for the input data HS, HAWS, HR, HAWR that follows, such that if

0= wavelengths

1= meters

2= feet

3= inches

Note the default is meters. If the wavelength option is specified, then the length and width of the antenna in meters is determined based on the frequency in effect at the time the source or receiver is defined. If the frequency is changed later, the length and width of the source or receiver in meters will not change based on the new frequency. If this is desired, the source and/or receiver command will have to be redefined.

EXAMPLE:

US
0

The antenna size dimensions are to be input in wavelengths.

4.43 Command VD: Volumetric Far Zone

This command enables the user to define the far zone volumetric pattern coordinate system, the pattern cut, and the angular range that is desired. The angular range is restricted to integer steps. This command is superseded by the **VF** command, which allows non-integer steps, is therefore more general. The geometry is illustrated in Figure 4.4, 4.5, and 4.6. See Appendix A on how to adjust the number of observation points (NOX) available.

READ: THCZ, PHCZ, THCX, PHCX

_____ where _____

THCZ,PHCZ These are real variables. They are input in degrees as spherical angles that define the z_p -axis of the pattern coordinate system as if it was a radial vector in the reference coordinate system.

THCX,PHCX These are real variables. They are input in degrees as spherical angles that define the x_p -axis of the pattern coordinate system as if it was a radial vector in the reference coordinate system.

Note that the new x_p -axis and z_p -axis must be defined orthogonal to each other. The new y_p -axis is found from the cross product of the x_p - and z_p -axes.

READ: LCNPAT, TPPD, TPPV, NPV

_____ where _____

LCNPAT This is a logical variable that defines the pattern cut desired, such that

VD

143

T= The theta angle is held fixed while the phi angle is varied. The theta angle will then be incremented and another cut will be calculated.

F= The phi angle is held fixed while the theta angle is varied. The phi angle will then be incremented and another cut will be calculated.

TPPD This is a real variable. It defines the starting angle of the "fixed" angle specified by LCNPAT.

TPPV This is a real variable. It defines the incremental angle of the "fixed" angle specified by LCNPAT.

NPV This is an integer variable. It defines the number of pattern points of the "fixed" angle specified by LCNPAT.

READ: IB, IE, IS

_____ where _____

IB,IE,IS These are integer variables used to define angles in degrees. They are, respectively, the beginning, ending, and incremental values of the pattern angle.

4.44 Command VF: Far Zone Volumetric Pattern

This command enables the user to define the far zone volumetric pattern coordinate system, the pattern cut, and the angular range that is desired. The geometry is illustrated in Figure 4.4, 4.5, and 4.6. See Appendix A on how to adjust the number of observation points (NOX) available.

READ: THCZ, PHCZ, THCX, PHCX

_____ where _____

THCZ,PHCZ These are real variables. They are input in degrees as spherical angles that define the z_p -axis of the pattern coordinate system as if it was a radial vector in the reference coordinate system.

THCX,PHCX These are real variables. They are input in degrees as spherical angles that define the x_p -axis of the pattern coordinate system as if it was a radial vector in the reference coordinate system.

Note that the new x_p -axis and z_p -axis must be defined orthogonal to each other. The new y_p -axis is found from the cross product of the x_p - and z_p -axes.

READ: LCNPAT, TPPD, TPPV, NPV

_____ where _____

LCNPAT This is a logical variable that defines the pattern cut desired, such that

T= The theta angle is held fixed while the phi angle is varied. The theta angle will then be incremented and another cut will be calculated.

F= The phi angle is held fixed while the theta angle is varied. The phi angle will then be incremented and another cut will be calculated.

TPPD This is a real variable. It defines the starting angle of the "fixed" angle specified by LCNPAT.

TPPV This is a real variable. It defines the incremental angle of the "fixed" angle specified by LCNPAT.

NPV This is an integer variable. It defines the number of pattern points of the "fixed" angle specified by LCNPAT.

READ: TPPS, TPPI, NPN

_____ where _____

TPPS This is a real variable. It defines the starting angle of the "varying" angle specified by LCNPAT.

TPPI This is a real variable. It defines the incremental angle of the "varying" angle specified by LCNPAT.

NPN This is an integer variable. It defines the number of pattern points of the "varying" angle specified by LCNPAT.

EXAMPLE:

VF
0.,0.,90.,0.
T,-90.,15.,13
0.,15.,13

This specifies a far zone scan over the entire upper half plane ($z > 0$) by sweeping in ϕ for various θ cuts.

EXAMPLE:

VF

0.,0.,90.,0.

F,0.,15.,13

-90.,15.,13

This specifies the same scan as above
but sweeps θ for various ϕ cuts.

4.45 Command VN: Volumetric Near Zone

This command enables the user to define the near zone pattern coordinate system, the volumetric pattern cut, and the spacial range that is desired. The geometry is illustrated in Figures 4.8, 4.9, and 4.10. See Appendix A on how to adjust the number of observation points (NOX) available.

READ: (XPC(N),N=1,3)

_____ where _____

XPC(N) This is a dimensioned real variable. It is used to specify the origin of the near zone pattern coordinate system relative to the reference coordinate system. It is input on a single line with the real numbers being the x, y, z coordinates of the origin which corresponds to $N=1,2,3$, respectively.

READ: THCZ, PHCZ, THCX, PHCX

_____ where _____

THCZ,PHCZ These are real variables. They are input in degrees as spherical angles that define the z_p -axis of the pattern coordinate system as if it was a radial vector in the reference coordinate system.

THCX,PHCX These are real variables. They are input in degrees as spherical angles that define the x_p -axis of the pattern coordinate system as if it was a radial vector in the reference coordinate system.

Note that the new x_p -axis and z_p -axis must be defined orthogonal to each other. The new y_p -axis is found from the cross product of the x_p - and z_p -axes.

READ: LRECT

_____ where _____

LRECT This is a logical variable that defines whether a spherical or linear pattern cut is desired. It is designated as follows:

T= linear pattern cut

F= spherical pattern cut

READ: RXS, TYS, PZS

_____ where _____

RXS,TYS,PZS These are real variables. They define the starting position of the pattern trace. If **LRECT=F**, they are the radial, theta, and phi coordinates of the start location, respectively. If **LRECT=T**, they are the x , y , and z coordinates of the starting location, respectively.

READ: RXI, TYI, PZI

_____ where _____

RXI,TYI,PZI These are real variables. They define the size of the incremental steps for the pattern trace. If **LRECT=F**, they are the radial, theta, and phi step sizes, respectively. If **LRECT=T**, they are the x , y , and z step sizes, respectively.

READ: IVPN, NPV, NPN

_____ where _____

IVPN This is an integer variable. It is used to specify the type of rasterization for the volumetric pattern cut.

1 = r and θ or x and y is varied.

2 = r and ϕ or x and z is varied.

3 = θ and ϕ or y and z is varied.

NPV This is an integer variable used to define the number of pattern points that are processed in the outer loop.

IVPN > 0 NPV specifies the number of r , r , or θ steps or x , x , or y steps respectively, as defined by the IVPN above.

IVPN < 0 NPV specifies the number of θ , ϕ , or ϕ steps or y , z or z steps, respectively, as defined by the IVPN above.

NPN This is an integer variable used to define the number of pattern points that are processed in the inner loop.

IVPN > 0 NPN specifies the number of θ , ϕ , or ϕ steps or y , z or z steps, respectively, as defined by the IVPN above.

IVPN < 0 NPN specifies the number of r , r , or θ steps or x , x , or y steps respectively, as defined by the IVPN above.

EXAMPLE:

VN

0., 0., 0.

0., 0., 90., 0.

F

20., 0., 0.

0., 15., 15.

3, 7, 24

This specifies a scan of the entire upper half plane ($z > 0$) at $r = 20$.

EXAMPLE:

VN

0.,0.,25.

0.,0.,90.,0.

T

-25.,-25.,0.

5.,5.,0.

-1,11,11

This specifies a scan over a flat plane
parallel to the $x - y$ plane at $z = 25$.

The scan plane covers the values of
 $-25 < x < 25$ and $-25 < y < 25$.

4.46 Command VP: Volumetric Plot Data

This command enables the user to specify whether binary output is written to the disk eventually to be plotted. Information about the type of plot desired is specified. A rectangular or polar plot can be defined along with the size of the plot and viewing window. It is like the **PP** command except that it is designed for volumetric information, so to conserve space on the disk or other device the type of field and polarization desired can be specified.

READ: LPLT

_____ where _____

LPLT This is a logical variable defined by T or F. It is used to indicate if a plot of the results are desired.

READ: LPPREC, PPXL, PPYL

_____ where _____

LPPREC This is a logical variable defined by T or F that is used to specify whether a rectangular or polar plot is desired. If LPPREC is TRUE, a rectangular plot is specified. If LPPREC is FALSE, a polar plot is specified.

PPXL This is a real variable. If LPPREC is TRUE, this is the length of the x -axis. The x -axis is the angle definition axis. If LPPREC is FALSE, this is the angular position of the zero angle axis.

PPYL This is a real variable. If LPPREC is TRUE, this is the length of the y -axis. The y -axis is the dB definition axis. If LPPREC is FALSE, this is the radius of the polar plot.

READ: PPXB, PPXE, PPXS

_____ where _____

PPXB This is a real variable that defines the beginning value of the grid's x -axis.

PPXE This is a real variable that defines the end value of the grid's x -axis.

PPXS This is a real variable that defines the step size of the grid's x -axis.

READ: PPYB, PPYE, PPYS

_____ where _____

PPYB This is a real variable that defines the beginning value of the grid's y -axis.

PPYE This is a real variable that defines the end value of the grid's y -axis.

PPYS This is a real variable that defines the step size of the grid's y -axis.

READ: IVTYP, IVPOL

_____ where _____

IVTYP This is an integer variable. It is used to specify the type of field output to the file. If a receiver is present, only the coupling is supplied; therefore, this option has no action. If just the field are being studied, then IVTYP can be used to reduce the amount of information written on the file.

1= Output only the electric field.

2= Output only the magnetic field.

3= Output both the electric and magnetic fields.

IVPOL This is an integer variable. It is used to specify the type of polarization to be output to the file. If a receiver is present, the coupling has no polarization; therefore, this option has no action. If a field is being output, then the polarization can be chosen with the following options.

1= r or x polarized field is output.

2= θ or y polarized field is output.

3= ϕ or z polarized field is output.

4= r and θ or x and y polarized fields are output.

5= r and ϕ or x and z polarized fields are output.

6= θ and ϕ or y and z polarized fields are output.

7= r , θ , and ϕ or x , y , and z polarized fields are output.

4.47 Command XQ: Execute Code

This command is used to execute the code so that the results may be computed. After execution the code returns for another possible command word.

4.48 Command XT: Execute Terms

This command is used to execute the code. It enables a term processor, that allows the user to compute only the UTD terms from the specific diffraction locations desired. It can be used to include all of a particular type of term, to include only some of the scattering centers of the term, or to exclude some of the centers. It reads the information from a file assigned to logical unit IUT. It is used in place of the **XQ** command. Further information is given in Section 5.6 for the **XT** command and Section 4.47 for the **XQ** command.

In the file assigned to IUT all the field terms to be included in the analysis must be listed. The present choices are:

- INCFLD = incident field.
- RP = reflected fields off plates.
- RPRP = reflected-reflected fields off plates.
- DP = diffracted fields off plates.
- RPDP = reflected-diffracted fields off plates.
- DPRP = diffracted-reflected fields off plates.
- RC = reflected fields off curved surfaces.
- DC = diffracted fields off curved surfaces.
- RN = reflected fields off curved surface end caps.
- DN = diffracted fields off curved surface end caps.

Following each field listed in the file the user tells the code which of the scattering centers are to be used. If the field is followed by 'ALL' then the code includes all the fields of that type. If only certain of the terms of the field are to be included then the field is followed by 'SOM', which is followed by a list of the desired terms. If all the terms except for certain ones are desired the field is followed by 'EXC' and a list of the terms to exclude. The term 'END' must be the last item in the file. The individual terms for each of the field types are:

INCFLD

no choice

RP

i

i=plate number

RPRP

i,j

i= plate number of first plate

j= plate number of second plate

DP

i,n

i=plate number

n=edge number

RPDP

i,j,n

i=reflecting plate number

j=diffraction plate number

n=diffraction edge number

DPRP

j,n,i

j=diffraction plate number

n=diffraction edge number

i=reflecting plate number

RC

i,j

i=curved surface cylinder number

j=section number

DC

i,j

i=curved surface cylinder number

j=section number

RN

i,j

i=curved surface cylinder number

j=end cap number

DN

i,j

i=cylinder number

j=rin number

The number 999 in the first place, with the appropriate number of places after it, is the end of list indicator for the list of terms for each field type.

EXAMPLE:

XT

Using this command only the terms specified in the file shown are included.

EXAMPLE:

INCFLD
RP
ALL
DP
EXC
1,2
999,0
RPDP
SOM
1,2,3
999,0,0
END

This separate file instructs the code to include the incident field, all the reflection from plates, all the diffraction from plates except from plate 1 edge 2 and only the reflected-diffracted term for reflection from plate 1 and diffraction from plate 2 edge 3.

Chapter 5

Interpretation Of Input Data

This computer code is written to require a minimal amount of user information such that the burden associated with organizing the details of a complex geometry internal to the computer code will be accomplished opaque to the user. An attempt has been made to make as many of the geometry decisions that have to be made as automatic as possible. The code has been tested on a large class of problems over the years, but, as can be imagined with a code as complex as this, it is not possible to anticipate all possible geometry situation that can arise in practice. Therefore, some rules have to be followed to help the code properly interpret the particular situation desired. Many of these rules are governed by the numerical accuracy of the computer that is being used, since most of the decisions are based on logical statements that compare small numbers. This chapter is intended to point out the subtle rules that the user needs to be aware of when he defines his geometry and to alert him to many of the situations that can arise and how to avoid or interpret them.

5.1 Moving Antennas

The orientation and location of moving antennas is handled differently then stationary ones. For stationary antennas, the location and orientation input by the user defines the antenna in the definition coordinate system, or more precisely in the reference coordinate system after performing any rotation or translation required by an active **RT**. For moving antennas, this is not the case. The displacement and orientation data input by the user is still

acted upon by any active **RT** to give what we will call here \vec{d}_a for the displacement and $\theta_{x,a}, \phi_{x,a}, \theta_{z,a}$ and $\phi_{z,a}$ for the orientation, but this data is not used to locate the axes in the reference coordinate system. Instead the moving antenna's coordinate system $(\hat{x}_a, \hat{y}_a, \hat{z}_a)$ is defined using this data in the moving pattern coordinate system $(\hat{x}_p, \hat{y}_p, \hat{z}_p)$. The moving pattern system is the coordinate system defined by the pattern commands. The axes definitions are done for each pattern point, \vec{r}_p .

For linear pattern motion, this definition is straight forward. The code uses the \vec{d}_a to translate the origin linearly in the $(\hat{x}_p, \hat{y}_p, \hat{z}_p)$ directions from the pattern point. At this point, the two θ and ϕ angles define the orientation of the $(\hat{x}_a, \hat{y}_a, \hat{z}_a)$ relative to the same axes, using the standard definitions for θ (measured from \hat{z}) and ϕ (measured from \hat{x}). For circular patterns the translation is still performed first but not in the same directions. The \vec{d}_a defines a linear translation from the pattern point in the $\hat{r}_p, \hat{\theta}_p, \hat{\phi}_p$ directions. For example, a translation of 1,1,0 would mean a linear shift of 1 unit each in the \hat{r}_p and $\hat{\theta}_p$ directions. The rotation is also taken in terms of the $\hat{r}_p, \hat{\theta}_p, \hat{\phi}_p$ directions. The θ_x and θ_z are the angles measured from the $\hat{\phi}_p$ direction and the ϕ_x and ϕ_z are measured from the \hat{r}_p direction. What this means is that the antenna coordinate system is rotated and translated about axes aligned so that: \hat{x} is \hat{r}_p , \hat{y} is $\hat{\theta}_p$ and \hat{z} is $\hat{\phi}_p$. Therefore if \hat{x}_a is to be $\hat{\phi}_p$ directed then the user would set $\theta_x, \phi_x = 0, 0$. For more on both linear and circular motion coordinates see Figures 5.1 and 5.2, respectively. Remember that the antenna is defined in the antenna coordinate system depending on its shape. Rectangular elements have currents that are directed in the \hat{z}_a directions and lie in the $x_a - z_a$ plane, while the circular elements lie in the $x_a - y_a$ plane.

5.2 Plates

The operator need not instruct the code that two plates are attached to form a convex or concave structure. The code flags this situation by recognizing that two plates have a common set of corners (i.e., a common edge). So if the operator wishes to attach two plates together he needs only define the two plates as though they were isolated, but, the two plates will have two identical corners. All the geometrical information associated with plates with common edges is then generated by the code.

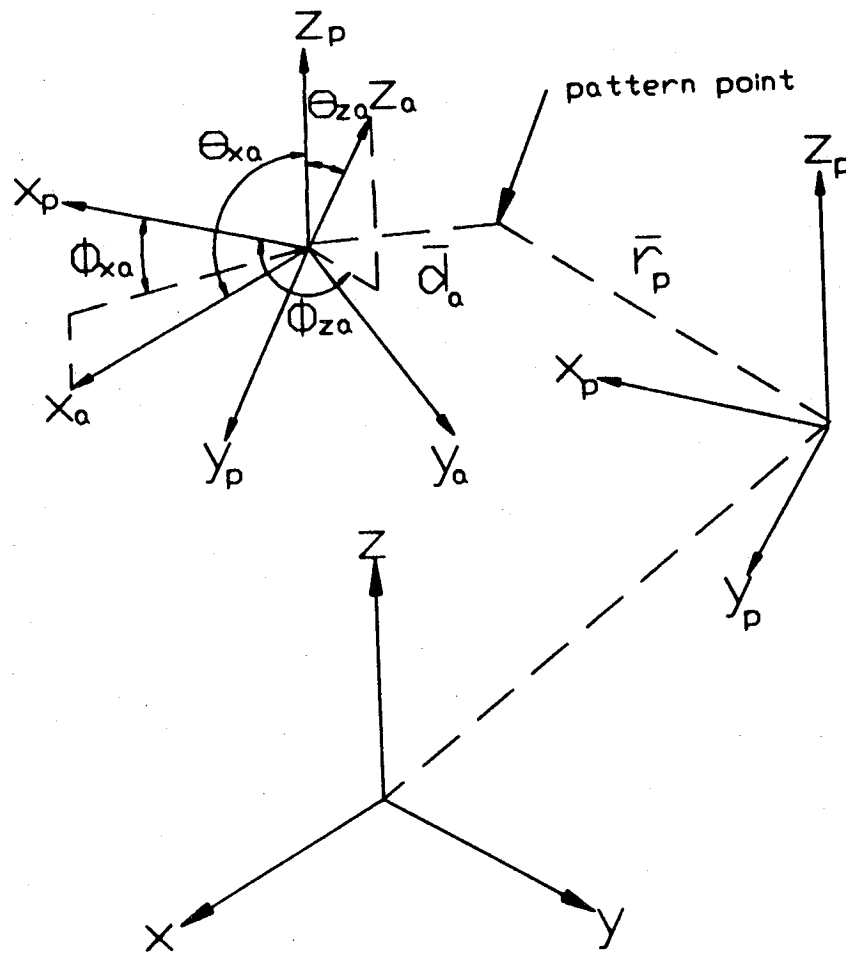


Figure 5.1: Definition of antenna coordinate system for a linearly moving antenna.

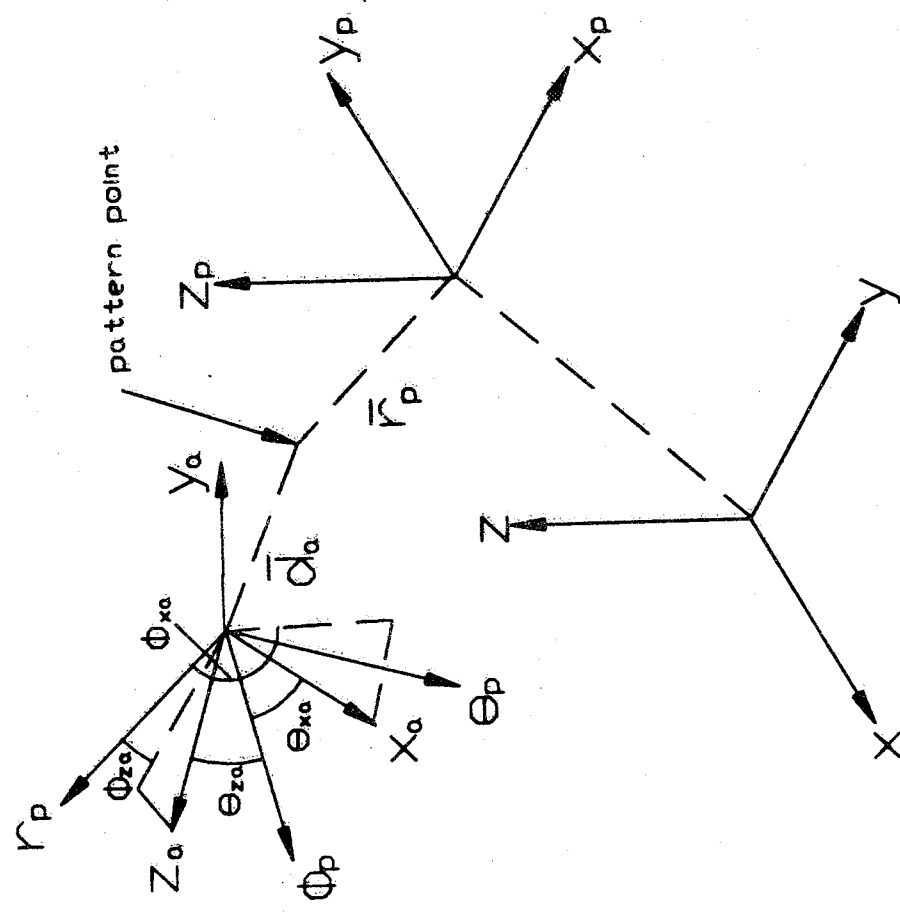


Figure 5.2: Definition of antenna coordinate system for a circularly moving antenna.

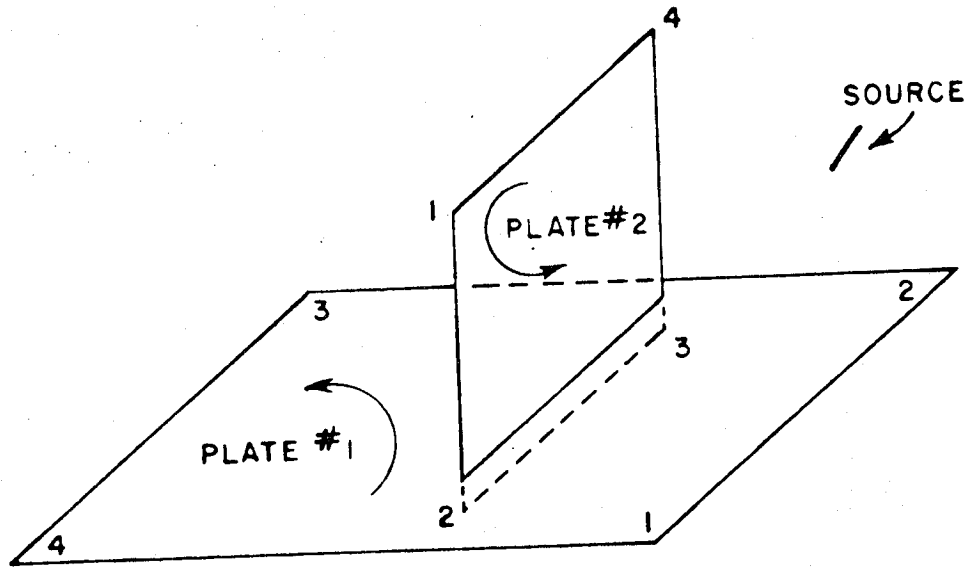


Figure 5.3: Data format used to define a flat plate intersecting another flat plate.

If the geometry being defined is rather complex, such that the corners of the plate can not be specified in nice round numbers, the code sometimes will flag the the plate as not being flat. It may be possible to get around this situation in a couple of ways. First, it may be possible to add a few more significant digits of accuracy to the definition of the corners. Second, the plates can be defined in the $x - y$ plane of a definition coordinate system using the **RT** command to rotate - translate the plate into place. Thirdly, the plate can be broken up into triangular plates. Finally, the user could find the appropriate IF statement governing the flatness test in the GEOMP subroutine and change the logical test number slightly to eliminate the problem.

The present code also will allow a plate to intersect another plate as shown in Figure 5.3. It is necessary that the corners defining the attachment be positioned a small amount (approximately $10^{-5}\lambda$) through the plate surface to which it is being connected. If a larger amount ($\sim 0.1\lambda$) of corner is positioned through the plate, the code will print a warning and not attach the plates.

In defining the plate corners it is necessary to be aware of a subtlety

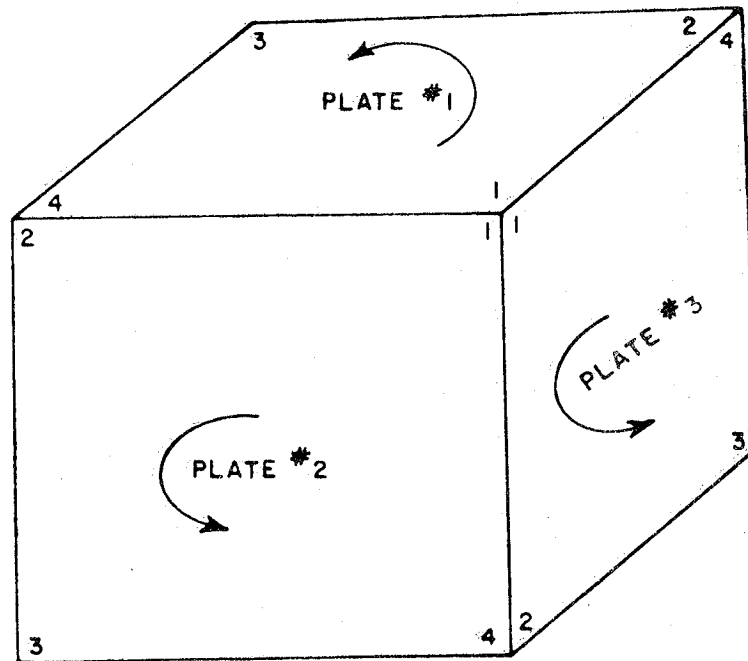


Figure 5.4: Data format used to define a box structure.

associated with simulating convex or concave structures in which two or more plates are used in the computation. This problem results in that each plate has two sides. If the plates are used to simulate a closed or semi-closed structure, then possibly only one side of the plate will be illuminated by the antenna. Consequently, the operator must define the data in such a way that the code can infer which side of the plate is illuminated by the antenna. This is accomplished by defining the plate according to the right-hand rule. As one's fingers of the right hand follow the edges of the plate around in the order of their definition, his thumb should point toward the illuminated region above the plate. To illustrate this constraint associated with the data format, let us consider the definition of a rectangular box. In this case, all the plates of the box must be specified such that they satisfy the right-hand rule with the thumb pointing outward as illustrated in Figure 5.4. If this rule were not satisfied the code attempts to figure out the intended wedge number from what it knows. It is possible, however, that it can misinterpret the situation. Caution in interpreting the results would be strongly advised.

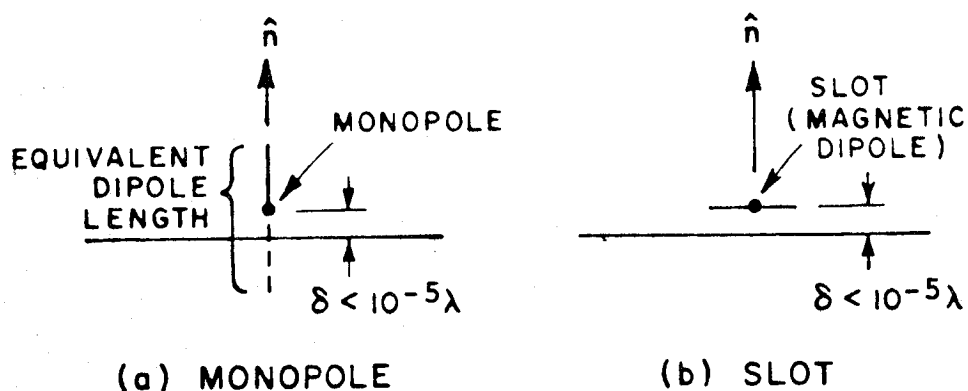


Figure 5.5: Illustration of geometry for plate-mounted antennas.

5.3 Plate Mounted Antennas

Another situation which must be kept in mind is associated with antenna elements mounted on a plate. The code automatically determines that the antenna element is mounted on the plate. It assumes that the element will radiate on the side of the plate into which the normal points. This is accomplished in the code by automatically positioning the source a small distance ($10^{-5}\lambda$) above the plate in the direction of the normal as illustrated in Figure 5.5. This can be overridden by placing the element a slightly larger distance than this small number. It is important, therefore, to follow the simple rules above for defining the plate normals when dealing with plate mounted antennas. There is, also, another point associated with antennas mounted on perfectly - conducting flat structures. If a plate - mounted monopole is considered in the computation, one should input the equivalent dipole length and not the monopole length (i.e., the monopole plus image length should be used as shown in Figure 5.5a). The code automatically handles the half dipole modes associated with the monopole. The plate - mounted slot is, also, automatically taken care of by the code as shown in Figure 5.5b if a magnetic dipole is used.

5.4 Curved Surfaces

The same situation, as for a plate, arises when the antenna is mounted on the end cap of a curved surface. It should also be remembered that the antenna can not be mounted on the curved surface. In general, the antenna should be kept a wavelength away, however, this can often be relaxed to approximately a quarter - wavelength.

In the present code, the attachment of a plate corner to the curved surface is automatically detected, however, a diffracted field from the plate - curved surface junction is not considered in this version. If the plate - cylinder junction forms a straight, orthogonal edge, image theory alone will give the correct results. The diffracted fields, therefore, are not needed. If the plate - cylinder junction forms a curved edge or one in which the plate and curved surface are not orthogonal a diffracted field from that edge will be required in the solution. This will be added when time and effort permit.

5.5 Geometry Warning Messages

Occasionally, the code will try to trace out ray paths associated with geometrical situations that give the algorithms numerical problems. It checks most of its ray path calculation against the laws of reflection and diffraction. If the code thinks that the laws have not been satisfied to a given degree of accuracy it will warn the user if the LWARN flag is set in the **TO** command. If a warning message arises it may or may not indicate a problem has occurred. It may be possible that the geometry is not defined in the proper manner. The user should check the input data set to make sure that none of the geometry has been incorrectly defined. If this is not the case, it is possible that the code could be trying to define degenerate ray paths, that is ray paths that are associated with small distance and tight angles. These ray paths may not actually be a significant contributor to the over all result. This can be checked by setting the flag associated with that particular mechanism false in the **TO** command and recalculate the result. If the answers do not change significantly, the results are probably reasonable. If the answers do appear to be significant, then the algorithm that is causing problems probably needs to be improved to handle the class of geometries the users is studying or the user can attempt to extrapolate the

results based on the fundamental principles of UTD, that is, the continuity of fields.

Chapter 7 has a set of sample problems to illustrate how the operator can realize the versatility of the code and still satisfy the few constraints associated with the input data format.

5.6 Term Interpreter Input

The new term interpreter command, **XT**, gives a flexible way to tailor the calculations of the UTD field terms. See Chapter 5 for how to call the **XT** command. When using the SOM or EXC features, which allows just some of the individual terms or exclusion of some of the individual terms, requires that the user list the particular geometrical components desired. The numbering scheme used to accomplish this and some of the subtle interpretation of the resultant fields needs to be understood.

The numbering scheme for the plates is rather straight forward. The first plate in the list is numbered one and each succeeding plate in the command list is incremented by one. If the user should remove a plate at the top of a previously used input set, the succeeding plates in the new run will be renumbered. Therefore, the user must remember to change the term processor list also. The edge numbering scheme is similar. The edge numbered one is between the first and second corner points defined. Each succeeding edge is up by one.

For the plate diffraction, however, it must be remembered that in order to avoid duplication of diffracted fields for jointed plate edges, it does the diffraction from the lowered numbered plate and does not do the diffracted field calculation for the higher numbered plate that has the same edge joined together. This is done automatically in the code. Trying to call the higher numbered plate representation of the same edge will result in no field calculation. The lower numbered edge must be used. See below for the interpretation of the fields in these instances.

The curved surface scheme is similar, except now the first call to a command such as **CG**, **CC**, or **CF** will be numbered one and each succeeding call to one of these different commands will increment the curved surface unit by one. The different sections of the curved surface within the command have their own numbering scheme similar to the edges. The rims, as

they are called, are obvious for the cylinder and cones. They are the junctions between the end caps and different cone frustum sections. The most positive one being numbered one and each succeeding one is increment by one as its position moves to more negative values. The ellipsoid rims are similar, except now a rim may also be the junction between the front and back z -axis radii of curvatures if there is a difference in curvature.

There is always one more surface than there is rims. A call to the field term associated with the reflection from the curved surface (RC) with an end cap in the front would start at a section number of "2". The call to the field term associated with the reflection for the end cap (RN) would start at a section of "1". No other end cap can be define except at the back of the sections so the next call to RN would be at the number of rims plus one, that is a the highest number for that particular curved surface command call. In all of the above cases, a 999 in the first column will terminate the list for that term.

As far as the resultant diffracted fields are concerned, the pattern for a single plate or curved surface will not necessarily be the some for that same plate attached to a more complex structure with the term processor set to provide the fields from only that plate or curved surface. The reason is that the wedge angle can be different for the isolated plate or curved surface than for the attached one. The diffraction coefficient will be different and include information about the other surface although the surface and edge number may be the same.

Chapter 6

Interpretation Of Output Data

The basic output from the computer code is a line printer listing of the results. The results are referenced to the pattern coordinate system that is described in Chapter 5 and is illustrated in Figure 4.4 and 4.8. The code has three basic options for computing a result, that is a far zone option (**PD**, **PF**, **VD**, or **VF**), near zone option (**PN** or **VN**), and an antenna to antenna coupling option (**PN** or **VN**, and **RG**, **RA**, **RM** or **RI**). Each of these options have a different format for their output. In each case a swept frequency option is available (**FM**). In addition, there are different normalization options (**PR**) that will be detailed for the individual cases below. If a moving source is specified using the **BP** command, than an additional line of information will be printed in all of the cases below. It contains information about the source position only, similar to the format for the observer position information.

6.1 Far Zone Case

The total far zone electric field is given by

$$\vec{E}(\theta_p, \phi_p) = \hat{\theta}_p E_{\theta_p} + \hat{\phi}_p E_{\phi_p}.$$

In the default case the fields are assumed to have the factor $\frac{e^{-jkR}}{R}$ suppressed. The fields therefore are assumed to be peak values given in volts/unit. The far zone range and phase factor can be included by specifying the **RD** command. The results will then be peak values given in

volts/meter. The magnetic field is not displayed in the far zone case but is easily determined by the formula

$$\vec{H}(\theta_p, \phi_p) = \frac{\hat{R}_p \times \vec{E}}{Z_0}$$

The results are displayed in two sections. The first section gives the electric field and radiation intensity (or gain) in terms of the theta and phi pattern coordinates. The second section gives the total radiation intensity (or gain) along with its major and minor components, axial ratio, tilt angle, and sense. The results are displayed as follows:

6.1.1 Far Zone Electric Field Theta And Phi Components

1. Angular position or frequency

- (a) theta angle in degrees, θ_p
- (b) phi angle in degrees, ϕ_p

*** or if FM specified ***

- (a) frequency in GHz

2. Theta components

- (a) magnitude of theta electric field in volts/unit or volts/meter, $|E_{\theta_p}|$
- (b) phase of theta electric field in degrees, $\angle E_{\theta_p}$
- (c) radiation intensity theta component in dB,

$$U_{\theta_p} = \frac{R^2 |E_{\theta_p}|^2}{2Z_0}$$

or the directive gain or power gain theta component in dB, if option 1 of the **PR** command is specified,

$$G_{\theta_p} = \frac{4\pi U_{\theta_p}}{P_t}$$

where P_t is the power radiated for the directive gain or the power input for the power gain.

3. Phi components

- (a) magnitude of theta electric field in volts/unit or volts/meter,
 $|E_{\phi_p}|$
- (b) phase of theta electric field in degrees, $\angle E_{\phi_p}$
- (c) radiation intensity theta component in dB,

$$U_{\phi_p} = \frac{R^2 |E_{\phi_p}|^2}{2Z_o}$$

or the directive gain or power gain theta component in dB, if the option 1 of the **PR** command is specified,

$$G_{\phi_p} = \frac{4\pi U_{\phi_p}}{P_t}$$

where P_t is the power radiated for the directive gain or the power input for the power gain.

6.1.2 Far Zone Total Field Components

1. Angular position or frequency

- (a) theta angle in degrees, θ_p
- (b) phi angle in degrees, ϕ_p

*** or if **FM** specified ***

- (a) frequency in GHz

2. Radiation intensity or gain components

- (a) major component in dB,

$$U_{major} = \frac{R^2 |E_{major}|^2}{2Z_o},$$

or G_{major} with **PR**, where

$$E_{major} = \left[\left(|E_{\theta_p}| \cos \tau + |E_{\phi_p}| \cos \psi \sin \tau \right)^2 + |E_{\phi_p}|^2 \sin^2 \psi \sin^2 \tau \right]^{1/2},$$

and

$$\psi = \angle E_{\phi_p} - \angle E_{\theta_p},$$

and

$$\tau = \frac{1}{2} \arctan \left[\frac{2|E_{\theta_p}||E_{\phi_p}|\cos\psi}{|E_{\theta_p}|^2 - |E_{\phi_p}|^2} \right]$$

(b) minor component in dB,

$$U_{minor} = \frac{R^2 |E_{minor}|^2}{2Z_o},$$

or G_{minor} with **PR**, where

$$E_{minor} = \left[\left(|E_{\theta_p}| \sin \tau - |E_{\phi_p}| \cos \phi \cos \tau \right)^2 + |E_{\phi_p}|^2 \sin^2 \psi \cos^2 \tau \right]^{1/2}$$

(c) total component in dB,

$$U = \frac{R^2 \vec{E} \cdot \vec{E}^*}{2Z_o},$$

or G with **PR**

3. Polarization information

(a) axial ratio of the polarization ellipse,

$$axial\ ratio = \left| \frac{E_{minor}}{E_{major}} \right|$$

(b) tilt angle, τ , as defined above

(c) polarization sense, either linear, right, left

6.2 Near Zone Case

The total near zone electric field is given by

$$\vec{E}(r_p, \theta_p, \phi_p) = \hat{r}_p E_{r_p} + \hat{\theta}_p E_{\theta_p} + \hat{\phi}_p E_{\phi_p}$$

if the spherical pattern cut option of the **PN** or **VN** command is chosen, or it is given by

$$\vec{E}(x_p, y_p, z_p) = \hat{x}_p E_{x_p} + \hat{y}_p E_{y_p} + \hat{z}_p E_{z_p}$$

if the linear pattern cut option of the **PN** or **VN** command is chosen. The fields are assumed to be peak values given in volts/meter. The total magnetic field can not be easily defined from the total electric field like in the far zone case so the magnetic fields are displayed explicitly and are given in amperes/meter. It can be noted that the individual UTD rays obey the far zone plane wave definition of the magnetic field as given in the far zone section above, in fact that is how the magnetic field is computed in the code; however, the sum of these individual rays in the near zone of the scattering structure do not as stated. The results are displayed in three sections. The first section gives the electric field, the second gives the magnetic fields and the third gives the power densities defined by the Poynting vector. The results are displayed as follows:

6.2.1 Near Zone Electric Field Components

1. Spherical position, linear position, or frequency

*** if spherical option in **PN** is specified ***

- (a) radial position in meters, r_p
- (b) theta angle in degrees, θ_p
- (c) phi angle in degrees, ϕ_p

*** if linear option in **PN** is specified ***

- (a) x_p -axis position in meters, x_p
- (b) y_p -axis position in meters, y_p
- (c) z_p -axis position in meters, z_p

*** or if **FM** is specified ***

- (a) frequency in GHz

2. r or x components

- (a) magnitude of the r or x oriented electric field in volts/meter,
 $|E_{r_p}|$ or $|E_{x_p}|$
- (b) phase of the r or x oriented electric field in degrees $\angle E_{r_p}$ or $\angle E_{x_p}$
- (c) magnitude of the r or x oriented electric field represented in dB,
that is, $20 \log |E_{r_p}|$ or $20 \log |E_{x_p}|$

3. θ or y components

- (a) magnitude of the θ or y oriented electric field in volts/meter,
 $|E_{\theta_p}|$ or $|E_{y_p}|$
- (b) phase of the θ or y oriented electric field in degrees $\angle E_{\theta_p}$ or $\angle E_{y_p}$
- (c) magnitude of the θ or y oriented electric field represented in dB,
that is, $20 \log |E_{\theta_p}|$ or $20 \log |E_{y_p}|$

4. ϕ or z components

- (a) magnitude of the ϕ or z oriented electric field in volts/meter,
 $|E_{\phi_p}|$ or $|E_{z_p}|$
- (b) phase of the ϕ or z oriented electric field in degrees $\angle E_{\phi_p}$ or
 $\angle E_{z_p}$
- (c) magnitude of the ϕ or z oriented electric field represented in dB,
that is, $20 \log |E_{\phi_p}|$ or $20 \log |E_{z_p}|$

6.2.2 Near Zone Magnetic Field Components

1. Spherical position, linear position, or frequency

*** if spherical option in PN is specified ***

- (a) radial position in meters, r_p
- (b) theta angle in degrees, θ_p
- (c) phi angle in degrees, ϕ_p

*** if linear option in **PN** is specified ***

- (a) x_p -axis position in meters, x_p
- (b) y_p -axis position in meters, y_p
- (c) z_p -axis position in meters, z_p

*** or if **FM** is specified ***

- (a) frequency in GHz

2. r or x components

- (a) magnitude of the r or x oriented magnetic field in amperes/meter, $|H_{r_p}|$ or $|H_{x_p}|$
- (b) phase of the r or x oriented magnetic field in degrees $\angle H_{r_p}$ or $\angle H_{x_p}$
- (c) magnitude of the r or x oriented magnetic field represented in dB, that is, $20 \log |H_{r_p}|$ or $20 \log |H_{x_p}|$

3. θ or y components

- (a) magnitude of the θ or y oriented magnetic field in amperes/meter, $|H_{\theta_p}|$ or $|H_{y_p}|$
- (b) phase of the θ or y oriented magnetic field in degrees $\angle H_{\theta_p}$ or $\angle H_{y_p}$
- (c) magnitude of the θ or y oriented magnetic field represented in dB, that is, $20 \log |H_{\theta_p}|$ or $20 \log |H_{y_p}|$

4. ϕ or z components

- (a) magnitude of the ϕ or z oriented magnetic field in amperes/meter, $|H_{\phi_p}|$ or $|H_{z_p}|$
- (b) phase of the ϕ or z oriented magnetic field in degrees $\angle H_{\phi_p}$ or $\angle H_{z_p}$
- (c) magnitude of the ϕ or z oriented magnetic field represented in dB, that is, $20 \log |H_{\phi_p}|$ or $20 \log |H_{z_p}|$

6.2.3 Near Zone Power Density Components

1. Spherical position, linear position, or frequency

*** if spherical option in **PN** is specified ***

- (a) radial position in meters, r_p
- (b) theta angle in degrees, θ_p
- (c) phi angle in degrees, ϕ_p

*** if linear option in **PN** is specified ***

- (a) x_p -axis position in meters, x_p
- (b) y_p -axis position in meters, y_p
- (c) z_p -axis position in meters, z_p

*** or if **FM** is specified ***

- (a) frequency in GHz

2. Average power flow per square meter,

$$\vec{P}_r = \text{Re}(\frac{1}{2} \vec{E} \times \vec{H}^*)$$

- (a) radial or x oriented power flow per square meter in dB
- (b) theta or y oriented power flow per square meter in dB
- (c) phi or z oriented power flow per square meter in dB

3. Average reactive power per square meter,

$$\vec{P}_i = \text{Im}(\frac{1}{2} \vec{E} \times \vec{H}^*)$$

- (a) radial or x oriented reactive power per square meter in dB
- (b) theta or y oriented reactive power per square meter in dB
- (c) phi or z oriented reactive power per square meter in dB

6.3 Coupling Case

The coupling in this code is calculated based on the reaction principle. The reaction between two antennas can be thought of in this case as the terminal current of the transmitter times the open circuit voltage produced at the receiver. The reaction coupling power is then given by

$$C_t = I_m V_{oc}.$$

This quantity can be normalized in a manner that presents the data in a more useful form for the antenna designer by using the **PR** command. The **PR** command has four options. The first option is for the far zone case and is not useful here. The second option displays the coupling in terms of the mutual coupling impedance, the third option displays the coupling in terms of the modified Frii's transmission equation, and the fourth option displays the results in terms of the Linville method. The results are displayed in one section as follows:

6.3.1 Near Zone Coupling

1. Spherical position, linear position, or frequency

*** if spherical option in **PN** is specified ***

- (a) radial position in meters, r_p
- (b) theta angle in degrees, θ_p
- (c) phi angle in degrees, ϕ_p

*** if linear option in **PN** is specified ***

- (a) x_p -axis position in meters, x_p
- (b) y_p -axis position in meters, y_p
- (c) z_p -axis position in meters, z_p

*** or if **FM** is specified ***

- (a) frequency in GHz

2. Reaction information

- (a) magnitude of the average reaction coupling power, $\frac{1}{2}|C_t|$
- (b) phase of the reaction coupling power, $\angle C_t$

3. Coupling information

*** unnormalized coupling with no **PR** or option 1 ***

- (a) magnitude of the coupling power squared, $(\frac{1}{2}|C_t|)^2$
- (b) magnitude of the coupling power squared in dB

*** mutual coupling impedance with **PR** option 2 ***

- (a) magnitude of the mutual impedance in ohms,

$$Z_{12} = \left| \frac{I_m V_{oc}}{I_{11} I_{22}} \right|$$

where values I_{11} and I_{22} are the transmitter and receiver terminal currents.

- (b) phase of the mutual impedance in degrees, $\angle Z_{12}$

*** modified Frii's coupling with **PR** option 3 ***

- (a) coupling gain into a conjugate matched load,

$$\frac{P_o}{P_i} = \frac{|\frac{1}{2}I_m V_{oc}|^2}{P_{rt} P_{rr}} \left[\frac{R_r R_l}{|Z_r + Z_l|^2} \right]$$

where P_{rt} is the power radiated by the transmitter and P_{rr} is the power radiated by the receiver as if it were acting as a transmitter. The radiation impedance and the load impedances are assumed to be conjugately matched so that the quantity in the large bracket above goes to a factor of one fourth.

- (b) coupling gain into a matched load in dB

*** Linville coupling with **PR** option 4 ***

(a) maximum coupling gain, G_{max}

where the code first finds the mutual impedance between the antennas as given above and uses it to find the maximum coupling gain where

$$L = \frac{|Z_{12}^2|}{2\text{Re}(Z_{11})\text{Re}(Z_{22}) - \text{Re}(Z_{12}^2)}$$

so

$$G_{max} = \frac{1 - \sqrt{1 - L^2}}{L}.$$

The terminal current is I_{11} and I_{22} and terminal impedance is Z_{11} and Z_{22} .

(b) maximum coupling gain in dB

A very convenient means of displaying the results of the code is through a rectangular or polar plot representation. This is discussed in more detail in Appendix D.

The next chapter displays the results in either polar or rectangular dB plots to compare against measured results whenever possible.

Chapter 7

Applications

The following examples are used to illustrate the various features of the computer code. Each example is designed to show how a set of commands can be put together to solve a single problem or a group of problems. In most cases, the input data sets can be constructed in more than one way to accomplish the same results. The particular form of these examples have been chosen so that all the commands are used. As an aid to the user, an echo of the input data is given on the line printer, terminal, or in a file for later reference, in the form that the computer code has interpreted the data. This is useful for checking that the correct problem has been properly constructed. Also, messages are given when the code misinterprets the data or when an error has been made in the input set. This makes it easier to debug the input data sets. Example 1A illustrates this type of print out. The other examples do not show this output in order to save space in this report.

The computer code has a default list at the beginning of the main program. This list can be set up at the convenience of the user. If the defaults are set up correctly for the particular applications of the user, the same data will not have to be input in the data sets every time. For example, the default list is set up initially to have the code give a line printer output of the results. Since most user's will want this output all the time the **LP** command need never be specified as shown in the examples that follow. However, the **LP** command can be used to suppress this output if desired. The pen plotter command, **PP**, on the other hand, has been set false initially. This is because most computer facilities have different

procedures for plotter output. Once the user determines the best way to use this command for his needs and the appropriate plot routines are included in the code, the **PP** command can be called to instate the plots or the default list can be changed accordingly.

In the examples that follow, all the results have been shown graphically in some form. The plots are usually normalized, but for some of the figures the maximum value of the absolute fields are given (for comparison purposes). This is the most concise way to show the results and to illustrate the validity of the codes operation by comparing against measurements. A few of the examples, however, contain the line printer output of the results so that the output numbers can be checked to verify that the computer being used is giving correct results. Different computers have different accuracies so that the numbers may not check in the last few decimal places. In particular, the cross polarized fields of some problems may be many orders of magnitude less than the co-polarized fields. These results may not check even in the first few digits if at all; however, this just indicates the difference in the accuracies between the two computers especially when the numbers are in the noise level and does not indicate that the code is operating incorrectly on your machine. These examples have been run on a DEC - VAX 8550, VAX 11/780, and/or VAX 11/750 digital computer. The CPU times are given for the specified computer for some of the examples.

Ex. 1A

181

7.1 Example 1A: Plate - Dipole

This example illustrates how to set up a data set to calculate the far zone pattern of an electric dipole in the presence of a finite perfectly conducting ground plane as shown in Figure 7.1. The input data for the *H*-plane pattern is given by

```
CE:  FAR ZONE PLATE TEST, EXAMPLE 1A.
UN:  UNITS IN INCHES
3
US:  SOURCE UNITS IN WAVELENGTHS
0
FR:  FREQUENCY IN GHZ
8.0
PF:  PATTERN CUT
0.,0.,90.,0.
T,90.
0.,1.,361
PG:  PLATE GEOMETRY
4,0
0.,3.5,3.5
0.,-3.5,3.5
0.,-3.5,-3.5
0.,3.5,-3.5
SG:  SOURCE GEOMETRY
5.12,0.,0.
0.,0.,90.,0.
-2,0.5,0.
1.,0.
PP:  PLOTTABLE OUTPUT
T
T,5.33,2.66
0.,360.,36.
-40.,0.,10.
XQ:  EXECUTE CODE
EN:  END CODE
```

The computer code prints out on the line printer, terminal, or disk file for later printing the information in Figure 7.2 pertaining to the input

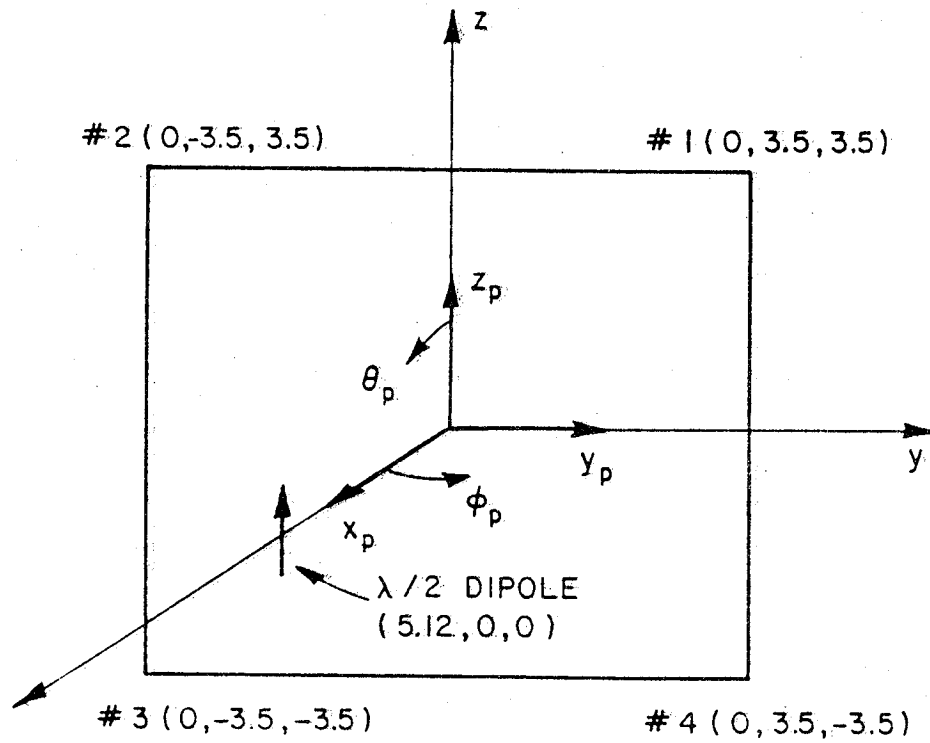


Figure 7.1: Dipole in presence of a square ground plane.

data. This information can help the user decipher how the computer code interpreted the input data. It also provides messages to the user if the input data is found to be incorrect by the code.

The E_{θ_p} pattern is compared with the measured results in Figure 7.6. The E_{ϕ_p} pattern is not plotted because it is of negligible value.

Ex. 1A

```
*****
*
* NEC-BSC      3.1-9, 20-MAY-88
*
* THE OHIO STATE UNIVERSITY
* ELECTROSCIENCE LABORATORY
* 1320 KINNREAR RD.
* COLUMBUS, OHIO 43212
*
* WRITTEN BY RONALD J. MARHEFKA
*
*****
```

```
*****
*
* CE:  FAR ZONE PLATE TEST, EXAMPLE 1A.
*
*
*****
```

```
*****
*
* UN:  UNITS IN INCHES
*
*
* ALL THE LINEAR DIMENSIONS BELOW ARE ASSUMED TO BE IN INCHES
*
*****
```

```
*****
*
* US:  SOURCE UNITS IN WAVELENGTHS
*
*
* SOURCE LENGTH HS AND WIDTH HAWS ARE ASSUMED TO BE IN WAVELENGTHS
*
*****
```

Figure 7.2: Line printer output for the code's interpretation of the input data set of Example 1A. The figure is continued on the following pages.

ORIGINAL PAGE IS
OF POOR QUALITY

184

Ex. 1A

```
*****
*
* FR:  FREQUENCY IN GHZ
*
*
* FREQUENCY=  8.000 GIGAHERTZ
*
* WAVELENGTH=  0.037474 METERS
*
*****
```

```
*****
*
* PF:  PATTERN CUT
*
*
* PATTERN AXES ARE AS FOLLOWS:
*
* VPC(1,1)=  1.00000 VPC(1,2)=  0.00000 VPC(1,3)=  0.00000
*
* VPC(2,1)=  0.00000 VPC(2,2)=  1.00000 VPC(2,3)=  0.00000
*
* VPC(3,1)=  0.00000 VPC(3,2)=  0.00000 VPC(3,3)=  1.00000
*
* PHI IS BEING VARIED WITH THETA=  90.00000
*
* START=  0.00000 STEP=  1.00000 NUMBER=  361
*
*****
```

```
*****
*
* PG:  PLATE GEOMETRY
*
*
* THIS IS PLATE NO.  1 IN THIS SIMULATION.
*
*
* METAL PLATE USED IN THIS SIMULATION
*
* PLATE#  CORNER#  INPUT LOCATION IN INCHES  ACTUAL LOCATION IN METERS
* -----
*
* 1      1      0.000,  3.500,  3.500  0.000,  0.089,  0.089
*
* 1      2      0.000, -3.500,  3.500  0.000, -0.089,  0.089
*
* 1      3      0.000, -3.500, -3.500  0.000, -0.089, -0.089
*
* 1      4      0.000,  3.500, -3.500  0.000,  0.089, -0.089
*
*****
```

Figure 7.3: Figure 7.2 continued.


```

*****
*
* SG: SOURCE GEOMETRY
*
* THIS IS SOURCE NO. 1 IN THIS COMPUTATION.
*
* THIS IS AN ELECTRIC SOURCE OF TYPE -2
*
* SOURCE LENGTH= 0.50000 AND WIDTH= 0.00000 WAVELENGTHS
*
* SOURCE LENGTH= 0.01874 AND WIDTH= 0.00000 METERS
*
* THE SOURCE WEIGHT HAS MAGNITUDE= 1.00000 AND PHASE= 0.00000
*
*
* SOURCE# INPUT LOCATION IN INCHES ACTUAL LOCATION IN METERS
* -----
* 1 5.120, 0.000, 0.000 0.130, 0.000, 0.000
*
*
* THE FOLLOWING SOURCE ALIGNMENT IS USED:
*
* VISS(1,1, 1)= 1.00000 VISS(1,2, 1)= 0.00000 VISS(1,3, 1)= 0.00000
*
* VISS(2,1, 1)= 0.00000 VISS(2,2, 1)= 1.00000 VISS(2,3, 1)= 0.00000
*
* VISS(3,1, 1)= 0.00000 VISS(3,2, 1)= 0.00000 VISS(3,3, 1)= 1.00000
*
*****

```

Figure 7.4: Figure 7.2 continued.

```

*****
*
* PP:  PLOTTABLE OUTPUT
*
*
* DATA WILL BE OUTPUT FOR A PLOT !!!
*
* LPPREC=  T      PPXL=  5.33000      PPYL=  2.66000
* PPXB=  0.00000      PPXE= 360.00000      PPIS= 36.00000
* PPYB= -40.00000      PPYE=  0.00000      PPYS= 10.00000
*
*****

*****
*
* XQ:  EXECUTE CODE
*
*
* INCFLD  =  0.00533 CPU MINUTES
* RP      =  0.00400 CPU MINUTES
* RPRP    =  0.00233 CPU MINUTES
* DP      =  0.08817 CPU MINUTES
* RPDP    =  0.00250 CPU MINUTES
* DPRP    =  0.00283 CPU MINUTES
* END
*
* CPU TIME FOR FIELD EXECUTION =  0.10633 MINUTES
*
*****

*****
*
* EN:  END CODE
*
*
*****

```

Figure 7.5: Figure 7.2 continued.

Ex. 1A

187

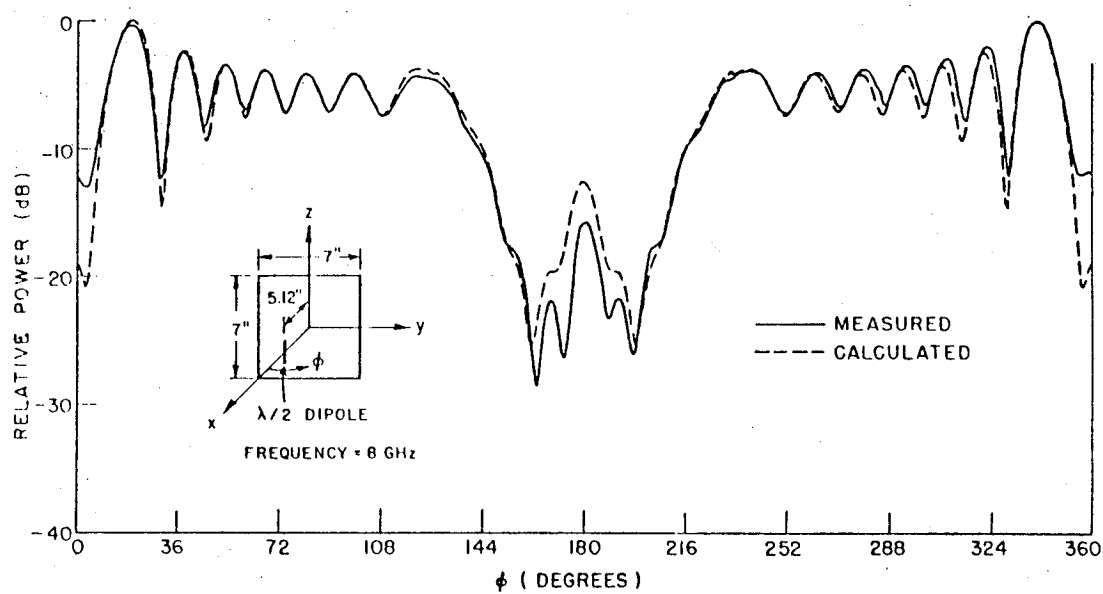


Figure 7.6: Comparison of measured and calculated H -plane pattern (E_{θ_p}) for a half-wave dipole located above a square plate. (VAX 8550 run time is 0.106 min and VAX 11/750 run time is 1.2 min.)

7.2 Example 1B: Plate - Dipole

This example considers the far zone E -plane pattern of the electric dipole in the presence of the finite perfectly conducting ground plane as shown in Figure 7.1. This problem is the same as Example 1A except that the pattern cut information is changed so that the ϕ angle is fixed and the θ angle is varied. The input data is given by

```
CE:  FAR ZONE PLATE TEST, EXAMPLE 1B.
UN:  UNITS IN INCHES
3
US:  SOURCE UNITS IN WAVELENGTHS
0
FR:  FREQUENCY IN GHZ
8.0
PF:  PATTERN CUT
0.,0.,90.,0.
F,0.
0.,1.,361
PG:  PLATE GEOMETRY
4,0
0.,3.5,3.5
0.,-3.5,3.5
0.,-3.5,-3.5
0.,3.5,-3.5
SG:  SOURCE GEOMETRY
5.12,0.,0.
0.,0.,90.,0.
-2,0.5,0.
1.,0.
PP:
T
T,5.33,2.66
0.,360.,36.
-40.,0.,10.
XQ:  EXECUTE CODE
EN:  END CODE
```

The E_{θ_p} pattern is compared with the measured results in Figure 7.7. The E_{ϕ_p} pattern is not plotted because it is of negligible value.

Ex. 1B

189

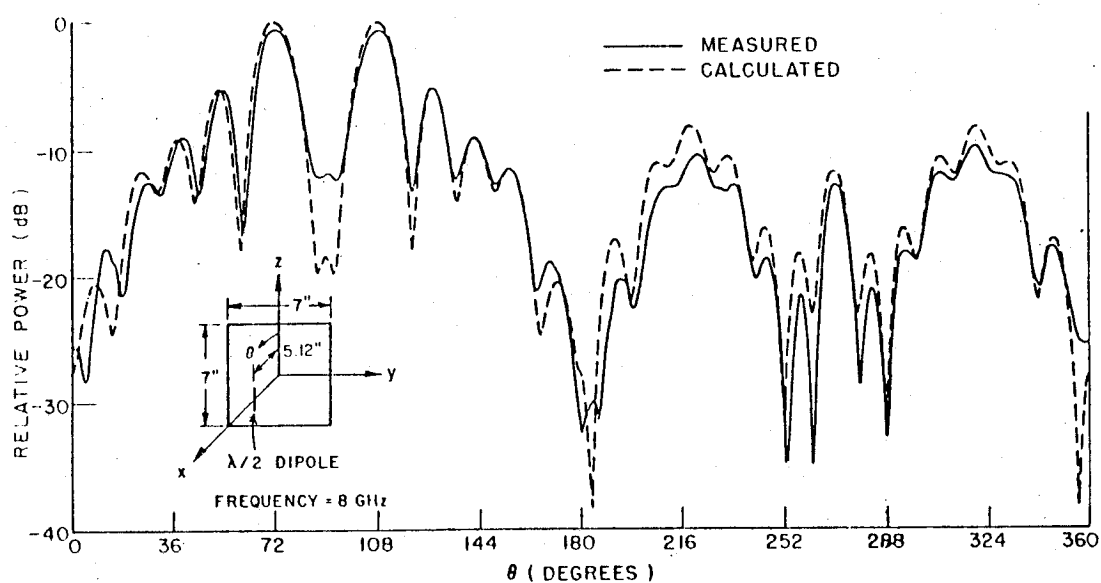


Figure 7.7: Comparison of measured and calculated E -plane pattern (E_{θ_p}) for a half-wave dipole located above a square plate. (VAX 11/750 run time is 1.15 min.)

7.3 Example 1C: Plate - Dipole

This example considers the far zone pattern of the electric dipole taken across the corner of the finite perfectly conducting ground plane in Figure 7.8. This problem is the same as in Example 1A except that the pattern cut coordinate system is changed. The input data is given by

```
CE:  FAR ZONE PLATE TEST, EXAMPLE 1C.
UN:  UNITS IN INCHES
3
US:  SOURCE UNITS IN WAVELENGTHS
0
FR:  FREQUENCY IN GHZ
8.0
PF:  PATTERN CUT
45.,90.,90.,0.
T,90.
0.,1.,361
PG:  PLATE GEOMETRY
4,0
0.,3.5,3.5
0.,-3.5,3.5
0.,-3.5,-3.5
0.,3.5,-3.5
SG:  SOURCE GEOMETRY
5.12,0.,0.
0.,0.,90.,0.
-2,0.5,0.
1.,0.
LP:  LINE PRINTER OUTPUT
T
PP:  PLOTTABLE OUTPUT
T
T,5.33,2.66
0.,360.,36.
-40.,0.,10.
XQ:  EXECUTE CODE
EN:  END CODE
```

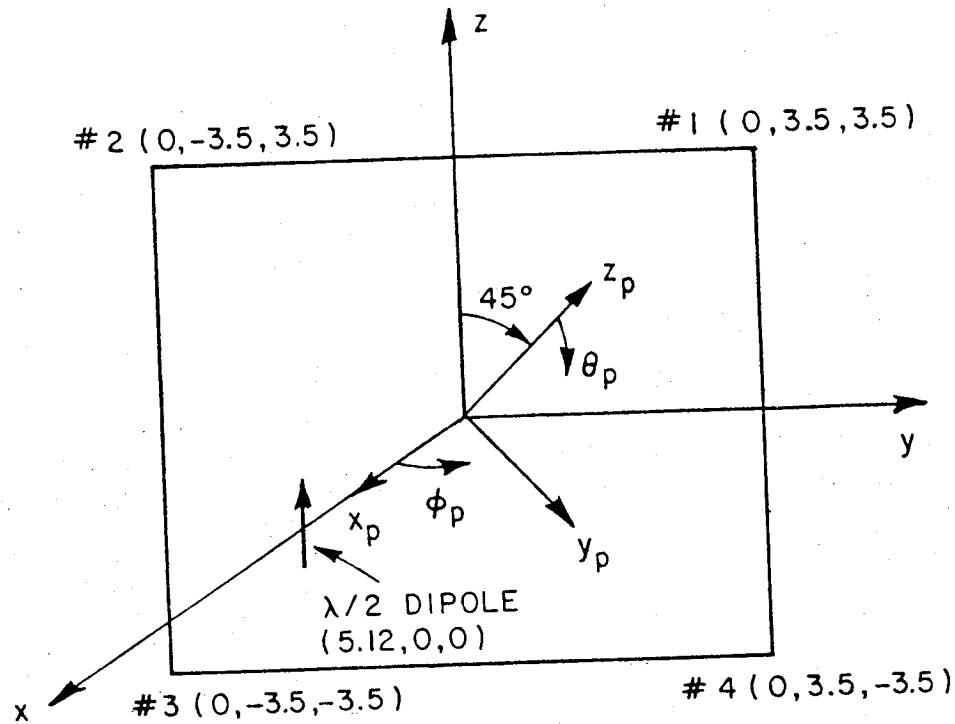


Figure 7.8: Dipole in presence of a square ground plane with a pattern cut corresponding to Example 1C.

The E_{θ_p} pattern is compared with its measured result in Figure 7.9, and the E_{ϕ_p} pattern is compared with its measured result in Figure 7.10.

If the **LP** command is used, the calculated results for the electric field are printed out on the line printer or terminal as shown in Figures 7.11 and 7.12. The output shown in Figures 7.11 and 7.12 is for 10 degree increments from 0 to 180 degrees. This is to save space in this document.

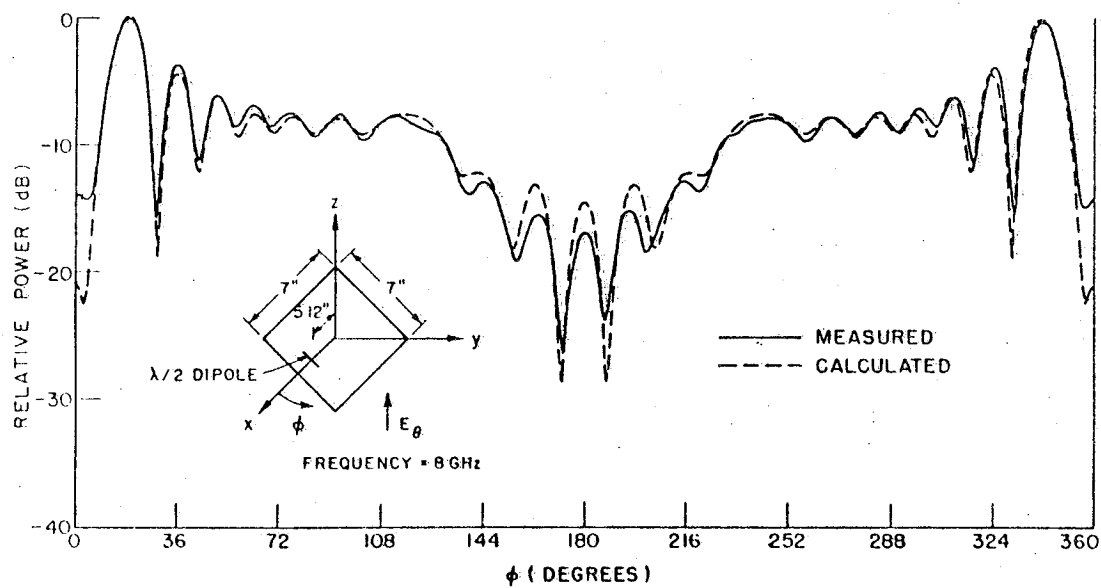


Figure 7.9: Comparison of measured and calculated E_{θ} pattern taken over the corner of a square plate with a half-wave dipole mounted above it. (VAX 11/750 run time is 1.7 min.)

Ex. 1C

193

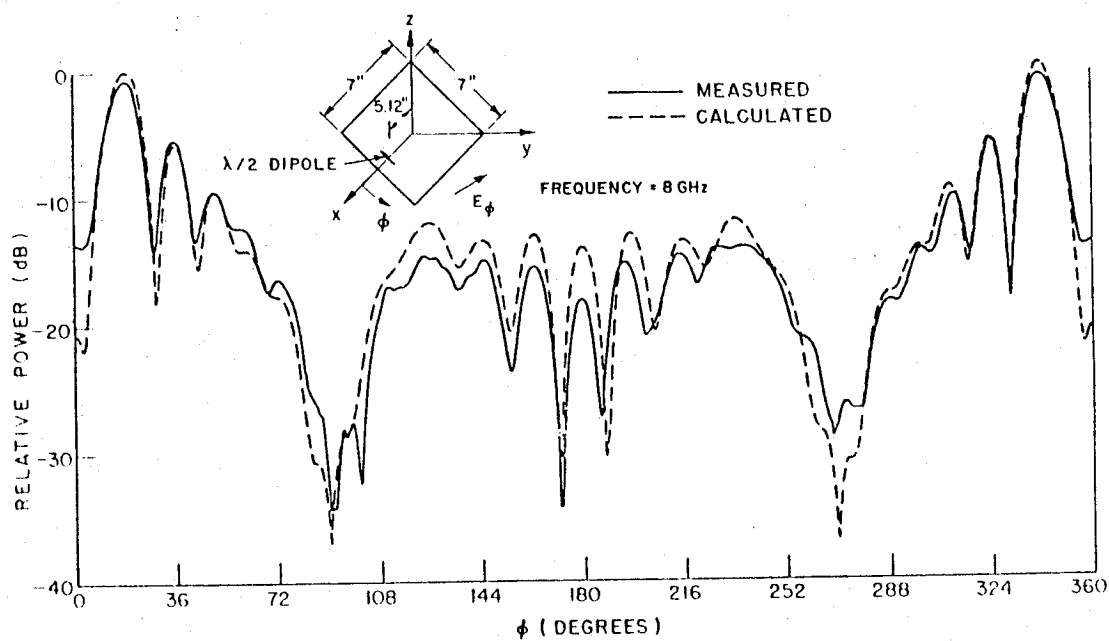


Figure 7.10: Comparison of measured and calculated E_{ϕ} pattern taken over the corner of a square plate with a half-wave dipole mounted above it.

ORIGINAL PAGE IS
OF POOR QUALITY

194

Ex. 1C

THE FAR ZONE ELECTRIC FIELD

THE FIELDS ARE REFERENCED TO THE PATTERN COORDINATE SYSTEM

THETA	PHI	H-THETA			H-PHI		
		MAGNITUDE	PHASE	DB	MAGNITUDE	PHASE	DB
90.00	0.00	8.8940E+00	-84.45	-9.79	8.8940E+00	-84.45	-9.79
90.00	10.00	4.7239E+01	174.14	4.73	4.6800E+01	175.80	4.63
90.00	20.00	9.7978E+01	-171.28	13.05	9.2693E+01	-171.70	10.57
90.00	30.00	1.6908E+01	61.19	-4.21	1.4054E+01	68.78	-5.82
90.00	40.00	4.5705E+01	-10.26	4.43	3.4954E+01	-8.62	2.10
90.00	50.00	4.6741E+01	167.18	4.98	3.2245E+01	164.18	1.40
90.00	60.00	3.7481E+01	-11.56	2.70	1.8403E+01	-8.88	-3.48
90.00	70.00	3.4858E+01	157.66	2.07	1.2208E+01	152.74	-7.04
90.00	80.00	3.8895E+01	-48.68	3.02	6.0098E+00	-38.92	-15.20
90.00	90.00	3.9183E+01	86.42	3.09	1.3009E+00	-97.21	-26.49
90.00	100.00	3.5275E+01	-124.09	2.18	4.9598E+00	49.57	-14.86
90.00	110.00	4.0487E+01	19.10	3.37	1.4391E+01	-157.13	-5.61
90.00	120.00	4.1283E+01	-169.52	3.54	2.0671E+01	7.90	-2.47
90.00	130.00	3.2899E+01	19.19	1.57	2.1388E+01	-155.73	-2.17
90.00	140.00	2.4249E+01	-160.39	-1.08	1.8163E+01	16.76	-3.59
90.00	150.00	1.8421E+01	53.53	-3.47	1.5101E+01	-119.83	-5.19
90.00	160.00	1.9975E+01	-131.93	-2.76	1.8839E+01	45.26	-3.27
90.00	170.00	7.0623E+00	136.90	-11.79	6.4577E+00	-32.04	-12.57
90.00	180.00	1.8794E+01	-28.10	-3.29	1.8794E+01	151.90	-3.29

Figure 7.11: Line printer output of the electric fields of Example 1C.

Ex. 1C

195

.....

.....

TOTAL RADIATION INTENSITY IN DB

THE FIELDS ARE REFERENCED TO THE PATTERN COORDINATE SYSTEM

TNETA	PKI	MAJOR	MINOR	TOTAL	AXIAL RATIO	TYLT ANG	SENSE
90.00	0.00	-6.78	-100.00	-6.78	0.00000	45.00	LINEAR
90.00	10.00	7.68	-29.07	7.68	0.01453	44.73	LEFT
90.00	20.00	13.83	-34.83	13.83	0.00369	43.41	RIGHT
90.00	30.00	-1.95	-25.66	-1.93	0.06523	39.69	LEFT
90.00	40.00	6.42	-30.78	6.43	0.01379	37.41	LEFT
90.00	50.00	6.56	-25.80	6.56	0.02412	33.47	RIGHT
90.00	60.00	3.64	-31.02	3.64	0.01849	26.14	LEFT
90.00	70.00	2.57	-28.87	2.57	0.02678	19.25	RIGHT
90.00	80.00	3.12	-28.71	3.13	0.02562	8.66	LEFT
90.00	90.00	3.09	-50.45	3.09	0.00210	-1.90	LEFT
90.00	100.00	2.26	-34.09	2.26	0.01523	-7.96	LEFT
90.00	110.00	3.89	-29.79	3.89	0.02071	-19.64	RIGHT
90.00	120.00	4.51	-30.36	4.51	0.01804	-26.68	LEFT
90.00	130.00	3.09	-24.75	3.10	0.04053	-32.99	RIGHT
90.00	140.00	0.85	-31.60	0.85	0.02384	-36.82	LEFT
90.00	150.00	-1.25	-26.15	-1.23	0.05685	-39.31	RIGHT
90.00	160.00	0.00	-32.22	0.00	0.02450	-43.32	LEFT
90.00	170.00	-9.20	-29.51	-9.16	0.09644	-42.39	RIGHT
90.00	180.00	-0.28	-100.00	-0.28	0.00000	-45.00	LINEAR

.....

.....

Figure 7.12: Line printer output of the total radiation intensity of Example 1C.

7.4 Example 2: Plate - Slot

Consider the pattern of a half - wavelength cavity backed slot antenna mounted in the center of a square perfectly conducting ground plane as shown in Figure 7.13. The pattern cut is taken across the corners of the plate. This example illustrates how the **TP** command can be used to show the strength of a particular diffraction mechanism by removing the mechanism from the computation for comparison. In this case the corner diffracted fields are removed in the second execution by setting **LCORNR=FALSE**. Of course, other fields can be modified in other problems by using the appropriate logical variables in the **TP** command. The input data for this example is given by

```
CE:  FAR ZONE PLATE TEST, EXAMPLE 2.
UN:
3
US:
0
FR:
10.
PF:  PATTERN CUT OVER CORNER
0.,0.,90.,0.
F,45.
0.,1.,361
PG:
4,0
6.,6.,0.
-6.,6.,0.
-6.,-6.,0.
6.,-6.,0.
SG:
0.,0.,0.
90.,90.,90.,0.
3,0.5,0.
1.,0.
PP:
T
F,90.,2.55
0.,360.,30.
```

-40.,0.,10.

XQ: EXECUTE CODE

TP: REMOVE CORNER DIFFRACTION

T,F

XQ: EXECUTE CODE

EN:

The results with and without the corner diffracted fields included are compared in Figures 7.14 and 7.15 for the E_{θ_p} and E_{ϕ_p} fields, respectively.

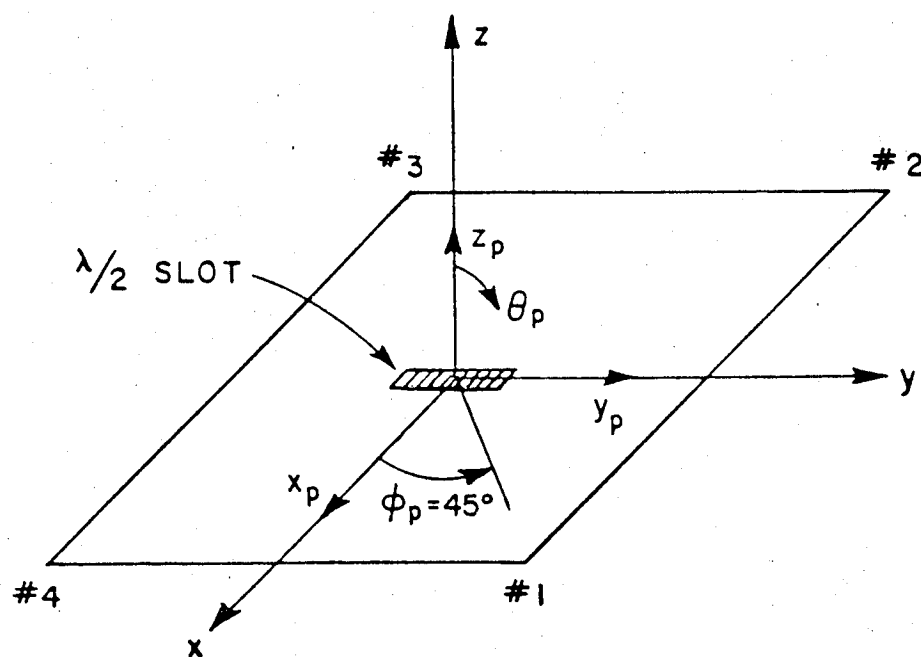


Figure 7.13: A half-wavelength cavity backed slot mounted on top of a perfectly conducting square ground plane.

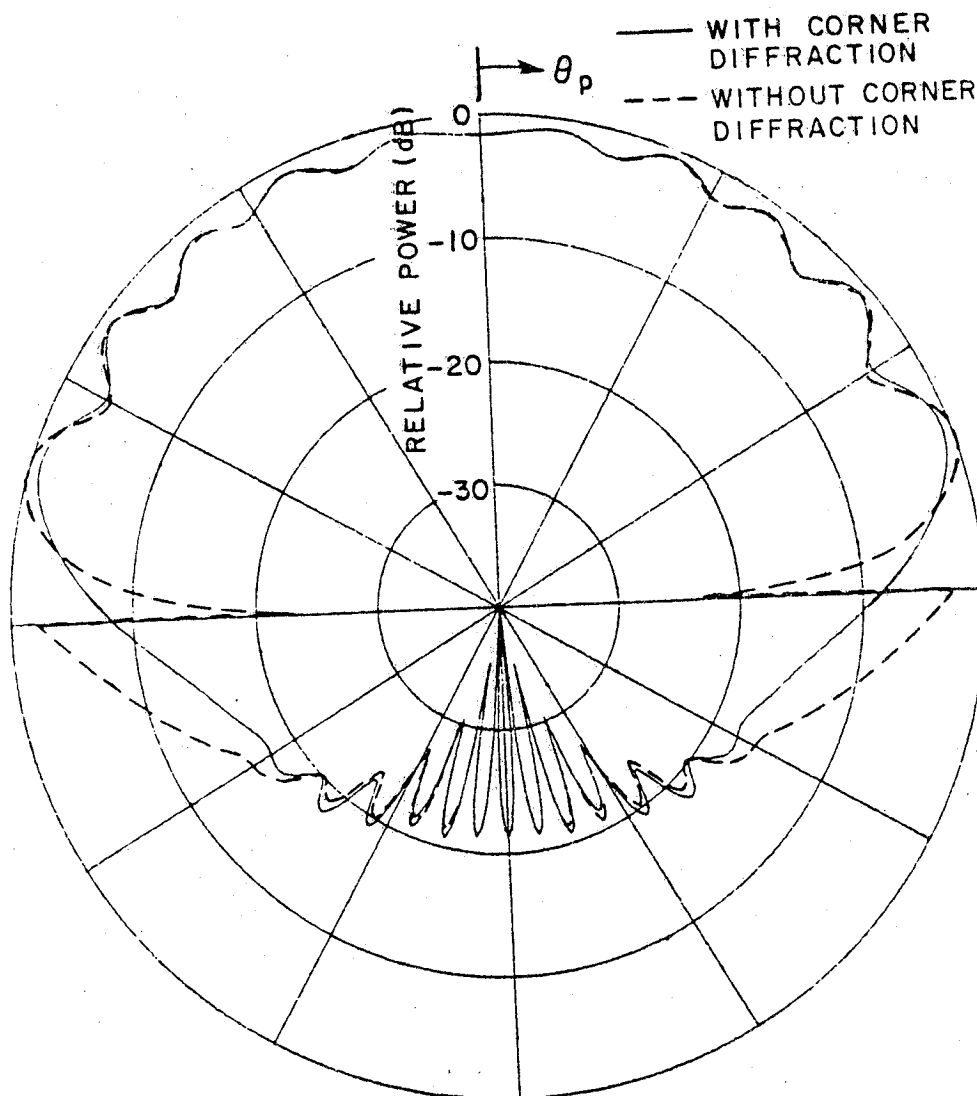


Figure 7.14: Comparison of E_{θ_p} pattern with and without corner diffracted fields for a half-wave slot antenna mounted on a square plate. (VAX 11/750 run time for case with corner diffracted fields is 1.3 min and the peak value of the E_{θ} is -11.45 dB.)

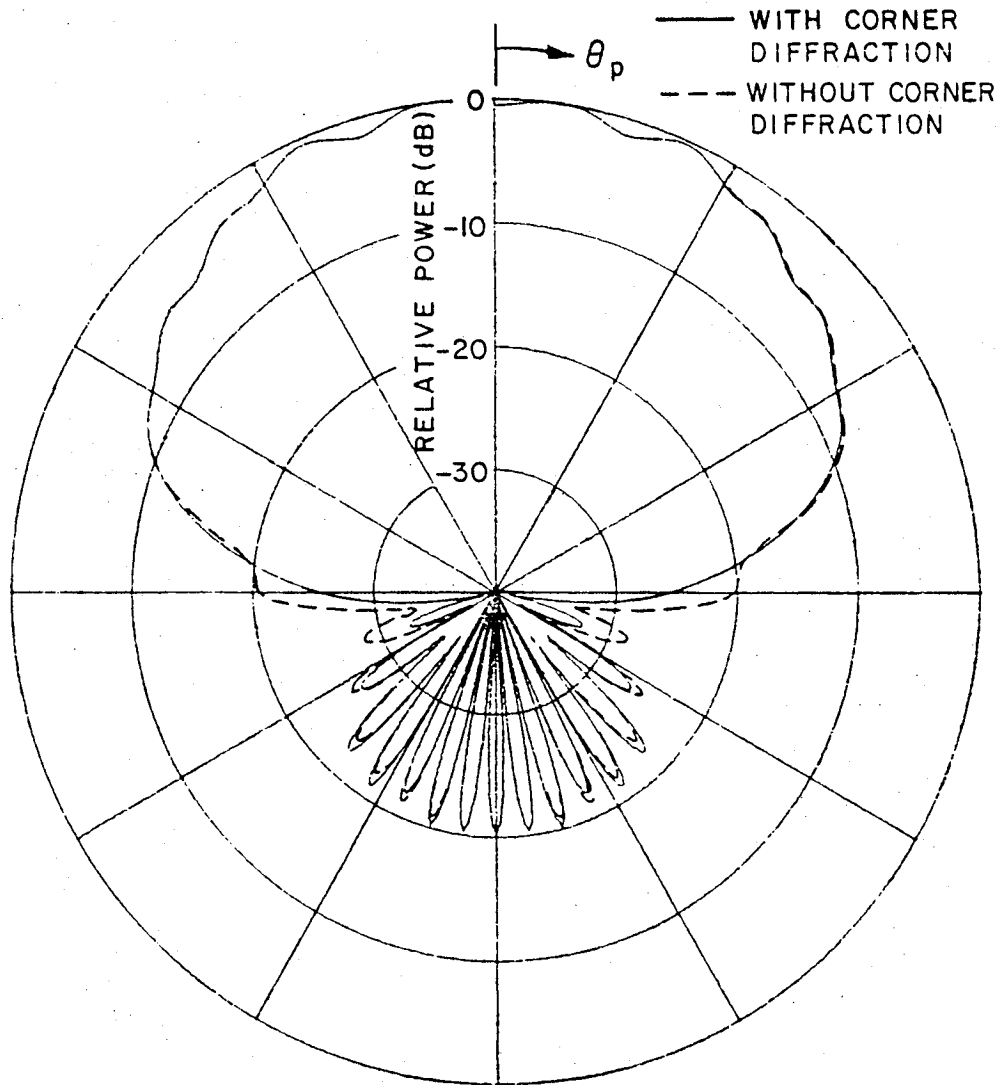


Figure 7.15: Comparison of E_{ϕ_p} pattern with and without corner diffracted fields for a half-wave slot antenna mounted on a square plate.

7.5 Example 3: Near Zone Plate

This example illustrates the near zone pattern effects of a dipole in the presence of a perfectly conducting square plate. The pattern of the antenna is checked first and then two different pattern origins and two different pattern ranges are shown. The geometries are illustrated in the inserts of Figures 7.16 to 7.19. The input data is given by

```
CM:  EXAMPLE 3.
CE:  NEAR ZONE PLATE TEST
UN:
3
US:
3
FR:
3.985
SG:
5.625,0.,0.
90.,90.,0.,0.
-2,1.5,0.
1.,0.
PN:
5.625,0.,0.
0.,0.,90.,0.
F
37.,90.,0.
0.,0.,1.
361
LP:
T
PP:
T
T,4.2,2.1
0.,360.,36.
-40.,0.,10.
XQ:  EXECUTE CODE
LP:
F
PG:
```


Ex. 3

```
4,0
0.,5.,5.
0.,-5.,5.
0.,-5.,-5.
0.,5.,-5.
XQ:  EXECUTE CODE
PN:
0.,0.,0.
0.,0.,90.,0.
F
37.,90.,0.
0.,0.,1.
361
XQ:  EXECUTE CODE
PN:
0.,0.,0.
0.,0.,90.,0.
F
26.125,90.,0.
0.,0.,1.
361
XQ:  EXECUTE CODE
EN:
```

The E_{ϕ_p} near zone pattern of the source antenna is compared with measured results in Figure 7.16. The E_{ϕ_p} pattern for a source in the presence of the plate with the center of pattern rotation at the source and with a range of 37 inches is shown in Figure 7.17. The E_{ϕ_p} near zone pattern with the center of pattern rotation at the center of the plate and at a range of 37 inches is shown in Figure 7.18. The E_{ϕ_p} near zone pattern with the center of pattern rotation at the center of the plate and at a range of 26.125 inches is shown in Figure 7.19. Note that changing the pattern origin and range results in relatively small shifts in the position of the peaks and the fine detail. Also note that the radial and theta components of the field are present but they are not shown since they are much smaller than the phi component. The magnitude of these cross polarized terms for the pattern corresponding to Figure 7.17 can be seen in the print out of the fields in Figures 7.20, 7.21, and 7.22. The print out is for a range of phi angles of 0 to 180 degrees in steps of 10 degrees in order to save space.

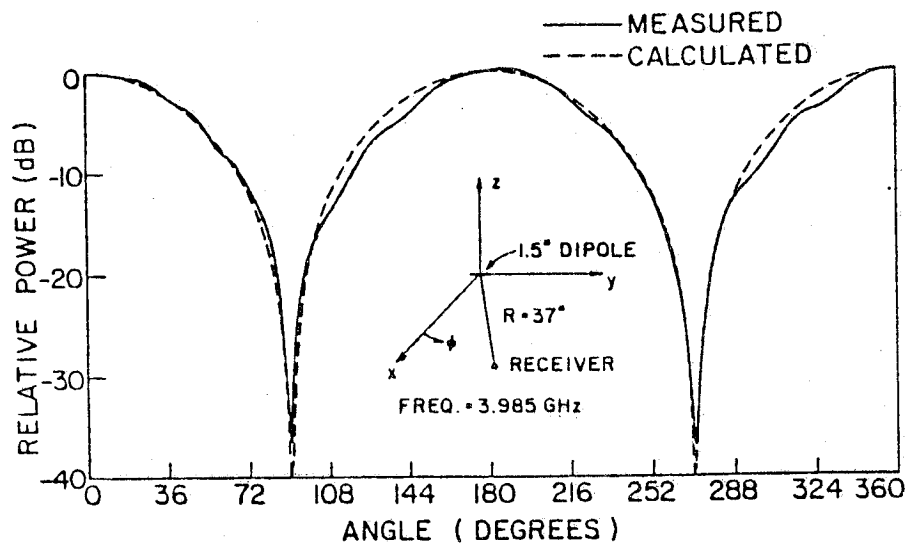


Figure 7.16: Comparison of the measured and calculated E_{ϕ_p} radiation pattern of a dipole.

Ex. 3

203

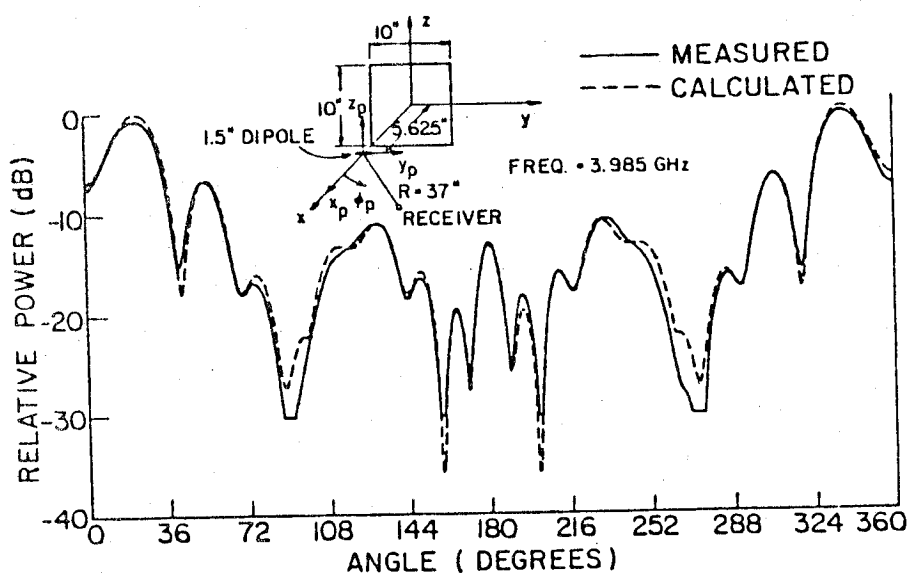


Figure 7.17: Comparison of the measured and calculated E_{ϕ_p} radiation pattern in the $x - y$ plane 37" from a dipole in the presence of a square plate.

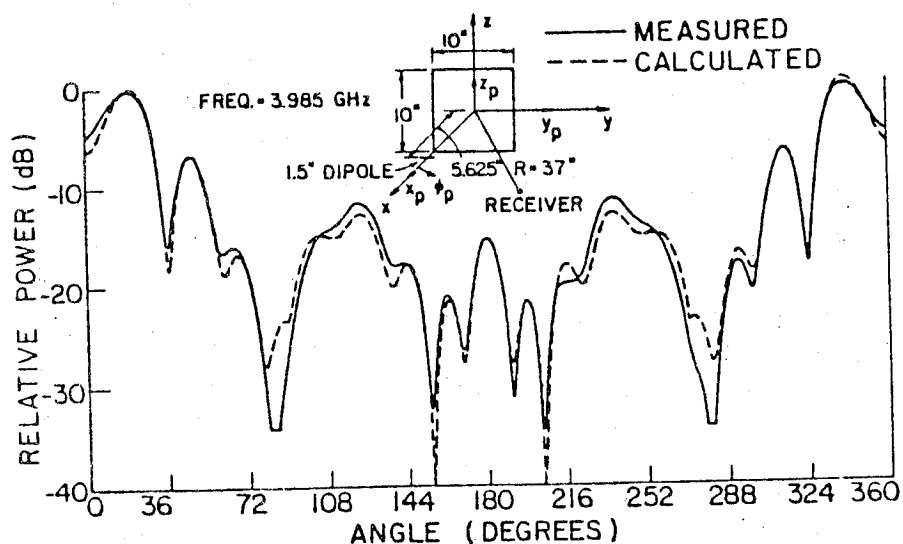


Figure 7.18: Comparison of the measured and calculated E_{ϕ_p} radiation pattern in the $x - y$ plane 37" from a square plate in the presence of a dipole.

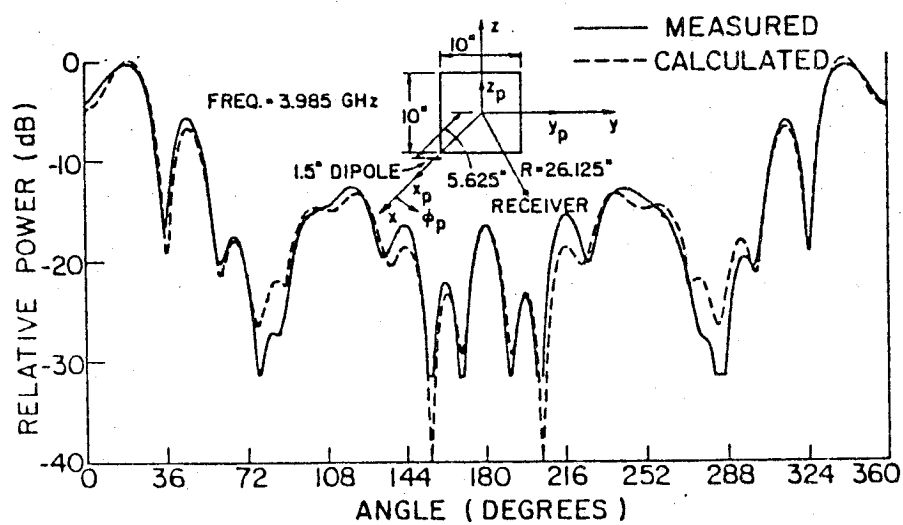


Figure 7.19: Comparison of the measured and calculated E_{ϕ_p} radiation pattern in the $x - y$ plane 26.125" from a square plate in the presence of a dipole.

Ex. 3

205

NEAR ZONE ELECTRIC FIELD

THE FIELDS ARE REFERENCED TO THE PATTERN COORDINATE SYSTEM

R	THETA	PHI	R			THETA			PHI		
			MAGNITUDE	PHASE	DB	MAGNITUDE	PHASE	DB	MAGNITUDE	PHASE	DB
0.940	90.000	0.000	3.4345E-07	40.60	-129.28	2.1948E-06	52.79	-113.17	5.0727E+01	54.51	34.10
0.940	90.000	10.000	3.1833E+00	-24.91	10.06	2.4847E-06	55.45	-112.09	7.3103E+01	52.54	37.28
0.940	90.000	20.000	4.5316E+00	48.17	13.13	3.0091E-06	66.12	-110.43	1.0808E+02	70.92	40.67
0.940	90.000	30.000	5.4788E+00	139.86	14.77	2.4875E-06	101.08	-112.08	9.2100E+01	108.03	39.29
0.940	90.000	40.000	4.9400E+00	-114.09	13.87	8.5355E-07	141.17	-121.38	2.0944E+01	126.56	28.42
0.940	90.000	50.000	4.1920E+00	9.90	12.45	8.3021E-07	51.02	-121.62	4.7587E+01	60.43	33.55
0.940	90.000	60.000	2.8328E+00	145.93	9.04	6.5631E-07	119.96	-123.66	3.8543E+01	105.58	31.72
0.940	90.000	70.000	1.4146E+00	-55.60	5.01	2.2519E-07	-27.43	-132.95	1.4688E+01	81.57	23.33
0.940	90.000	80.000	1.0720E+00	114.95	0.60	3.2503E-07	114.36	-129.76	1.4448E+01	106.48	23.20
0.940	90.000	90.000	8.9534E-01	-101.29	-0.96	5.0770E-04	92.78	-65.89	5.8848E+00	-103.49	15.09
0.940	90.000	100.000	6.2681E-01	-165.78	-4.06	3.2712E-07	44.80	-129.71	1.1124E+01	-108.72	20.93
0.940	90.000	110.000	9.0806E-01	-48.07	-0.84	4.1748E-07	122.30	-127.59	2.3303E+01	-77.47	27.35
0.940	90.000	120.000	6.7733E-01	76.85	-3.38	3.3366E-07	146.84	-129.53	2.3977E+01	-74.65	27.60
0.940	90.000	130.000	6.4282E-01	-66.18	-3.84	4.1208E-07	128.16	-127.70	3.1171E+01	-72.99	29.88
0.940	90.000	140.000	1.0644E+00	70.40	0.54	1.2395E-07	13.28	-138.14	1.6844E+01	-73.21	24.53
0.940	90.000	150.000	4.8235E-01	-140.57	-6.33	2.9470E-07	78.05	-130.61	1.7320E+01	-121.43	24.77
0.940	90.000	160.000	1.8257E+00	0.22	5.23	4.3185E-07	167.60	-127.29	4.2467E+00	61.29	12.56
0.940	90.000	170.000	2.0003E+00	-155.84	6.02	4.1170E-07	121.83	-127.71	5.8505E+00	39.87	15.34
0.940	90.000	180.000	2.0727E-06	-54.47	-113.67	1.0555E-06	135.52	-119.53	2.3545E+01	-50.25	27.44

Figure 7.20: Line printer output of the near zone electric fields of Example 3.

NEAR ZONE MAGNETIC FIELD

THE FIELDS ARE REFERENCED TO THE PATTERN COORDINATE SYSTEM

R	THETA	PHI	MAGNITUDE	PHASE	DB	MAGNITUDE	PHASE	DB	MAGNITUDE	PHASE	DB
0.940	90.000	0.000	1.0657E-09	147.58	-179.45	1.3447E-01	-125.49	-17.43	5.8228E-09	52.83	-164.70
0.940	90.000	10.000	1.0856E-09	-177.79	-179.29	1.9408E-01	-127.51	-14.24	6.6112E-09	54.72	-163.59
0.940	90.000	20.000	1.2021E-09	-149.63	-178.40	2.8740E-01	-109.09	-10.83	8.0239E-09	65.55	-161.91
0.940	90.000	30.000	6.7414E-10	-79.96	-183.43	2.4499E-01	-71.81	-12.22	6.6984E-09	101.48	-163.48
0.940	90.000	40.000	6.0817E-10	119.05	-184.32	5.4982E-02	-52.63	-25.20	2.1978E-09	143.65	-173.16
0.940	90.000	50.000	2.9101E-10	-147.23	-190.72	1.2692E-01	-119.91	-17.93	2.2062E-09	48.83	-173.13
0.940	90.000	60.000	3.0277E-10	-90.00	-190.38	1.0278E-01	-74.09	-19.76	1.8409E-09	118.44	-174.70
0.940	90.000	70.000	1.2762E-10	-90.00	-197.88	3.8594E-02	-98.87	-28.27	6.0449E-10	-30.57	-184.37
0.940	90.000	80.000	1.0000E-10	0.00	-200.00	3.8578E-02	-73.48	-28.27	8.4120E-10	113.87	-181.50
0.940	90.000	90.000	1.0000E-10	0.00	-200.00	1.5265E-02	76.63	-36.33	1.3467E-06	92.77	-117.41
0.940	90.000	100.000	2.6161E-10	35.24	-191.65	2.9566E-02	71.08	-30.58	8.6529E-10	47.14	-181.26
0.940	90.000	110.000	1.9994E-10	143.58	-193.98	6.1952E-02	102.63	-24.16	1.0587E-09	121.23	-179.50
0.940	90.000	120.000	1.6049E-10	-90.00	-195.89	6.3414E-02	105.35	-23.96	8.4407E-10	147.99	-161.47
0.940	90.000	130.000	1.0000E-10	0.00	-200.00	8.2866E-02	106.96	-21.63	1.0846E-09	128.15	-179.29
0.940	90.000	140.000	5.5106E-10	-156.13	-185.18	4.4419E-02	106.88	-27.05	3.6934E-10	21.11	-188.65
0.940	90.000	150.000	3.6555E-10	16.49	-188.74	4.6358E-02	58.36	-26.68	7.8881E-10	72.68	-182.06
0.940	90.000	160.000	1.0249E-09	-177.04	-179.79	1.1437E-02	-117.59	-38.83	1.1637E-09	166.14	-178.68
0.940	90.000	170.000	6.6874E-10	-37.96	-183.49	1.5418E-02	-137.98	-36.24	1.1308E-09	125.68	-178.93
0.940	90.000	180.000	3.0081E-10	-4.37	-190.43	6.2673E-02	129.77	-24.06	2.8251E-09	155.16	-170.98

Figure 7.21: Line printer output of the near zone magnetic fields of Example 3.

.....

.....

NEAR ZONE POWER DENSITY IN DB

THE FIELDS ARE REFERENCED TO THE PATTERN COORDINATE SYSTEM

			RADIATED			REACTIVE		
R	THETA	PMI	R	THETA	PMI	R	THETA	PMI
0.940	90.000	0.000	5.33	-88.39	-76.49	-33.22	-75.69	-82.56
0.940	90.000	10.000	8.51	-75.65	-11.71	-21.51	-76.95	-5.21
0.940	90.000	20.000	11.91	-71.76	-2.21	-25.28	-74.34	-5.99
0.940	90.000	30.000	10.52	-73.46	-2.43	-15.21	-78.04	-4.53
0.940	90.000	40.000	-2.40	-81.27	-11.88	-20.92	-83.50	-9.23
0.940	90.000	50.000	4.80	-80.12	-7.69	-17.50	-95.09	-6.90
0.940	90.000	60.000	2.97	-81.34	-9.53	-19.46	-83.80	-10.29
0.940	90.000	70.000	-5.48	-89.35	-17.02	-26.56	-91.52	-17.28
0.940	90.000	80.000	-5.55	-96.95	-16.89	-37.68	-93.08	-25.19
0.940	90.000	90.000	-13.63	-82.33	-21.66	-40.25	-68.35	-36.07
0.940	90.000	100.000	-7.84	-90.23	-22.95	-32.57	-89.99	-21.10
0.940	90.000	110.000	-1.42	-88.91	-16.10	-28.92	-87.91	-18.61
0.940	90.000	120.000	-1.19	-88.03	-17.24	-41.28	-89.08	-19.89
0.940	90.000	130.000	1.11	-93.57	-15.78	-29.24	-89.27	-24.97
0.940	90.000	140.000	-4.27	-93.53	-17.21	-32.34	-83.51	-18.52
0.940	90.000	150.000	-3.96	-86.60	-19.76	-28.25	-86.52	-24.40
0.940	90.000	160.000	-16.15	-99.50	-23.12	-33.23	-87.98	-20.35
0.940	90.000	170.000	-13.46	-97.29	-18.33	-27.71	-90.95	-23.25
0.940	90.000	180.000	-1.32	-86.08	-71.89	-35.76	-85.95	-83.18

.....

.....

Figure 7.22: Line printer output of the near zone power density of Example 3.

7.6 Example 4: Frequency Sweep

This example illustrates the swept frequency option. The geometry is that of the plate and source shown in the insert of Figure 7.19. The frequency is varied from 3 GHz to 5 GHz at two pattern locations. The first location is directly in front of the plate where the fields are dominated by the direct and reflected fields. The second location is directly behind the plate where the diffracted fields are the only fields present. Note that the frequency response of the antenna is assumed to be totally represented by the change in the current on the antenna based on a piece-wise sinusoidal approximation. The input data is given by

```

CM:  EXAMPLE 4.
CE:  NEAR ZONE SWEPT FREQUENCY PLATE TEST
UN:
3
US:
3
FM:
37,3.,0.05556
SG:
5.625,0.,0.
90.,90.,0.,0.
-2,1.5,0.
1.,0.
PN:
0.,0.,0.
0.,0.,90.,0.
F
26.125,90.,0.
0.,0.,1.
1
PG:
4,0
0.,5.,5.
0.,-5.,5.
0.,-5.,-5.
0.,5.,-5.
PP:

```



```
T
T,4.2,2.1
3.,5.,.5
10.,50.,10.
XQ:  EXECUTE CODE
PN:
0.,0.,0.
0.,0.,90.,0.
F
26.125,90.,180.
0.,0.,1.
1
XQ:  EXECUTE CODE
EN:
```

The E_{ϕ_p} component of the field is shown in Figure 7.23 for a pattern location directly in front of the dipole and plate geometry of Figure 7.19 as the frequency is swept from 3 GHz to 5 GHz. The E_{ϕ_p} component of the field is shown in Figure 7.24 for a pattern location directly behind the plate.

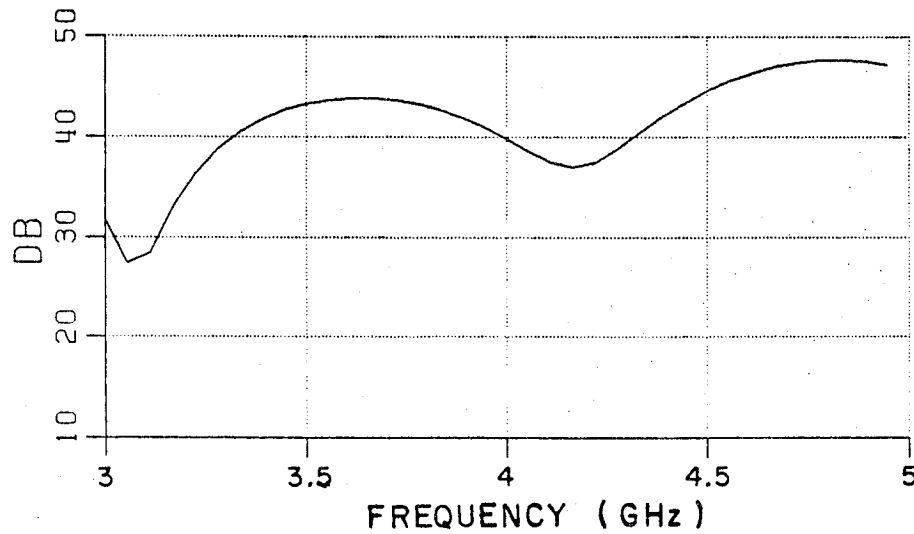


Figure 7.23: The E_{ϕ_p} component of the field for a pattern location directly in front of the plate. (VAX 11/750 run time is 0.8 min.)

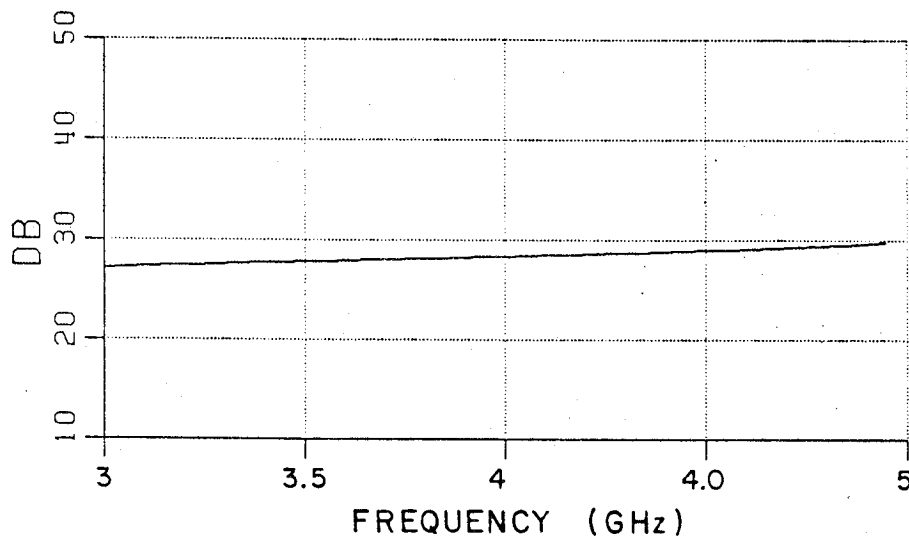


Figure 7.24: The E_{ϕ_p} component of the field for a pattern location directly behind the plate.

7.7 Example 5: Corner Reflector

This example shows the near zone pattern of a corner reflector antenna. The corner reflector is represented by two plates joined together at a common edge. The geometry is illustrated in Figure 7.25. The input data is given by

```
CM:  EXAMPLE 5.
CE:  NEAR ZONE CORNER REFLECTOR TEST
FR:
3.985
UN:
3
US:
3
SG:
3.5,0.,0.
0.,0.,90.,0.
-2,1.5,0.
1.,0.
PG:
4,0
0.,0.,-6.5
0.,0.,6.5
3.36,-3.36,6.5
3.36,-3.36,-6.5
PG:
4,0
0.,0.,6.5
0.,0.,-6.5
3.36,3.36,-6.5
3.36,3.36,6.5
PN:
0.,0.,0.
0.,0.,90.,0.
F
36.75,90.,0.
0.,0.,1.
361
```

```
PP:
T
T,4.2,2.1
0.,360.,36.
-40.,0.,10.
XQ:  EXECUTE CODE
EN:
```

The E_{θ_p} near zone radiation pattern in the $x - y$ plane of a corner reflector is compared with measurements in Figure 7.26. The pattern is taken at a distance of 36.75" from the corner of the plates. The radial and phi components are not shown since they are small compared to the theta component.

Ex. 5

213

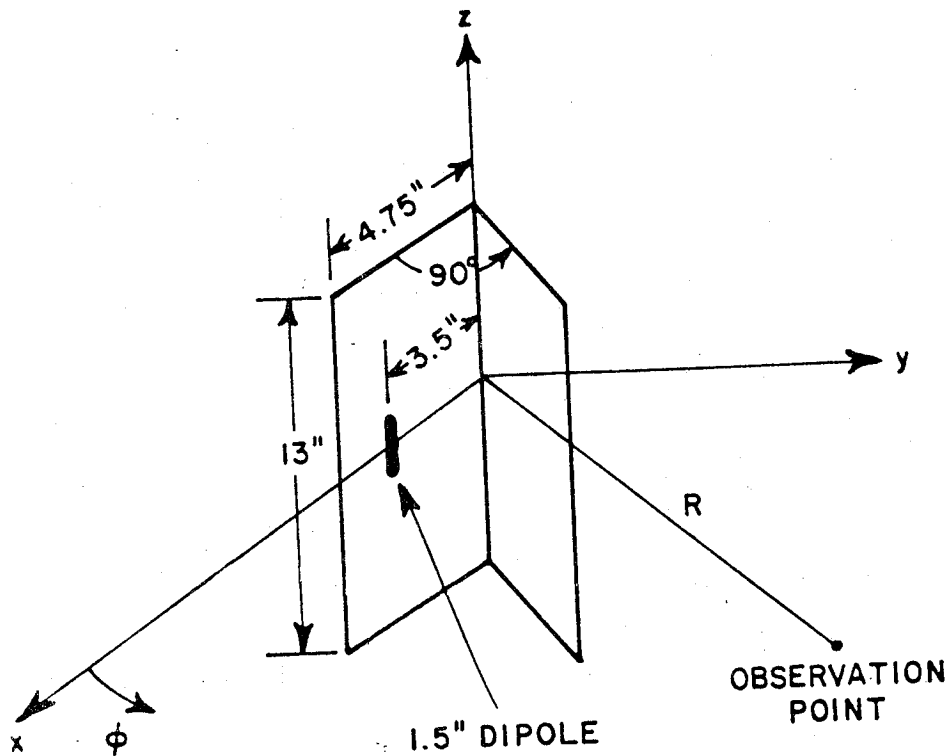


Figure 7.25: Geometry of a corner reflector antenna.

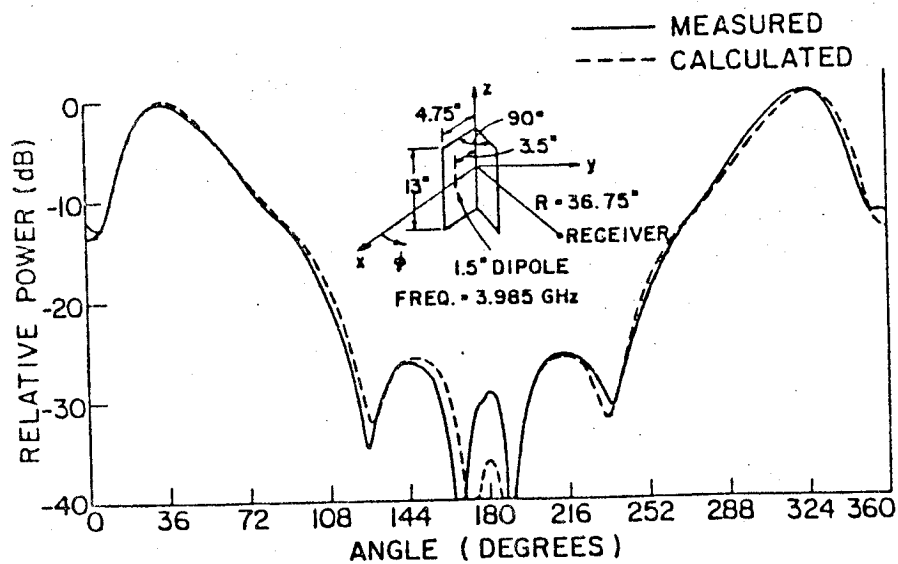


Figure 7.26: Comparison of the E_{θ} radiation pattern in the $x - y$ plane 36.75" from the junction of two plates forming a corner reflector antenna (the maximum value of the E_{θ} is 45.28 dB).

7.8 Example 6: Eight Sided Box

Consider the far zone pattern of an electric dipole in the presence of an perfectly conducting eight-sided box as shown in Figure 7.27. The input data is given by

CE: EIGHT SIDED BOX TEST, EXAMPLE 6.

US:

0

FR:

9.94

PF:

0.,0.,90.,0.

T,90.

0.,1.,361

SG:

0.212,0.,0.

0.,0.,90.,0.

-2,0.5,0.

1.,0.

PG: FRONT

4,0

0.122,0.1023,-0.1

0.122,0.1023,0.1

0.122,-0.1023,0.1

0.122,-0.1023,-0.1

PG: RIGHT FRONT

4,0

0.,0.1707,-0.1

0.,0.1707,0.1

0.122,0.1023,0.1

0.122,0.1023,-0.1

PG: RIGHT BACK

4,0

-0.122,0.1023,-0.1

-0.122,0.1023,0.1

0.,0.1707,0.1

0.,0.1707,-0.1

PG: BACK

```
4,0
-0.122,-0.1023,-0.1
-0.122,-0.1023,0.1
-0.122,0.1023,0.1
-0.122,0.1023,-0.1
PG:  LEFT BACK
4,0
0.,-0.1707,-0.1
0.,-0.1707,0.1
-0.122,-0.1023,0.1
-0.122,-0.1023,-0.1
PG:  LEFT FRONT
4,0
0.122,-0.1023,-0.1
0.122,-0.1023,0.1
0.,-0.1707,0.1
0.,-0.1707,-0.1
PG:  TOP
6,0
0.,0.1707,0.1
-0.122,0.1023,0.1
-0.122,-0.1023,0.1
0.,-0.1707,0.1
0.122,-0.1023,0.1
0.122,0.1023,0.1
PG:  BOTTOM
6,0
0.,0.1707,-0.1
0.122,0.1023,-0.1
0.122,-0.1023,-0.1
0.,-0.1707,-0.1
-0.122,-0.1023,-0.1
-0.122,0.1023,-0.1
PP:
T
T,5.1,2.5
0.,360.,90.
-40.,0.,10.
XQ:  EXECUTE CODE
```

EN:

The E_{θ_p} pattern is compared with measured results [22] in Figure 7.28. The E_{ϕ_p} pattern is not plotted because it is of negligible value.

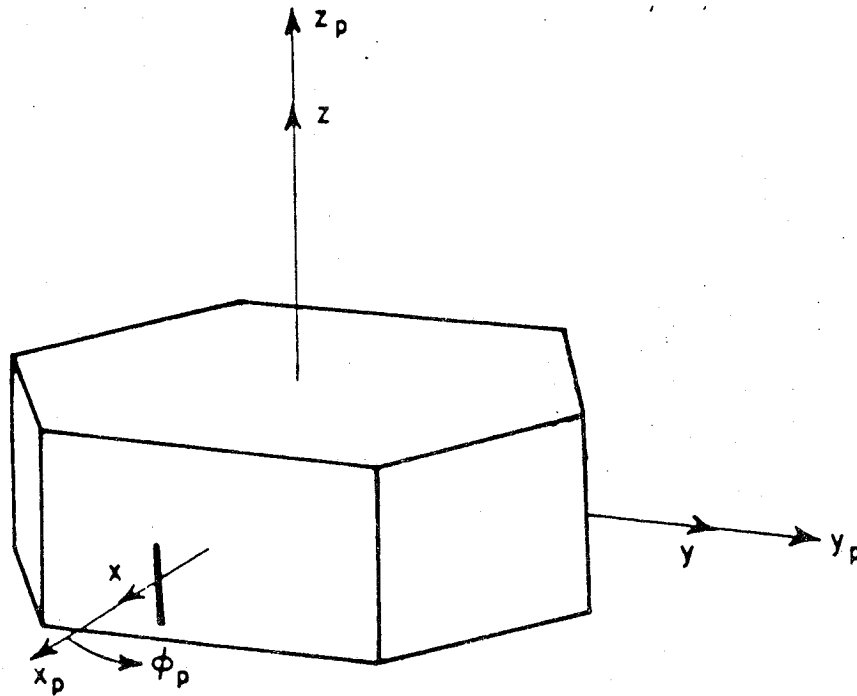


Figure 7.27: Electric dipole in the presence of an eight sided box.

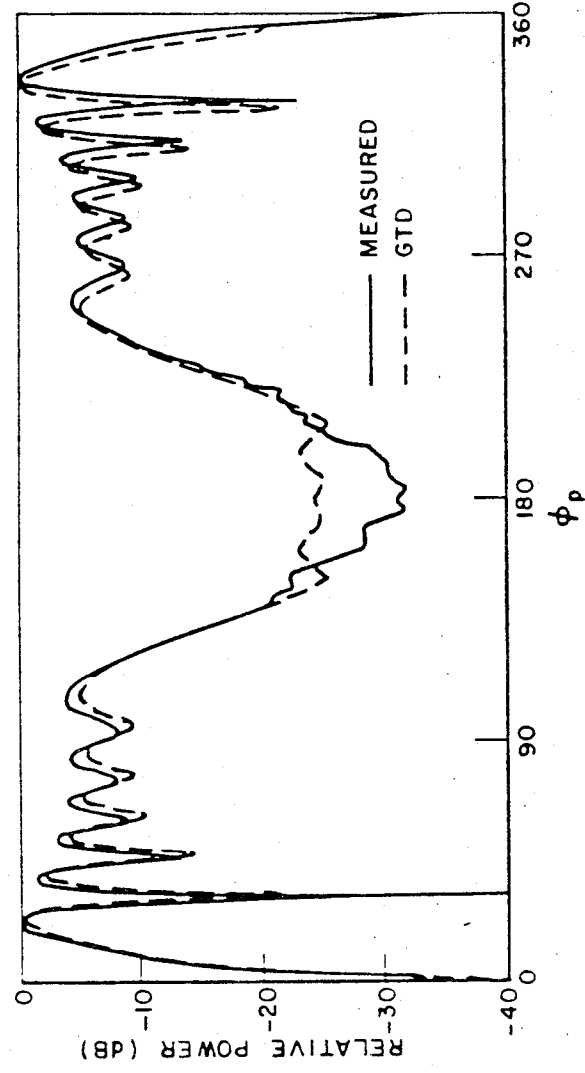


Figure 7.28: Comparison of measured (Bach) and calculated radiation E_{θ_p} pattern for an electric dipole in the presence of an eight sided box. (VAX 11/750 run time is 11.5 min and the maximum value of E_θ is 42.5 dB.)

7.9 Example 7: Dielectric Plate

This example considers a dipole mounted above a dielectric covered metallic ground plane. The geometry is illustrated in Figure 7.29. The dielectric is composed of a polystyrene slab which is 0.2715" thick with a relative dielectric constant of 2.55 and is mounted flush on a square metallic plate. The antenna is mounted 5.15" above the center of the plate. The input data is given by

```
CM: EXAMPLE 7.
CM: THIS DATA SET IS USED TO GENERATE A SET OF PATTERNS FOR
CE: A DIPOLE ANTENNA MOUNTED ABOVE A DIELECTRIC GROUND PLANE
UN:
3
US:
3
FR:
8.
PF: E PLANE PATTERN
180.,0.,90.,180.
F,0.
0.,1.,361
PG: GROUND PLANE WITH POLYSTYRENE LAYER
4,-2
1
0.2715,2.55,0.,1.,0.
3.5,3.5,0.
-3.5,3.5,0.
-3.5,-3.5,0.
3.5,-3.5,0.
SG: DIPOLE MOUNTED ABOVE DIELECTRIC SURFACE
0.,0.,4.8485
90.,0.,90.,90.
-2,0.738,0.0
1.,.0
PP:
T
T,3.92,1.95
0.,360.,30.
```

```

-40.,0.,10.
XQ: EXECUTE CODE
PF: H PLANE PATTERN
180.,0.,90.,180.
F,90.
0.,1.,361
XQ: EXECUTE CODE
PF: DIAGONAL PATTERN CUT
180.,0.,90.,180.
F,45.
0.,1.,361
XQ: EXECUTE CODE
EN:

```

The E_{θ_p} (E -plane) pattern is compared with measurements in Figure 7.30. The E_{ϕ_p} (H -plane) pattern is compared with measurements in Figure 7.31. The E_{ϕ_p} component of the field for a pattern across the corners is compared with measurements in Figure 7.32 and the E_{θ_p} component of the field is shown in Figure 7.33.

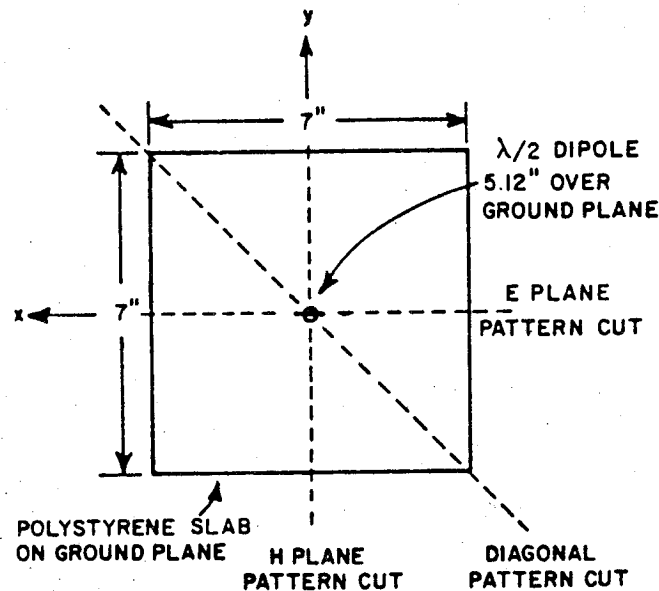


Figure 7.29: Geometry for a dielectric cover metallic square ground plane.

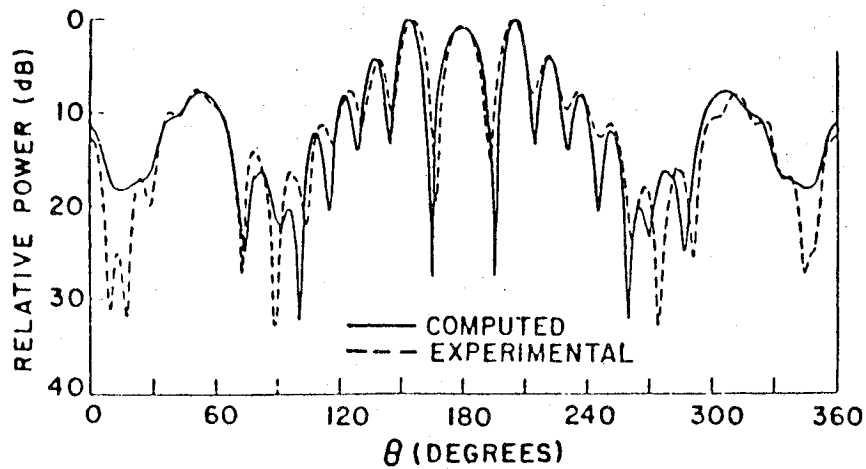


Figure 7.30: *E*-plane patterns ($\phi = 0^\circ$) for a dipole over a polystyrene covered ground plate at 8 GHz.

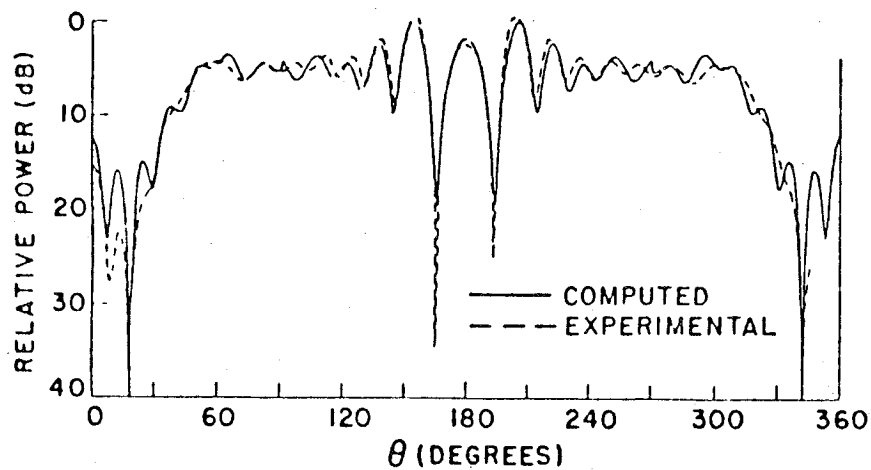


Figure 7.31: *H*-plane patterns ($\phi = 90^\circ$) for a dipole over a polystyrene covered ground plate at 8 GHz.

Ex. 7

221

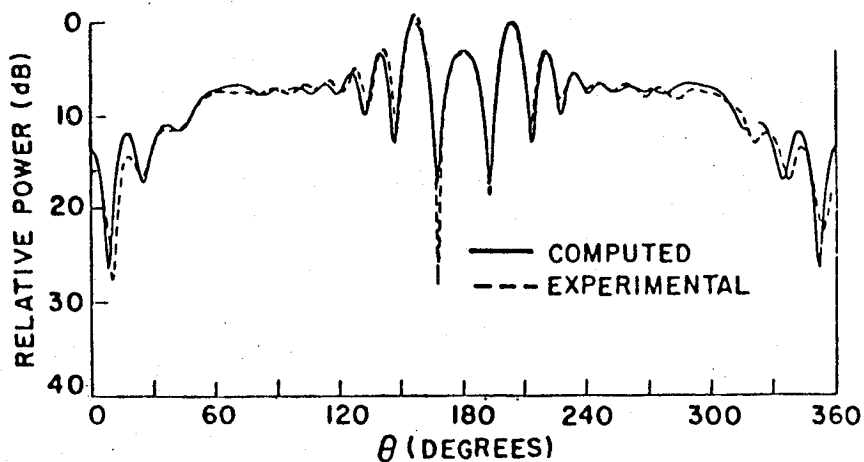


Figure 7.32: E_ϕ component for a diagonal pattern ($\phi = 45^\circ$) for a dipole over a polystyrene covered ground plate at 8 GHz.

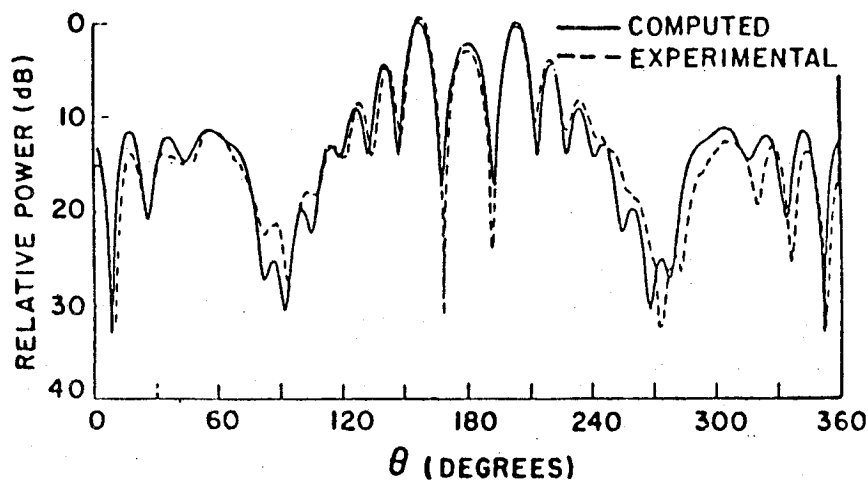


Figure 7.33: E_θ component for a diagonal patterns ($\phi = 45^\circ$) for a dipole over a polystyrene covered ground plate at 8 GHz.

7.10 Example 8: Dielectric Plate

This example is used to show the effects on having or not having the dielectric layer on the metallic ground plane of Example 7. The geometry is illustrated in Figure 7.29. In addition, the effect of the diffracted fields is illustrated by including and not including those terms, using the **XT** command. The input data is given by

```

CM: EXAMPLE 8.
CM: THIS DATA SET IS USED TO SHOW EFFECTS OF HAVING OR NOT
CM: HAVING THE DIELECTRIC LAYER. NEXT THE PATTERN WITHOUT
CM: DIFFRACTIONS IS SHOWN TO ILLUSTRATE HOW MUCH A ROLE
CE: THE DIFFRACTIONS PLAY.
UN:
3
US:
3
FR:
8.
PF: E PLANE PATTERN
180.,0.,90.,180.
F,0.
0.,1.,361
PG: GROUND PLANE ALONE
4,0
3.5,3.5,0.
-3.5,3.5,0.
-3.5,-3.5,0.
3.5,-3.5,0.
SG: DIPOLE ABOVE GROUND PLANE
0.,0.,5.12
90.,0.,90.,90.
-2.,.738,0.0
1.,.0
PP:
T
T,2.96,1.5
0.,360.,30.
-40.,0.,10.

```

```

XQ: EXECUTE CODE
NP: GET RID OF PREVIOUS PLATE!!!
NS: GET RID OF PREVIOUS SOURCE!!!
PG: GROUND PLANE WITH POLYSTYRENE LAYER
4,-2
1
0.2715,2.55,0.,1.,0.
3.5,3.5,0.
-3.5,3.5,0.
-3.5,-3.5,0.
3.5,-3.5,0.
SG:
0.,0.,4.8485
90.,0.,90.,90.
-2,0.738,0.0
1.,.0
XT: RUN ONLY SOURCE AND REFLECTED FIELDS. NO DIFFRACTIONS
EN:

```

in file unit IUG:

```

INCFLD
RP
ALL
END

```

The E_{θ_p} (E -plane) pattern of the dielectric covered metallic ground plane of Example 7 is compared with the bare metallic ground plane pattern in Figure 7.34. The E_{θ_p} pattern of the dielectric covered metallic ground plane is compared with the pattern with the diffracted field terms removed from the calculations in Figure 7.35.

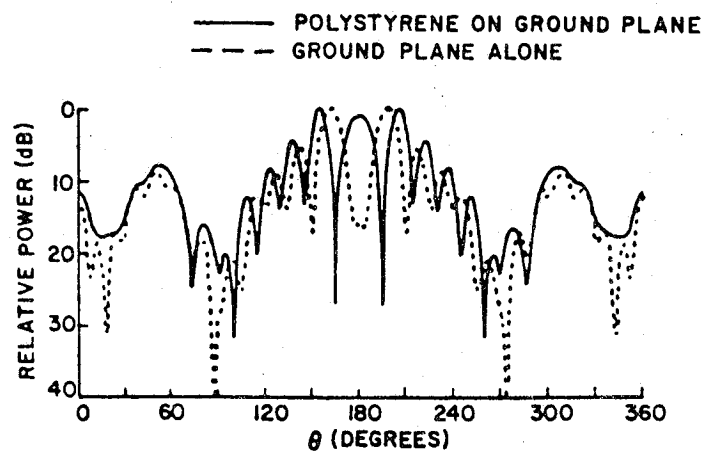


Figure 7.34: Comparison of the *E*-plane patterns of a bare metallic ground plane with a polystyrene covered metallic ground plane.

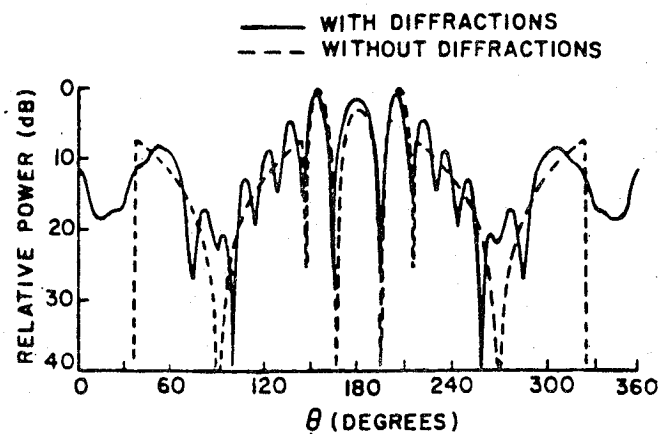


Figure 7.35: Comparison of the *E*-plane pattern of a polystyrene covered ground plane with and without the diffraction terms included. (VAX 11/750 run time is 0.8 min for the case without diffractions)

7.11 Example 9: Lossy Dielectric

This example is used to show the effects of a thin ferrite absorber covering a metallic plate. The properties of the thin ferrite absorber have been obtained from the Avionics Laboratory at Wright Patterson Air Force Base. The input data is given by

```
CM: EXAMPLE 9.
CM: THIS DATA SET IS USED TO SHOW THE UTD SOLUTION ACCURACY
CM: WHEN DEALING WITH ABSORBER MATERIAL. THE ELECTRICAL
CM: PROPERTIES OF THE THIN FERRITE ABSORBER WERE OBTAINED
CE: FROM THE AVIONICS LAB. AT WRIGHT PATTERSON AFB.
UN:
3
US:
3
FR: FREQUENCY OF 9 GHZ
9.
PN:
-1.8,0.,0.
0.,0.,90.,0.
F
99.,90.,0.
0.,0.,1.
361
PG: GROUND PLANE ALONE
4,0
0.,5.,5.
0.,-5.,5.
0.,-5.,-5.
0.,5.,-5.
SG: DIPOLE ABOVE GROUND PLANE
4.87,.0,.0
0.,0.,90.,90.
-2,0.74,0.2
1.,.0
PP:
T
T,5.25,2.6
```

```

0.,360.,36.
-40.,0.,10.
XQ: EXECUTE CODE
NP: GET RID OF PREVIOUS PLATE!!!
NS: GET RID OF PREVIOUS SOURCE!!!
FR: CHANGE FREQUENCY TO 8 GHZ
8.
PN: DEFINE NEW ORIGIN
-1.84,0.,0.
0.,0.,90.,0.
F
99.,90.,0.
0.,0.,1.
361
PG: GROUND PLANE WITH ABSORBER LAYER
4,-2
1
0.04,19.65,0.11,1.77,1.24
0.,5.,5.
0.,-5.,5.
0.,-5.,-5.
0.,5.,-5.
SG: NEW SOURCE LOCATION RELATIVE TO FRONT OF ABSORBER
4.83,.0,.0
0.,0.,90.,90.
-2,0.74,0.2
1.,.0
XQ: EXECUTE CODE
EN:

```

The E_{θ_p} pattern of a 10" square metallic ground plane is compared with measurements in Figure 7.36. The E_{θ_p} pattern of this ground plane cover with a thin ferrite absorber is compared with measurements in Figure 7.37.

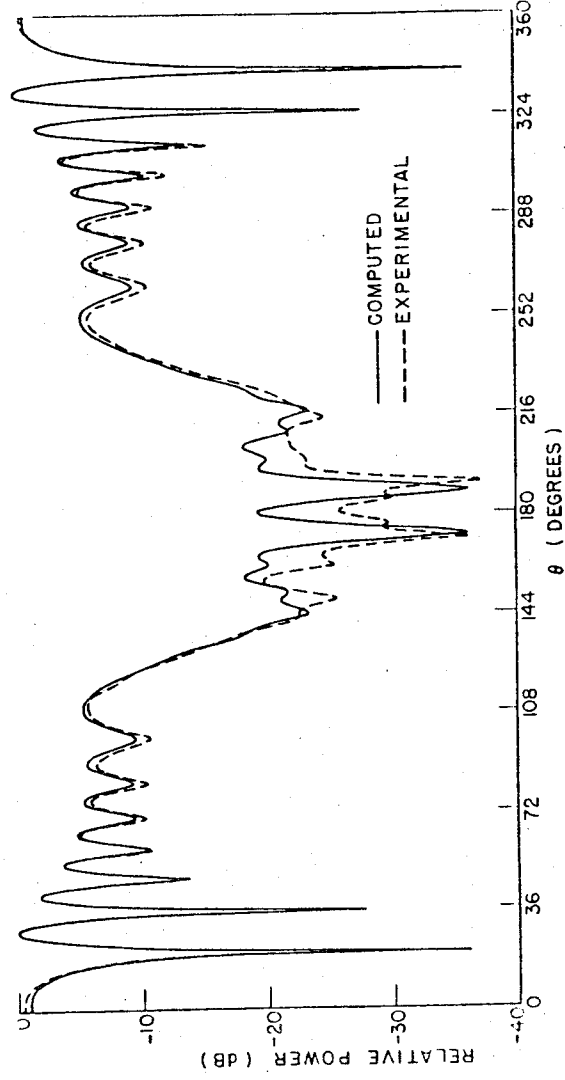


Figure 7.36: Comparison of E_{θ} , measured and calculated patterns for a perfectly conducting metallic plate.

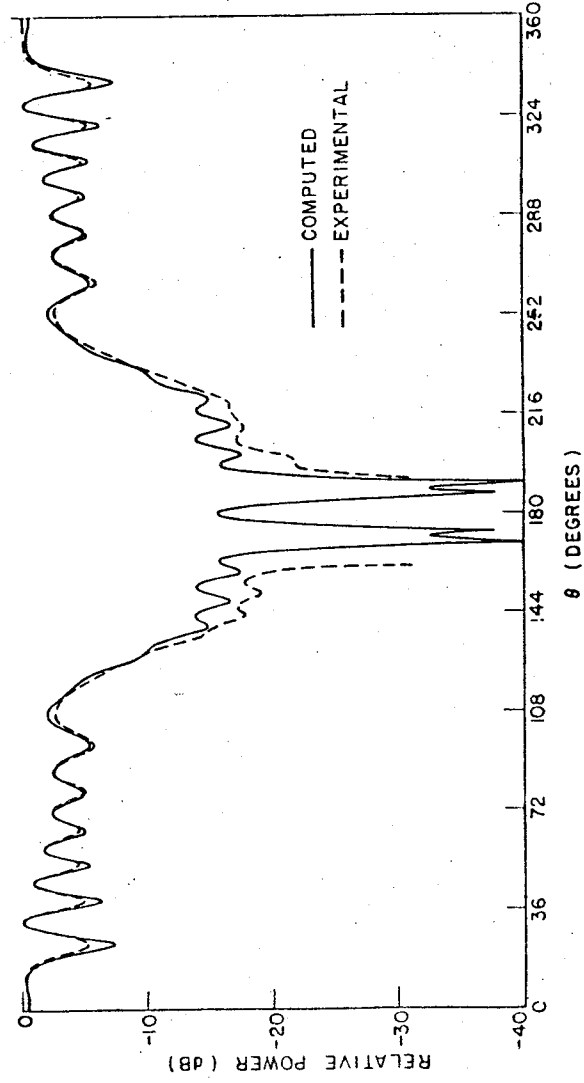


Figure 7.37: Comparison of E_{θ} , measured and calculated patterns for a thin ferrite absorber covered metallic plate. (VAX 11/750 run time is 2.4 min and the maximum value of E_{θ} is -14.9 dB.)

7.12 Example 10: Radome and Horn

This example is used to illustrate the prediction of the performance of an radome covered horn antenna mounted on the belly of an aircraft. The circular polarized horn is approximated by two magnetic sources mounted on a plate. The belly of the aircraft is modeled by a finite perfectly conducting ground plane. The radome is simulated by using a three layer dielectric panel. The geometry is illustrated in Figure 7.38. The input data is given by

```

CM: EXAMPLE 10.
CE: HORN RADIATION PATTERN
UN:
3
US:
3
FR:
7.
PF:
0.,0.,90.,0.
T,90.
0.,1.,181
SG: VERTICAL POLARIZATION MAGNETIC DIPOLE MOMENT
6.25,.0,.0
90.,330.,0.,0.
1,1.8,2.25
1.,.0
SG: HORIZONTAL POLARIZATION MAGNETIC DIPOLE MOMENT
6.25,.0,.0
180.,.0,90.,330.
1,1.8,2.25
1.,90.
RT: ROTATE COORDINATES FOR PLATE BACKING DIPOLE MOMENTS.
6.2,-.086,.0
0.,0.,90.,330.
PG: ANTENNA BLOCKAGE PLATE. GIVES PROPER BACK LOBES.
4,0
-1.25,0.,1.25
1.25,0.,1.250

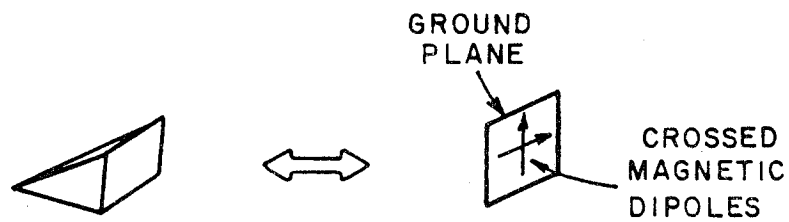
```

```

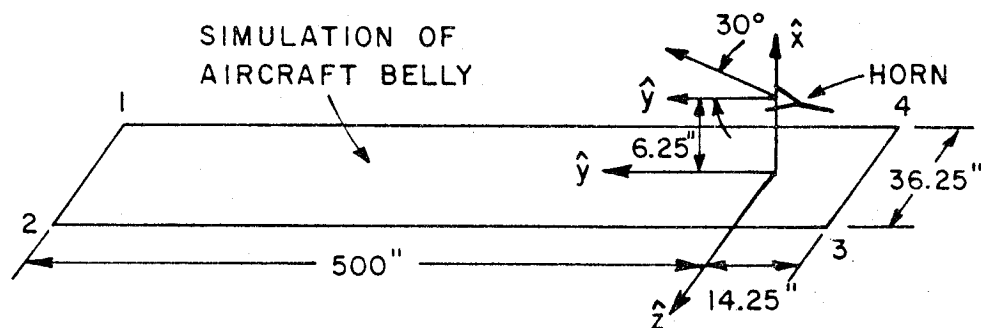
1.25,0.,-1.25
-1.25,0.,-1.25
PP:
T
F,0.,2.55
0.,360.,30.
-40.,0.,10.
XQ: EXECUTE CODE
RT: RESET ROTATE TRANSLATE TO ORIGINAL COORDINATE SYSTEM
0.,0.,0.
0.,0.,90.,0.
PG: GROUND PLANE SIMULATING BELLY OF AIRCRAFT
4,0
0.,500.,-18.125
0.,500.,18.125
0.,-14.25,18.125
0.,-14.25,-18.125
XQ: EXECUTE CODE
CE: ELEVATION PATTERN WITH TOP SECTION OF RADOME PRESENT
PG: TOP RADOME MODEL USING 3 LAYER DIELECTRIC PANEL
4,1
3
0.02,3.9,0.015,1.,0.
0.34,1.15,0.005,1.,0.
0.02,3.9,0.015,1.,0.
13.8,7.5,8.125
13.8,-100.,8.125
13.8,-100.,-8.125
13.8,7.5,-8.125
XQ: EXECUTE CODE
EN:

```

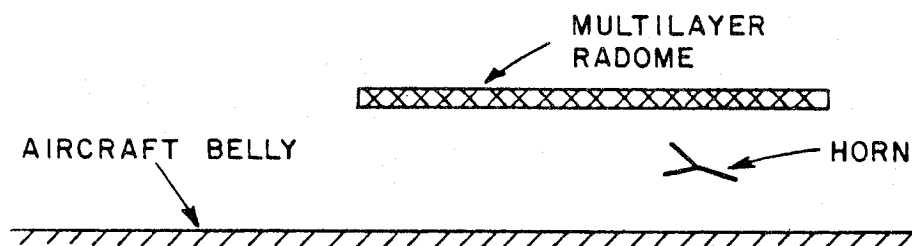
The E_{θ_p} and E_{ϕ_p} radiation patterns of the simulated horn in free space are shown in Figure 7.39 and 7.40, respectively. The E_{θ_p} and E_{ϕ_p} radiation patterns of the horn mounted above the ground plane representing the belly of the aircraft are shown in Figure 7.41 and 7.42, respectively. The E_{θ_p} and E_{ϕ_p} radiation patterns of the radome covered horn above the aircraft belly are shown in Figure 7.43 and 7.44, respectively.



(a) SIMULATION OF HORN



(b) HORN ABOVE AIRCRAFT BELLY



(c) HORN ON AIRCRAFT WITH RADOME

Figure 7.38: Geometry of radome and horn over aircraft belly model.

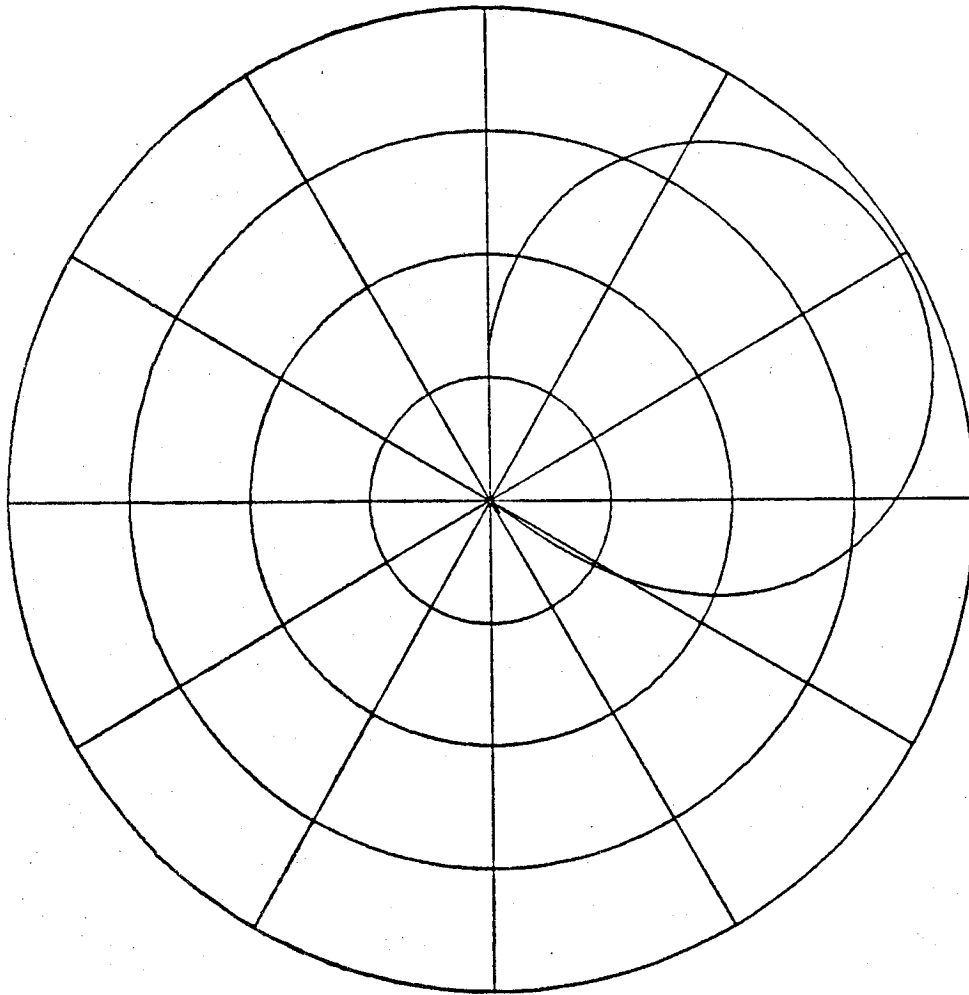


Figure 7.39: The E_{θ_p} radiation pattern of the simulated horn in free space.

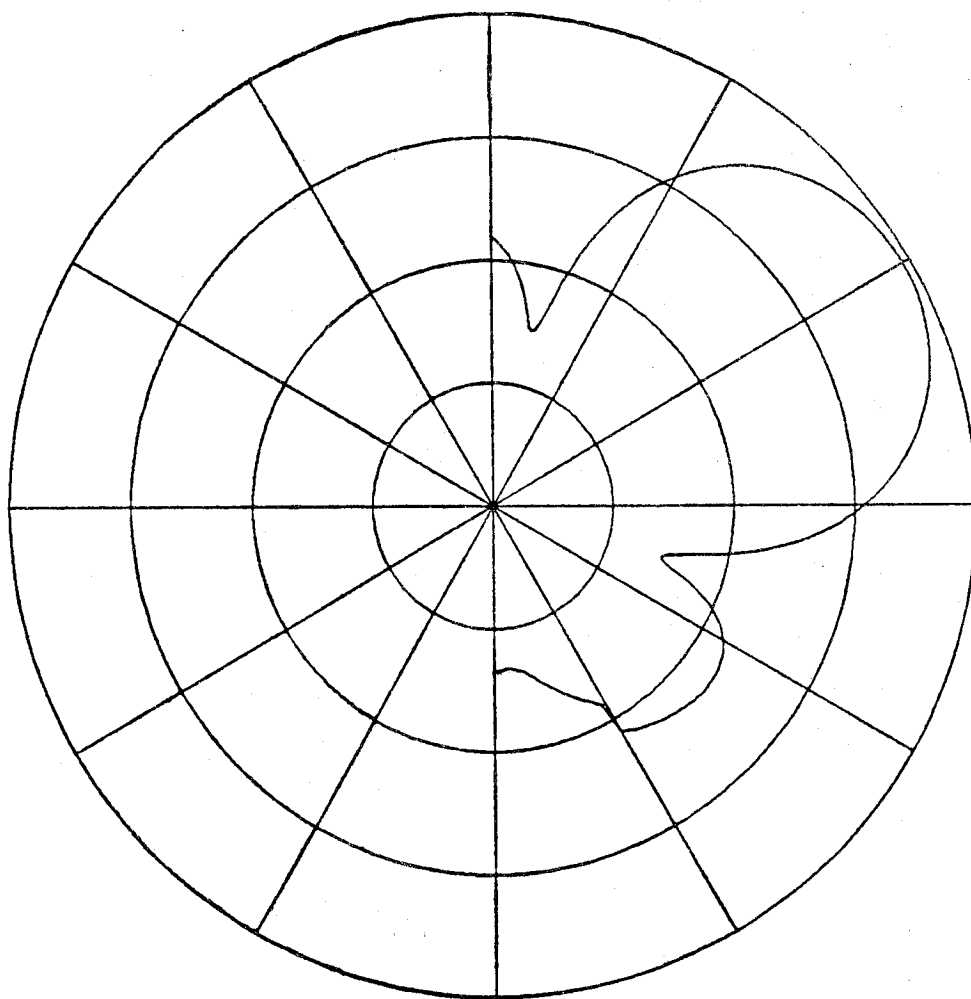


Figure 7.40: The E_{ϕ_r} radiation pattern of the simulated horn in free space.

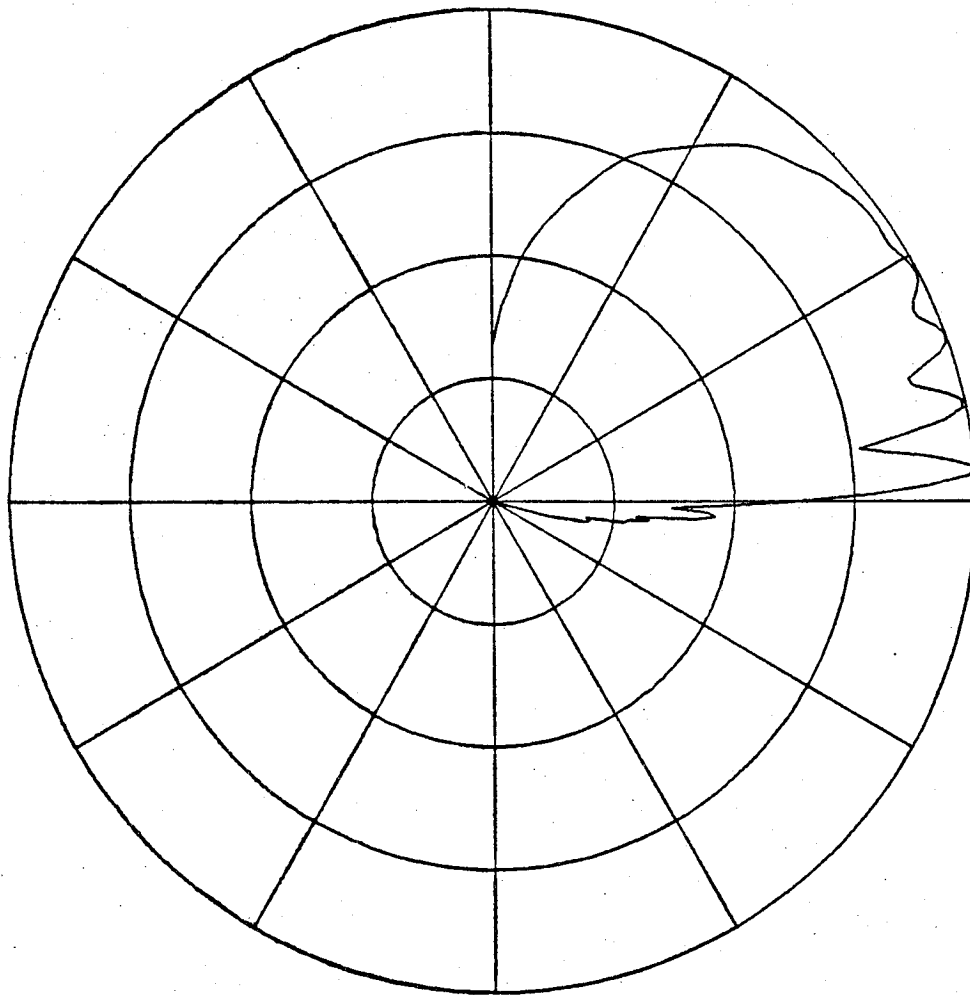


Figure 7.41: The E_{θ_p} radiation pattern of the horn over the plate model of the belly of the aircraft.

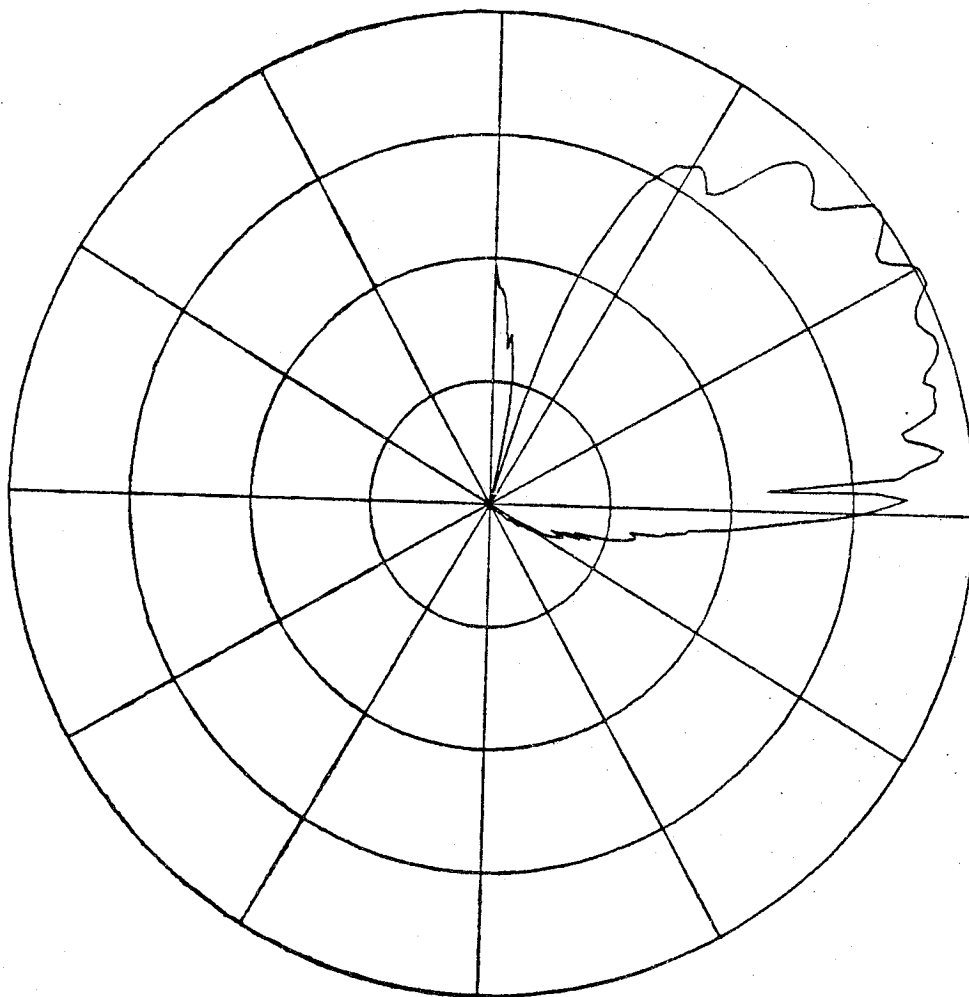


Figure 7.42: The E_{ϕ_p} radiation pattern of the horn over the plate model of the belly of the aircraft.

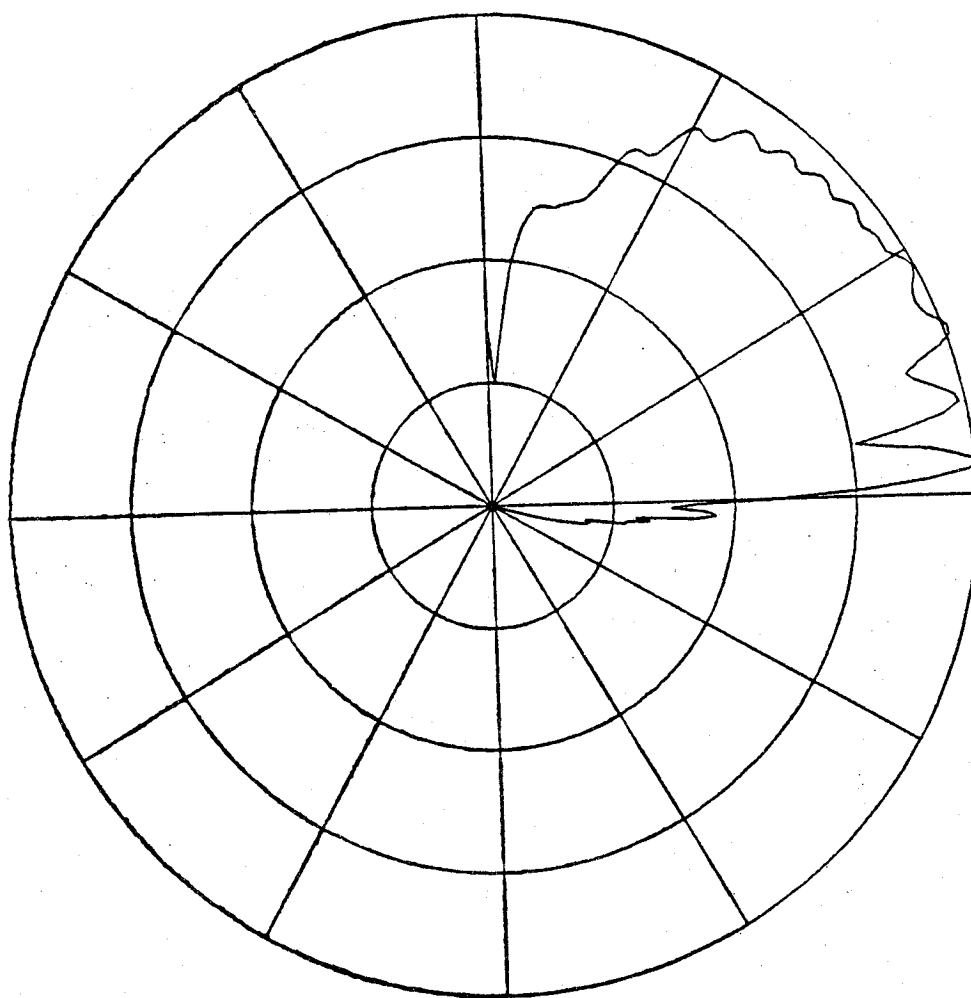


Figure 7.43: The E_{θ} radiation pattern of the radome covered horn over the belly of the aircraft. (VAX 11/750 run time is 11 min.)

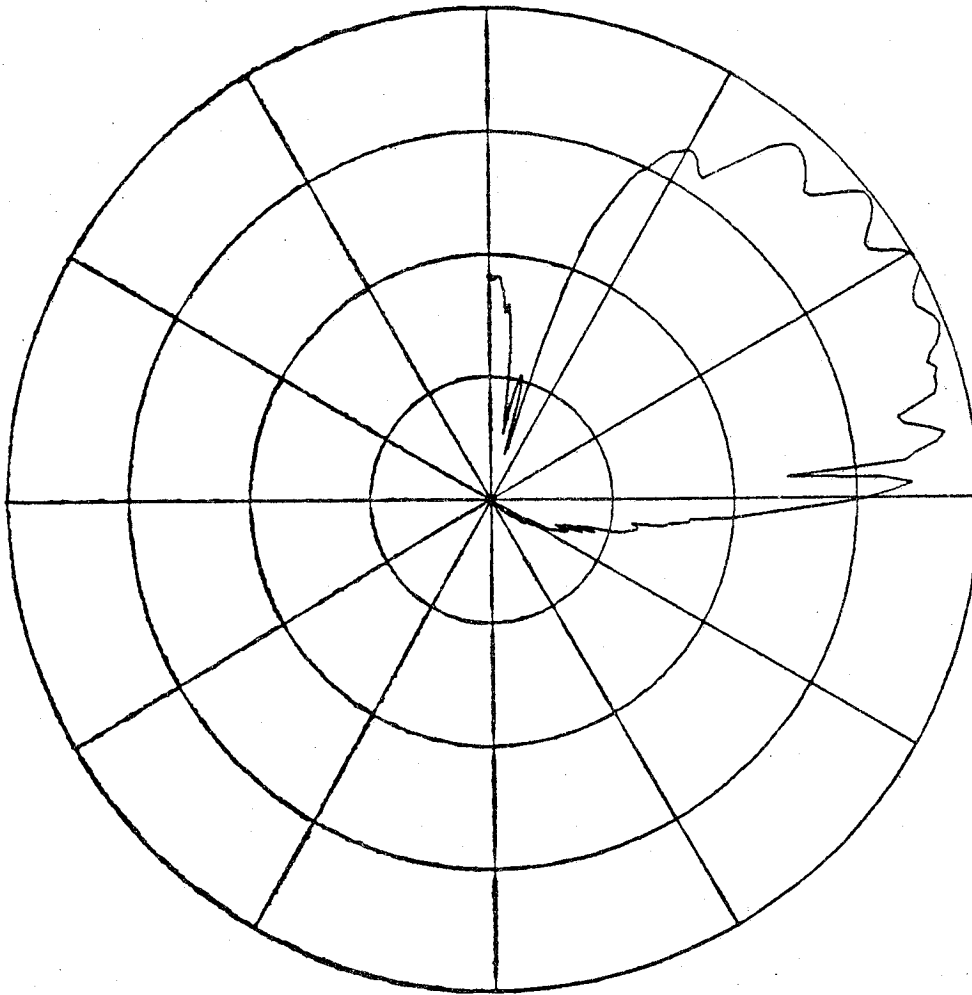


Figure 7.44: The E_{ϕ_p} radiation pattern of the radome covered horn over the belly of the aircraft.

7.13 Example 11A: Antenna Coupling

This example is used to illustrate the different methods of simulating a source and a receiver. In addition, the different methods of representing the coupling between the source and receiver are shown. Four different geometries are studied. The basic geometry is shown in Figure 7.45. The coupling between the two dipoles is compared with the moment method solution when the dipoles are separated in the x direction and z direction in free space and in the x and z direction over a perfectly conducting infinite ground plane. This example uses a seven segment model of the source and receiver. The currents for the dipoles have been obtained from the NEC - Moment Method Code [14] for an isolated dipole. This represents a numerical integration of the currents of the dipoles. Examples 11B and 11C will explore alternative representations for the dipoles. The input data is given by

```
CM: EXAMPLE 11A.
CE: TWO HALF-WAVELENGTH DIPOLE ANTENNAS: CASE 1.
US:
0
SG: SOURCE GEOMETRY(SEGMENT 1.)--TRANSMITTER
0.,0.,0.
0.,0.,90.,0.
-1.,.07143,0.
0.010551,-29.246
SG: SOURCE GEOMETRY(SEGMENT 2.)--TRANSMITTER
0.,0.,-.07143
0.,0.,90.,0.
-1.,.07143,0.
9.8472E-3,-31.777
SG: SOURCE GEOMETRY(SEGMENT 3.)--TRANSMITTER
0.,0.,-.1429
0.,0.,90.,0.
-1.,.07143,0.
7.2367E-3,-33.996
SG: SOURCE GEOMETRY(SEGMENT 4.)--TRANSMITTER
0.,0.,-.2143
0.,0.,90.,0.
-1.,.07143,0.
```

2.9010E-3,-35.584

SG: SOURCE GEOMETRY(SEGMENT 5.)--TRANSMITTER

0.,0.,.0714

0.,0.,90.,0.

-1.,.07143,0.

9.8472E-3,-31.777

SG: SOURCE GEOMETRY(SEGMENT 6.)--TRANSMITTER

0.,0.,.1429

0.,0.,90.,0.

-1.,.07143,0.

7.2367E-3,-33.996

SG: SOURCE GEOMETRY(SEGMENT 7.)--TRANSMITTER

0.,0.,.2143

0.,0.,90.,0.

-1.,.07143,0.

2.9010E-3,-35.584

RG: RECEIVE GEOMETRY(SEGMENT 1.)--RECEIVER

0.,0.,0.

0.,0.,90.,0.

-1.,.07143,0.

1.0551E-2,-29.246

RG: RECEIVE GEOMETRY(SEGMENT 2.)--RECEIVER

0. 0.,-.07143

0.,0.,90.,0.

-1.,.07143,0.

9.8472E-3,-31.777

RG: RECEIVE GEOMETRY(SEGMENT 3.)--RECEIVER

0.,0.,-.1429

0.,0.,90.,0.

-1.,.07143,0.

7.2367E-3,-33.996

RG: RECEIVE GEOMETRY(SEGMENT 4.)--RECEIVER

0.,0.,-.2143

0.,0.,90.,0.

-1.,.07143,0.

2.9010E-3,-35.584

RG: RECEIVE GEOMETRY(SEGMENT 5.)--RECEIVER

0.,0.,.0714

0.,0.,90.,0.

```
-1,.07143,0.
9.8472E-3,-31.777
RG: RECEIVE GEOMETRY(SEGMENT 6.)--RECEIVER
0.,0.,.1429
0.,0.,90.,0.
-1,.07143,0.
7.2367E-3,-33.996
RG: RECEIVE GEOMETRY(SEGMENT 7.)--RECEIVER
0.,0.,.2143
0.,0.,90.,0.
-1,.07143,0.
2.9010E-3,-35.584
PN: NEAR-ZONE PATTERN
0.,0.,0.
0.,0.,90.,0.
T
0.5,0.,0.
0.5,0.,0.
19
PR: POWER RADIATED (MODIFIED FRIL'S METHOD)
3
4.6029E-3,4.6029E-3
PP:
T
T,5.0,6.0
0.,10.,1.
-70.,-10.,10.
LP:
T
XQ: EXECUTE CODE
CE: TWO HALF-WAVELENGTH DIPOLE ANTENNAS: CASE 2.
PN: NEAR-ZONE PATTERN
0.,0.,0.
0.,0.,90.,0.
T
1.0,0.,0.
0.,0.,.5
19
XQ: EXECUTE CODE
```

```

CE: TWO HALF-WAVELENGTH DIPOLE ANTENNAS: CASE 3.
RT: TRANSLATE AXES 1.25 METERS DOWN
0.,0.,-1.25
0.,0.,90.,0.
GP: INFINITE GROUND PLANE
0
PN: NEAR-ZONE PATTERN
0.,0.,0.
0.,0.,90.,0.
T
0.5,0.,0.
0.5,0.,0.
19
XQ: EXECUTE CODE
CE: TWO HALF-WAVELENGTH DIPOLE ANTENNAS: CASE 4.
PN: NEAR-ZONE PATTERN
0.,0.,0.
0.,0.,90.,0.
T
1.0,0.,0.
0.,0.,.5
19
XQ: EXECUTE CODE
EN: END CODE

```

The coupling between two dipoles represented by three different methods and calculated by the Modified Frii's and Linville methods for four different geometrical cases are shown in Figures 7.46 through 7.49. Figure 7.46 is for the dipoles moving apart in the x direction in free space. Figure 7.47 is for the dipoles moving apart in the z direction in free space. Figure 7.48 is for the dipoles moving apart in the x direction over a perfectly conducting infinite ground plane. Figure 7.49 is for the dipoles moving apart in the z direction over a perfectly conducting infinite ground plane. The dots represent the moment method result using the Linville method. The results for the particular data set in this example is shown in the Figure 7.46, 7.47, 7.48, and 7.49 by the solid line for the Frii's normalization and the short dashed lines for the Linville normalization method. Note that in all the case run, this method matches best with with the method of moments. The Linville and Frii's normalization methods disagree slightly

Ex. 11A

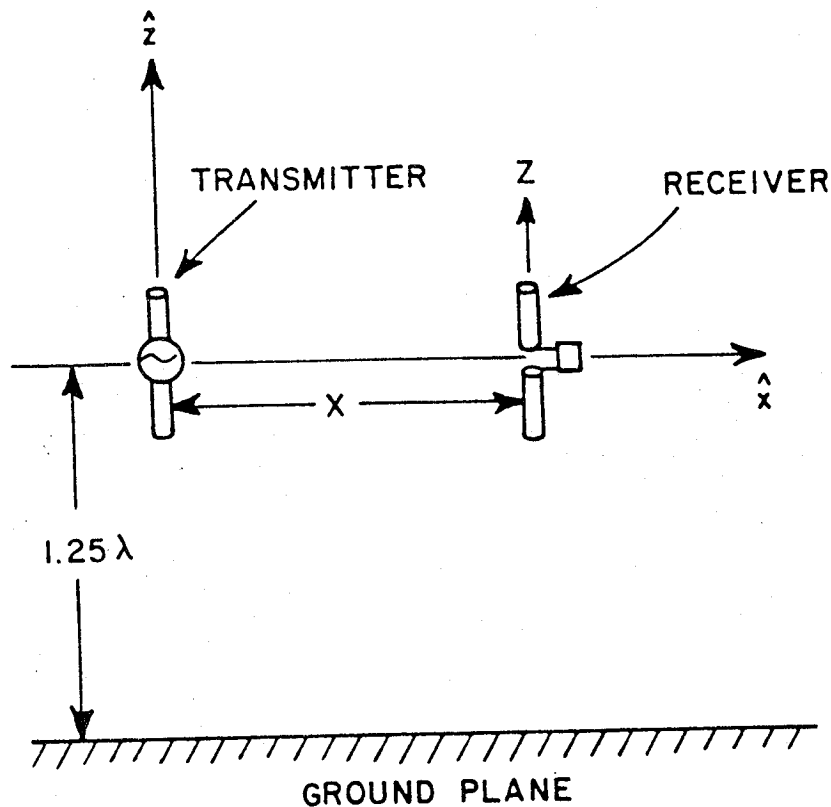


Figure 7.45: Illustration of the geometry used to find the coupling between two dipole antennas.

as the dipoles get close together, but on the whole they agree well. The print out for the coupling of the two dipoles moving apart in the x direction in free space calculated using the Modified Frii's method is shown in Figure 7.50.

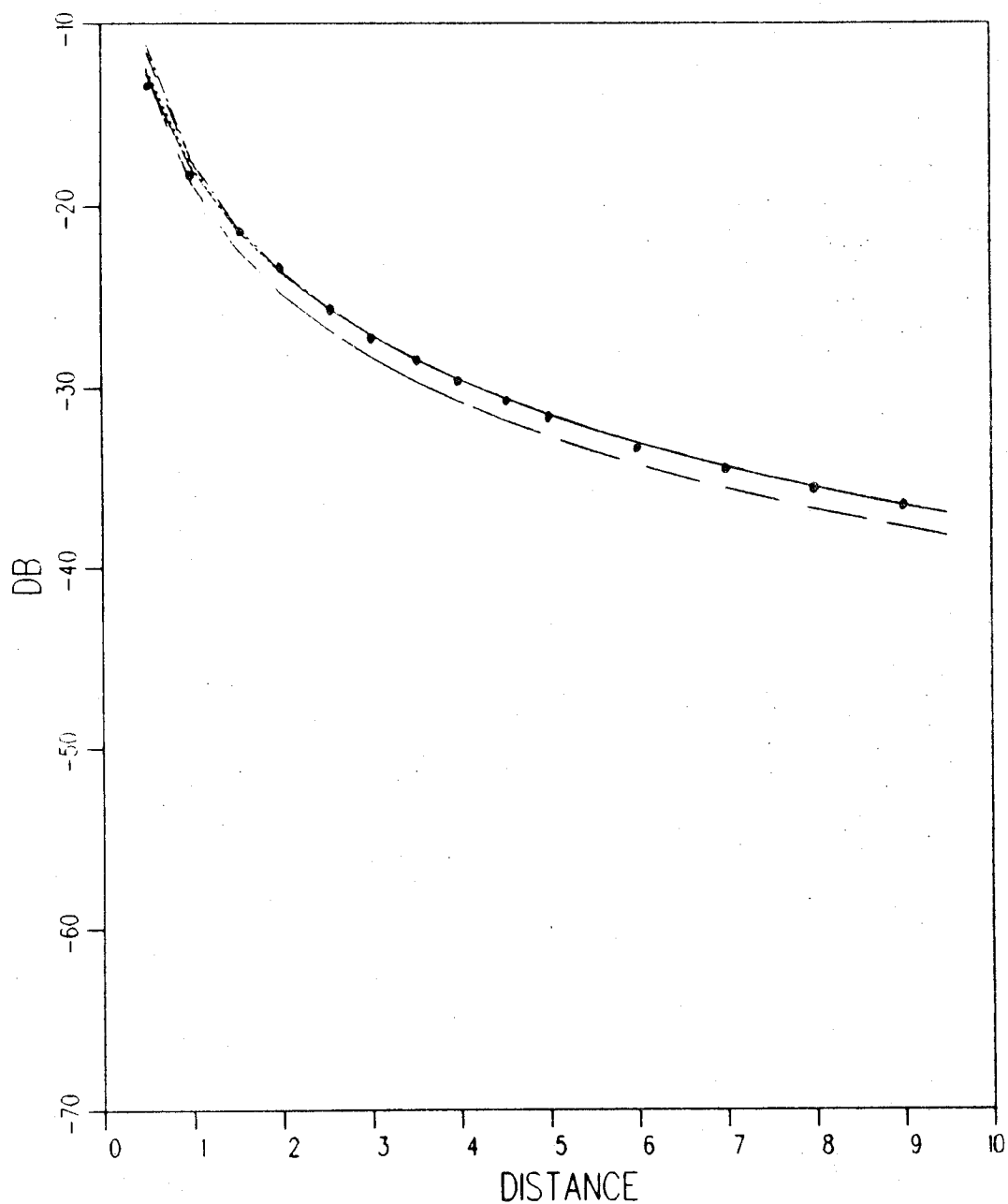


Figure 7.46: The coupling between two half wavelength dipoles in free space as they move apart along the x -axis. The NEC - Method of Moments results are shown as dots.

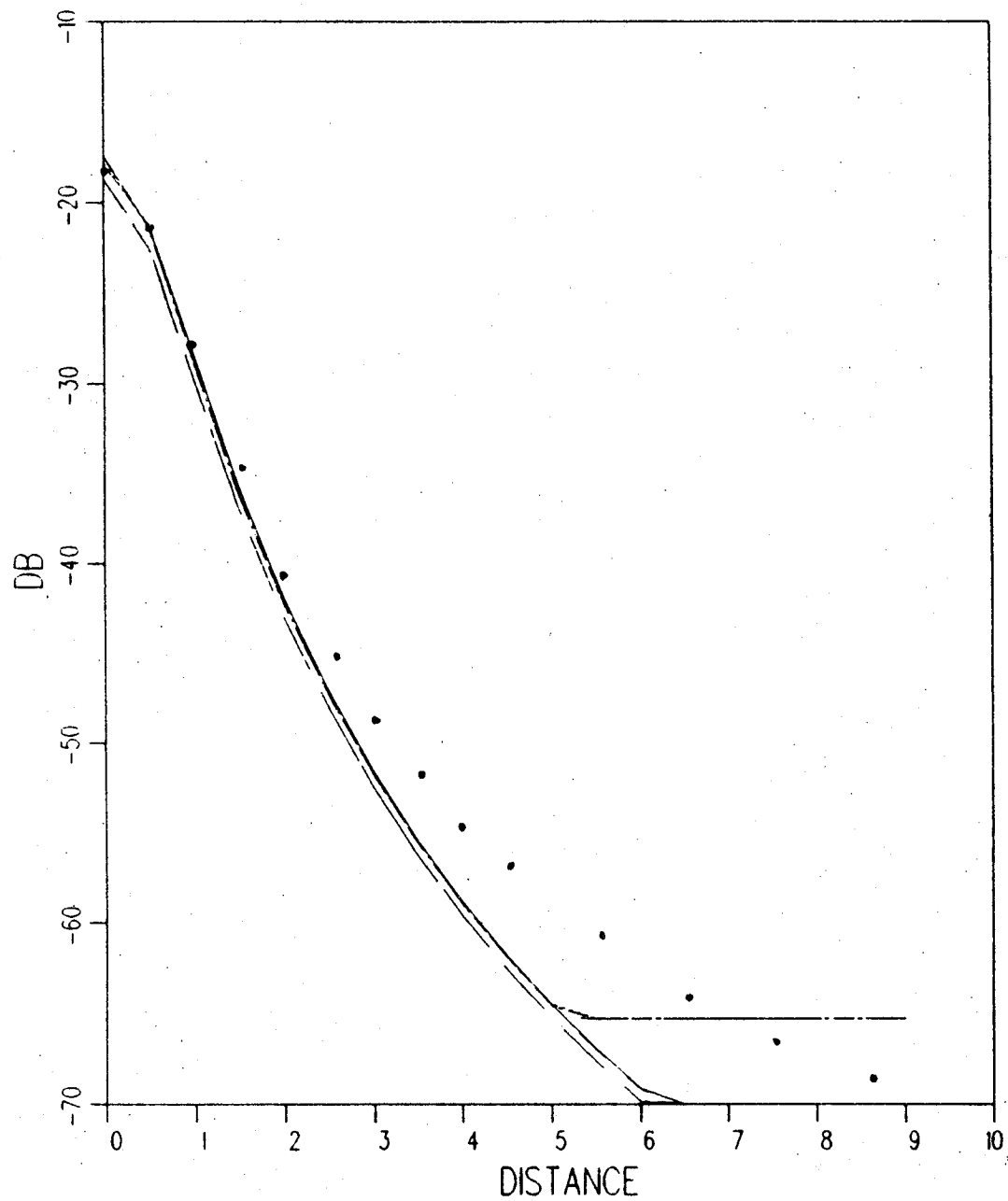


Figure 7.47: The coupling between two half wavelength dipoles in free space as they move apart along the z -axis. The NEC - Method of Moments results are shown as dots.

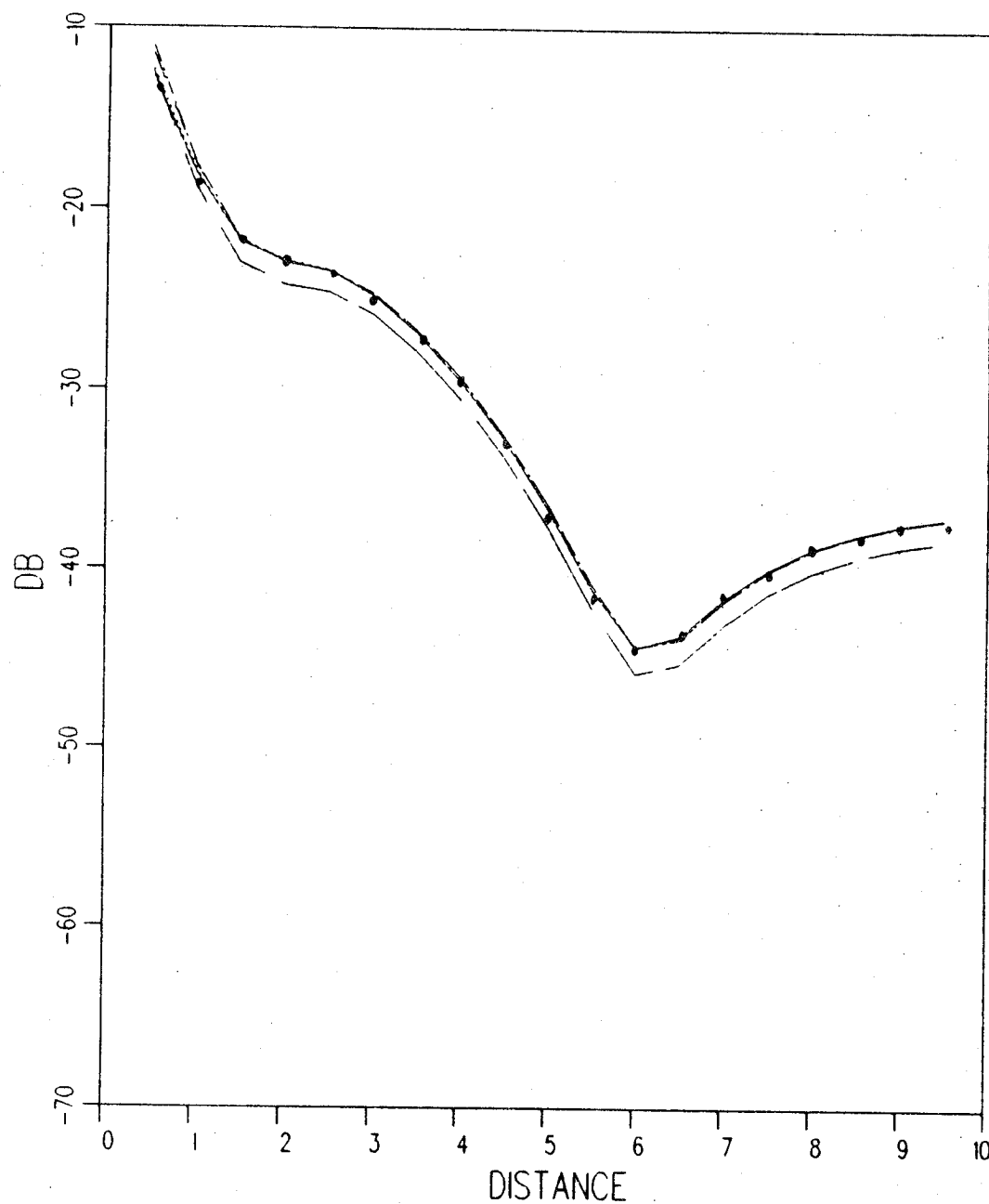


Figure 7.48: The coupling between two half wavelength dipoles over a infinite ground plane as they move apart along the x -axis. The NEC - Method of Moments results are shown as dots.

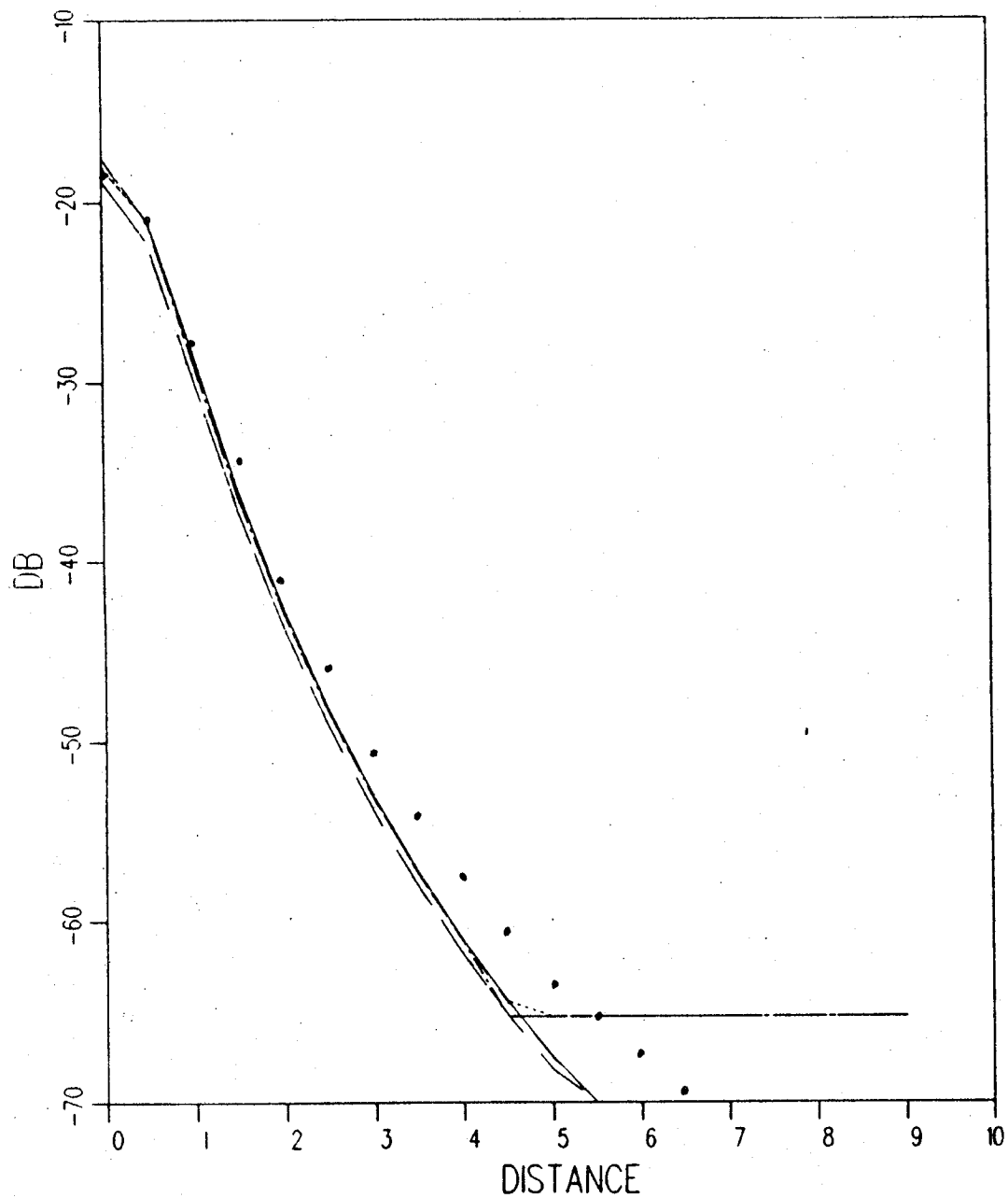


Figure 7.49: The coupling between two half wavelength dipoles over a infinite ground plane as they move apart along the z-axis. The NEC - Method of Moments results are shown as dots.

ORIGINAL PAGE IS
OF POOR QUALITY

246

Ex. 11A

.....

.....

ANTENNA COUPLING VIA THE REACTION PRINCIPLE

THE FIELDS ARE REFERENCED TO THE PATTERN COORDINATE SYSTEM

X	Y	Z	MAGNITUDE	PHASE	MAG. $\times 10^2$	DB
0.500	0.000	0.000	2.1186E-03	-161.65	5.2964E-02	-12.76
1.000	0.000	0.000	1.1724E-03	21.08	1.6220E-02	-17.90
1.500	0.000	0.000	8.0008E-04	-157.64	7.5533E-03	-21.22
2.000	0.000	0.000	6.0533E-04	23.07	4.3238E-03	-23.64
2.500	0.000	0.000	4.8630E-04	-156.49	2.7905E-03	-25.84
3.000	0.000	0.000	4.0620E-04	23.81	1.9470E-03	-27.11
3.500	0.000	0.000	3.4868E-04	-155.97	1.4346E-03	-28.43
4.000	0.000	0.000	3.0638E-04	24.19	1.1004E-03	-29.58
4.500	0.000	0.000	2.7163E-04	-155.68	8.7063E-04	-30.60
5.000	0.000	0.000	2.4459E-04	24.42	7.0589E-04	-31.51
5.500	0.000	0.000	2.2243E-04	-155.50	5.8381E-04	-32.34
6.000	0.000	0.000	2.0395E-04	24.58	4.9083E-04	-33.09
6.500	0.000	0.000	1.8831E-04	-155.37	4.1841E-04	-33.78
7.000	0.000	0.000	1.7489E-04	24.69	3.6090E-04	-34.43
7.500	0.000	0.000	1.6325E-04	-155.27	3.1498E-04	-35.02
8.000	0.000	0.000	1.5307E-04	24.77	2.7646E-04	-35.58
8.500	0.000	0.000	1.4408E-04	-155.20	2.4494E-04	-36.11
9.000	0.000	0.000	1.3608E-04	24.83	2.1852E-04	-36.61
9.500	0.000	0.000	1.2893E-04	-155.14	1.9615E-04	-37.07

.....

.....

Figure 7.50: Line printer output for the coupling between two dipoles in free space as they move apart in the x direction. The dipoles are represented by a numerical integration of seven segments apiece and the modified Frii's transmission formula is used to represented the coupling.

7.14 Example 11B: Antenna Coupling

This example illustrates the use of an array factor approximation to represent the source and receiver dipoles in the same situation as Example 11A. The same currents obtained from the method of moments as are used here. The data set is shown using the Linville method of representing the coupling. The input data is given by

```

CM:  EXAMPLE 11B.
CE:  TWO HALF-WAVELENGTH DIPOLE ANTENNAS:  CASE 1.
US:
0
SA:  SOURCE ARRAYED
F,F,F
7
0.,0.,0.
0.,0.,-.07143
0.,0.,-.1429
0.,0.,-.2143
0.,0.,.07143
0.,0.,.1429
0.,0.,.2143
0.,0.,90.,0.
-1.,.07143,0.
1.0551E-02,-29.246
9.8472E-03,-31.777
7.2367E-03,-33.996
2.9010E-03,-35.584
9.8472E-03,-31.777
7.2367E-03,-33.996
2.9010E-03,-35.584
RA:  RECEIVER ARRAYED
F,F,F
7
0.,0.,0.
0.,0.,-.07143
0.,0.,-.1429
0.,0.,-.2143
0.,0.,.07143

```

0.,0.,.1429
0.,0.,.2143
0.,0.,90.,0.
-1.,.07143,0.
1.0551E-02,-29.246
9.8472E-03,-31.777
7.2367E-03,-33.996
2.9010E-03,-35.584
9.8472E-03,-31.777
7.2367E-03,-33.996
2.9010E-03,-35.584
PN: NEAR-ZONE PATTERN
0.,0.,0.
0.,0.,90.,0.
T
0.5,0.,0.
0.5,0.,0.
19
PR: TERMINAL CURRENT AND IMPEDANCE (LINVILLE METHOD)
4
(9.20585E-03,-5.15474E-03),(9.20585E-03,-5.15474E-03)
(82.6979,46.3060),(82.6979,46.3060)
PP:
T
T,5.0,6.0
0.,10.,1.
-70.,-10.,10.
XQ: EXECUTE CODE
CE: TWO HALF-WAVELENGTH DIPOLE ANTENNAS: CASE 2.
PN: NEAR-ZONE PATTERN
0.,0.,0.
0.,0.,90.,0.
T
1.0,0.,0.
0.,0.,.5
19
XQ: EXECUTE CODE
CE: TWO HALF-WAVELENGTH DIPOLE ANTENNAS: CASE 3.
RT: TRANSLATE AXES 1.25 METERS DOWN


```
0.,0.,-1.25
0.,0.,90.,0.
GP: INFINITE GROUND PLANE
0
PN: NEAR-ZONE PATTERN
0.,0.,0.
0.,0.,90.,0.
T
0.5,0.,0.
0.5,0.,0.
19
XQ: EXECUTE CODE
CE: TWO HALF-WAVELENGTH DIPOLE ANTENNAS: CASE 4.
PN: NEAR-ZONE PATTERN
0.,0.,0.
0.,0.,90.,0.
T
1.0,0.,0.
0.,0.,.5
19
XQ: EXECUTE CODE
EN: END CODE
```

The results for this particular data set are shown in Figure 7.46, 7.47, 7.48, and 7.49. The results for the Frii's normalization is shown as intermediate sized dashes and the Linville normalization method by a dot dashed line.

7.15 Example 11C: Antenna Coupling

This example used to illustrate the pattern factor representation of the dipoles in Example 11A. The current at the terminal of the dipoles are obtained from the method of moments code. The input data is given by

```

CM:  EXAMPLE 11C.
CE:  TWO HALF-WAVELENGTH DIPOLE ANTENNAS:  CASE 1.
US:
0
SG:  SOURCE GEOMETRY--TRANSMITTER
0.,0.,0.
0.,0.,90.,0.
-2.,.5,0.
1.0551E-2,-29.246
RG:  RECEIVE GEOMETRY--RECEIVER
0.,0.,0.
0.,0.,90.,0.
-2.,.5,0.
1.0551E-2,-29.246
PN:  NEAR-ZONE PATTERN
0.,0.,0.
0.,0.,90.,0.
T
0.5,0.,0.
0.5,0.,0.
19
PP:
T
T,5.0,6.0
0.,10.,1.
-70.,-10.,10.
PR:  POWER RADIATED (MODIFIED FRII'S METHOD)
3
4.6029E-3,4.6029E-3
XQ:  EXECUTE CODE
CE:  TWO HALF-WAVELENGTH DIPOLE ANTENNAS:  CASE 2.
PN:  NEAR-ZONE PATTERN
0.,0.,0.

```

```
0.,0.,90.,0.
T
1.0,0.,0.
0.,0.,.5
19
XQ: EXECUTE CODE
CE: TWO HALF-WAVELENGTH DIPOLE ANTENNAS: CASE 3.
RT: TRANSLATE AXES 1.25 METERS DOWN
0.,0.,-1.25
0.,0.,90.,0.
GP: INFINITE GROUND PLANE
0
PN: NEAR-ZONE PATTERN
0.,0.,0.
0.,0.,90.,0.
T
0.5,0.,0.
0.5,0.,0.
19
XQ: EXECUTE CODE
CE: TWO HALF-WAVELENGTH DIPOLE ANTENNAS: CASE 4.
PN: NEAR-ZONE PATTERN
0.,0.,0.
0.,0.,90.,0.
T
1.0,0.,0.
0.,0.,.5
19
XQ: EXECUTE CODE
EN: END CODE
```

The results for this particular data set are shown in Figure 7.46, 7.47, 7.48, and 7.49. The results for the Frii's normalization is shown as long dashes and the Linville normalization method by a triple dot dashed line.

7.16 Example 12: NEC - MM Input

This example illustrates the use of the **SM** command. The geometry is four electric dipoles in the presence of a square plate over an infinite ground plane as shown in Figure 7.51. This represents a satellite type antenna. The currents in part A of this example are specified by the NEC - Moment Method Code [14] for four dipoles over an infinite ground plane. Part B of this example represents the dipoles by their analytic pattern using the **SG** command. The input data is given by

```

CE:  NEC INPUT TEST, EXAMPLE 12A.
PF:  PHI=0  PATTERN CUT
0.,0.,90.,0.
F,0.
0.,1.,91
FR:
0.2998
UN:
3
US:
0
RD:
150.
GP:  GROUND PLANE
0
RT:
0.,0.,28.5
0.,0.,90.,0.
PG:
4,0
25.,-25.,0.
25.,25.,0.
-25.,25.,0.
-25.,-25.,0.
UN:
1
PP:
T
F,90.,4.35

```

0,90,30

-25.,15.,10.

SM: NEC MOMENT METHOD INPUT

.001535

20

-.47752	-.35560	.20637	.06096	.00000	.00000
-.41656	-.35560	.20637	.06096	.00000	.00000
-.35560	-.35560	.20637	.06096	.00000	.00000
-.29464	-.35560	.20637	.06096	.00000	.00000
-.23368	-.35560	.20637	.06096	.00000	.00000
.23368	-.35560	.20637	.06096	.00000	.00000
.29464	-.35560	.20637	.06096	.00000	.00000
.35560	-.35560	.20637	.06096	.00000	.00000
.41656	-.35560	.20637	.06096	.00000	.00000
.47752	-.35560	.20637	.06096	.00000	.00000
-.47752	.35560	.20637	.06096	.00000	.00000
-.41656	.35560	.20637	.06096	.00000	.00000
-.35560	.35560	.20637	.06096	.00000	.00000
-.29464	.35560	.20637	.06096	.00000	.00000
-.23368	.35560	.20637	.06096	.00000	.00000
.23368	.35560	.20637	.06096	.00000	.00000
.29464	.35560	.20637	.06096	.00000	.00000
.35560	.35560	.20637	.06096	.00000	.00000
.41656	.35560	.20637	.06096	.00000	.00000
.47752	.35560	.20637	.06096	.00000	.00000
.3288E-3	.1796E-2				
.6564E-3	.4092E-2				
.7673E-3	.5621E-2				
.6735E-3	.4089E-2				
.3462E-3	.1794E-2				
.3462E-3	.1794E-2				
.6735E-3	.4089E-2				
.7673E-3	.5621E-2				
.6564E-3	.4092E-2				
.3288E-3	.1796E-2				
.3288E-3	.1796E-2				
.6564E-3	.4092E-2				
.7673E-3	.5621E-2				
.6735E-3	.4089E-2				

```

      .3462E-3   .1794E-2
      .3462E-3   .1794E-2
      .6735E-3   .4089E-2
      .7673E-3   .5621E-2
      .6564E-3   .4092E-2
      .3288E-3   .1796E-2
XQ:
NG:  REMOVE GROUND PLANE
XQ:
CE:  NEC TEST, EXAMPLE 12B.
RT:  RESET ORIGIN FOR GROUND PLANE
     0.,0.,0.
     0.,0.,90.,0.
GP:  REPLACE GROUND PLANE
     0
RT:  RESET FOR SOURCES
     0.,0.,28.5
     0.,0.,90.,0.
NS:  REMOVE NEC SOURCES
US:
     1
PR:
     1
     .001535
SG:  SOURCE #1
     -.35560,-.35560,.20637
     90.,0.,90.,90.
     -2,0.3048,0.
     0.005673,82.2
SG:  SOURCE #2
     .35560,-.35560,.20637
     90.,0.,90.,90.
     -2,0.3048,0.
     0.005673,82.2
SG:  SOURCE #3
     -.35560,.35560,.20637
     90.,0.,90.,90.
     -2,0.3048,0.
     0.005673,82.2

```

```
SG:  SOURCE #4
0.35560,.35560,.20637
90.,0.,90.,90.
-2,0.3048,0.
0.005673,82.2
XQ:
EN:
```

The directive gain normalized to isotropic is plotted in Figure 7.52 for the $\phi = 0$ degree plane using the method of moments representation for the dipoles. The result is compared against the infinite ground plane case and the case for the plate in free space which is given as the second execution in the input set. Similarly, the directive gains for the three different cases are plotted in Figure 7.53 for the $\phi = 90$ degree plane. The calculations using the analytic representation of the dipoles gives approximately the same results. The directive gain is within approximately 0.5 dB throughout the entire pattern range. The pattern shape is essentially identical to the one in Figure 7.52 for the four dipoles over a plate over an infinite ground plane so the pattern is not shown.

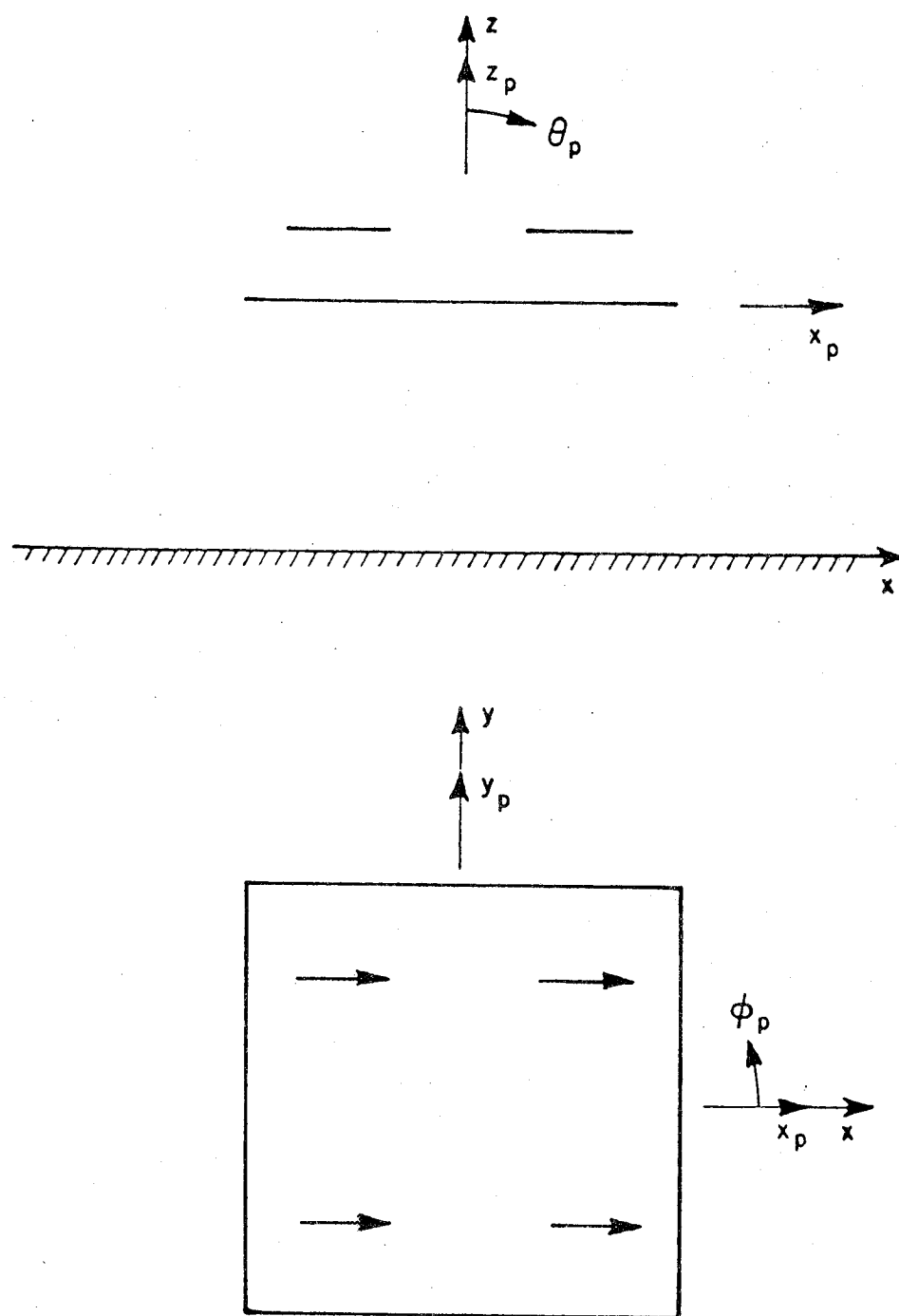


Figure 7.51: Geometry for the problems of dipoles over a square plate and infinite ground plane showing the side and top view.

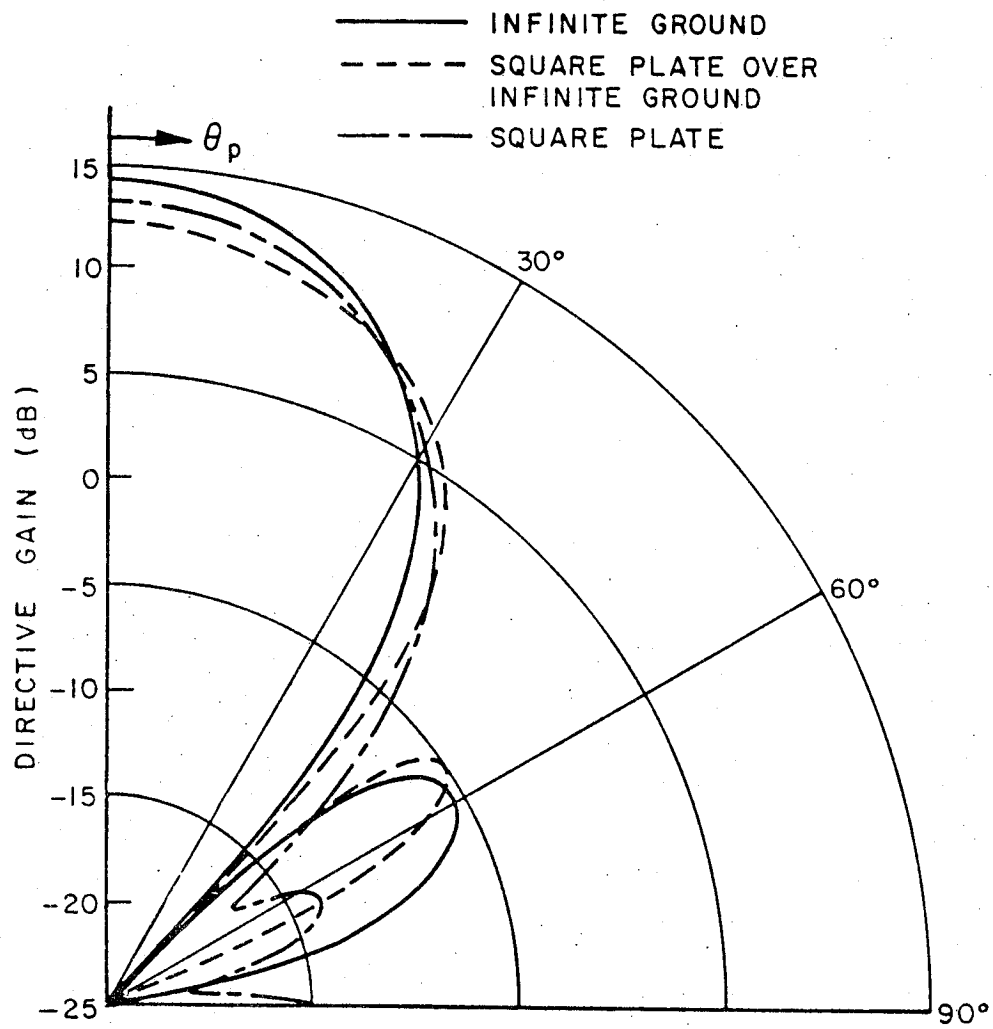


Figure 7.52: Comparison of the directive gain of four dipoles over an infinite ground with four dipoles over a square plate over an infinite ground and four dipoles over a square plate alone ($\phi = 0$ degrees, vertical polarization).

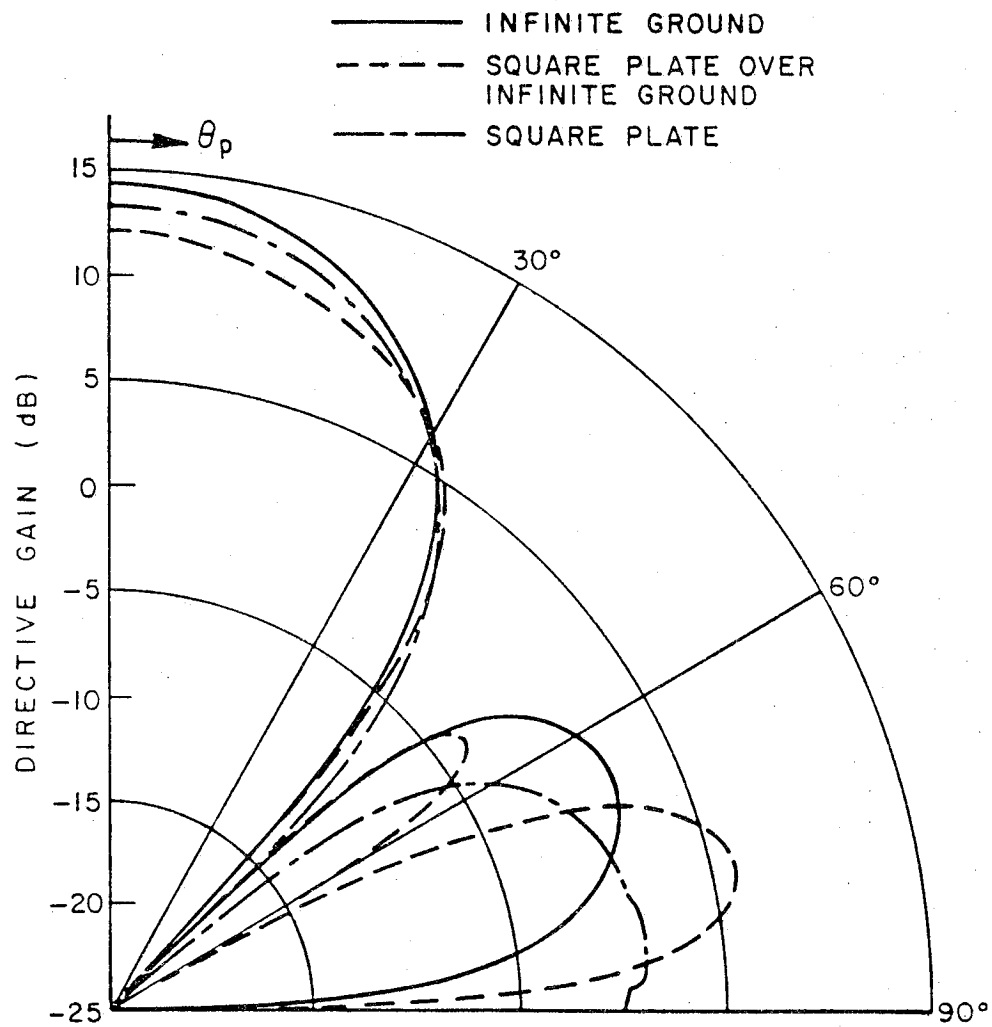


Figure 7.53: Comparison of the directive gain of four dipoles over an infinite ground with four dipoles over a square plate over an infinite ground and four dipoles over a square plate alone ($\phi = 90$ degrees, horizontal polarization).

7.17 Example 13: Cylinder - Dipole

This example considers an electric dipole in the presence of a finite circular cylinder as shown in Figures 7.54 and 7.55. The pattern is taken in two different cuts and the source is placed in two different positions. The input data is given by

CE: CYLINDER TEST, EXAMPLE 13A.

US:

0

FR:

9.94

PF:

0.,0.,90.,0.

T,90.

0.,1.,361

SG:

0.,0.19,0.

90.,0.,180.,0.

-2,0.5,0.

1.,0.

CG:

0.,0.,0.

0.,0.,90.,0.

0.1,0.1

-0.11,90.,0.11,90.

LP:

T

PP:

T

T,5.,2.5

0.,360.,30.

-40.,0.,10.

XQ:

CE: CYLINDER TEST, EXAMPLE 13B.

PF: CHANGE PATTERN CUT

0.,0.,90.,0.

F,90.

0.,1.,361

```
XQ:
CE:  CYLINDER TEST, EXAMPLE 13C.
NS:  CALL FOR NEW SOURCE
SG:
0.076,0.,0.2
90.,0.,180.,0.
-2,0.5,0.
1.,0.
XQ:
EN:
```

The line printer output of the results for Example 13A are shown in Figures 7.56 and 7.57. The print out is for only half the results in 10 degree increments associated with the geometry illustrated in Figure 7.58. The calculated results are compared with measured results [22] in the pattern figures. The E_{ϕ_r} pattern for Example 13A is shown in Figure 7.58. The E_{θ_r} pattern for Example 13B is shown in Figure 7.59. The E_{ϕ_r} pattern for Example 13C is shown in Figure 7.60. The E_{θ_r} pattern for all three cases are not shown because they are of negligible value.

Ex. 13

261

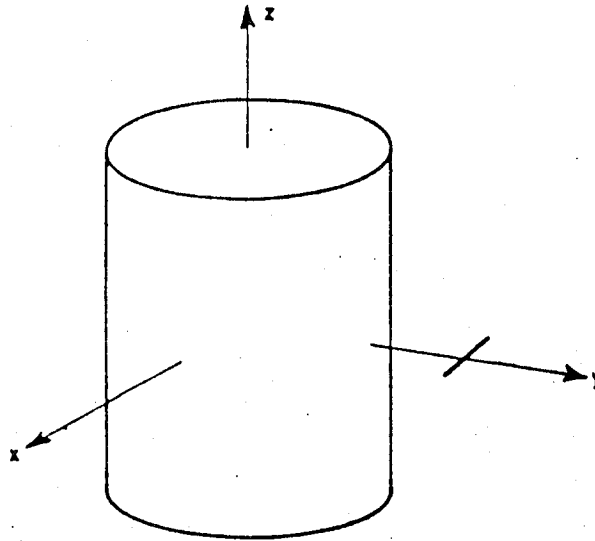


Figure 7.54: An electric dipole parallel to the x -axis on the side of a finite circular cylinder for Example 13A and 13B.

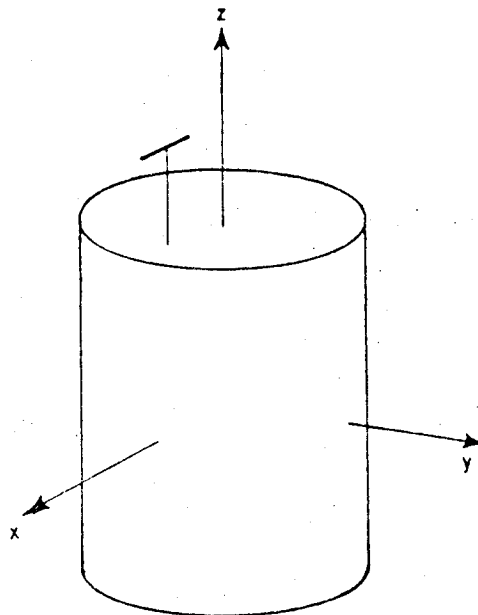


Figure 7.55: An electric dipole parallel to the x -axis on the top of a finite circular cylinder for Example 13C.

ORIGINAL PAGE IS
OF POOR QUALITY

262

Ex. 13

THE FAR ZONE ELECTRIC FIELD

THE FIELDS ARE REFERENCED TO THE PATTERN COORDINATE SYSTEM

		E-THETA			E-PHI		
THETA	PHI	MAGNITUDE	PHASE	DB	MAGNITUDE	PHASE	DB
90.00	90.00	5.3957E-06	-49.09	-134.13	2.6564E+01	-173.57	-0.29
90.00	100.00	2.0531E-06	-22.53	-142.53	3.4232E+01	132.40	1.91
90.00	110.00	3.7933E-06	-123.33	-137.19	6.7663E+01	31.31	7.83
90.00	120.00	3.1179E-06	81.86	-138.90	8.0613E+01	-96.63	9.35
90.00	130.00	3.5896E-06	-153.73	-137.67	1.2476E+01	62.82	-6.85
90.00	140.00	1.8402E-06	-72.00	-143.48	6.4112E+01	99.49	7.37
90.00	150.00	6.8031E-06	-15.20	-132.12	5.1980E+00	-13.10	-14.46
90.00	160.00	5.7322E-06	-51.55	-133.61	4.1858E+01	172.58	3.66
90.00	170.00	2.6275E-06	94.03	-140.38	2.5914E+01	50.55	-0.50
90.00	180.00	4.7427E-04	-89.37	-95.25	2.1538E+01	-136.08	-2.11
90.00	190.00	7.7974E-06	-147.43	-130.93	9.6212E+00	33.72	-9.11
90.00	200.00	3.0309E-06	-51.88	-139.14	2.9836E+01	-146.50	0.72
90.00	210.00	5.1042E-06	-153.45	-134.62	1.5646E+01	-131.22	-4.89
90.00	220.00	4.6260E-06	-91.49	-135.47	3.7199E+01	-117.25	2.64
90.00	230.00	2.6845E-06	-4.57	-140.20	4.1409E+01	-19.40	3.57
90.00	240.00	1.0269E-06	106.54	-148.54	2.7774E+01	102.34	0.10
90.00	250.00	4.0082E-07	-136.11	-156.71	1.4243E+01	-136.79	-5.70
90.00	260.00	1.5494E-07	-17.39	-164.97	1.4354E+01	-14.46	-5.63
90.00	270.00	1.6078E-05	116.52	-124.65	1.7089E+01	151.92	-4.12

Figure 7.56: Line printer output of the electric fields of Example 13A.

.....

.....

TOTAL RADIATION INTENSITY IN DB

THE FIELDS ARE REFERENCED TO THE PATTERN COORDINATE SYSTEM

YMET	PMI	MAJOR	MINOR	TOTAL	AXIAL RATIO	TYLT ANG	SENSE
90.00	90.00	-0.29	-100.00	-0.29	0.00000	-90.00	LINEAR
90.00	100.00	1.91	-100.00	1.91	0.00000	-90.00	LINEAR
90.00	110.00	7.83	-100.00	7.83	0.00000	-90.00	LINEAR
90.00	120.00	9.35	-100.00	9.35	0.00000	-90.00	LINEAR
90.00	130.00	-6.85	-100.00	-6.85	0.00000	-90.00	LINEAR
90.00	140.00	7.37	-100.00	7.37	0.00000	-90.00	LINEAR
90.00	150.00	-14.46	-100.00	-14.46	0.00000	90.00	LINEAR
90.00	160.00	3.66	-100.00	3.66	0.00000	-90.00	LINEAR
90.00	170.00	-0.50	-100.00	-0.50	0.00000	90.00	LINEAR
90.00	180.00	-2.11	-100.00	-2.11	0.00000	90.00	LINEAR
90.00	190.00	-9.11	-100.00	-9.11	0.00000	-90.00	LINEAR
90.00	200.00	0.72	-100.00	0.72	0.00000	-90.00	LINEAR
90.00	210.00	-4.89	-100.00	-4.89	0.00000	90.00	LINEAR
90.00	220.00	2.64	-100.00	2.64	0.00000	90.00	LINEAR
90.00	230.00	3.57	-100.00	3.57	0.00000	90.00	LINEAR
90.00	240.00	0.10	-100.00	0.10	0.00000	90.00	LINEAR
90.00	250.00	-5.70	-100.00	-5.70	0.00000	90.00	LINEAR
90.00	260.00	-5.63	-100.00	-5.63	0.00000	90.00	LINEAR
90.00	270.00	-4.12	-100.00	-4.12	0.00000	90.00	LINEAR

.....

.....

Figure 7.57: Line printer output of the total radiation intensity of Example 13A.

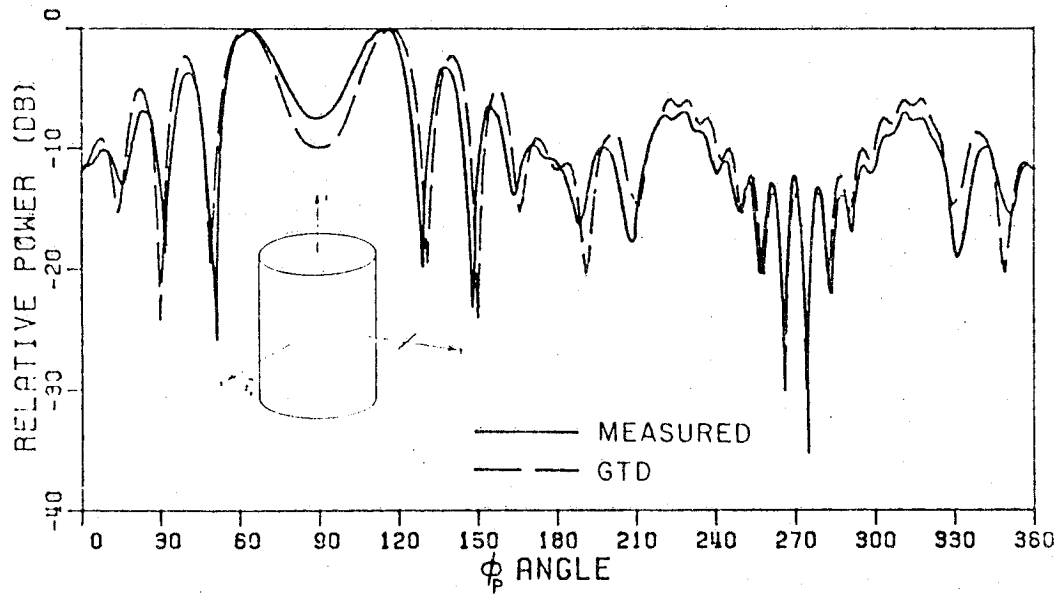


Figure 7.58: Comparison of measured (Bach) and calculated E_{ϕ_p} radiation pattern of an electric dipole on the y -axis parallel to the x -axis in the presence of a finite circular cylinder (pattern taken in the $x - y$ plane).

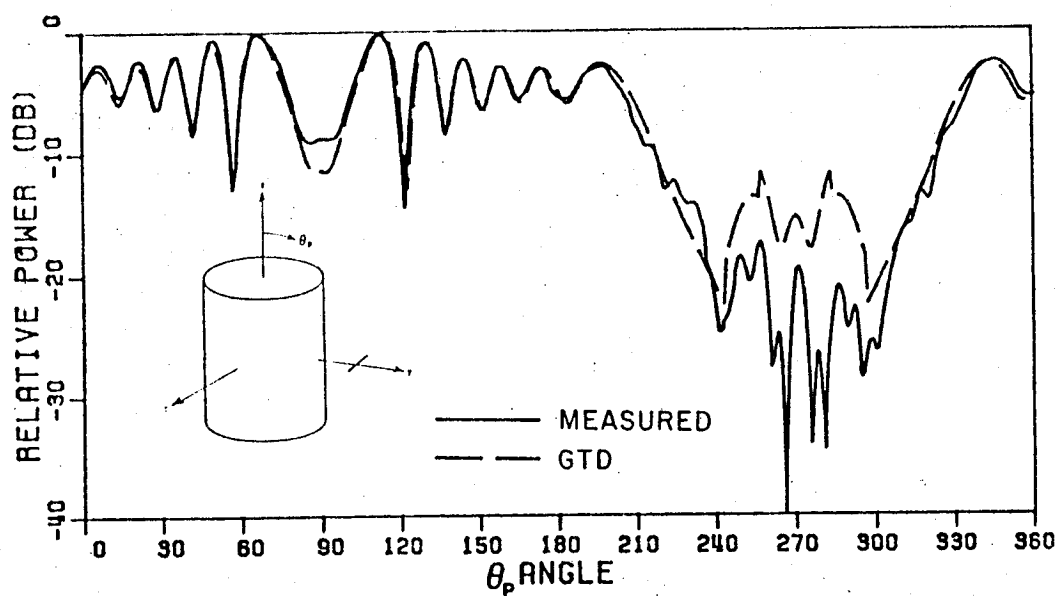


Figure 7.59: Comparison of measured (Bach) and calculated E_{ϕ_r} radiation pattern of an electric dipole on the y -axis parallel to the x -axis in the presence of a finite circular cylinder (pattern taken in the $y - z$ plane).

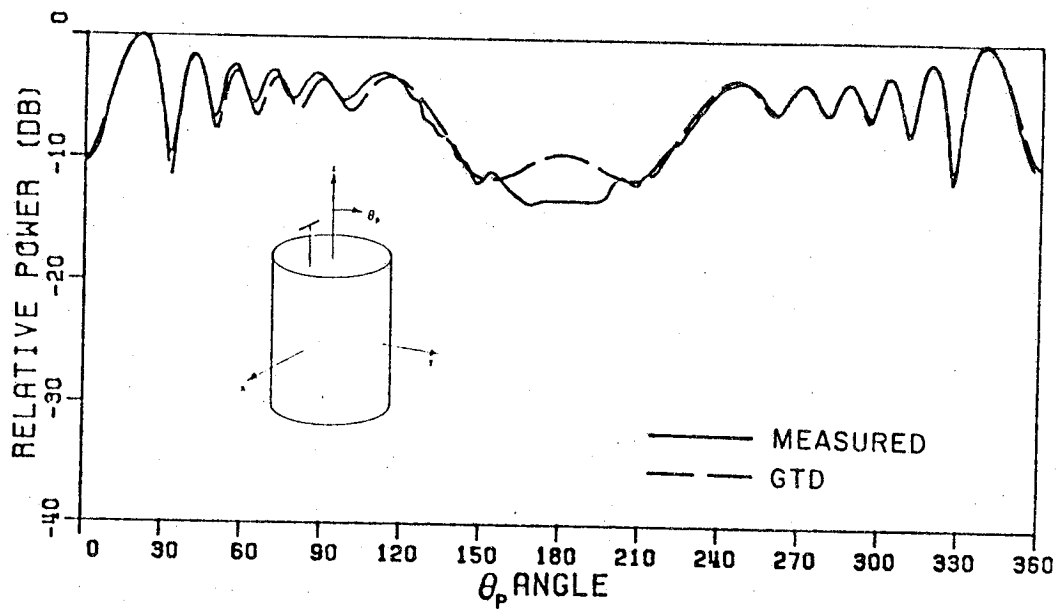


Figure 7.60: Comparison of measured (Bach) and calculated E_{ϕ_p} radiation pattern of an electric dipole parallel to the x -axis mounted above the end cap of a finite circular cylinder (pattern taken in the $y-z$ plane). (VAX 11/750 run time is 2.1 min.)

7.18 Example 14: Elliptic Cylinder

This example considers the pattern of a magnetic dipole in the presence of an elliptic cylinder as shown in Figure 7.61. This example illustrates how the LOUT parameter in the TO command can be used to print out the individual fields reflected and diffracted by the body under consideration. Note, also, that since the units and frequency are not specified in the data set the input is assumed to be given in wavelengths. The input data is given by

```
CE:  ELLIPTIC CYLINDER TEST, EXAMPLE 14.
US:
0
PF:
0.,0.,90.,0.
T,90.
0.,1.,361
CG:
0.,0.,0.
0.,0.,90.,0.
2.,1.
-500.,90.,500.,90.
SG:
2.828,2.828,0.
0.,0.,90.,0.
2,0.5,0.
1.,0.
PP:
T
F,90.,2.5
0.,360.,30.
-40.,0.,10.
XQ:
TO:  PRINT INDIVIDUAL FIELDS AROUND SHADOW BOUNDARY
F,F,T,F
PF:  REDUCE ANGULAR RANGE
0.,0.,90.,0.
T,90.
204.,1.,6
```

XQ:

EN:

The reflected and diffracted fields in the region close to one of the shadow boundaries of the elliptic cylinder, as printed by the line printer, are shown in Figure 7.62. The different types of fields can be interpreted by looking at Tables 4.1 and 4.2. The three pairs of columns of real numbers are the magnitude and phase of the x , y , and z components of the electric fields. The polarization is referred to the reference coordinate system for this type of print out. Notice that the VAX cpu times are interwoven in with the field values.

The E_{ϕ_p} pattern is plotted in Figure 7.63 compared with a moment method solution. The E_{θ_p} pattern is not plotted because it is of negligible value.

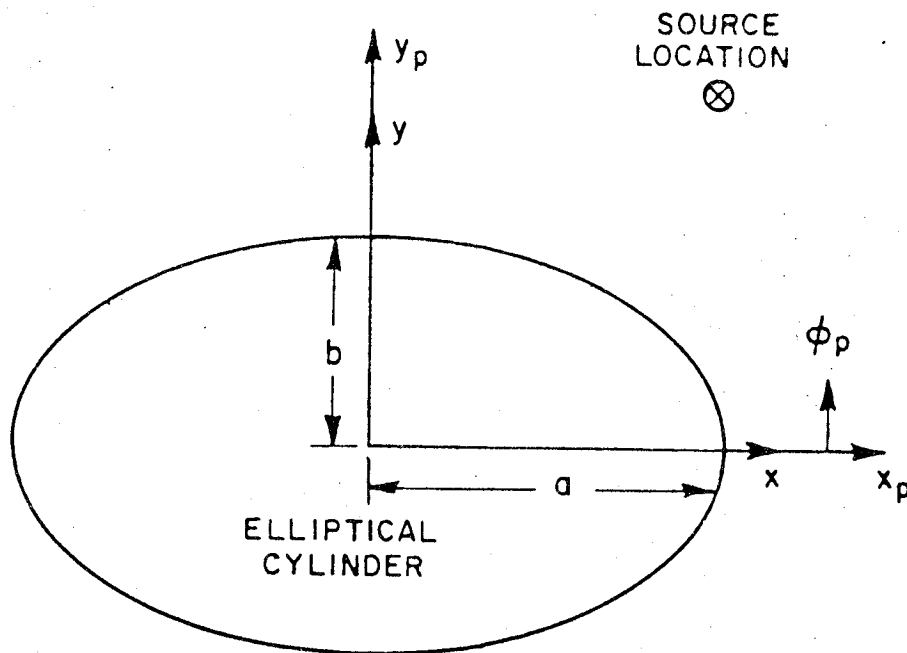


Figure 7.61: Elliptic cylinder configuration excited by a magnetic source parallel to the z -axis.

Ex. 14

269

.....										
* IQ:										
* INCFLD										
INCFLD	0	0	0	0	6.47341E-02	5.847	1.45395E-01	-174.153	1.00000E-10	0.000
SUBTOTAL	1	1	0	0	6.47341E-02	5.847	1.45395E-01	-174.153	1.00000E-10	0.000
INCFLD	0	0	0	0	6.72618E-02	-2.953	1.44243E-01	177.047	1.00000E-10	0.000
SUBTOTAL	1	2	0	0	6.72618E-02	-2.953	1.44243E-01	177.047	1.00000E-10	0.000
INCFLD	0	0	0	0	6.99086E-02	-11.341	1.43334E-01	168.659	1.00000E-10	0.000
SUBTOTAL	1	3	0	0	6.99086E-02	-11.341	1.43334E-01	168.659	1.00000E-10	0.000
* INCFLD = 0.00050 CPU MINUTES										
* RC										
RC	1	2	0	0	1.80137E-02	-179.851	4.04594E-02	0.149	2.77182E-10	176.574
GO	1	2	0	0	4.54787E-03	4.148	1.02147E-02	-175.852	1.00000E-10	0.000
SUBTOTAL	12	1	0	0	1.80137E-02	-179.851	4.04594E-02	0.149	2.77182E-10	176.574
RC	1	2	0	0	2.07452E-02	176.390	4.44882E-02	-3.610	1.77988E-10	171.536
GO	1	2	0	0	3.64205E-03	-3.586	7.81039E-03	176.414	1.00000E-10	0.000
SUBTOTAL	12	2	0	0	2.07452E-02	176.390	4.44882E-02	-3.610	1.77988E-10	171.536
RC	1	2	0	0	2.38092E-02	172.440	4.88162E-02	-7.560	1.00000E-10	0.000
GO	1	2	0	0	2.23463E-03	-11.424	4.58167E-03	168.576	1.00000E-10	0.000
SUBTOTAL	12	3	0	0	2.38092E-02	172.440	4.88162E-02	-7.560	1.00000E-10	0.000
* RC = 0.00050 CPU MINUTES										
* DC										
DC	1	2	0	0	9.64846E-03	-111.448	2.16708E-02	68.552	1.00000E-10	0.000
SUBTOTAL	13	1	0	0	9.64846E-03	-111.448	2.16708E-02	68.552	1.00000E-10	0.000
DC	1	2	0	0	1.02710E-02	-102.821	2.20263E-02	77.179	1.00000E-10	0.000
SUBTOTAL	13	2	0	0	1.02710E-02	-102.821	2.20263E-02	77.179	1.00000E-10	0.000
DC	1	2	0	0	1.09114E-02	-94.132	2.23716E-02	85.868	1.00000E-10	0.000
SUBTOTAL	13	3	0	0	1.09114E-02	-94.132	2.23716E-02	85.868	1.00000E-10	0.000
DC	1	2	0	0	5.23290E-02	-34.080	1.03998E-01	146.107	1.00000E-10	0.000
SUBTOTAL	13	4	0	0	5.23290E-02	-34.080	1.03998E-01	146.107	1.00000E-10	0.000
DC	1	2	0	0	5.46804E-02	-43.010	1.02839E-01	136.990	1.00000E-10	0.000
SUBTOTAL	13	5	0	0	5.46804E-02	-43.010	1.02839E-01	136.990	1.00000E-10	0.000
DC	1	2	0	0	5.64682E-02	-49.915	1.01871E-01	130.085	1.00000E-10	0.000
SUBTOTAL	13	6	0	0	5.64682E-02	-49.915	1.01871E-01	130.085	1.00000E-10	0.000
* DC = 0.00150 CPU MINUTES										
* DU										
* DW										
* DW = 0.00017 CPU MINUTES										
* DE										
DE	1	2	0	0	1.00000E-10	0.000	1.00000E-10	0.000	2.92633E-07	178.433
SUBTOTAL	15	1	0	0	1.00000E-10	0.000	1.00000E-10	0.000	2.92633E-07	178.433
DE	1	2	0	0	1.00000E-10	0.000	1.00000E-10	0.000	2.89034E-07	-177.743
SUBTOTAL	15	2	0	0	1.00000E-10	0.000	1.00000E-10	0.000	2.89034E-07	-177.743
DE	1	2	0	0	1.00000E-10	0.000	1.00000E-10	0.000	2.85322E-07	-173.783
SUBTOTAL	15	3	0	0	1.00000E-10	0.000	1.00000E-10	0.000	2.85322E-07	-173.783
DE	1	2	0	0	1.00000E-10	0.000	1.00000E-10	0.000	2.81488E-07	-169.688
SUBTOTAL	15	4	0	0	1.00000E-10	0.000	1.00000E-10	0.000	2.81488E-07	-169.688
DE	1	2	0	0	1.00000E-10	0.000	1.00000E-10	0.000	2.77525E-07	-165.463
SUBTOTAL	15	5	0	0	1.00000E-10	0.000	1.00000E-10	0.000	2.77525E-07	-165.463
DE	1	2	0	0	1.00000E-10	0.000	1.00000E-10	0.000	2.73421E-07	-161.109
SUBTOTAL	15	6	0	0	1.00000E-10	0.000	1.00000E-10	0.000	2.73421E-07	-161.109
* DE = 0.00183 CPU MINUTES										
* END										
TOTAL	1	1	1	1	5.82077E-09	0.000	2.92910E-07	-1.569	1.05534E-01	-3.249
TOTAL	2	2	2	2	1.86265E-09	0.000	2.89209E-07	2.251	1.08456E-01	-15.403
TOTAL	3	3	3	3	9.31323E-10	90.000	2.85385E-07	6.213	1.12029E-01	-25.960
TOTAL	4	4	4	4	6.08514E-04	-19.364	2.81485E-07	10.314	1.16420E-01	-33.931
TOTAL	5	5	5	5	3.72529E-09	0.000	2.77525E-07	14.537	1.16472E-01	-43.010
TOTAL	6	6	6	6	1.00000E-10	0.000	2.73421E-07	18.891	1.16475E-01	-49.915
* CPU TIME FOR FIELD EXECUTION = 0.00533 MINUTES										
*										

Figure 7.62: See Tables 4.1 and 4.2 for help in interpreting the results. The real numbers represents the magnitude and phase fo the E_x , E_y and E_z fields, respectively.

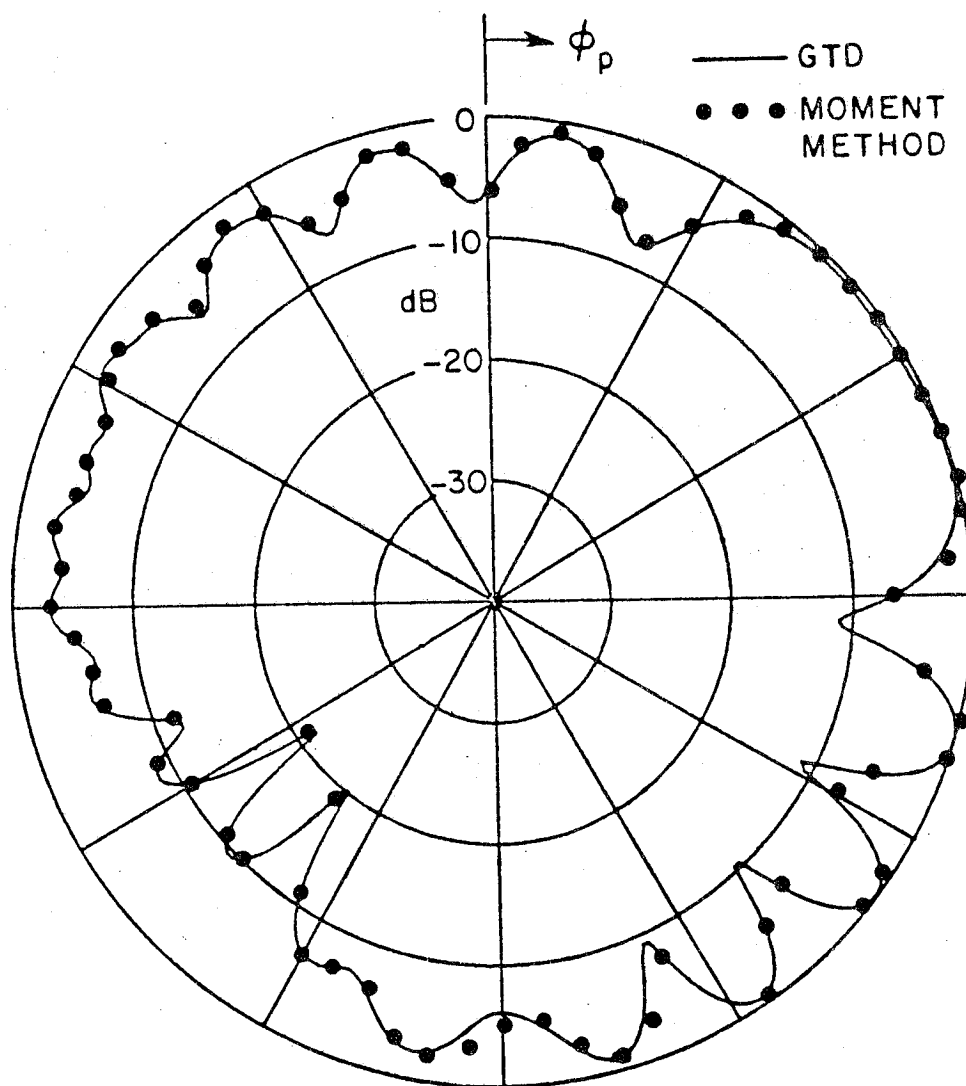


Figure 7.63: Comparison of UTD and moment method results for E_{ϕ_p} pattern. (VAX 8550 run time is 0.23 min and VAX 11/750 run time is 2.7 min.)

7.19 Example 15: Near Zone Cylinder

This example illustrates the near zone pattern effects of a dipole in the presence of a perfectly conducting finite circular cylinder. The results for two different pattern origins and two different ranges are shown. The geometries are illustrated in the inserts of Figures 7.64 to 7.67. The input data is given by

CM: EXAMPLE 15.

CE: NEAR ZONE CYLINDER TEST

UN:

3

FR:

3.985

US:

3

SG:

0.,0.,0.

90.,90.,0.,0.

-2,1.5,0.

1.,0.

CG:

6.5625,0.,0.

0.,0.,90.,0.

1.25,1.25

-9.,90.,8.,90.

PN:

0.,0.,0.

0.,0.,90.,0.

F

36.75,90.,0.

0.,0.,1.

361

LP:

T

PP:

T

T,4.2,2.1

0.,360.,36.

-40.,0.,10.
XQ:
PN:
0.,0.,0.
0.,0.,90.,0.
F
26.25,90.,0.
0.,0.,1.
361
XQ:
PN:
6.5625,0.,0.
0.,0.,90.,0.
F
36.75,90.,0.
0.,0.,1.
361
XQ:
PN:
6.5625,0.,0.
0.,0.,90.,0.
F
26.25,90.,0.
0.,0.,1.
361
XQ:
EN:

The E_{ϕ_p} near zone pattern for a source in the presence of the cylinder with the center of pattern rotation at the source and with a range of 36.75 inches is shown in Figure 7.64. The E_{ϕ_p} near zone pattern with the center of pattern rotation at the source and with a range of 26.25 inches is shown in Figure 7.65. The E_{ϕ_p} near zone pattern with the center of pattern rotation at the center of the cylinder and with a range of 36.75 inches is shown in Figure 7.66. The E_{ϕ_p} near zone pattern with the center of pattern rotation at the center of the cylinder and with a range of 26.25 inches is shown in Figure 7.67. Note that as in Example 7-3 for the near zone plate patterns, changing the pattern origin and range results in relatively small shifts in the position of the peaks and the fine detail. The radial component of the

pattern is present but is not shown since it is much smaller than the ϕ component. In addition, the θ component is negligible and is not shown. The magnitude of the cross polarized terms for the pattern corresponding to Figure 7.64 can be seen in the print out of the fields in Figures 7.68, 7.69 and 7.70. The print out is for a range of ϕ angles of 0 to 180 degrees in steps of 10 degrees in order to save space.

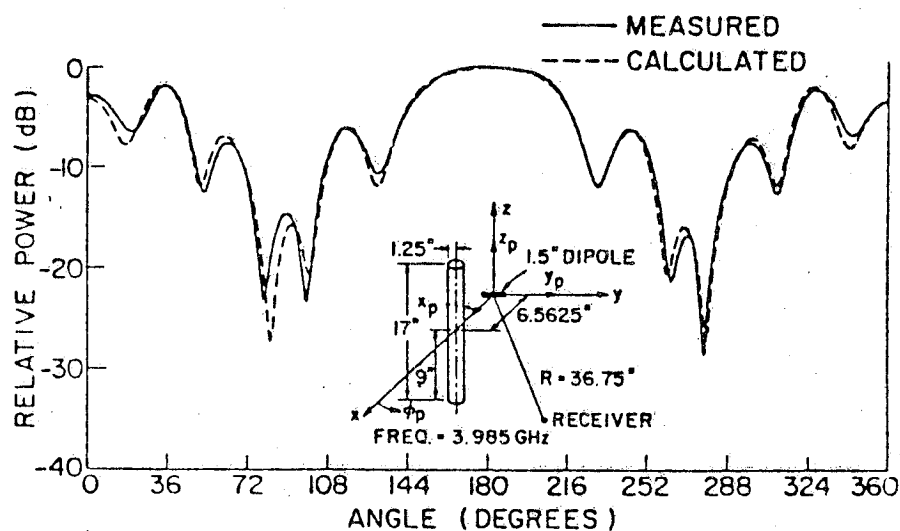


Figure 7.64: Comparison of the measured and calculated E_ϕ radiation pattern in the $x - y$ plane 36.75" from a dipole in the presence of a circular cylinder.

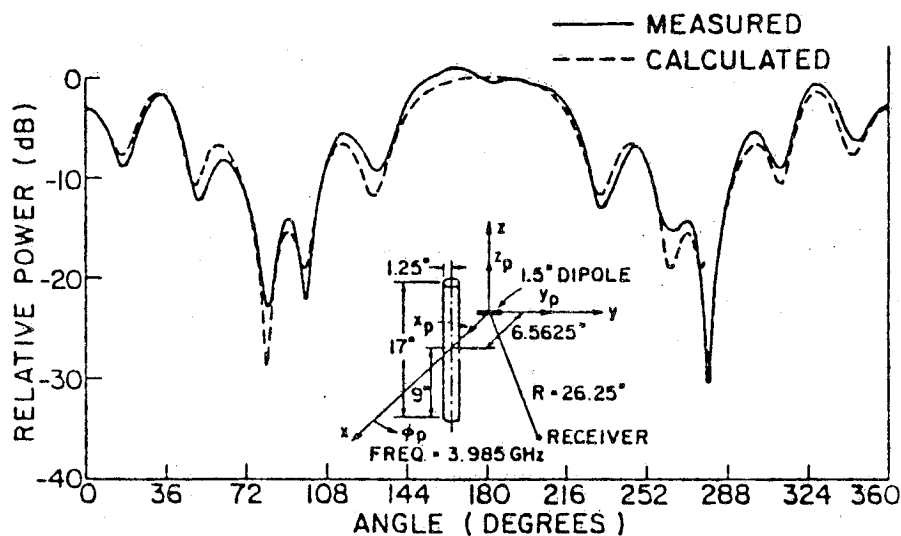


Figure 7.65: Comparison of the measured and calculated E_ϕ radiation pattern in the $x - y$ plane 26.25" from a dipole in the presence of a circular cylinder.

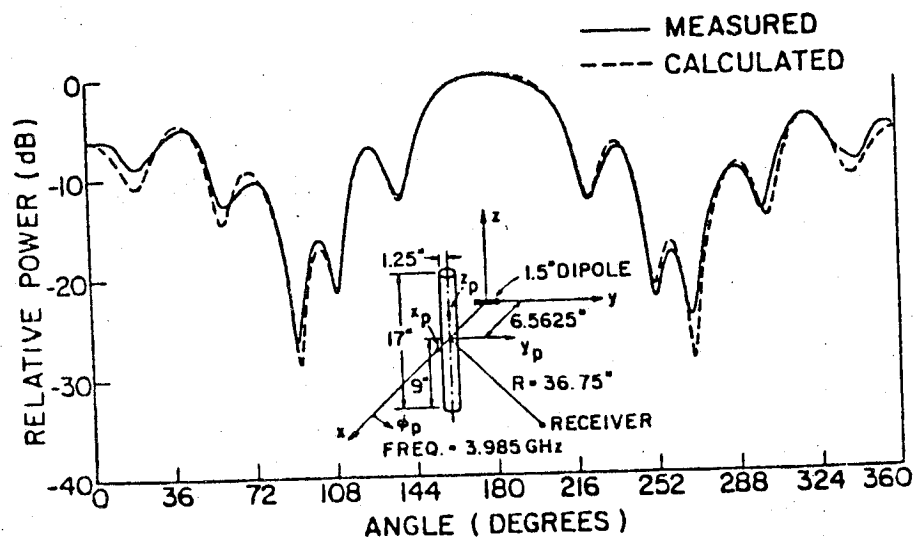


Figure 7.66: Comparison of the measured and calculated E_ϕ radiation pattern in the $x - y$ plane $36.75''$ from a circular cylinder in the presence of a dipole.

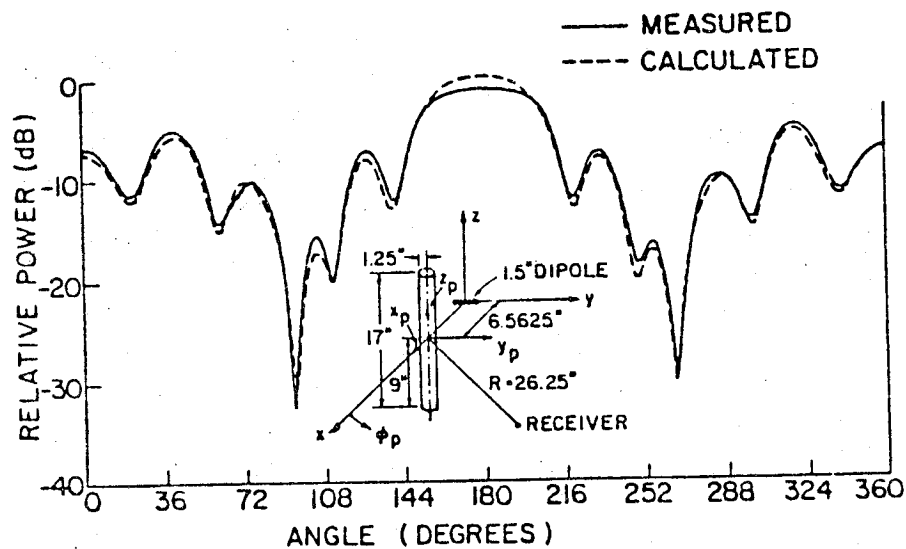


Figure 7.67: Comparison of the measured and calculated E_ϕ radiation pattern in the $x - y$ plane $26.25''$ from a circular cylinder in the presence of a dipole.

ORIGINAL PAGE IS
OF POOR QUALITY

276

Ex. 15

NEAR ZONE ELECTRIC FIELD

THE FIELDS ARE REFERENCED TO THE PATTERN COORDINATE SYSTEM

R	THETA	PHI	MAGNITUDE	PHASE	DB	MAGNITUDE	PHASE	DB	MAGNITUDE	PHASE	DB
0.933	90.000	0.000	1.1921E-07	90.00	-138.47	9.7848E-07	84.48	-120.19	5.5758E+01	85.03	34.93
0.933	90.000	10.000	1.6085E+00	-156.34	4.13	7.2616E-07	97.15	-122.78	4.4610E+01	90.75	32.99
0.933	90.000	20.000	2.0716E+00	119.89	6.33	8.4354E-07	160.74	-121.48	3.5352E+01	132.53	30.97
0.933	90.000	30.000	2.0980E+00	15.46	6.44	1.4222E-06	158.17	-116.94	6.1845E+01	138.49	35.83
0.933	90.000	40.000	2.2258E+00	-112.33	6.95	1.3533E-06	137.56	-117.37	5.5728E+01	109.47	34.92
0.933	90.000	50.000	2.3747E+00	117.43	7.51	9.7038E-07	113.84	-120.26	2.1009E+01	124.30	26.45
0.933	90.000	60.000	1.8058E+00	-15.90	5.13	2.7776E+00	118.59	8.87	3.5945E+01	141.28	31.11
0.933	90.000	70.000	1.0393E+00	-130.82	0.34	2.8531E+00	2.33	9.11	2.5220E+01	105.91	28.04
0.933	90.000	80.000	9.4597E-01	159.85	-0.48	2.5918E+00	-119.24	8.27	5.1828E+00	41.53	14.29
0.933	90.000	90.000	1.6632E+00	51.82	4.42	2.2860E+00	118.20	7.18	1.2732E+01	-156.95	22.10
0.933	90.000	100.000	2.1829E+00	-73.06	6.78	1.9717E+00	-1.25	5.90	7.9653E+00	77.66	18.02
0.933	90.000	110.000	2.3147E+00	165.63	7.29	1.6775E+00	-114.98	4.49	3.2989E+01	-37.30	30.37
0.933	90.000	120.000	2.1403E+00	54.57	6.61	1.4003E+00	140.40	2.92	3.7246E+01	-82.63	31.42
0.933	90.000	130.000	1.7935E+00	-42.36	5.07	1.1398E+00	47.49	1.14	2.0754E+01	-69.55	26.34
0.933	90.000	140.000	1.3895E+00	-122.67	2.86	8.9396E-01	-31.52	-0.97	4.0975E+01	-36.15	32.25
0.933	90.000	150.000	1.0031E+00	175.24	0.03	6.6003E-01	-94.82	-3.61	6.3821E+01	-45.50	36.10
0.933	90.000	160.000	6.6089E-01	131.84	-3.73	4.3505E-01	-141.02	-7.23	7.4965E+01	-54.85	37.50
0.933	90.000	170.000	3.6484E-01	107.63	-8.76	2.1604E-01	-169.13	-13.31	7.9745E+01	-60.06	38.03
0.933	90.000	180.000	5.8988E-07	-97.44	-124.58	1.1624E+00	-153.73	1.31	8.0458E+01	-62.15	38.11

Figure 7.68: Line printer output of the near zone electric fields of Example 15.

NEAR ZONE MAGNETIC FIELD

THE FIELDS ARE REFERENCED TO THE PATTERN COORDINATE SYSTEM

R	TNETA	PHI	I			TNETA			PHI		
			MAGNITUDE	PHASE	DB	MAGNITUDE	PHASE	DB	MAGNITUDE	PHASE	DB
0.933	90.000	0.000	1.0000E-10	0.00	-200.00	1.4803E-01	-94.97	-16.59	2.5933E-09	84.48	-171.72
0.933	90.000	10.000	1.0809E-10	-161.06	-199.32	1.1841E-01	-89.32	-18.53	1.9247E-09	97.29	-174.31
0.933	90.000	20.000	2.0471E-10	90.00	-193.78	9.3499E-02	-47.44	-20.58	2.2450E-09	160.55	-172.98
0.933	90.000	30.000	2.3138E-10	32.49	-192.71	1.6424E-01	-41.40	-15.89	3.7608E-09	157.99	-168.49
0.933	90.000	40.000	1.5095E-10	-90.00	-196.42	1.4816E-01	-70.64	-18.59	3.5794E-09	137.75	-168.92
0.933	90.000	50.000	1.0000E-10	0.00	-200.00	5.5227E-02	-55.61	-25.16	2.5864E-09	113.84	-171.75
0.933	90.000	60.000	1.5613E-03	-63.97	-56.13	9.5711E-02	-38.72	-20.38	7.4599E-03	118.77	-42.55
0.933	90.000	70.000	1.5173E-03	179.88	-56.38	6.6845E-02	-74.24	-23.50	7.6574E-03	2.51	-42.32
0.933	90.000	80.000	1.2766E-03	58.43	-57.88	1.3808E-02	-138.58	-37.20	6.9585E-03	-119.08	-43.15
0.933	90.000	90.000	9.9820E-04	-63.63	-60.02	3.4035E-02	43.26	-29.36	6.1477E-03	118.33	-44.23
0.933	90.000	100.000	7.2332E-04	176.52	-62.81	2.1462E-02	-101.67	-33.37	5.3160E-03	-1.12	-45.49
0.933	90.000	110.000	4.6875E-04	62.36	-66.58	8.7892E-02	142.83	-21.12	4.5376E-03	-114.86	-46.86
0.933	90.000	120.000	2.4306E-04	-43.88	-72.29	9.9068E-02	97.23	-20.08	3.8011E-03	160.51	-48.40
0.933	90.000	130.000	5.1724E-05	-150.56	-85.73	5.4811E-02	110.32	-25.22	3.1049E-03	47.59	-50.16
0.933	90.000	140.000	1.1051E-04	-23.84	-79.13	1.0869E-01	143.94	-19.28	2.4432E-03	-31.42	-52.24
0.933	90.000	150.000	2.3543E-04	-91.38	-72.64	1.6937E-01	134.52	-15.42	1.8088E-03	-94.72	-54.85
0.933	90.000	160.000	3.2141E-04	-138.60	-69.86	1.9890E-01	125.15	-14.03	1.1948E-03	-140.92	-58.45
0.933	90.000	170.000	3.7416E-04	-167.09	-68.54	2.1156E-01	119.94	-13.49	5.9408E-04	-169.03	-64.52
0.933	90.000	180.000	3.9173E-04	-176.62	-68.14	2.1344E-01	117.85	-13.41	3.0832E-03	-153.73	-60.22

Figure 7.69: Line printer output of the near zone magnetic fields of Example 15.

NEAR ZONE POWER DENSITY IN DB

THE FIELDS ARE REFERENCED TO THE PATTERN COORDINATE SYSTEM

			RADIATED			REACTIVE		
R	YMET	PMI	R	YMET	PMI	R	YMET	PMI
0.933	90.000	0.000	6.16	-88.44	-80.56	-75.26	-100.00	-91.17
0.933	90.000	10.000	4.22	-95.00	-14.30	-24.82	-84.23	-10.57
0.933	90.000	20.000	2.18	-88.17	-10.25	-31.51	-85.20	-16.73
0.933	90.000	30.000	7.06	-89.36	-10.26	-20.15	-80.33	-8.41
0.933	90.000	40.000	6.16	-85.60	-9.10	-20.91	-85.44	-9.60
0.933	90.000	50.000	-2.36	-85.10	-11.86	-30.03	-93.54	-20.99
0.933	90.000	60.000	2.38	-16.85	-10.87	-42.08	-21.44	-14.73
0.933	90.000	70.000	-0.69	-20.96	-16.72	-26.47	-18.10	-15.39
0.933	90.000	80.000	-13.49	-25.77	-23.22	-43.63	-26.42	-22.46
0.933	90.000	90.000	-6.50	-36.72	-15.36	-30.94	-28.54	-23.72
0.933	90.000	100.000	-10.42	-26.49	-16.72	-29.99	-25.74	-19.49
0.933	90.000	110.000	1.62	-26.47	-10.26	-25.06	-26.09	-14.04
0.933	90.000	120.000	2.67	-24.89	-11.07	-23.40	-29.12	-11.44
0.933	90.000	130.000	-2.44	-40.90	-13.60	-29.14	-24.80	-16.47
0.933	90.000	140.000	3.48	-26.48	-23.46	-24.45	-29.16	-11.23
0.933	90.000	150.000	7.33	-22.85	-11.92	-26.91	-22.04	-12.56
0.933	90.000	160.000	8.72	-28.88	-11.92	-37.42	-19.08	-21.23
0.933	90.000	170.000	9.26	-23.58	-14.24	-35.35	-18.42	-20.85
0.933	90.000	180.000	9.34	-21.85	-36.78	-35.20	-18.43	-40.53

Figure 7.70: Line printer output of the near zone power density of Example 15.

7.20 Example 16: Ship Masts

This example illustrates the use of multiple cylinders to model ship masts. There are four dipoles mounted around one of the masts and they are nominally supposed to produce an omnidirectional pattern. The geometry used is illustrated in Figure 7.71. The input data is given by

```
CM:  EXAMPLE 16.
CE:  MULTIPLE CYLINDER TEST X-Y CUT NEAR FIELD
FR:
0.3125
US:
1
UN:
1
SG:
0.365,0.,23.05
0.,0.,90.,0.
-2,0.508,0.
1.,0.
SG:
0.,0.365,23.05
0.,0.,90.,0.
-2,0.508,0.
1.,0.
SG:
-0.365,0.,23.05
0.,0.,90.,0.
-2,0.508,0.
1.,0.
SG:
0.,-0.365,23.05
0.,0.,90.,0.
-2,0.508,0.
1.,0.
PN:
0.,0.,23.05
0.,0.,90.,0.
F
```

```

250.0,90.,0.
0.,0.,1.
361
CG:
0.,0.,10.
0.,0.,90.,0.
0.455,0.455
-10.,90.,10.,90.
CG:
0.,0.,24.75
0.,0.,90.,0.
0.14,0.14
-4.85,90.,4.75,90.
CG:
0.,12.8,13.66
0.,0.,90.,0.
0.455,0.455
-13.66,90.,13.66,90.
CG:
0.,12.8,32.07
0.,0.,90.,0.
0.14,0.14
-4.85,90.,4.75,90.
PP:
T
T,4.95,2.5
0.,360.,30.
-40.,0.,10.
XQ:
EN:

```

The frequency for this problem is 0.3125 GHz. Note that this means that the radius of the mast around which the antennas are mounted is only 0.1458 wavelengths. This is pushing the accuracy of UTD, so the solution should be checked against a known result first. This is accomplished by comparing the pattern for one of the dipoles in the presence of a infinite cylinder using the exact model solutions against the UTD result for a very long cylinder. The input set for this test is not shown. The results are compared in Figure 7.72 with excellent agreement verifying the validity of

the UTD solution. The azimuth plane pattern for the vertically polarized electric field in the presence of two masts without the multiple cylinder interaction terms is shown in Figure 7.73. Note that it is assumed that these higher order terms are initialized false. At present, the cylinder to cylinder interactions are not included in the present version. Version 2 had these terms available. To illustrate what correction can be obtained with their use, the resulting pattern with the multiple cylinder interaction terms is shown in Figure 7.74. Notice that the discontinuity at the 90 degree angle in Figure 7.73 has been smoothed out by the higher order terms included in Figure 7.74.

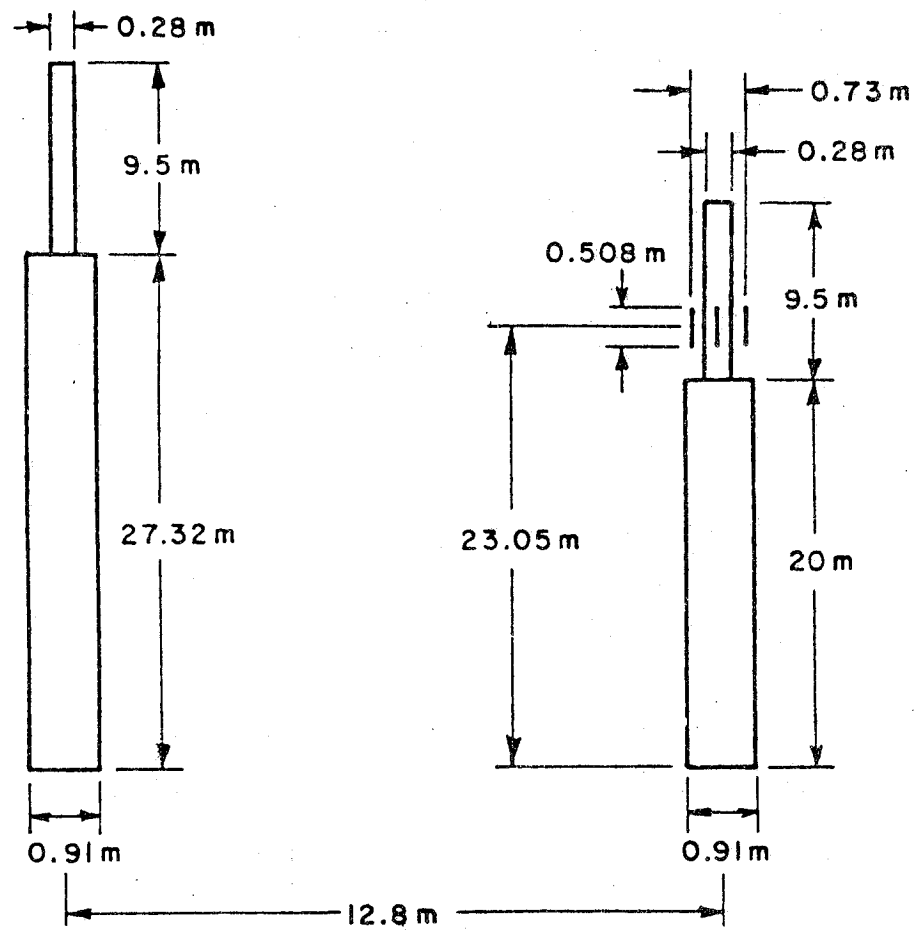


Figure 7.71: The geometry used to study the pattern of four antennas in the presence of two masts.

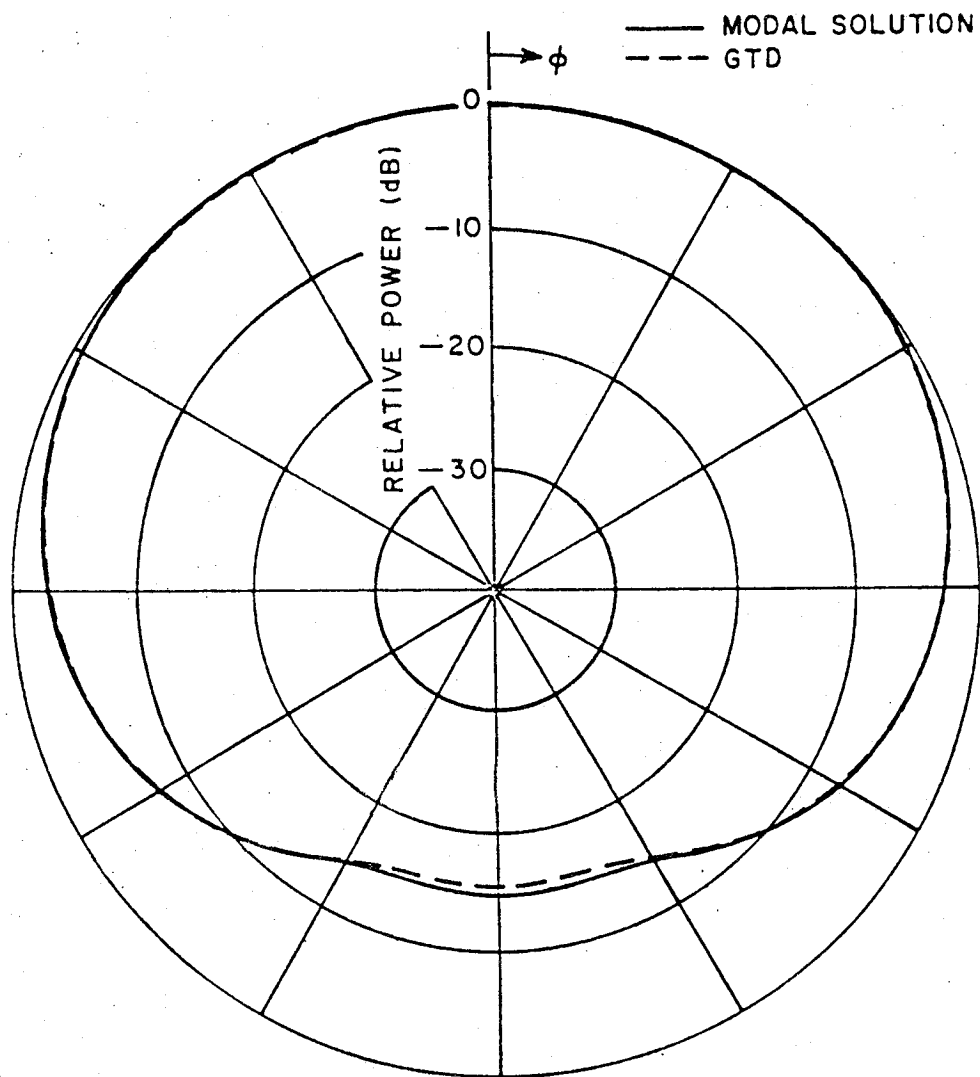


Figure 7.72: Comparison of the exact modal solution and the uniform asymptotic solution of the E_θ pattern in the azimuth plane for one dipole on one mast.

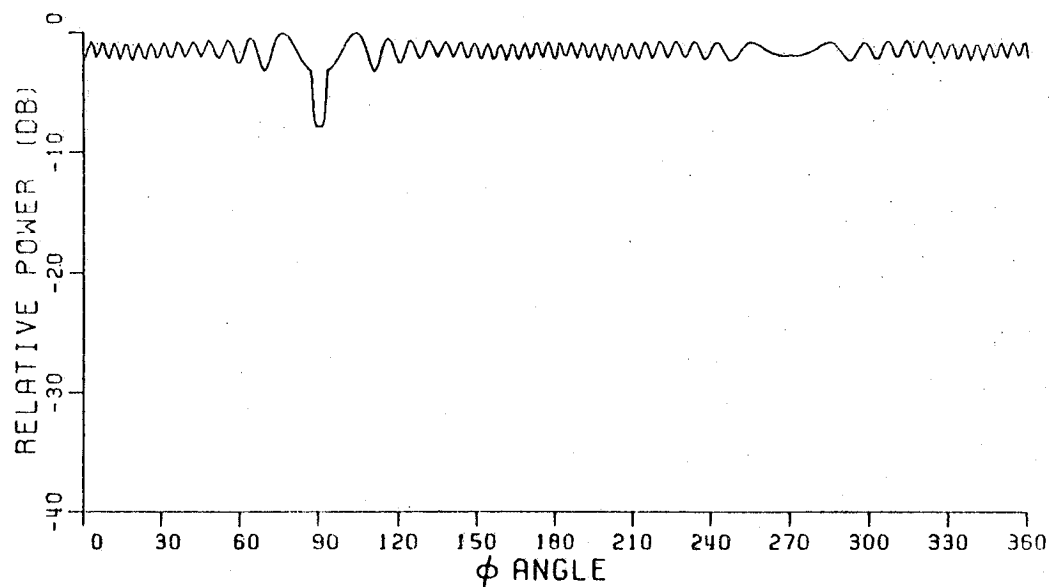


Figure 7.73: Calculated azimuth plane pattern at a range of 250 meters for four dipoles located around a mast in the presence of a second mast without higher order cylinder interactions terms (frequency = 0.3125 GHz) (VAX 11/750 run time is 47.3 min).

Ex. 16

285

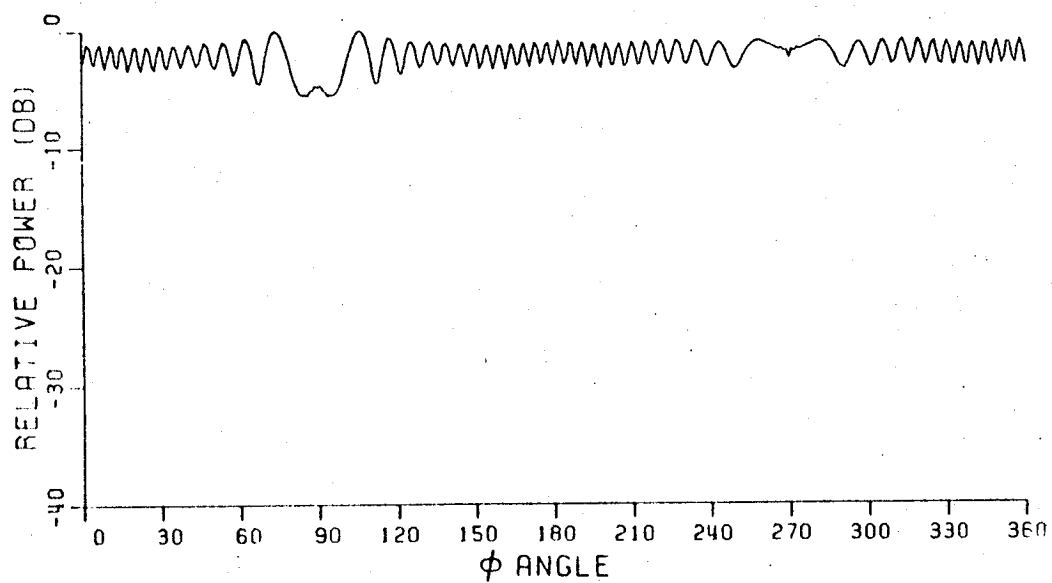


Figure 7.74: Calculated azimuth plane pattern at a range of 250 meters for four dipoles located around a mast in the presence of a second mast with higher order cylinder interactions terms (frequency = 0.3125 GHz).

7.21 Example 17: Plate - Cylinder

This example considers an electric dipole in the presence of a plate and a finite circular cylinder as shown in the inserts of Figures 7.75, 7.76, 7.77, 7.78, and 7.79. This example illustrates the effects of the far zone and near zone patterns cuts on such a geometry and also shows the effects of the plate - cylinder terms on the pattern. In addition, the use of the **NX** command in an input set is shown.

```

CM:  EXAMPLE 17A.
CE:  FAR ZONE PLATE AND CYLINDER TEST
PF:
0.,0.,90.,0.
T,90.
0.,1.,361
UN:
3
US:
0
FR:
4.
SG:
0.,5.625,0.
90.,0.,0.,0.
-2,0.508,0.0
1.,0.
PG:
4,0
5.,0.,5.
5.,0.,-5.
-5.,0.,-5.
-5.,0.,5.
CG:
0.,12.3125,-0.125
0.,0.,90.,0.
1.25,1.25
-8.5,90.,8.5,90.
PP:
T

```

T,4.62,2.32

0.,360.,36.

-40.,0.,10.

XQ: SOURCE AND PLATE TEST

NX:

CM: EXAMPLE 17B.

CE: NEAR ZONE PLATE AND CYLINDER TEST

UN:

3

FR:

3.985

US:

3

SG:

0.,0.,0.

90.,90.,0.,0.

-2,1.5,0.

1.,0.

PN:

0.,0.,0.

0.,0.,90.,0.

F

36.875,90.,0.

0.,0.,1.

361

CG:

6.5625,0.,0.

0.,0.,90.,0.

1.25,1.25

-9.,90.,8.,90.

PG:

4,0

-5.75,5.,5.

-5.75,-5.,5.

-5.75,-5.,-5.

-5.75,5.,-5.

XQ:

EN:

The far zone E_ϕ radiation pattern calculated without the plate - cylinder interaction terms is compared with measured results in Figure 7.75. The plate - cylinder interaction terms are not presently available in Version 3. They were, however, included in Version 1 and are shown here for comparison purposes. The same measured results compared with the calculated results including the plate - cylinder interaction terms is shown in Figure 7.76. The main features of the pattern are present without the plate - cylinder terms. The plate - cylinder terms add some of the small details and bring the overall levels into better agreement. The near zone E_ϕ radiation pattern calculated without the plate - cylinder interaction terms for two different pattern origins and two different ranges is shown next. The measured and calculated E_ϕ radiation pattern in the $x - y$ plane 36.875" from the dipole is shown in Figure 7.77. The measured and calculated E_ϕ radiation pattern in the $x - y$ plane 26.25" from the dipole is shown in Figure 7.78. The measured and calculated E_ϕ radiation pattern in the $x - y$ plane 36.875" from the center of the cylinder is shown in Figure 7.79. The E_θ pattern for all of the above case are not shown because they are of negligible value.

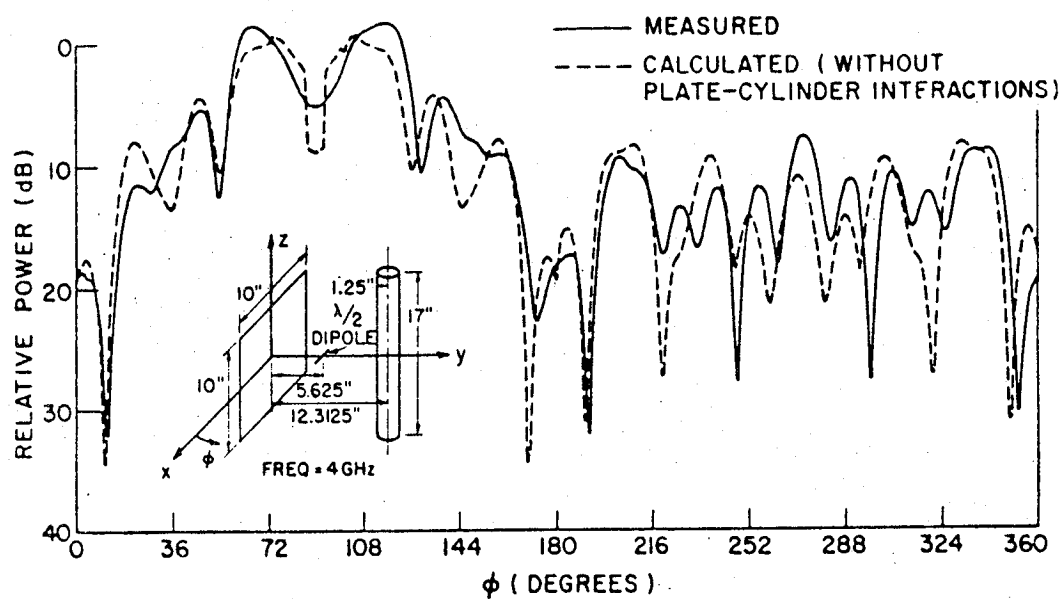


Figure 7.75: Comparison of the measured and calculated E_ϕ far zone radiation pattern of a dipole in the presence of a square plate and a finite circular cylinder (without plate - cylinder interactions).

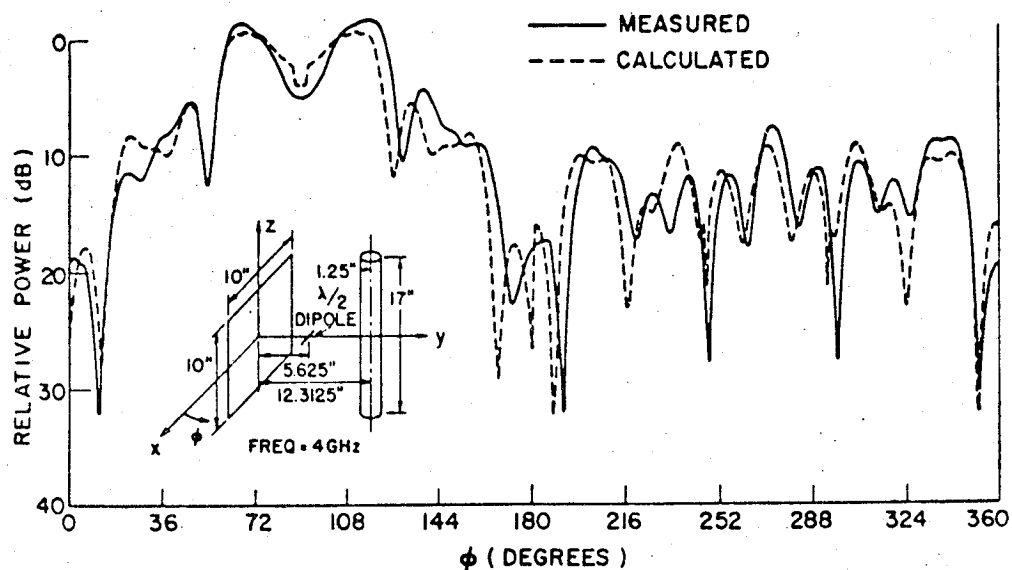


Figure 7.76: Comparison of the measured and calculated E_ϕ far zone radiation pattern of a dipole in the presence of a square plate and a finite circular cylinder (with plate - cylinder interactions).

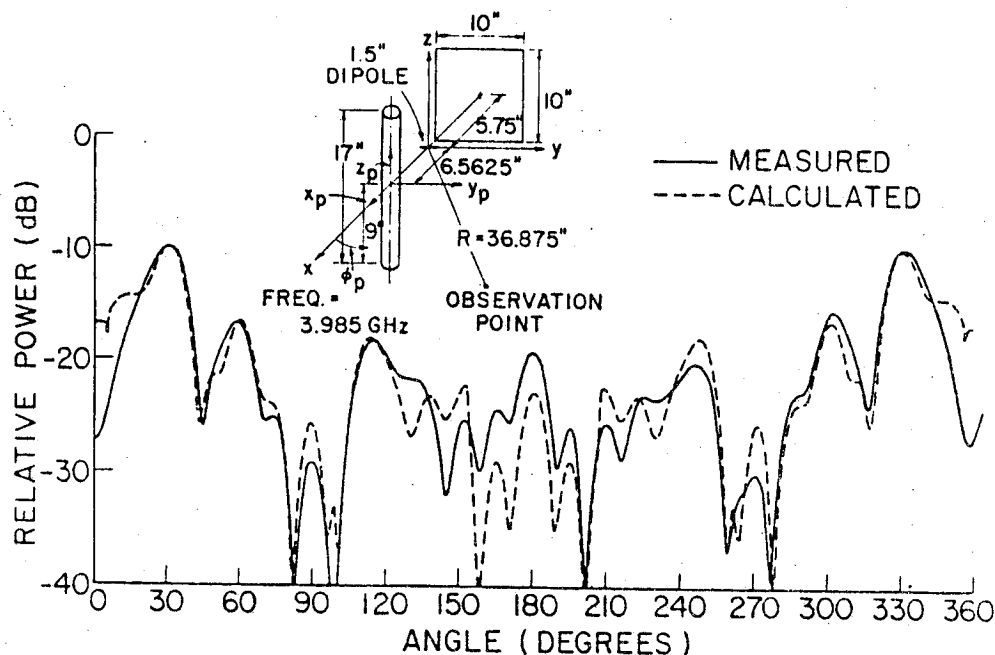


Figure 7.77: Comparison of the measured and calculated E_ϕ near zone radiation pattern 36.875" from a dipole in the presence of a square plate and a circular cylinder (without plate - cylinder interactions).

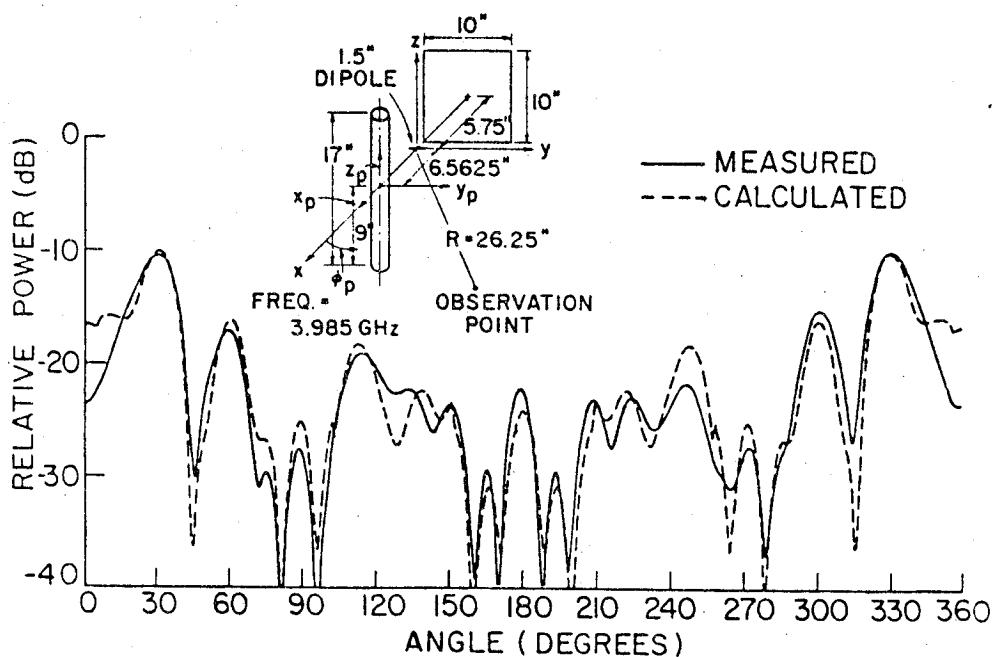


Figure 7.78: Comparison of the measured and calculated E_ϕ near zone radiation pattern 26.25" from a dipole in the presence of a square plate and a circular cylinder (without plate - cylinder interactions).

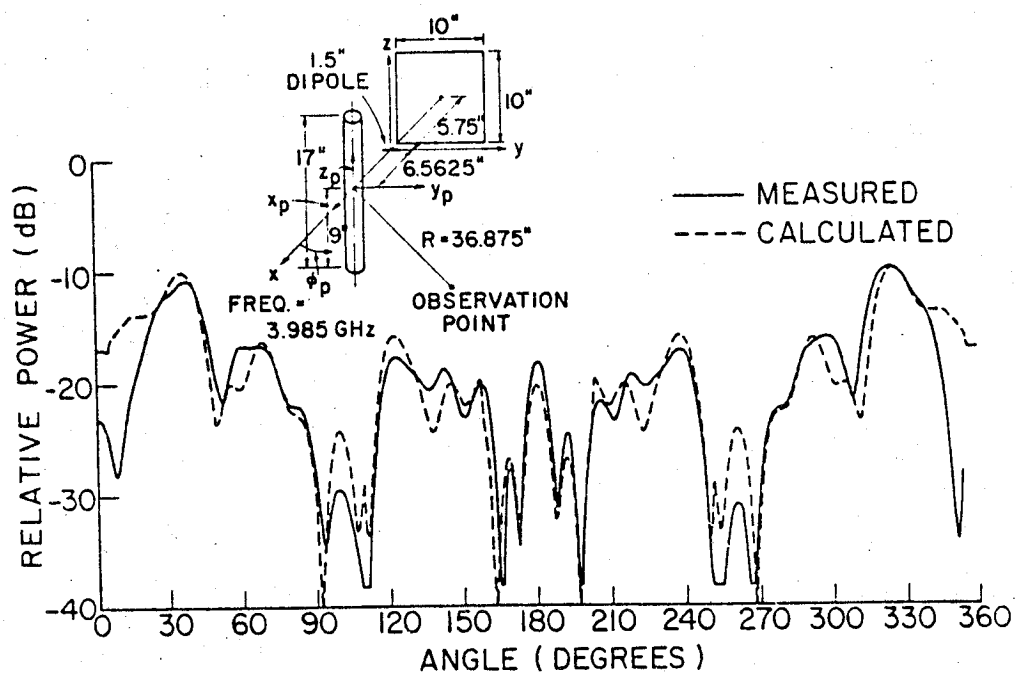


Figure 7.79: Comparison of the measured and calculated E_ϕ near zone radiation pattern $36.875''$ from a circular cylinder in the presence of a dipole and a square plate (without plate - cylinder interactions).

7.22 Example 18: Ship Yardarm

This example is used to illustrate the prediction of the far zone pattern of an antenna mounted on the yardarm of a mast as shown in Figure 7.80. Measurements were made on a 1/10 scale model of this geometry at NOSC [23]. The computer model used for this study is shown in Figure 7.81. The actual ship antenna is model by an equivalent dipole. The input data is given by

```

CM:  EXAMPLE 18.
CE:  YARDARM AND MAST EXAMPLE
PF:
0.,0.,90.,0.
T,89.5
0.,1.,361
FR:
4.
UN:
3
US:
3
SG:
-5.,0.,2.
0.,0.,90.,0.
-2,1.925,0.
1.,0.
CG:
0.,0.,0.
0.,0.,90.,0.
1.5625,1.5625
-43.625,90.,23.125,90.
PP:
T
T,5.,6.
0.,180.,10.
-22.,0.,1.
XQ:
PG:
4,0

```

-1.5625,0.625,0.
-32.75,0.625,0.
-32.75,-0.625,0.
-1.5625,-0.625,0.
XQ:
EN:

The vertically polarized radiation pattern in the azimuth plane calculated including the mast only is compared with the measured results for the completed model in Figure 7.82. The results for the mast - yardarm configuration are compared in Figure 7.83. The presence of the yardarm in the calculations makes the levels of the results compare better and gives more detail to the calculations around the 150 to 180 degree pattern region. The discrepancy in this region may be due to inadequate representation of the currents on the antenna in the presence of the mast, an inconsistent pattern cut with the measurements, the lack of some higher order terms in the calculations, or even to problems in the measurements. The agreement is good for engineering purposes, however.

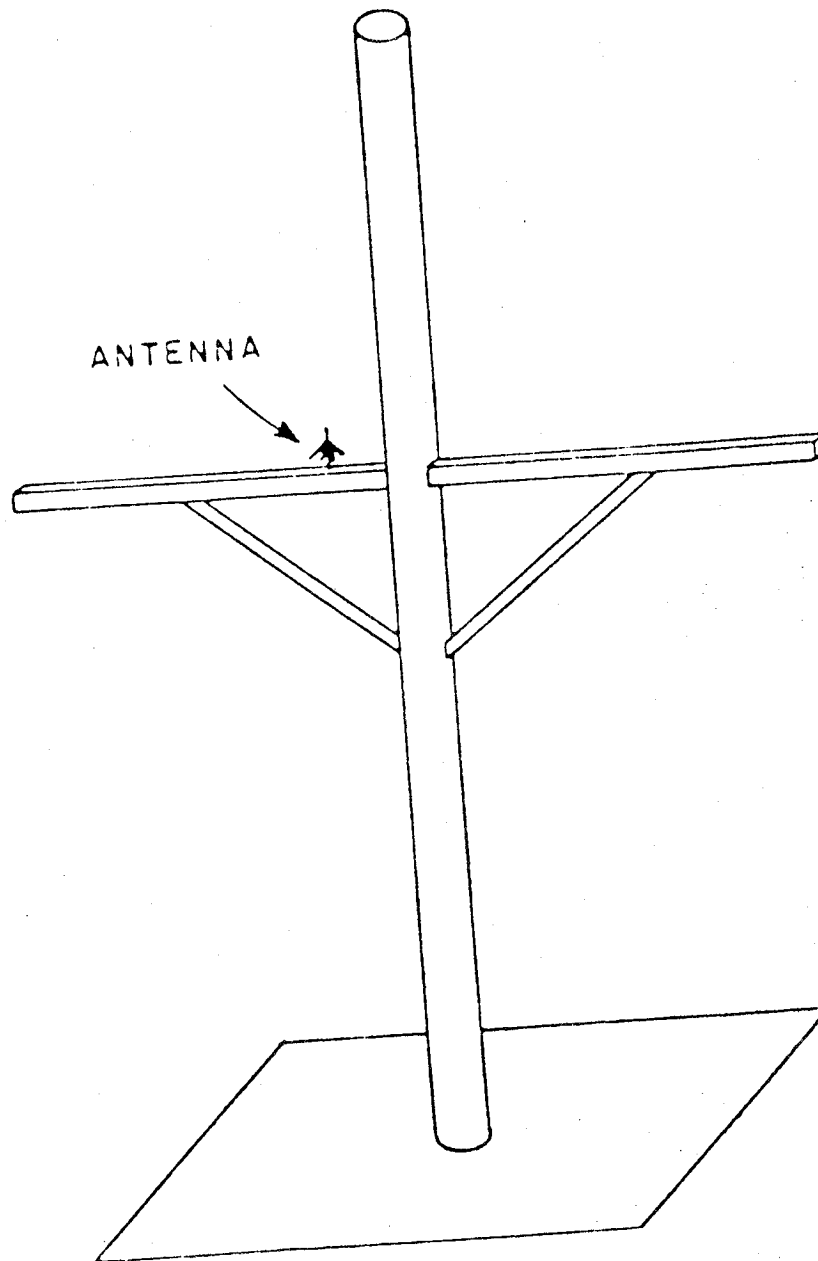


Figure 7.80: Geometry of an antenna in a mast and yardarm environment.

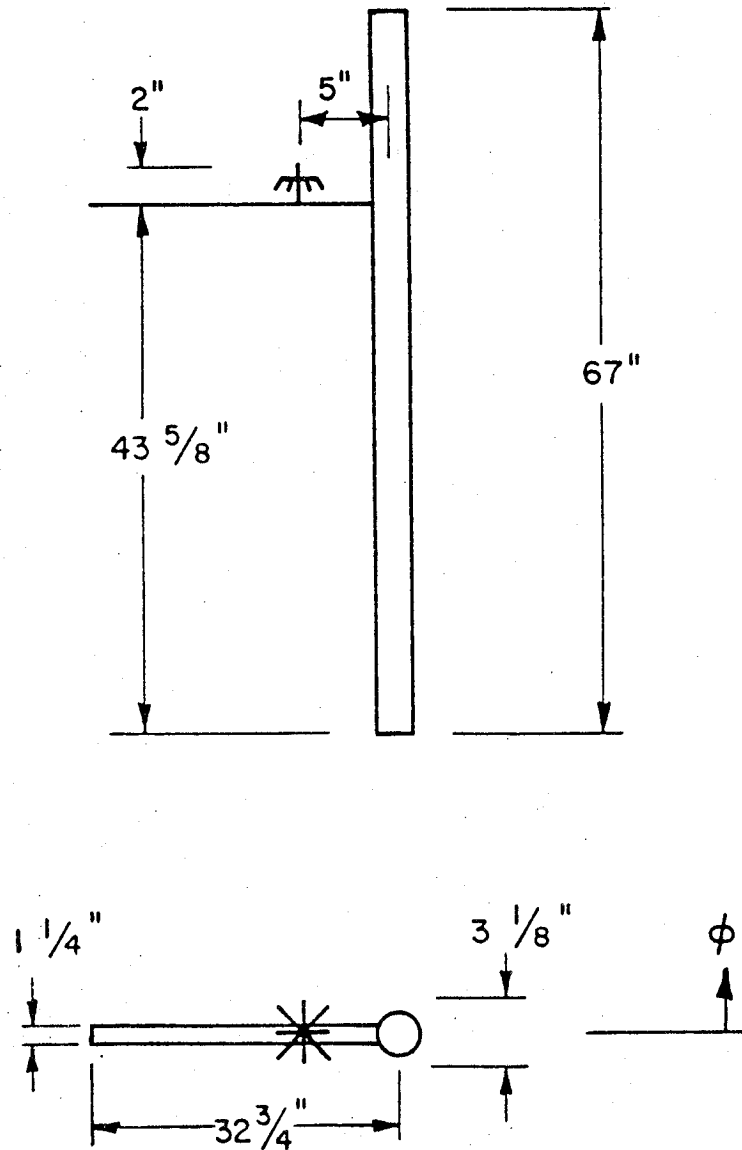


Figure 7.81: Top and side view of computer model corresponding to the mast and yardarm example.

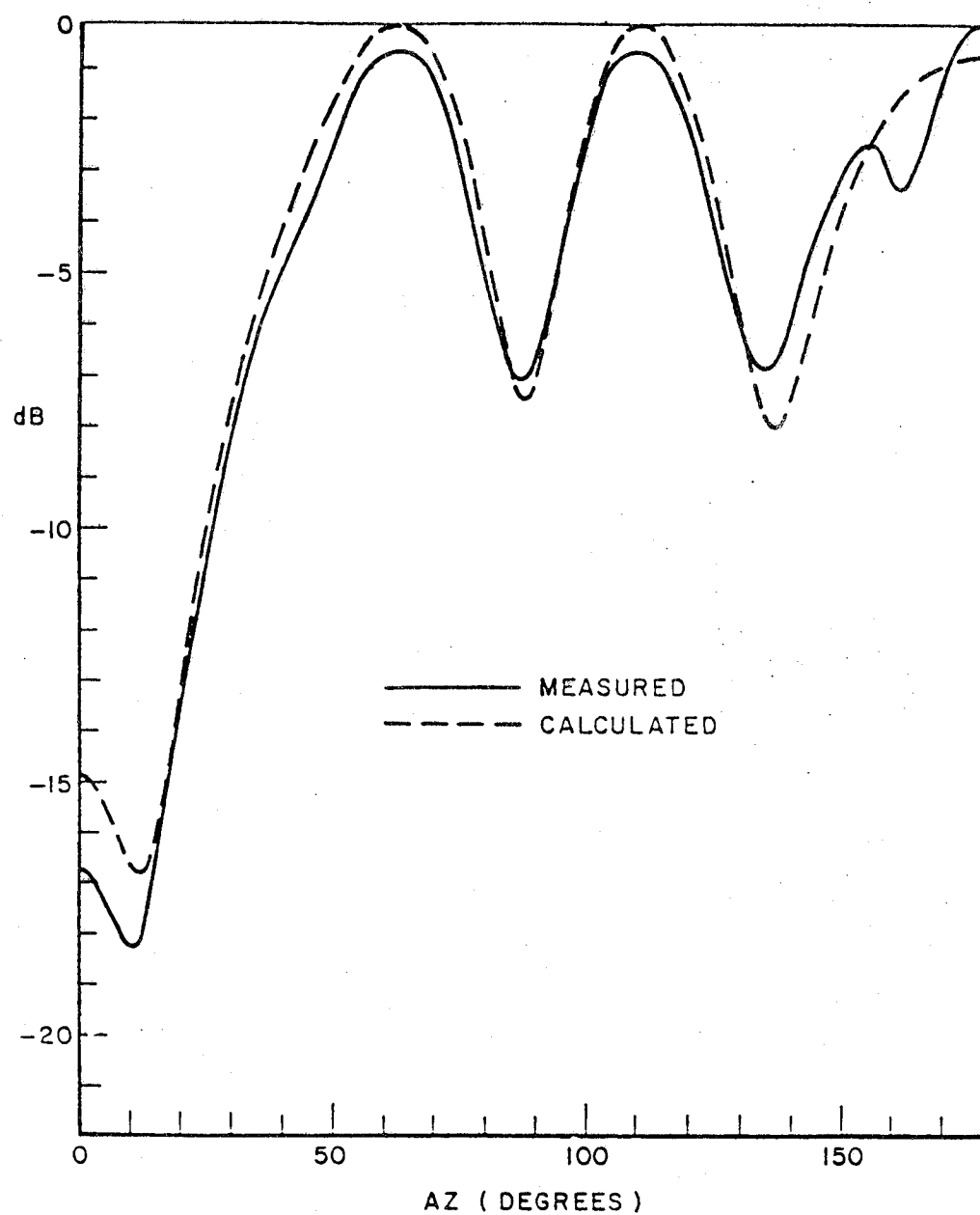


Figure 7.82: Comparison of the measured and calculated azimuth pattern for the mast and yardarm example. The calculated result includes the mast only. The measurements were made on a 1/10 scale model including the yardarms at NOSC [23]

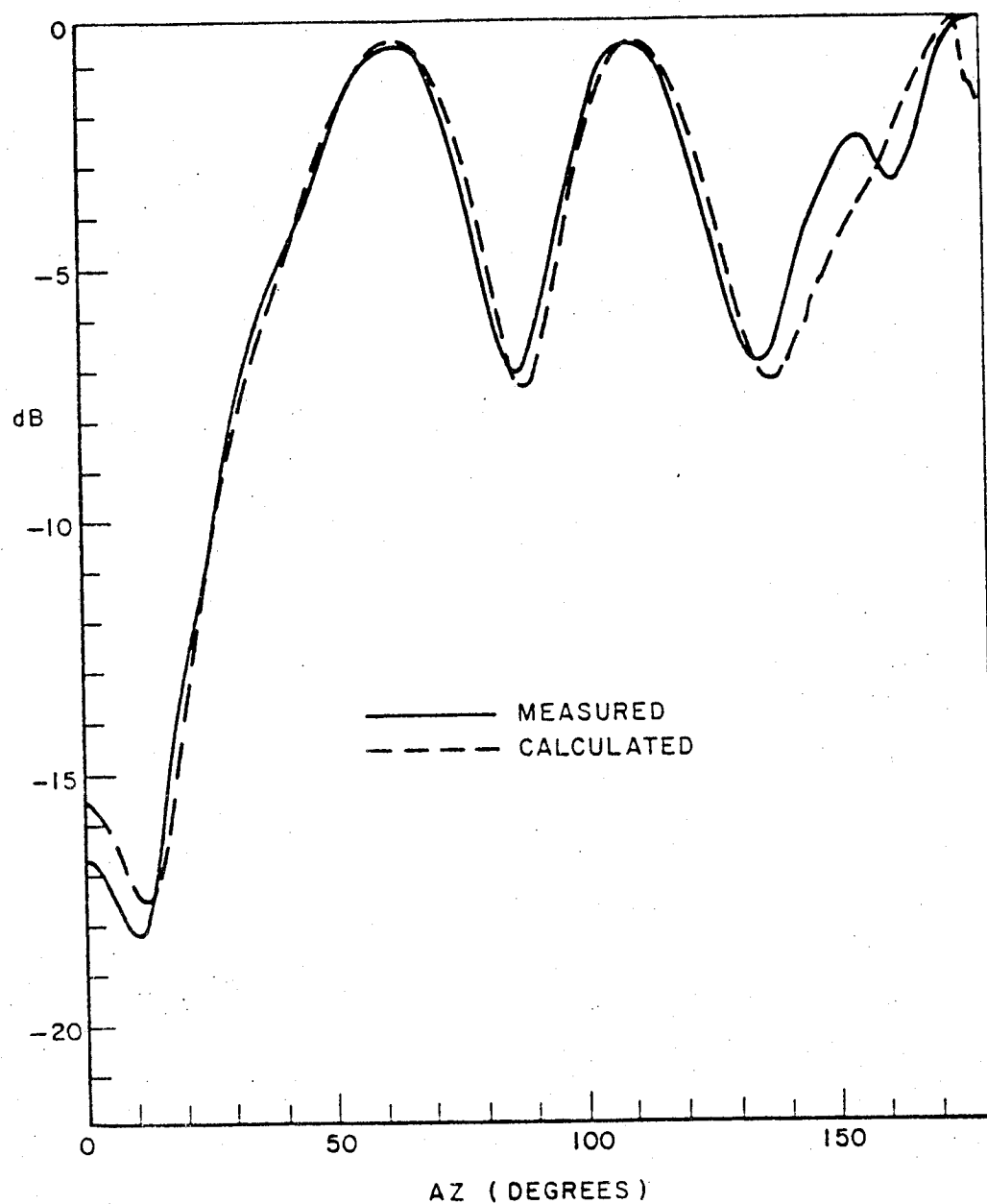


Figure 7.83: Comparison of the measured and calculated azimuth pattern for the mast and yardarm example. The calculated result includes both the mast and one yardarm. The measurements were made on a 1/10 scale model including the yardarms at NOSC [23].

7.23 Example 19: Aircraft

This example considers a slot mounted on the wing of a Boeing 737. The computer model of the Boeing 737 is illustrated in Figure 7.84. The input data is given by

```
CM:  AIRCRAFT TEST, EXAMPLE 19.
CE:  BOEING 737 COMPUTER MODEL
PF:
60.,90.,150.,90.
T,90.
0.,1.,361
FR:
1.746
UN:
3
US:
0
CG:
0.,0.,0.
0.,0.,90.,0.
104.1,74.7
-570.5,90.,260.4,20.
PG:  LEFT WING
5,0
0.,74.7,-212.8
0.,547.9,40.8
0.,547.9,95.1
0.,203.8,0.
0.,74.7,0.
PG:  RIGHT WING
5,0
0.,-74.7,0.
0.,-203.8,0.
0.,-547.9,95.1
0.,-547.9,40.8
0.,-74.7,-212.8
PG:  VERTICAL STABILIZER
4,0
```

104.1,0.,448.3
344.1,0.,516.2
344.1,0.,443.7
104.1,0.,235.5
SG: FINITE WIDTH SLOT
0.,312.4,-45.3
90.,90.,0.,0.
3,0.827837,0.413918
1.,0.
PP:
T
F,0.,2.5
0.,360.,30.
-40.,0.,10.
XQ:
EN:

The E_ϕ pattern is compared with its measured result in Figure 7.85. The measurement was made on a 1/20 scale model of a Boeing 737 at NASA (Hampton, Virginia). The antenna is a KA band waveguide mounted in the wing. The E_θ pattern is significant for this case, however, it is not shown.

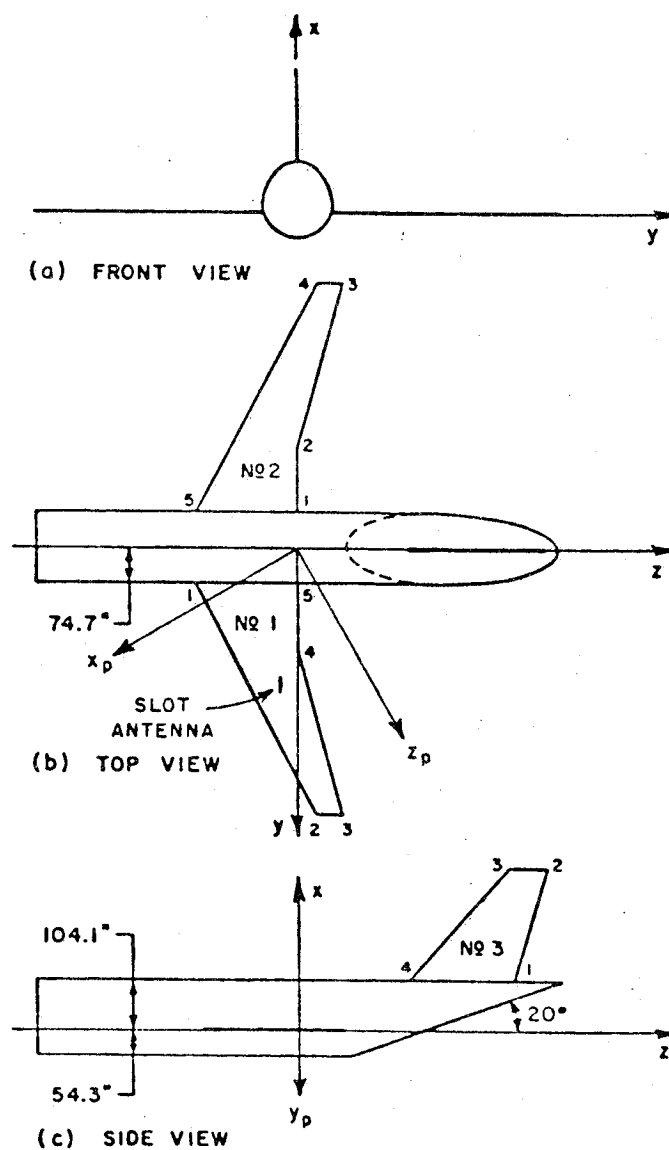


Figure 7.84: Illustration of geometry of Boeing 737 aircraft model used in finite elliptic cylinder model. The larger radius is used for an antenna mounted on the top of the wings and the smaller radius is used for an antenna mounted on the bottom.

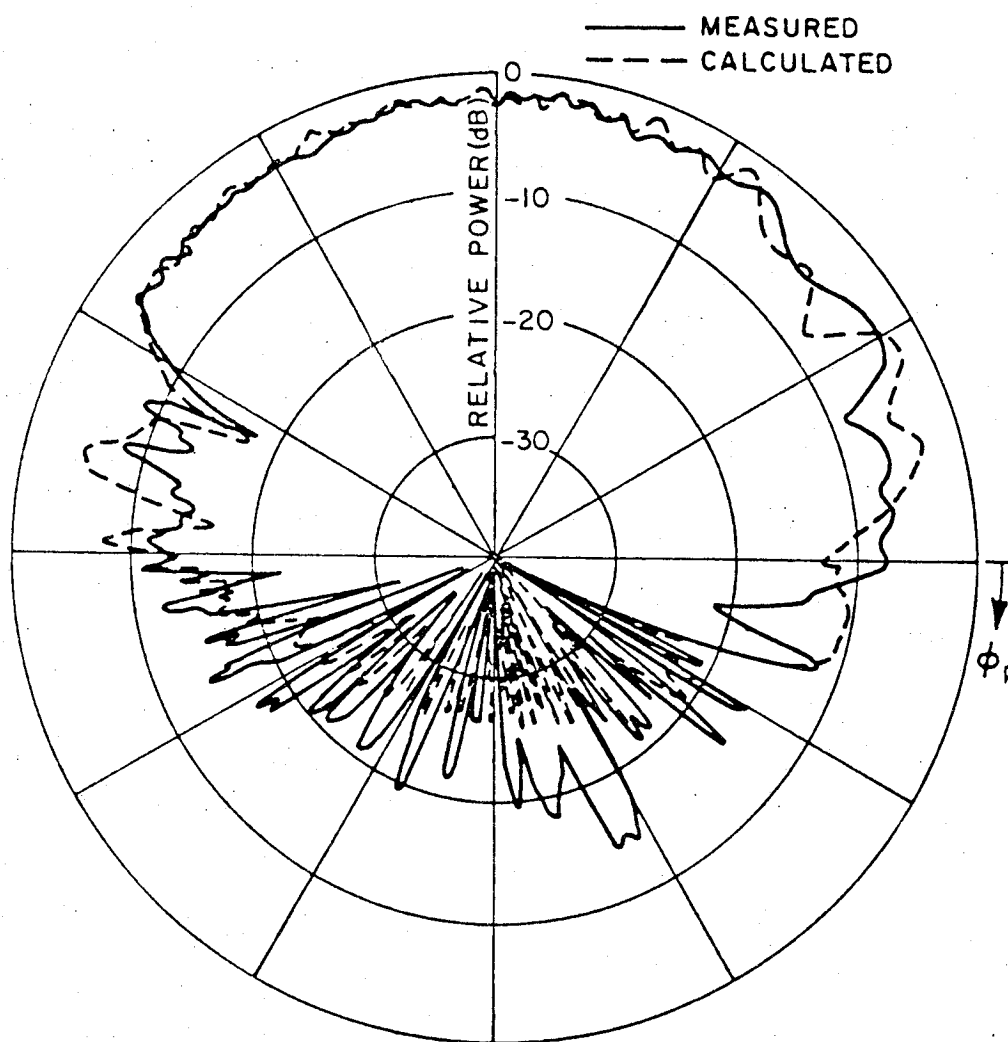


Figure 7.85: Comparison of measured and calculated E_{ϕ_p} results. (VAX 11/750 run time is 3 min and maximum E_{θ} value is -32.2 dB.)

7.24 Example 20A: Near Zone Scatter

This example illustrates the use of the backscatter option, **BP**. A simple aircraft model is used as shown in Figure 7.86. The measurements were made at Pacific Missile Test Center (Pt. Mugu, California) using this model [24]. Note that the computer model does not include the cone at the nose of the aircraft. The input data is given by

```

CM:  EXAMPLE 20A.
CE:  POLARIZATION HH, ROLL ANGLE 0.
UN:
3
US:
0
FR:
10.
CG: THE BODY OF THE PLANE
0.,0.,0.
90.,0.,0.,0.
6.,6.
-42.,90.,42.,90.
PG: RIGHT REAR STABILIZER
4,0
-42.,-6.,0.
-48.,-20.5,0.
-44.,-20.5,0.
-24.,-6.,0.
PG: LEFT REAR STABILIZER
4,0
-42.,6.,0.
-24.,6.,0.
-44.,20.5,0.
-48.,20.5,0.
PG: VERTICAL STABILIZER
4,0
-42.,0.,6.
-48.,0.,20.5
-44.,0.,20.5
-24.,0.,6.

```

PG: LEFT WING

4,0

3.,6.,0.

-25.,36.,0.

-12.,36.,0.

40.,6.,0.

PG: RIGHT WING

4,0

3.,-6.,0.

-25.,-36.,0.

-12.,-36.,0.

40.,-6.,0.

BP: RECEIVER AND SOURCE ARE TO MOVE TOGETHER

3

PN:

0.,0.,0.

0.,0.,90.,0.

F

864.,90.,0.

0.,0.,.5

361

SG: THE HH SOURCE

0.1,0.,0.

0.,0.,90.,90.

-2,0.5,0.

1.,0.

RG: THE HH RECEIVER

0.,0.,0.

0.,0.,90.,90.

-2,0.5,0.

1.,0.

PR: NORMALIZE TO A SQUARE METER

3

8.39E-5,8.39E-5

PP:

T

T,4.12,4.88

180.,0.,-30.

-60.,20.,10.

XT: TURN OFF DIRECT FIELD
EN:

in file unit IUG:

RP
ALL
DP
ALL
RPDP
ALL
DPRP
ALL
RC
ALL
DC
ALL
DN
ALL
RN
ALL
END

The measurements were made at 10 GHz. The calculated results for horizontal polarization in the azimuth plane is shown in Figure 7.87. The measured result is shown in Figure 7.88. Only half the patterns are shown because the patterns are symmetric. Both results are shown normalized with respect to a square meter. Note that the results agree very well. The lobe at the 80 degree angle in the measured result is missing in the calculated result because the measured model has a cone at the nose, whereas, the calculated result does not have this cone.

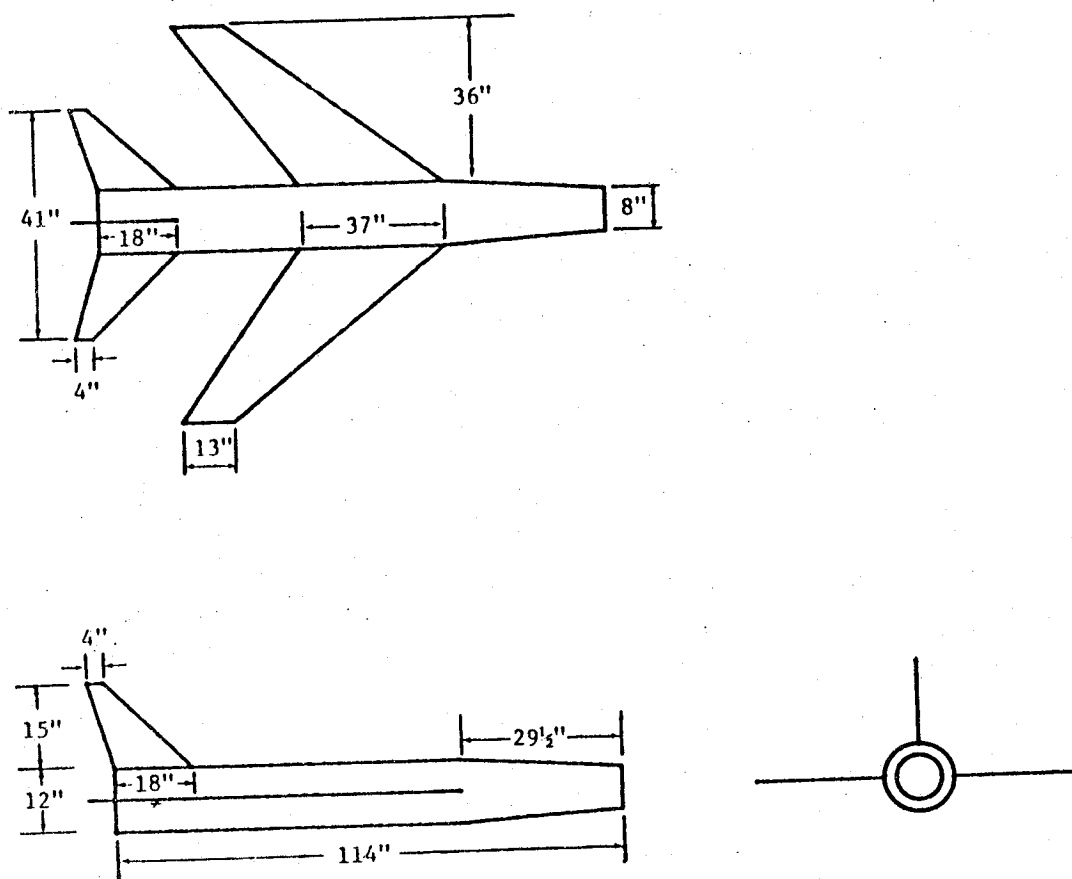


Figure 7.86: Simplified aircraft shape used in RCS example.

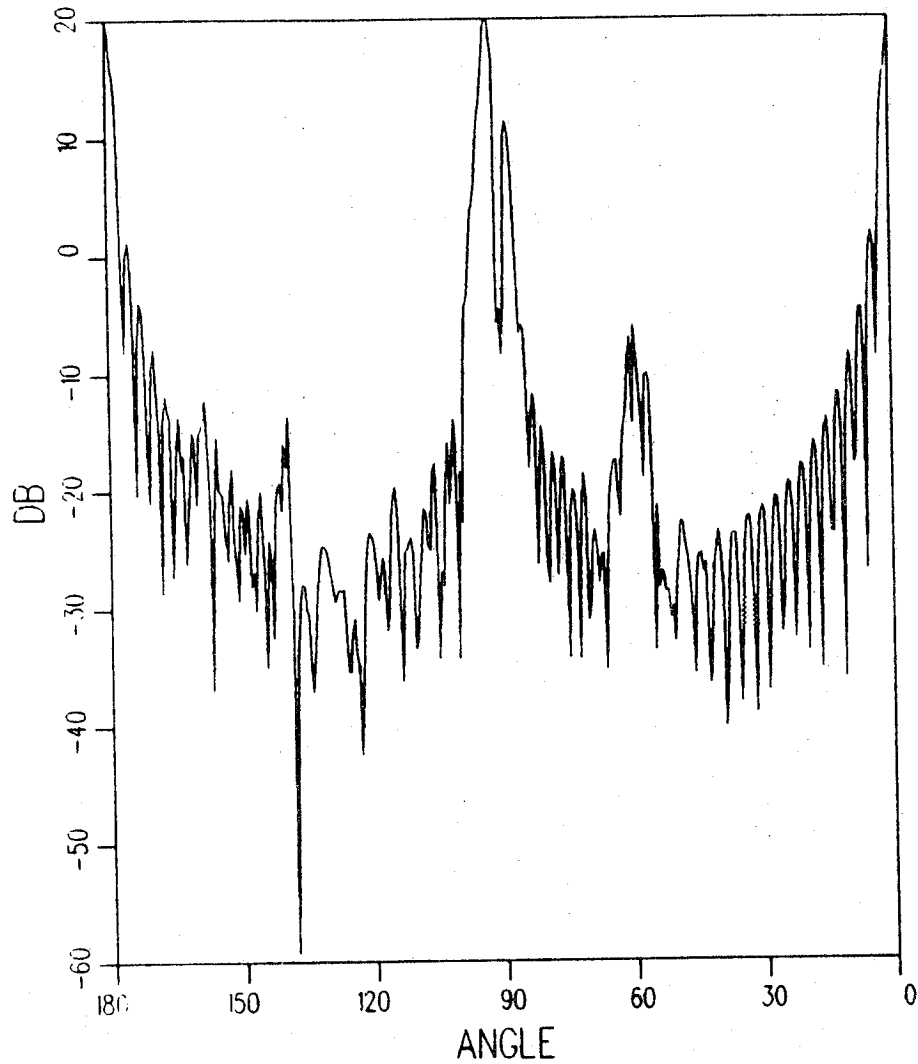


Figure 7.87: Calculated RCS result for horizontal polarization in the azimuth plane. The computer model does not include the nose cone. The results are normalized with respect to a square meter. (VAX 11/750 run time is 24.7 min. and VAX 8550 is 2.16 min.)

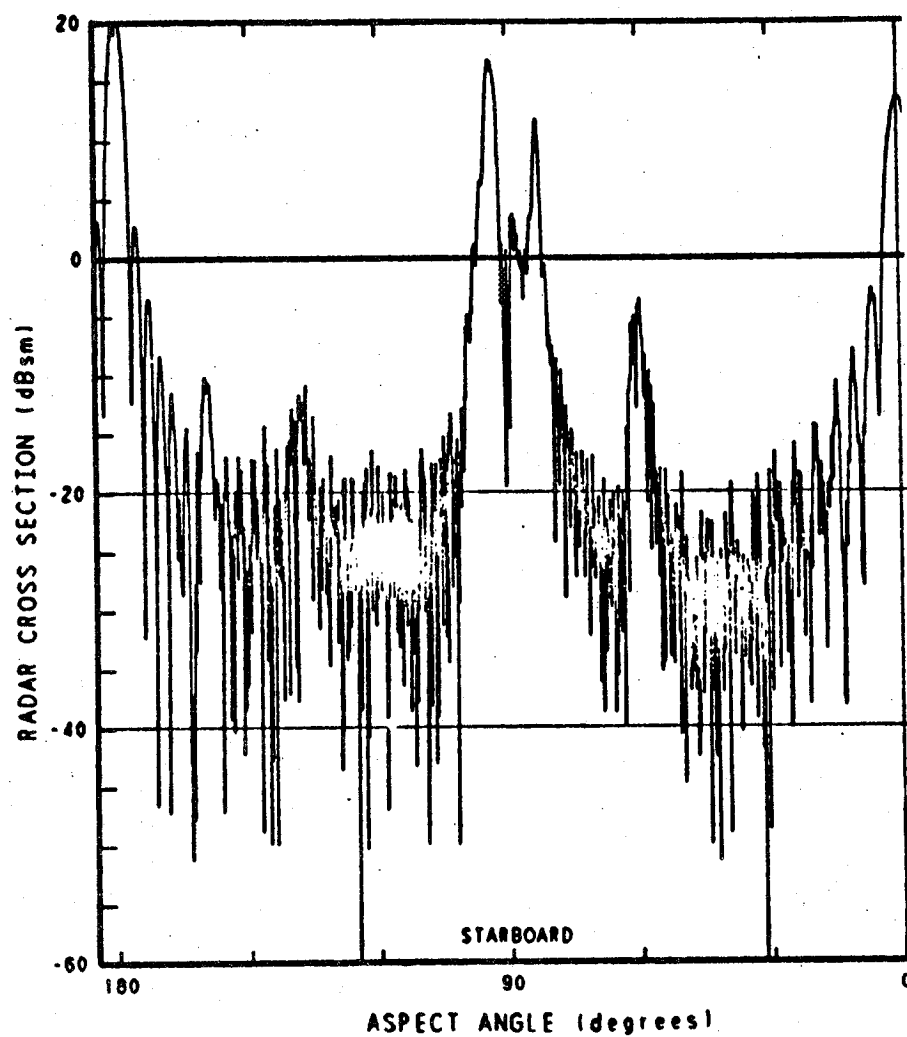


Figure 7.88: Measured RCS result made at Pacific Missile Test Center for horizontal polarization in the azimuth plane. The results are normalized with respect to a square meter.

7.25 Example 20B: Near Zone Scatter, Using an Ellipsoid

This example illustrates the use of the **CF** command. In this example the same plane will be modelled as for Example 20A, but with the cylinder used for the fuselage replaced by a truncated ellipsoid. Large values are used for the **CCN** and **CCP** in the **CF** call so that the truncated shape will approximate the cylinder it is replacing. The input data is given by

```

CM:   EXAMPLE 20B.
CE:   POLARIZATION HH, ROLL ANGLE 0.
UN:
3
US:
0
FR:
10.
CF: THE BODY OF THE PLANE
0.,0.,0.
90.,0.,0.,0.
6.,6.,80.,80.
T
-42.,90.,42.,90.
PG: RIGHT REAR STABILIZER
4,0
-42.,-6.,0.
-48.,-20.5,0.
-44.,-20.5,0.
-24.,-6.,0.
PG: LEFT REAR STABILIZER
4,0
-42.,6.,0.
-24.,6.,0.
-44.,20.5,0.
-48.,20.5,0.
PG: VERTICAL STABILIZER
4,0
-42.,0.,6.
-48.,0.,20.5

```

-44.,0.,20.5
-24.,0.,6.
PG: LEFT WING
4,0
3.,6.,0.
-25.,36.,0.
-12.,36.,0.
40.,6.,0.
PG: RIGHT WING
4,0
3.,-6.,0.
-25.,-36.,0.
-12.,-36.,0.
40.,-6.,0.
BP: RECEIVER AND SOURCE ARE TO MOVE TOGETHER
3
PN:
0.,0.,0.
0.,0.,90.,0.
F
864.,90.,0.
0.,0.,.5
361
SG: THE HH SOURCE
0.1,0.,0.
0.,0.,90.,90.
-2,0.5,0.
1.,0.
RG: THE HH RECEIVER
0.,0.,0.
0.,0.,90.,90.
-2,0.5,0.
1.,0.
PR: NORMALIZE TO A SQUARE METER
3
8.39E-5,8.39E-5
PP:
T
T,4.12,4.88

180.,0.,-30.

-60.,20.,10.

XT: TURN OFF DIRECT FIELD

EN:

in file unit IUG:

RP

ALL

DP

ALL

RPDP

ALL

DPRP

ALL

RC

ALL

DC

ALL

DN

ALL

RN

ALL

END

The calculated results for horizontal polarization in the azimuth plane using an ellipsoidal fuselage is shown in Figure 7.89. This can be compared with the measured result in Figure 7.88. As a note, an ellipsoid can be used to approximate a cylinder or a cylindrical section as was done above by setting CCN and CCP large and truncating, but care must be taken because if values are too large for the given model or the given path numerical inaccuracies may degrade the output.

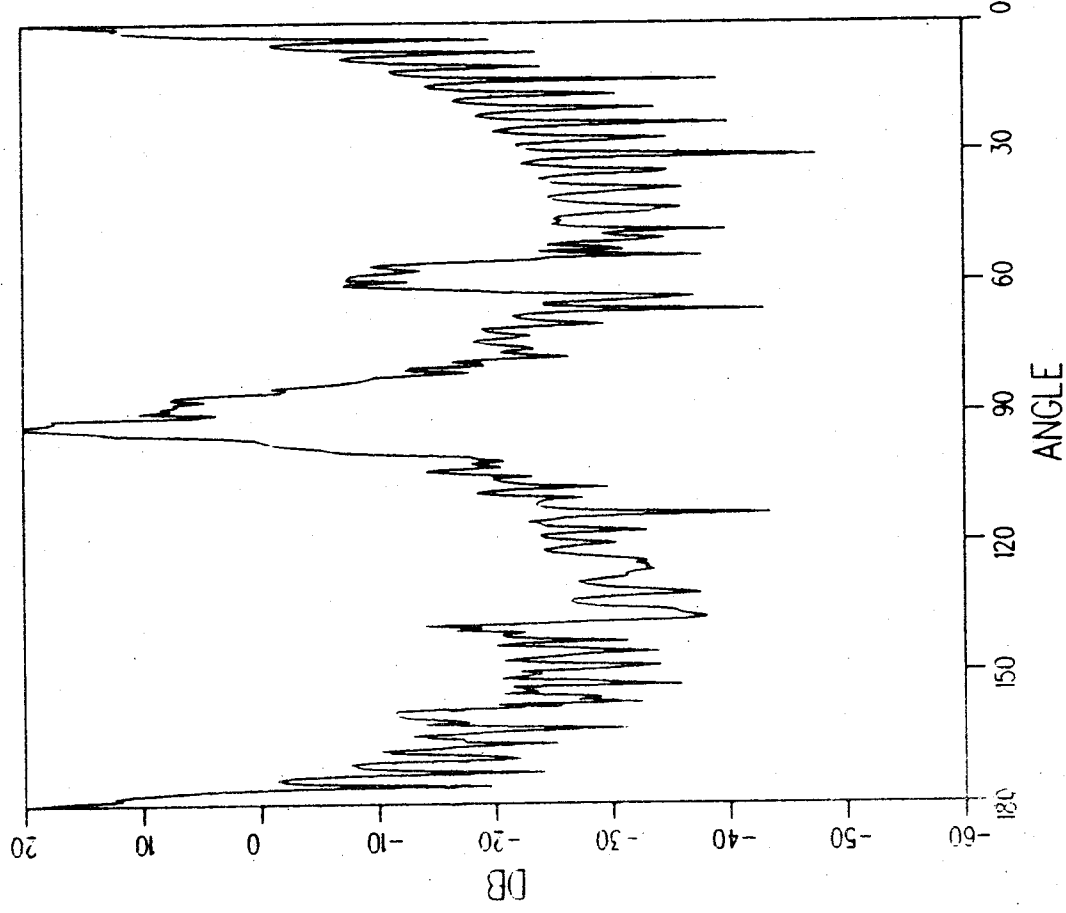


Figure 7.89: Calculated RCS result for horizontal polarization in the azimuth plane. The computer model does not include a nose cone and uses a truncated ellipsoid for the fuselage. (VAX 8550 run time is 2.20 min.)

7.26 Example 20C: Near Zone Scatter, Using a Cone Frustum

This example illustrates the use of the CC and the BF commands. In this example the same plane will be modelled as for Example 20A, but with the cylinder used for the fuselage replaced by a cone frustum that includes the nose cone. The RCS of the fuselage only will be considered first, and the RCS of the complete model second. The input data is given by

```
CM:  EXAMPLE 20C.
CM:  FUSELAGE ONLY.
CE:  POLARIZATION HH, ROLL ANGLE 0.
UN:
3
US:
0
FR:
10.
CC: THE BODY OF THE PLANE
0.,0.,0.
90.,0.,0.,0.
3
4.,4.,72.
5.9,5.9,42.
6.,6.,-42.
BP: RECEIVER AND SOURCE ARE TO MOVE TOGETHER
3
BF: CALCULATE SCATTERED FIELDS
T
PN:
0.,0.,0.
0.,0.,90.,0.
F
864.,90.,0.
0.,0.,.5
361
SG: THE HH SOURCE
0.1,0.,0.
0.,0.,90.,90.
```


-2,0.5,0.
1.,0.
RG: THE HH RECEIVER
0.,0.,0.
0.,0.,90.,90.
-2,0.5,0.
1.,0.
PR: NORMALIZE TO A SQUARE METER
3
8.39E-5,8.39E-5
PP:
T
T,4.12,4.88
180.,0.,-30.
-60.,20.,10.
XQ:
CE: ADD THE WINGS AND TAIL PLATES AND RERUN.
PG: RIGHT REAR STABILIZER
4,0
-42.,-6.,0.
-48.,-20.5,0.
-44.,-20.5,0.
-24.,-6.,0.
PG: LEFT REAR STABILIZER
4,0
-42.,6.,0.
-24.,6.,0.
-44.,20.5,0.
-48.,20.5,0.
PG: VERTICAL STABILIZER
4,0
-42.,0.,6.
-48.,0.,20.5
-44.,0.,20.5
-24.,0.,6.
PG: LEFT WING
4,0
3.,6.,0.
-25.,36.,0.

-12.,36.,0.
40.,6.,0.
PG: RIGHT WING
4,0
3.,-6.,0.
-25.,-36.,0.
-12.,-36.,0.
40.,-6.,0.
XQ:
EN:

The calculated result for horizontal polarization with the fuselage only composed of a multiple cone frustum model is shown in Figure 7.90. The corresponding measured result is shown in Figure 7.91. The calculated result for the complete model with cones and plates is shown in Figure 7.92. This can be compared with the measured result shown in Figure 7.88. Note that the main body of the fuselage, which is a cylinder, was approximated as a cone with a very gradual flare (a change of 0.1 inch over 84 inches). Care must be taken not to make the flare too gradual as numerical inaccuracies can occur.

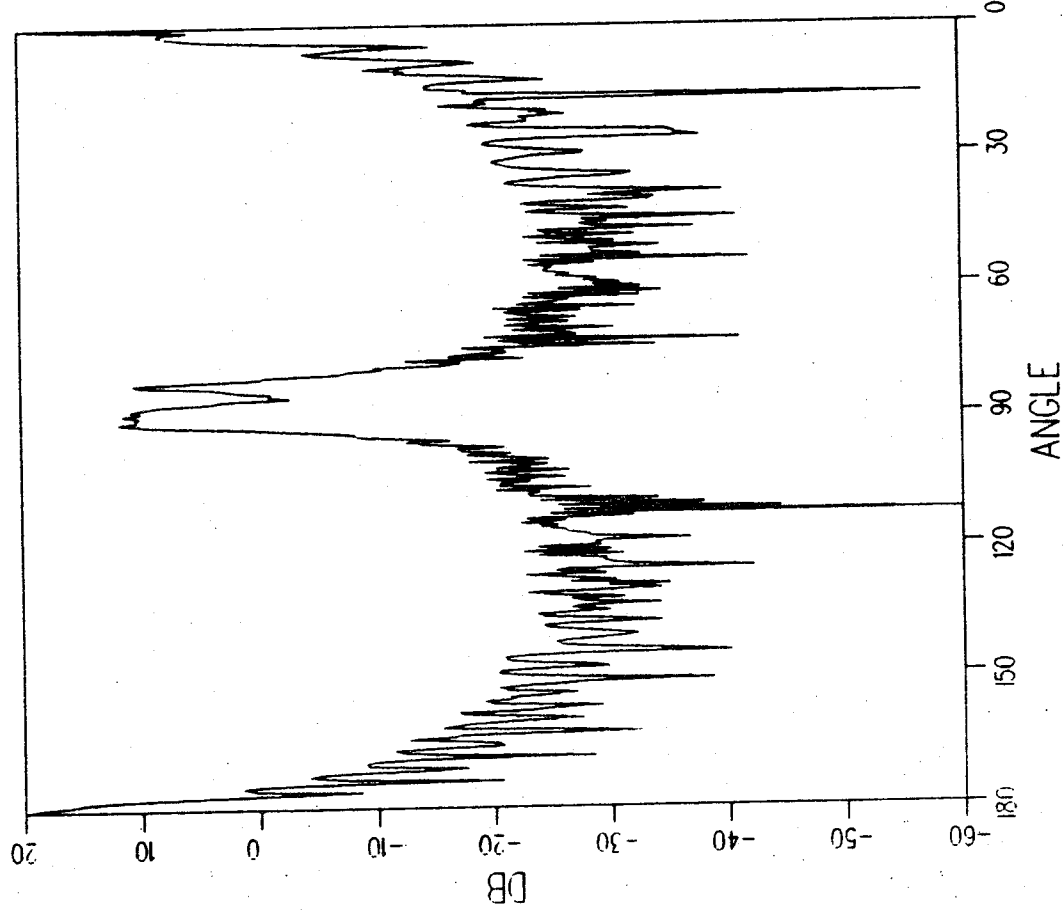


Figure 7.90: Calculated result for horizontal polarization in the azimuth plane of the fuselage only composed of multiple cone frustum sections. (VAX 8550 run time is 0.25 min.)

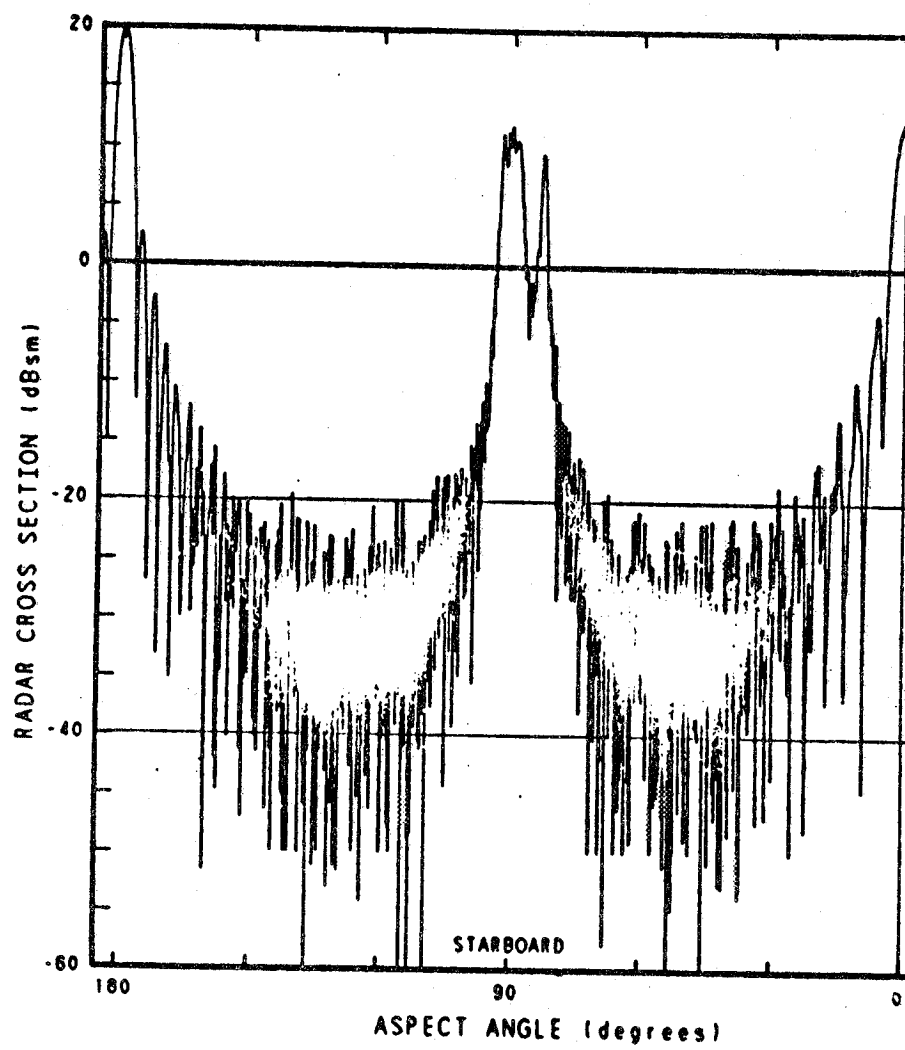


Figure 7.91: Measured RCS made at Pacific Missile Test Center for horizontal polarization in the azimuth plane of the fuselage only.

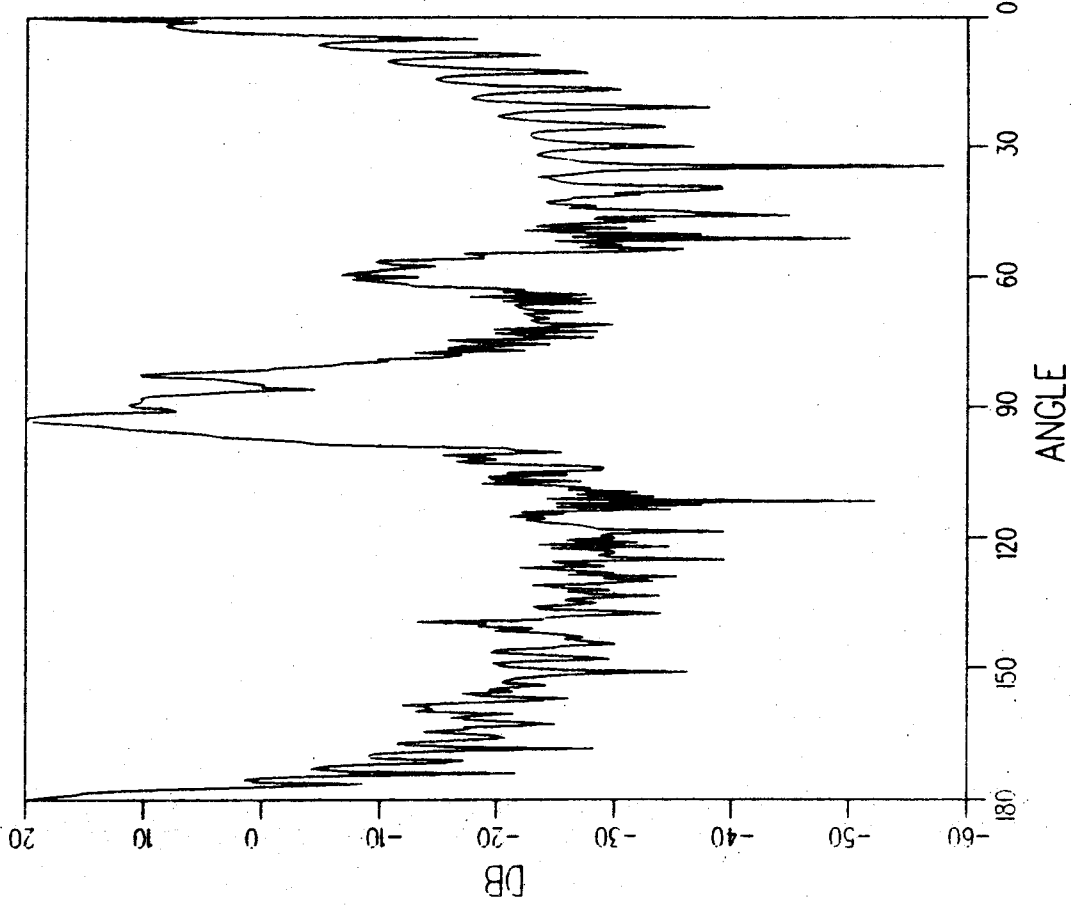


Figure 7.92: Calculated result for horizontal polarization in the azimuth plane of the complete model using a multiple cone frustum fuselage. (VAX 8550 run time is 2.83 min.)

Chapter 8

Space Station Applications

Antenna design considerations for the Space Station is a very large job, considering its size and the number of diverse antenna systems that are needed. NASA-LARC¹ has done extensive scale model measurements on various antennas and their locations. It illustrates the methodology that can be used to obtain meaningful design output information from the code's model capability. In addition, this chapter explores the comparisons of some this measured data with this code's predictions.

8.1 Description of Problem

Engineers involved with placing antennas on structures and ensuring that they meet performance goals are often faced with very cluttered environments. The Space Station is a fine example of this type of environment, as is illustrated in Figure 8.1. This figure only partially shows all of the antennas that will ultimately be involved. In addition, there will eventually be many more modules attached to the frame as well as necessary structures such as solar panels, power radiators, living quarters, etc., that cause blockage for the antennas.

The antennas must perform many functions and will span many frequency ranges. They must communicate with other satellites in various far

¹The calculations and measurements presented in this chapter, were provided by E. M. Bracalente and J. Sweet of National Aeronautics and Space Administration, Langley Research Center. The authors wish to recognize their efforts in obtaining this material and in their generosity in allowing their results to be presented here.

ORIGINAL PAGE IS
OF POOR QUALITY

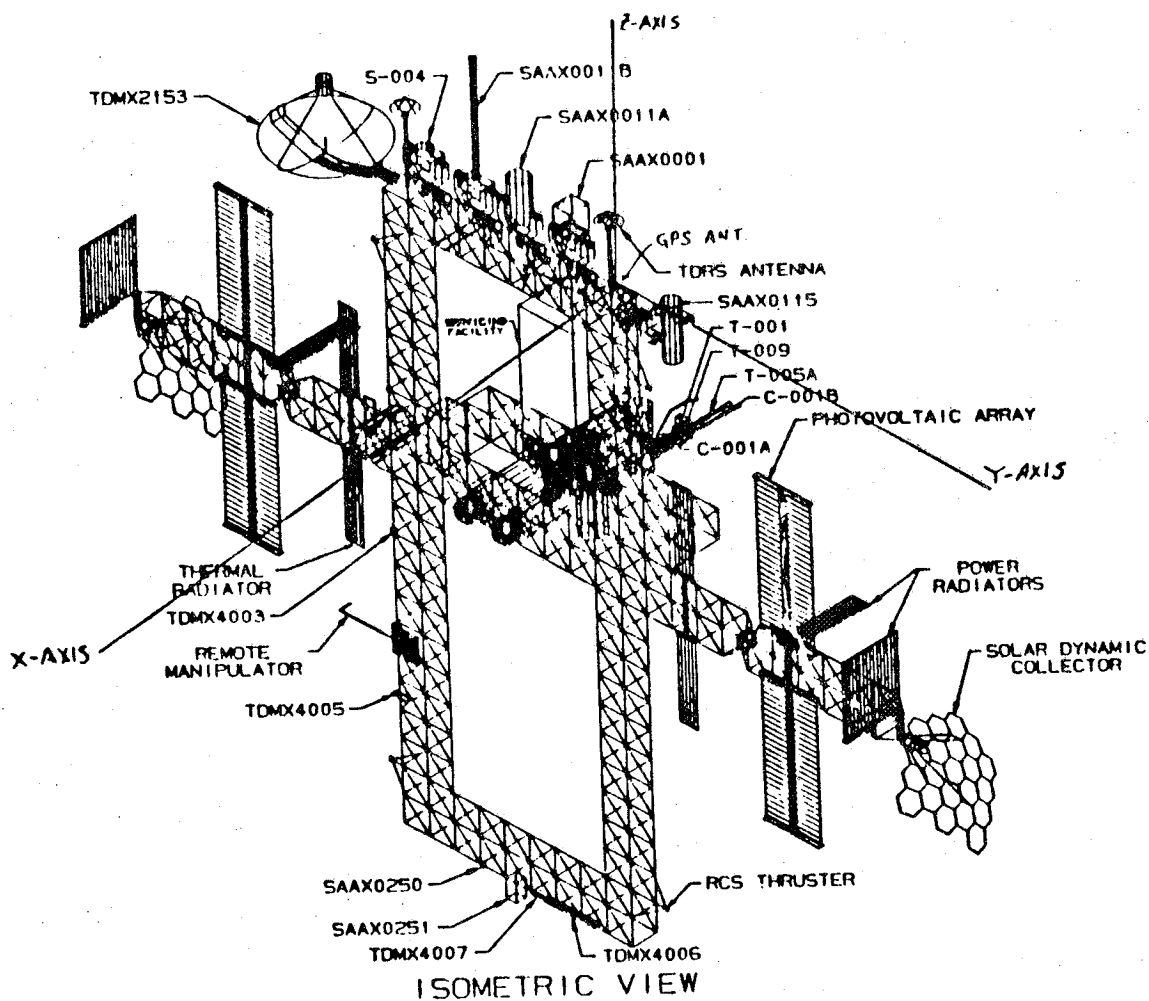


Figure 8.1: Illustration of the Space Station with some of its many antenna systems.

and near orbits, with in coming vehicles that will dock with it, and with men that can be outside working on experiments. The number of antennas and whether passive or active circuitry will be needed can greatly impact on the cost. Once the design is finalized and then put on the space station, it will be much more difficult to make a change, if it does not work correctly, since it will then be in orbit. Making wise choices based on sound data, therefore, is essential in the design process. To complicate things, as can be seen from the illustration, the space station is very large and even in a compact measurement range is difficult to model as an entire structure at reasonable scale model frequencies.

A typical design process on a couple of antenna placement situations will be shown here as a guide to how a code like the NEC-BSC can be used to help the antenna designer make decisions. Any general purpose user oriented code obviously has limitation, so understanding how to effectively use its strengths, avoid its weaknesses, validate the ensuing approximations, and understanding their implications is essential.

8.2 Sighting of Antennas

One of the first considerations of antenna placement is the direct line of sight coverage, especially at UHF and above. It is obvious that with a structure as large as the Space Station, there will be many chances for blockage of the signal from source to receiver. In addition, some of the structures must move relative to the antennas. The solar panels are an example whereby they must orient themselves to the location of the sun. The Space Station itself is moving in a low level orbit and can be communicating with other satellites in quite different orbits. In these cases, it is necessary to have three dimensional knowledge about the blockage for many different antenna locations and structural orientations.

It is not necessary at this phase of the process to worry about the total field values. The NEC-BSC has an obscuration option that allows the user to just obtain the blockage of the direct line of sight signal. This feature is relatively fast, since it only uses the shadowing algorithms in the code. It is, however, a brute force technique that is very appropriate for field calculations but not a wise choice for the large amount of obscuration information needed in this case. For this reason, a special purpose code [3]

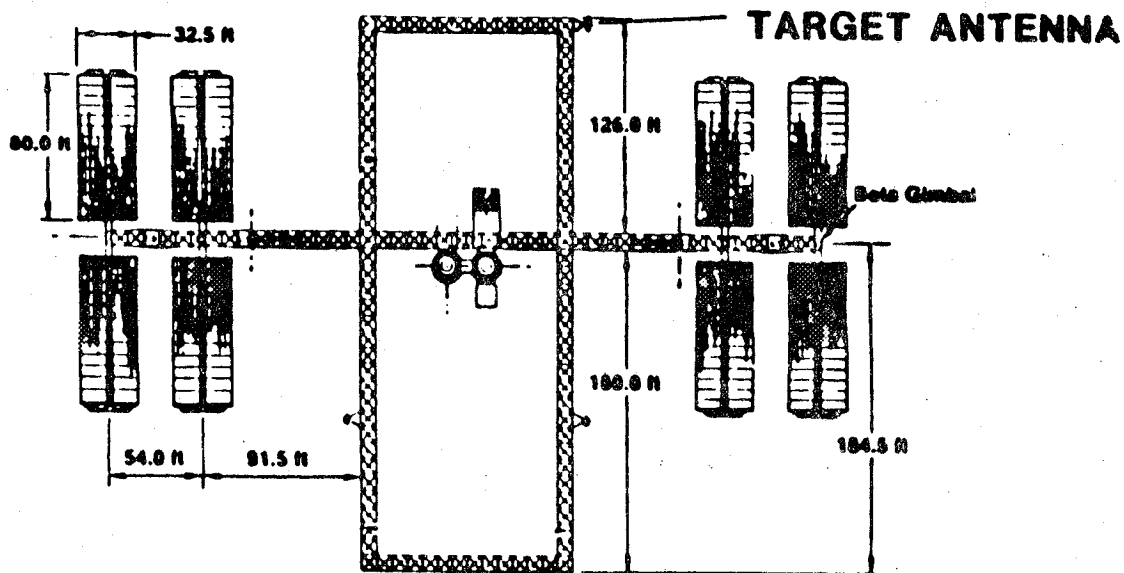


Figure 8.2: Space Station configuration showing antenna location used for shadowing example.

was written that directly projects the structures onto the far zone sphere as seen relative to the antenna. It uses a compatible input set with the NEC-BSC. More importantly, however, is that it provides several orders of magnitude speed improvement over the NEC-BSC for these purposes. The user can try many different candidate location with the structure in various configuration. Once a few choice candidate location are found than the user can move on to the next phase of determining whether the location is suitable in terms of other considerations as will be discussed below.

As an example of the use of the obscuration code, consider the Space Station configuration in Figure 8.2. The target location of an antenna is indicated in the illustration. An input set is first constructed, as indicated in this manual, consisting of a number of plates representing the frame and solar panels. Cylinders are used to represent the living quarters. The solar panels are rotated out of the paper at an angle of $\theta = 45^\circ$.

The Obscuration Code projects the above structure on to the far zone sphere, as illustrated in Figure 8.3. This figure represents a Mercator type projection with the shadowed regions for the particular antenna location

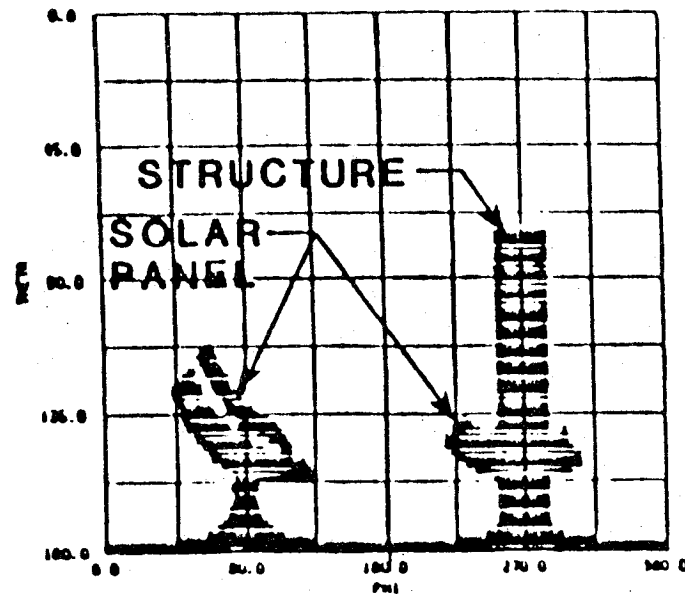


Figure 8.3: Calculated obscuration of the target antenna showing shadow of the Space Station.

and space station orientation represented as the darkened region. This figure indicates, that if all space is to be covered by an antenna system, four antenna locations would be needed at the four corners of the frame.

8.3 Volumetric Pattern Study

The next issue to be addressed is the type, orientation, and effect of the structure on the antenna pattern. For the results shown below a candidate antenna of a nine element three by three array of uniformly phased $\lambda/4$ crossed slots spaced $3/8\lambda$ apart with a cosine amplitude distribution is used. The antenna is first studied looking straight out to the right. The volumetric pattern of the antenna without the space station present is illustrated in contour and three dimensional plots in Figure 8.4. The volumetric pattern calculated in the NEC-BSC with the space station present is shown in Figure 8.5. Notice that a similar obscuration pattern due to the structure is visible in this field pattern plot as in the shadow map in Figure 8.3. In addition, there is a strong region of multipath interference from the solar

panels indicated in the upper region of the plot. As a potential fix to this situation, the antenna is rotate up at an angle of 45° . The pattern without the space station is indicated in Figure 8.6 and the pattern with the space station is indicated in Figure 8.7. Notice that the obscuration and multi-path have been greatly reduce by a wise use and positioning of the antenna pattern.

Other type of candidate antennas can now be tried for this location and orientation until the best match is found. For example, a higher gained antenna that can be actively scanned could be tried, etc.

8.4 Modeling Validation

The final step in all modeling problems is validation of the results and conclusions. As an illustration, a slightly different situation will be studied. Consider the Geosynchronous Positioning Satellite (GPS) antenna as indicated in Figure 8.1. It is in a very cluttered region on the top of the Space Station. This upper region is model using plates and cylinders as illustrated in Figure 8.8. A similar model has been constructed and measured at NASA-LARC. The Space Stations support frame has been modeled as solid flat plates in this example. It is assumed for now to be a worst case estimate. The antenna is a circular microstrip patch antenna measured at a scale frequency of 15.8 GHz. The full scale frequency is 1.22 GHz. The comparison of the antenna alone without the space station is illustrated in Figures 8.9 and 8.10 for the *E*-plane and *H*-plane pattern cuts, respectively. Note that it is a good idea to match the patterns of the source by itself to ensure. With the space station present, the comparison between measured and calculated patterns for the two principal cuts is illustrated in Figures 8.11 and 8.12. The results are also compared for various other pattern cuts in Figures 8.13–8.20 for $\theta = 60^\circ$ to $\theta = -60^\circ$ in 15° steps respectively. The results compare very well validating the model for this situation. It also illustrates the particular location may not be optimum for the GPS antenna placement.

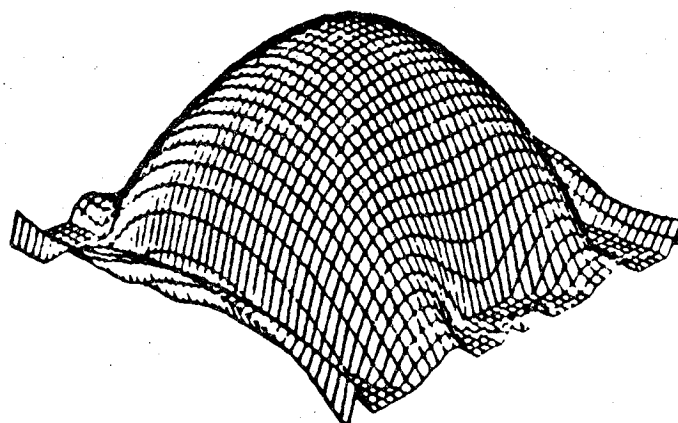
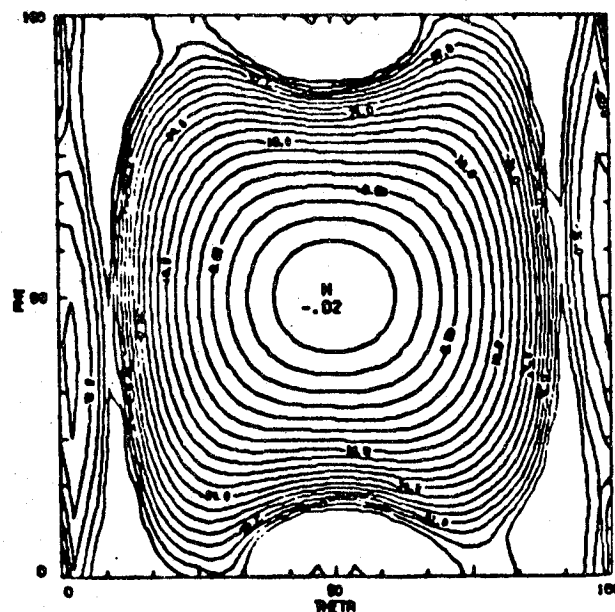


Figure 8.4: Contour and 3-D plot of volumetric E_θ pattern of target antenna mounted vertically without the Space Station.

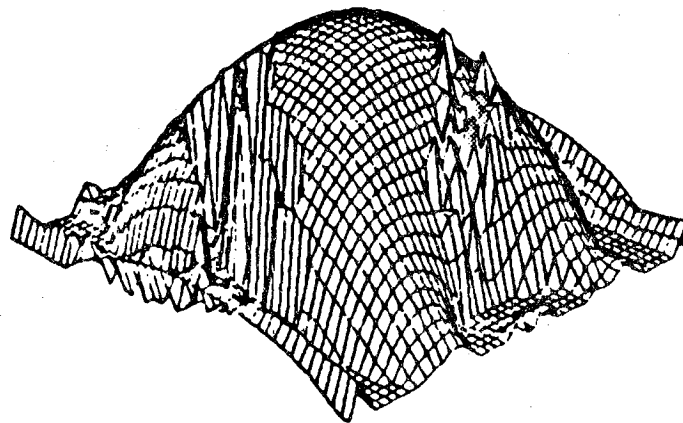
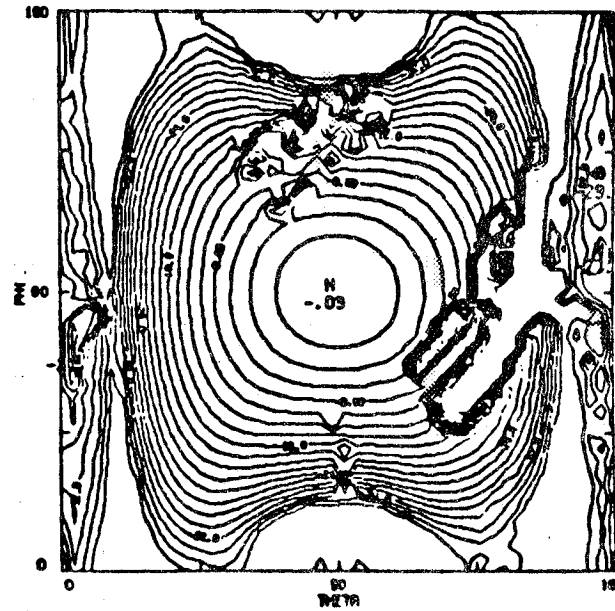


Figure 8.5: Contour and 3-D plot of volumetric E_θ pattern of target antenna mounted vertically on the Space Station.

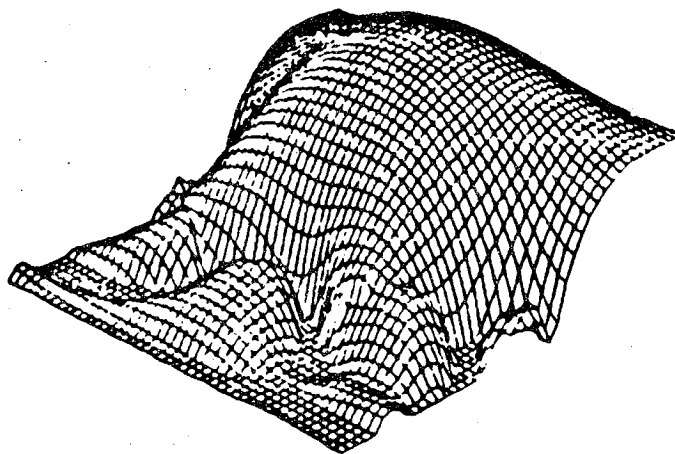
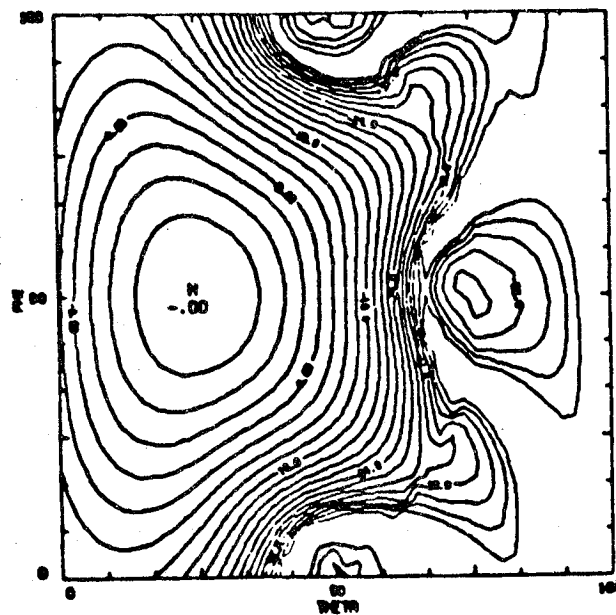


Figure 8.6: Contour and 3-D plot of volumetric E_θ pattern of target antenna mounted at a 45° angle without the Space Station.

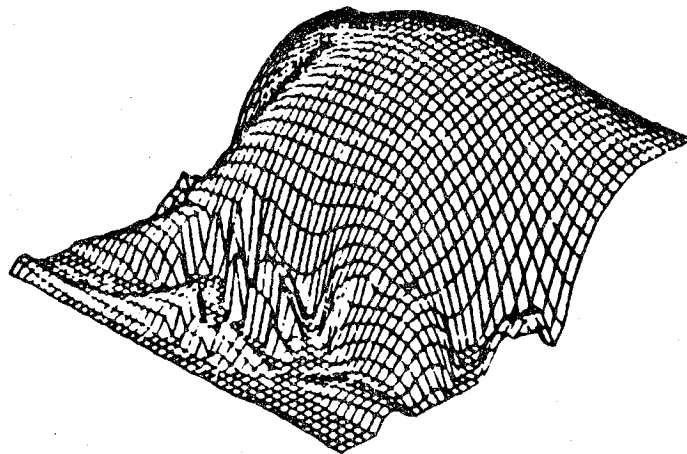
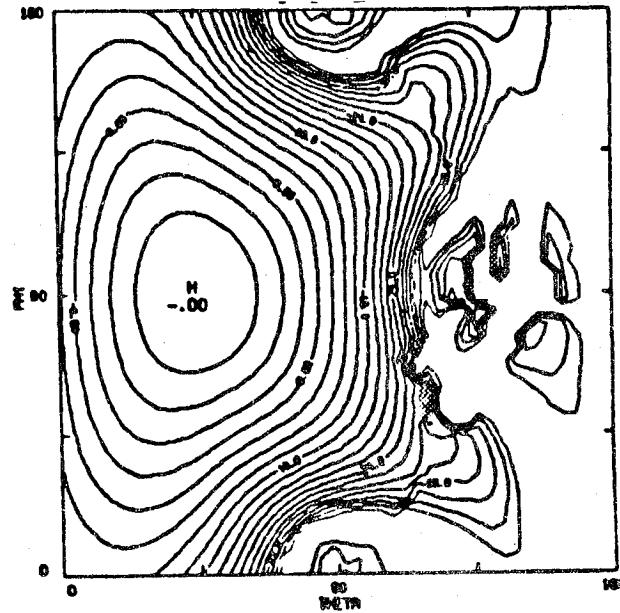


Figure 8.7: Contour and 3-D plot of volumetric E_θ pattern of target antenna mounted at a 45° angle on the Space Station.

ORIGINAL PAGE IS
OF POOR QUALITY

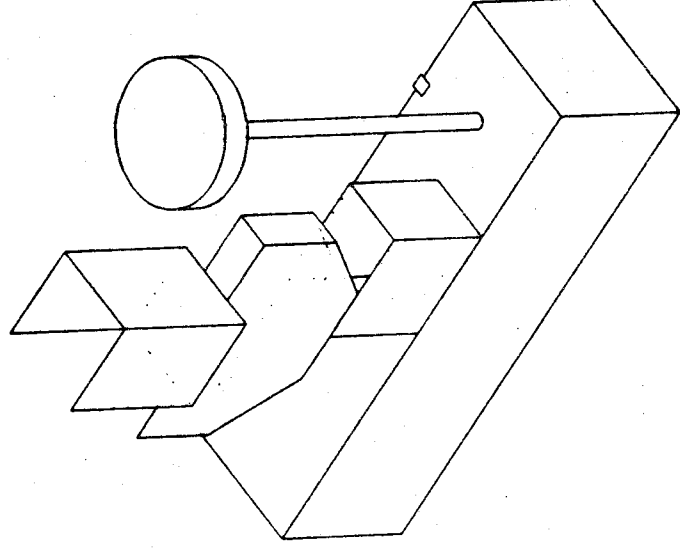


Figure 8.8: NEC-BSC model of portion of Space Station used to model GPS antenna environment.

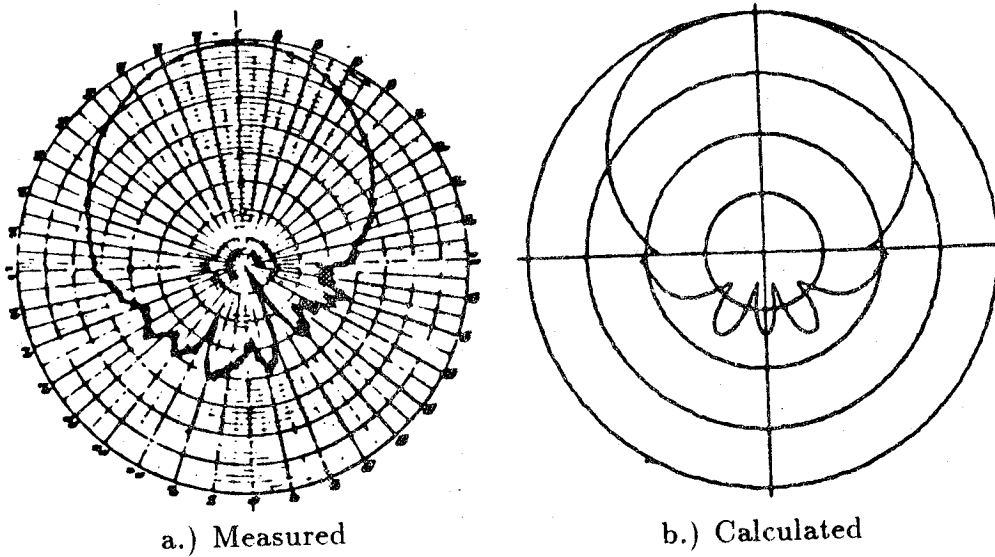


Figure 8.9: Comparison of *E*-plane cut ($\phi = 0^\circ$) measured and calculated patterns for the GPS antenna without the Space Station.

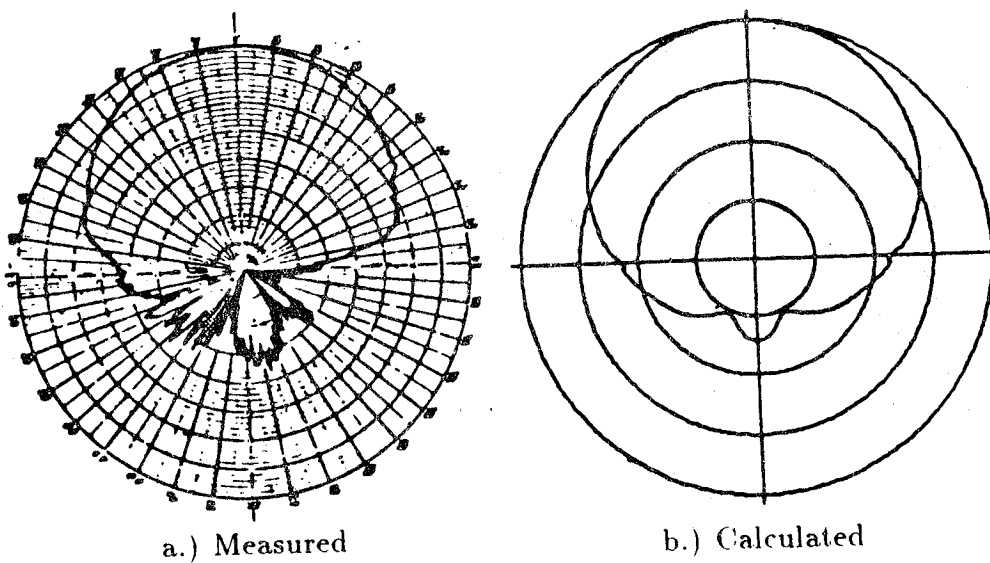


Figure 8.10: Comparison of *H*-plane cut ($\phi = 90^\circ$) measured and calculated patterns for the GPS antenna without the Space Station.

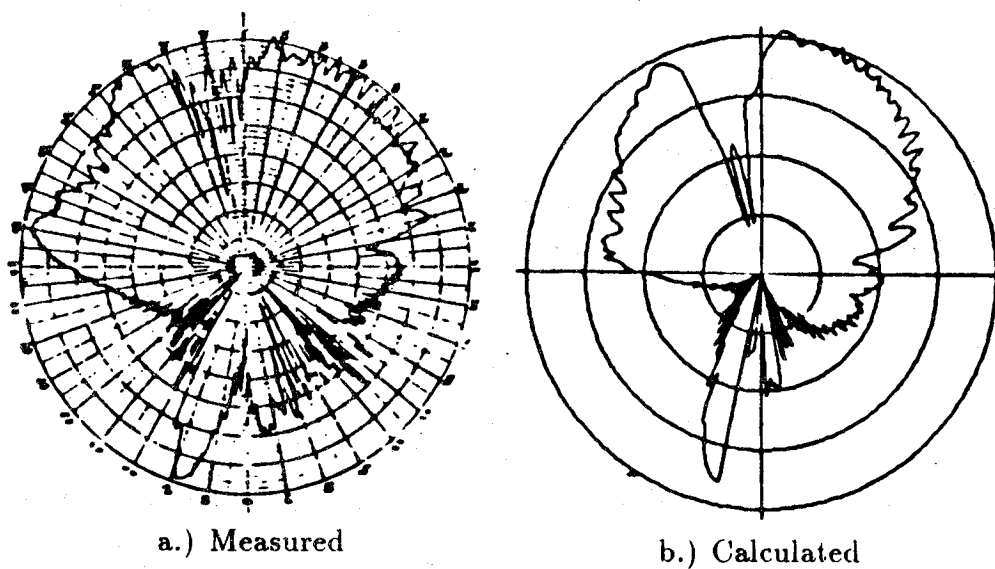


Figure 8.11: Comparison of *E*-plane cut ($\phi = 0^\circ$) measured and calculated patterns for the GPS antenna with the Space Station model.

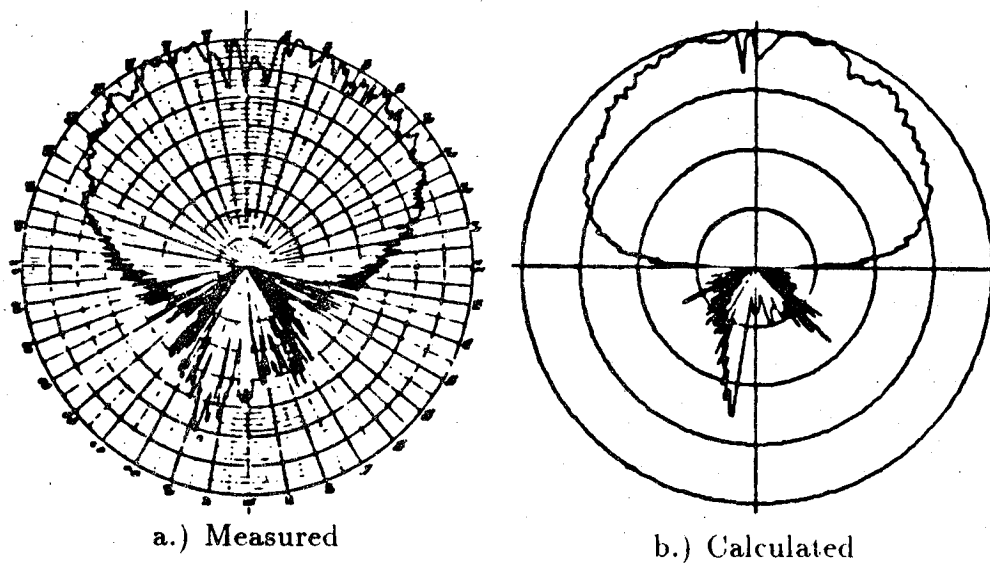


Figure 8.12: Comparison of *H*-plane cut ($\phi = 90^\circ$) measured and calculated patterns for the GPS antenna with the Space Station model.

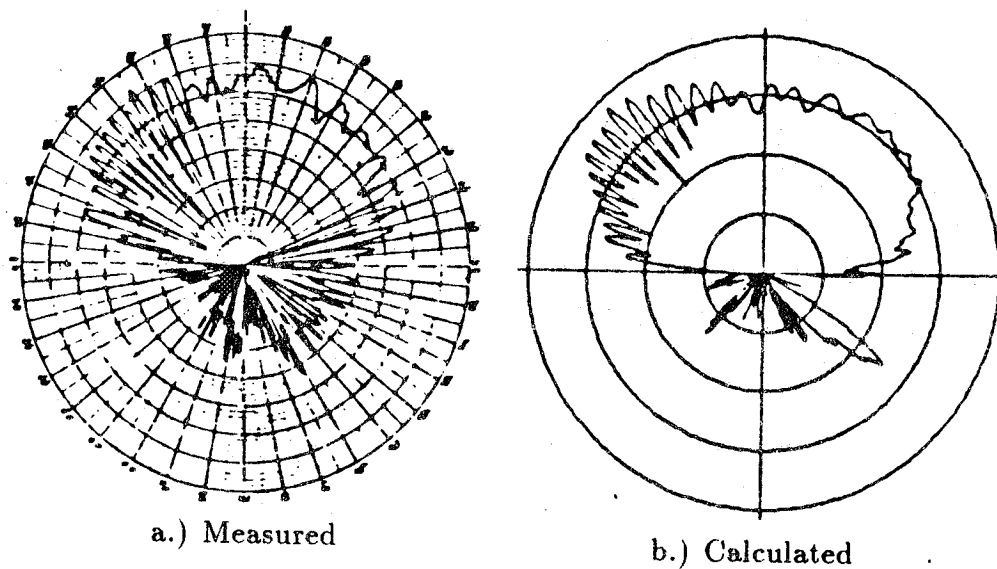


Figure 8.13: Comparison of elevation cut ($\phi = -60^\circ$) measured and calculated patterns for the GPS antenna with the Space Station model.

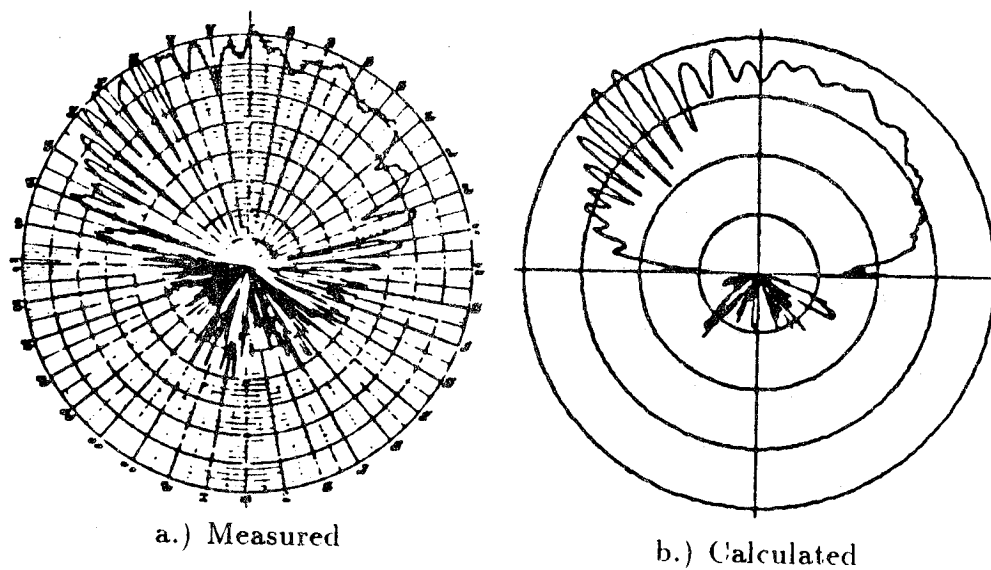


Figure 8.14: Comparison of elevation cut ($\phi = -45^\circ$) measured and calculated patterns for the GPS antenna with the Space Station model.

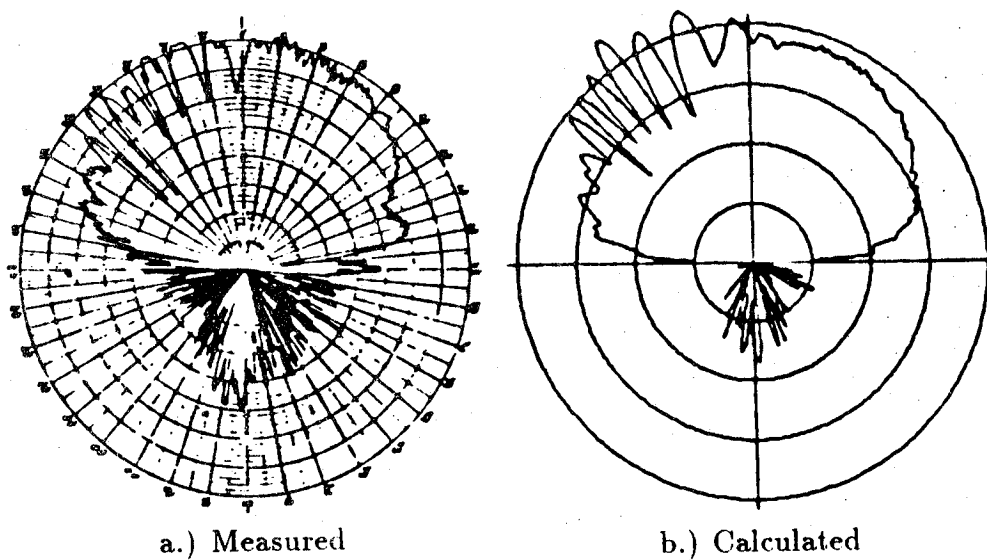


Figure 8.15: Comparison of elevation cut ($\phi = -30^\circ$) measured and calculated patterns for the GPS antenna with the Space Station model.

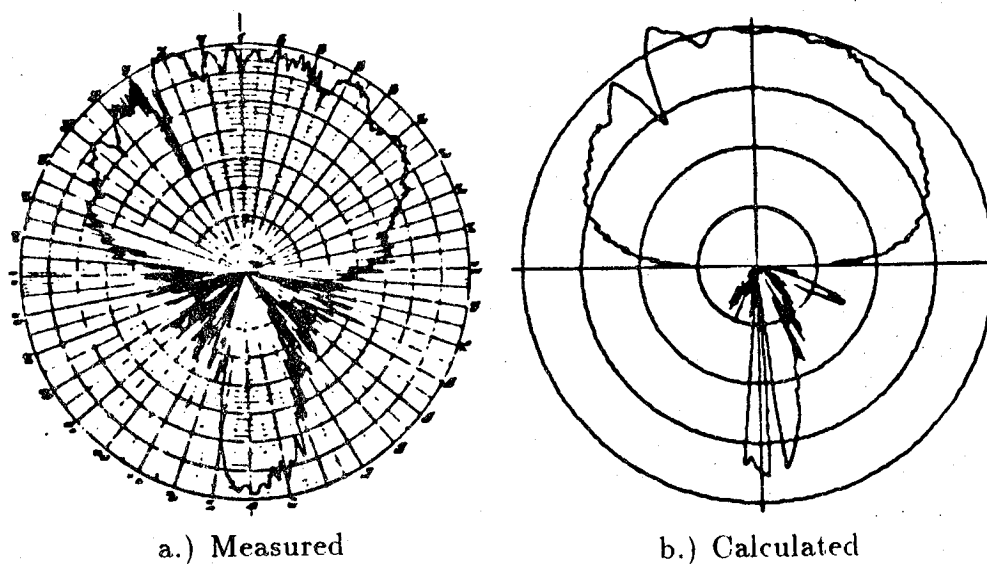


Figure 8.16: Comparison of elevation cut ($\phi = -15^\circ$) measured and calculated patterns for the GPS antenna with the Space Station model.

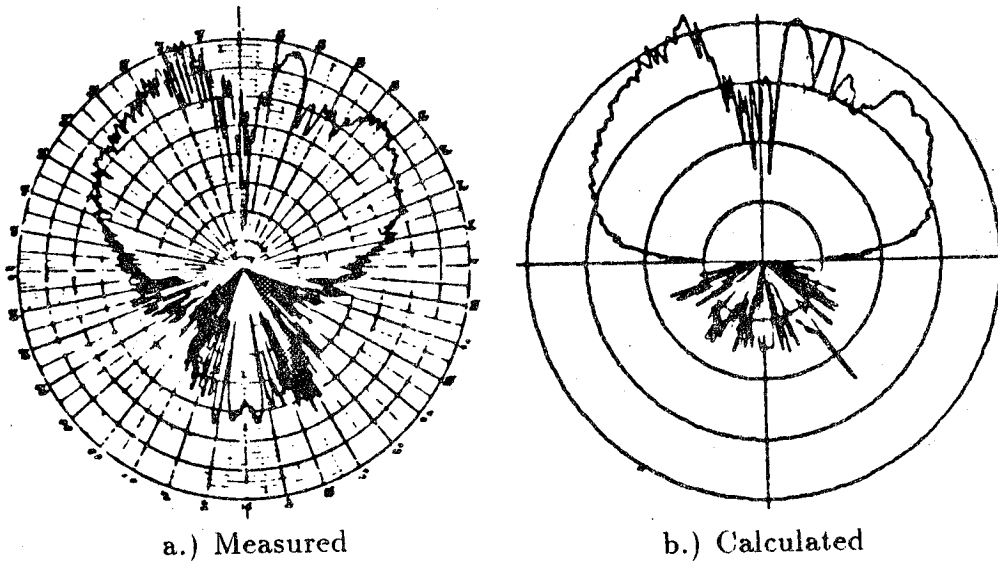


Figure 8.17: Comparison of elevation cut ($\phi = 15^\circ$) measured and calculated patterns for the GPS antenna with the Space Station model.

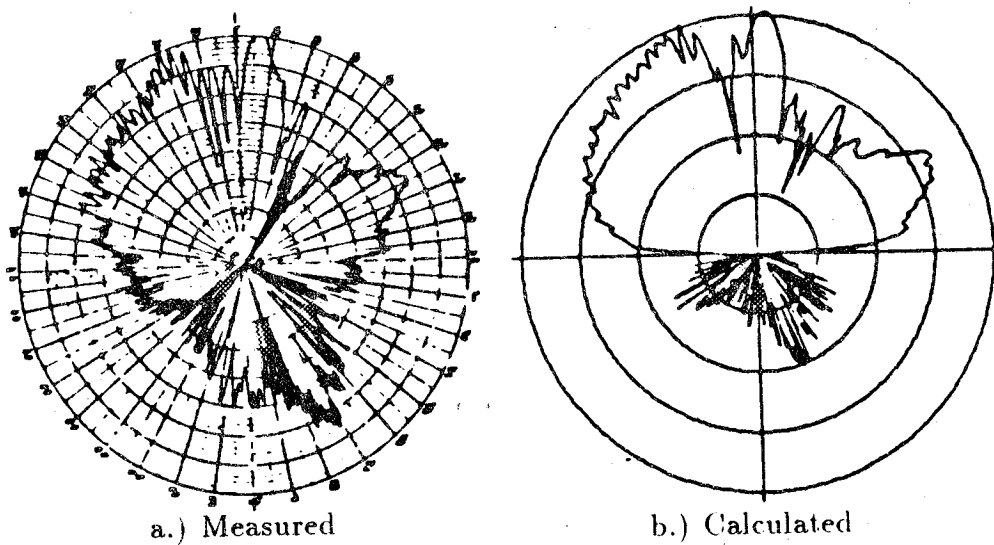


Figure 8.18: Comparison of elevation cut ($\phi = 30^\circ$) measured and calculated patterns for the GPS antenna with the Space Station model.

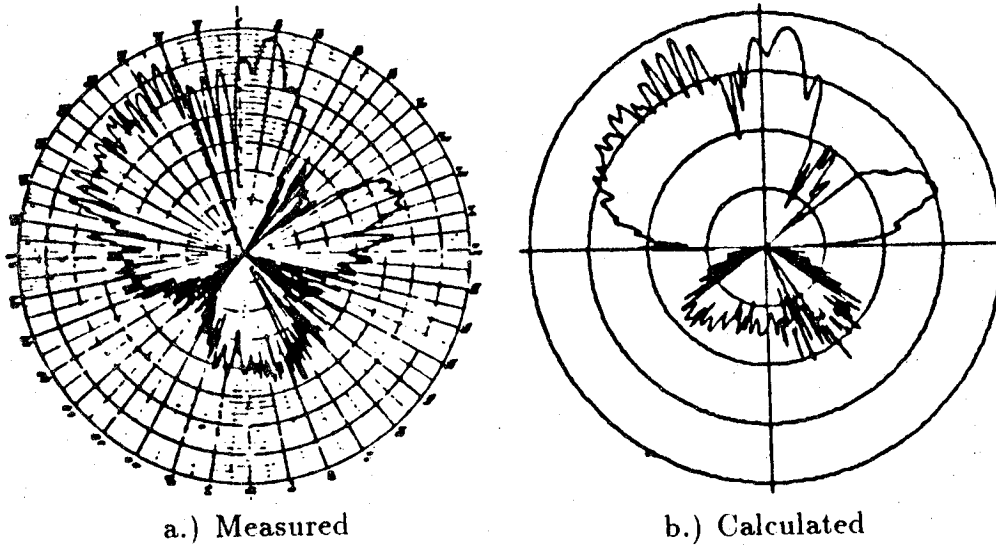


Figure 8.19: Comparison of elevation cut ($\phi = 45^\circ$) measured and calculated patterns for the GPS antenna with the Space Station model.

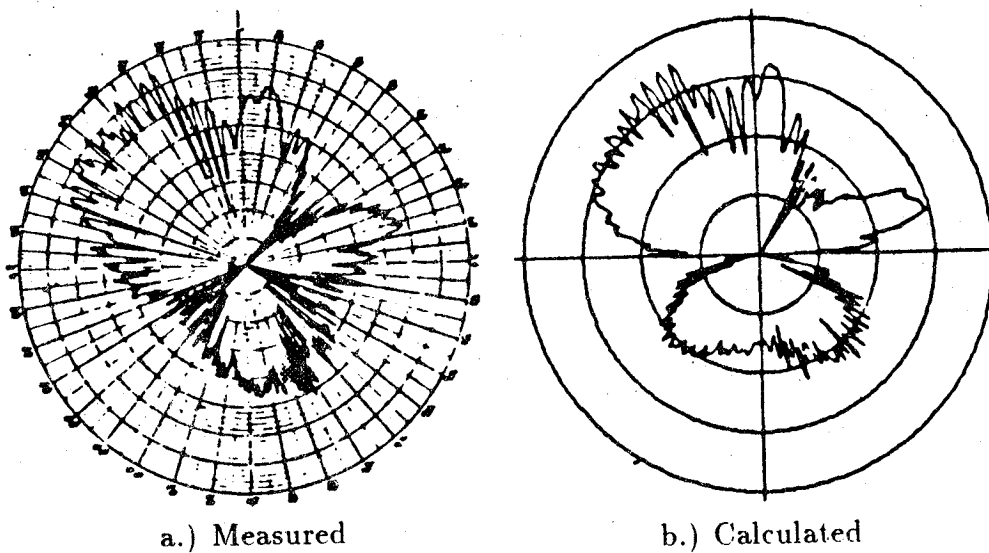


Figure 8.20: Comparison of elevation cut ($\phi = 60^\circ$) measured and calculated patterns for the GPS antenna with the Space Station model.

8.5 Overall Considerations

Many more details need to be considered before the antenna designer is finished. The above examples are meant to just illustrate some key points. In addition to pattern distortion effects, the engineer would potentially have to take in to consideration the coupling (electromagnetic compatibility) between antennas for the locations, frequencies, and antenna types chosen. In addition, the implications of the modeling approximations made need to be determined. In the above illustration, for example, it needs to be determined whether the solid plate model is an appropriate approximation for the lattice structure actually involved. Measurements to this effect are planned at NASA-LARC but are unavailable at the time of this printing.

In addition, many of the learning steps have been left out of the above examples for brevity. For example, it should be noticed that the validation measurements above include only a small area of the space station. This turns out to be appropriate because the rest of the space station will not greatly influence that pattern. Other consideration involved in the modeling decision process chosen is the size of model that can be conveniently measured and the calculation times involved for larger models. In addition, much can be learned by slowly adding details into the calculation model. It helps determine if and/or when an incorrect plate or cylinder dimension or orientation is input. It, also, gives physical insight into what parts of the structure are contributing to the overall resultant pattern.

Appendix A

Array Dimensions

The number of plates, edges, sources, receivers, etc., is determined by how large the arrays are dimensioned for the particular storage variable in the computer code. The array dimensions can be changed by the user to a desired maximum size in the code and then the code can be recompiled. This has been facilitated by using the `PARAMETER` statement which is standard FORTRAN 77. Unfortunately, standard FORTRAN requires that the particular variables defined by the `PARAMETER` statement be in each subroutine that they are needed. This means that the user can find a given storage variable by using an interactive editor, such as EDT, EVE, or LSE on a DEC computer and change every occurs of that variable. The variable defining the number of any given changeable parameter is the same throughout the code, and is not used for any other definition. The variables that can be changed and their description is given here:

NCX: The maximum number of curved surfaces that can be defined.

NEX: The maximum number of edges (or corners) that can be defined per plate.

NIX: The maximum number of interpolation points that can be defined for a look up table for antenna patterns.

NLX: The maximum number of layers of dielectric material that can be defined per plate.

NNX: The maximum number of rims that can be defined per curved surface unit.

NOX: The maximum number of observation points that can be defined by a given single pattern cut.

NPX: The maximum number of plates that can be defined.

NRX: The maximum number of receiver antennas that can be defined.

NSX: The maximum number of source antennas that can be defined.

NTX: The maximum number of UTD terms that are can be defined.

The PARAMETER statements are scattered throughout the code where ever they are needed to define array dimensions. A list of the location of these variables at the time this document is being written are given here. It is still a good idea to let the computer help the user find all occurrences, however, to insure that all have been found and change to exactly the same size.

NCX: Main, CAPINT, CMD, CSEP, CSNAT, CSRGP, CSRRP, CSURF, CSVAR, CTERMS, CYLINT, CYLROT, DFPTCL, DIFCYL, DIFRIM, FCT, FKARG, FLCS, FLDN, FLDS, FLG, FLGS, FLN, FLRS, FLS, FLSD, FLSR, FUNI, GEOMCS, GEOMPC, NANDB, RADCV, RCTEST, REFCAP, REFCYL, RFDFIN, RFPTCL, RFP TCS, RFP TFZ, RFTEST, SCFLD, SPT, TANG

NEX: Main, CMD, CTERMS, DFPTWD, DIFPLT, DIFTRM, DPLRPL, DPTNFW, DREFLD, DTRFLD, FLD, FLDD, FLDR, FLDRR, FLDS, FLR, FLRD, FLRDR, FLRR, FLRRD, FLRRR, FLRS, FLSD, FLSR, GEOMG, GEOMP, GEOMPC, GEOMPS, IMAGE, PLAINT, REFBP, REFPLA, RFPTCL, RPLDPL, RPLRPL

NIX: Main, CMD, RECEVR, SOURCE

NLX: Main, CMD, DIFPLT, DIFTRM, DPLRPL, DREFLD, GEOMG, GEOMP, PLAINT, REFPLA, RPLDPL, RPLRPL, SLABCF

NNX: Main, CAPINT, CMD, CSEP, CSNAT, CSRGP, CSRRP, CSURF, CSVAR, CTERMS, CYLINT, CYLROT, DFPTCL, DIFCYL, DIFRIM, FCT, FKARG, FLCS, FLDN, FLDS, FLG, FLGS, FLN, FLRS, FLS, FLSD, FLSR, FUNI, GEOMCS, GEOMPC, NANDB, RADCV, RCTEST, REFCAP, REFCYL, RFDFIN, RFPTCL, RFPTCS, RFPTFZ, RFTEST, SCFLD, SPT, TANG

NOX: Main, CMD, DIFPLT, FLDD, OUTPLT, OUTWRT

NPX: Main, CMD, CTERMS, DFPTWD, DIFPLT, DIFTRM, DPLRPL, DPTNFW, DREFLD, DTRFLD, FLD, FLDD, FLDR, FLDRR, FLDS, FLR, FLRD, FLRDR, FLRR, FLRRD, FLRRR, FLRS, FLSD, FLSR, GEOMG, GEOMP, GEOMPC, GEOMPS, IMAGE, PLAINT, REFBP, REFPLA, RFPTCL, RPLDPL, RPLRPL, SLABCF

NRX: Main, CMD, GEOMR, RECEVR

NSX: Main, CMD, GEOMCS, GEOMPS, GEOMS, SOURCE, SOURCP

NTX: Main, CTERMS

Appendix B

Logical Unit Numbers

The read and write operations in this code are done on different logical unit numbers depending on the situation. For example, the command words and UTD terms are read from different files. The assignment of these logical unit numbers are made in a common block called INOUT which is placed where needed throughout the code. The unit numbers may be changed by the user for his particular needs. This can be accomplished in the BLOCK DATA statement where the individual variables are set. The variables with their corresponding purpose are given as follows:

IUG: The logical unit number associated with reading the UTD terms to be calculated.

IUI: The logical unit number associated with reading of the input commands.

IUO: The logical unit number associated with writing the echoed information of the commands and the final printable results calculated by the code.

IUP: The logical unit number associated with writing the plottable output data to a file.

IURI: The logical unit number associated with reading the interpolated antenna pattern data look up table for the receiver.

IUSI: The logical unit number associated with reading the interpolated antenna pattern data look up table for the source.

IUT: The logical unit number associated with temporarily reading and writing the UTD as they are being processed.

IUW: The logical unit number associated with writing warning messages generated by the code.

The location at which these variables are used are given here. This gives an indication of where the read and write operations of the code are located. This listing may not be complete for the version being used. The safest approach is to let the computer search out the location of the variables desired.

IUG: Main, CTERMS

IUI: CMD, CREAD

IUO: Main, CAPINT, CFIELD, CMD, CREAD, CTERMS, CYLINT, DIFCYL, DIFPLT, DIFRIM, DPLRPL, FLDD, GEOMCS, GEOMG, GEOMP, GEOMPC, GEOMPS, GEOMR, GEOMS, OUTWRT PLAIN, PRIUC, PRIOUT, RECEVR, REFCAP, REFCYL, REFPLA, RPLDPL, RPLRPL, SCFLD, SOURCE, SOURCP, WD

IUP: Main, OUTPLT

IURI: CMD

IUSI: CMD

IUT: CFIELD, CTERMS, FLCS, FLD, FLDD, FLDN, FLDR, FLDRR, FLDS, FLG, FLGS, FLN, FLR, FLRD, FLRDR, FLRR, FLRRD, FLRRR, FLRS, FLS, FLSD, FLSR

IUW: CSNAT, CSURF, DFPTCL, GEOMP, POLYRT, RFPTCL, RPTCS, TANG

Appendix C

Installation and Operation (VAX)

This version of the code has been developed on a VAX computer. The coding is standard FORTRAN 77, however, so it should run on any machine. This section is intended to give some hints on using this code with a VAX operating system, in this case VMS version 4. Other computers most likely will have similar facilities.

The NEC-BSC code is usually supplied on a 9 track magnetic tape in one of two ways. If a VAX tape is requested, the code is placed on the tape with VAX ANSI tape label and headers at 1600 BPI. The label is usually "OSUESL". The "COPY" command is usually used instead of the "BACKUP" command. This file will contain tabs and continue statements will start with numbers in the first column after the tabs. The name of the code will be "NECBSC31.FOR" or possibly "NZBSC31.FOR". A paper label is normally on the external surface of the tape reel with the specific information.

The second way the code is placed on the tape is in unlabelled, unblocked or blocked at most likely 800, with 80 characters/record (card image format). The tabs will have been removed, the continued statements will be realigned, etc. This format takes up a lot of tape since it has many inter-record gaps. In addition, it will take up more disk space after it is read because of the trailing blanks. These may be removed during the time the tape is read or afterwards. Again a paper label is normally on the tape with the specific formatting information. No name is given to the code in

this case since there is no header information.

Once the code or codes are read off the tape and placed onto the computer disk, the code is ready to be used. It is self contained in one file. All that needs to be done is to "FORTRAN" and "LINK" the code to obtain an executable file. It is recommend at this printing to use the "/NOOPTIMIZE" option of the VAX compiler. Errors have occurred using the optimizer supplied that can not be easily traced.

The code is delivered entirely in FORTRAN 77, however, a couple of VAX specific subroutines are present but commented out. The first is the subroutine GETCP which gets the CPU time from the CPU clock. To use this feature on a VAX the commented lines just need to be reinstated. On another machine similar type lines can be place here for the CPU time. In addition, in the subroutine OUTPLT two subroutines for the date (DATE) and time (TIME) have been commented out. Similarly they can be uncommented on a VAX or a like statement can be used if this feature is desired for the plottable output file.

If the particular machine being used does not automatically save variable values and strange behavior is seen when running the code, a blanket "SAVE" may be necessary. This is automatically done on a VAX. Consult your local system manuals, if problems are detected.

Next it is suggested that the user get into an editor preferably a screen editor such as "EVE", "EDT", or "LSE" and type in one of the examples in Chapter 7. Upon exiting the editor, the user needs to make the association of the input file name with the logical unit number used to read the input file. On a VAX this can be done with something like:

```
$ASSIGN FILE.INP FOR005
```

The printable output will come out on the screen in this case. The complete list of logical unit numbers for input and output is given in Appendix B. A more convenient way to accomplish this on a VAX is to use a command procedure that makes all the assignments for you. An example of this is given here. It runs the code and makes all the assignments using the same name as the input file, but adding different file types for the different I/O operations. It prompts the user for the input file if he forgets. It assumes a ".INP" file type unless otherwise specified. In addition, if a return is given it uses the previous information. Typing "OUT" in the after

on blank on the line will send the printable output to a file "FILE.OUT" instead of the screen.

The following command procedure assigns the input (.INP) , printable output (as an option) (.OUT) , plottable output (.PLV), term processor (.INT), and term scratch file (.TEM). It also will initiate a "DEBUG" section, if the code has been compiled an linked with the debug option.

```

$IF F$MODE() .EQS. "BATCH" THEN GOTO NOINQ
$IF P1 .EQS. "" THEN INQUIRE P1 "INPUT FILE"
$IF P1 .EQS. "" THEN GOTO OLDIN
$NOINQ:
$D=F$PARSE(P1,,,"DEVICE")
$I=F$PARSE(P1,,,"DIRECTORY")
$N=F$PARSE(P1,,,"NAME")
$T=F$PARSE(P1,,,"TYPE")
$V=F$PARSE(P1,,,"VERSION")
$NN:='D'I'N'
$IF T .EQS. "." THEN NI:=$NN'.INP'
$IF T .NES. "." THEN NI:=$NN'T'V'
$ASSIGN 'NI' FOROO6
$IF F$MODE() .EQS. "BATCH" THEN GOTO AOUT
$IF P2 .EQS. "OUT" THEN GOTO AOUT
$IF F$LOGICAL("FOROO6") .NES. "" THEN DEASSIGN FOROO6
$GOTO NOUT
$AOUT:
$ASSIGN 'NN'.OUT FOROO6
$NOUT:
$ASSIGN 'NN'.PLV FOROO7
$ASSIGN 'NN'.INT FOROO8
$ASSIGN 'NN'.TEM FOROO9
$OLDIN:
$SHOW LOGICAL FOROO6
$SHOW LOGICAL FOROO8
$SHOW LOGICAL FOROO7
$SHOW LOGICAL FOROO8
$SHOW LOGICAL FOROO9
$IF P2 .EQS. "DEBUG" THEN GO TO DOUT
$RUN/NODEBUG USER1:[RJM]NECBSC31
$EXIT
$DOUT:
$DEFINE/USER_MODE SYS$INPUT SYS$COMMAND
$RUN/DEBUG USER1:[RJM]NECBSC31
$EXIT

```

Once the code is run the data can be check with the output in the example run. A few of the examples have numbers given. Most of the examples have just plots. An example for interfacing the plottable file with a plot program is given in Appendix D. A geometry drawing package that reads the input sets for this code is also useful for checking purposes before

the code is run. This is discussed in Appendix E. It is recommended that more than one example be run to verify the operation of the code.

Appendix D

Plottable Output

The NEC-BSC has an option that creates a output file that can be used for interfacing with other codes. This file is invoked using the **PP** command in the input data. One of the most useful codes that can be used with data is a plotting code. This has been set up as an external code because most plotting operations are not the same on different computer installations.

The information on this file is written unformatted. It is written and read on logical unit number IUP (see Appendix B). It contains information about the type of pattern that was taken, whether a receiver was present or what electric, magnetic, and polarizations are given. In addition, it gives data on the size and range of the plot window given in the **PP** command in the input set. This information can be obtained by using read statements similar to the ones given here.

```
C!!! Read plot information.
C!!!
C!!! Read plot file type index.
      READ(IUP,IOSTAT=IERR) ICODYP
      IF (IERR.GT.0) THEN
        WRITE(UNIT=IUO,FMT='(A,I4)') ' READ ERROR, IOSTAT= ',IERR
        STOP
      END IF
C!!! Read data type and polarization type.
      READ(IUP) IVTYP,IVPOL
C!!! Read pattern type and movement information.
      READ(IUP) LPATR,LPATS,LVOLP,NPN,NPV
      READ(IUP) LRCTR,IPTR,PATR
      READ(IUP) LRCTS,IPTS,PATS
C!!! Read frequency information.
      READ(IUP) LFQG,FRQG,NFQG,FQGS,FQGI
C!!! Read information for near or far zone
C!!! and whether or source of receiver is present.
```

348

```

      READ(IUP) LNEAR,LRCVR
      READ(IUP) LNEAS,LSORC
      READ(IUP) LSHDW
C!!! Read range distance information.
      READ(IUP) LRANG,RANG
C!!! Read normalization information.
      READ(IUP) LPRAD,IPRAD,PRADR,PRADS
      READ(IUP) CI11,CI22,Z11,Z22
C!!! Read plot size information.
      READ(IUP) LPPREC,PPXL,PPYL,PPGRD
C!!! Read pattern cut index.
      READ(IUP) IIV
C!!! Read fields.
      IF (LRCVR) THEN
C!!! Read coupling or shadowing.
      READ(IUP) (C(IJV),IJV=1,NFP)
      ELSE
      IF (IVTYP.EQ.1.OR.IVTYP.EQ.3) THEN
C!!! Read E-radial or -x.
      IF (IVPOL.EQ.1.OR.IVPOL.EQ.4.OR.IVPOL.EQ.5.OR.IVPOL.EQ.7) THEN
      READ(IUP) (E(1,IJV),IJV=1,NFP)
      END IF
C!!! Read E-theta or -y.
      IF (IVPOL.EQ.2.OR.IVPOL.EQ.4.OR.IVPOL.EQ.6.OR.IVPOL.EQ.7) THEN
      READ(IUP) (E(2,IJV),IJV=1,NFP)
      END IF
C!!! Read E-phi or -z.
      IF (IVPOL.EQ.3.OR.IVPOL.EQ.5.OR.IVPOL.EQ.6.OR.IVPOL.EQ.7) THEN
      READ(IUP) (E(3,IJV),IJV=1,NFP)
      END IF
      END IF
      IF (IVTYP.EQ.2.OR.IVTYP.EQ.3) THEN
C!!! Read H-radial or -x.
      IF (IVPOL.EQ.1.OR.IVPOL.EQ.4.OR.IVPOL.EQ.5.OR.IVPOL.EQ.7) THEN
      READ(IUP) (H(1,IJV),IJV=1,NFP)
      END IF
C!!! Read H-theta or -y.
      IF (IVPOL.EQ.2.OR.IVPOL.EQ.4.OR.IVPOL.EQ.6.OR.IVPOL.EQ.7) THEN
      READ(IUP) (H(2,IJV),IJV=1,NFP)
      END IF
C!!! Read H-phi or -z.
      IF (IVPOL.EQ.3.OR.IVPOL.EQ.5.OR.IVPOL.EQ.6.OR.IVPOL.EQ.7) THEN
      READ(IUP) (H(3,IJV),IJV=1,NFP)
      END IF
      END IF
      END IF
C!!! Read CPU time and run date and clock time.
IF (IIV.EQ.NPV) THEN
      READ(IUP,Iostat=ierr) CTIME
      IF (ierr.EQ.0) THEN
      READ(IUP) RUNDAT,RUNTIM
      END IF
END IF

```

A plot program is available that reads this information and plots it using

the ANSI standard Graphics Kernel System (GKS). It can be supplied at the user's own risk, since even though GKS is considered a standard, there is still installation specific startup and device information that needs to be supplied. It would be on the tape with a name like "NECBSCPT" or "NZPLT". It is mostly written in FORTRAN 77, with the exception of VAX specific file names, the "DATE" and "TIME" calls, and a "\$" used in the format statements that keeps the cursor on the same line after a question is asked.

The plotting code that can be supplied queries the user on the terminal in an interactive fashion. The questions follow in the following general order.

First it asks if more than one pattern trace is to be plotted on the same graph. Next it tells the user whether coupling or electric and or magnetic fields are contained in the file. If there is an option it will ask what type of field or power is to be plotted. The code next tells the user what range of the pattern angles, distance or frequency is contained on the file along with the maximum, minimum, and an average value for each polarization. The user can then choose if he wants to plot all the polarizations or a specific one. A symmetry option about zero is given if only half the data was calculated but a complete symmetric plot is desired.

The code then tells the user what the stored information for the plotting grid and window has been provided by the **PP** command. This can be overridden at this time with new information typed in. If the stored information is chosen, it gives the user the option to change the maximum grid window still preserving the same dynamic range on the stored list. The code is now ready to plot the results.

The user next needs to supply GKS with information about the type of device and workstation code number. This is installation dependent and the user should determine this for his computer system and change the subroutines PLTINI and PLTCLS for convenience, if necessary. A plot should result similar to those in the examples chapter.

Appendix E

Plottable Geometry

A code that draws the geometry of the structure under analysis can be provided. It is based on GKS like the pattern plot code discussed in Appendix D. It is placed on the tape with the name "NECBSCGM" or possibly "DRAWS3". It is supplied at the users own risk to get it running on their system. It is written primarily in FORTRAN 77, however, some non standard VAX specific options are present in subroutine NOTF77. These can be change if necessary. In addition, the GKS initialization can be system dependent. These can be changed in subroutine INIGKS.

The geometry plotting code uses the same input set as the EM code. It makes a good preprocessor to check the input sets. The command interpreter is the same as the EM code. In addition, it uses many of the same geometry subroutines to process the input so that it provides a visual validation of the algorithms in the EM code for the users particular geometry.

This code is highly interactive. The following discussion gives a brief overview of the commands available.

Overview

The geometry plotting uses the following three basic commands:

DRAW for displaying an object,

SET for changing parameter values, and

SHOW for examining parameter values.

A secondary set of general purpose commands are used for modifying the graphics environment or the state of the geometry plotting code. This set includes the following commands:

PATTERN CUT	NOPATTERN CUT	EXIT
SHADOWING	NOSHADOWING	SPAWN
TEXT_WINDOW	NOTEXT_WINDOW	FLUSH
BOX	NOBOX	HELP

All commands described in the following section are in response to the DRAWS> prompt.

Command Description

Command parameters or qualifiers separated by "," means one of the parameters or qualifiers should be chosen. Parameters in "[]" are optional. An uppercase parameter means it is a default. All output examples shown in the figures here are based on a Boeing 737 airplane input file. All the input files used by geometry plotting code are of the same format as the input files for the EM code. The Boeing 737 input file with only the geometry information needed to test the geometry plotting code is given here:

CE: THIS IS A TEST OF THE B737.

UN: INCHES

3

PG: RIGHT WING

6,0

3.9,4.9,-1.

3.9,-7.5,-1.

9.,-7.5,-1.

27.9,-13.6,-1.

27.9,-10.4,-1.

9.,.97,-1.

PG: LEFT WING

6,0

-3.9,4.9,-1.


```

-9.,.97,-1.
-27.9,-10.4,-1.
-27.9,-13.6,-1.
-9.,-7.5,-1.
-3.9,-7.5,-1.
PG: LEFT TAIL
4,0
-.6,-33.25,2.9
-2.,-26.45,2.9
-10.7,-32.6,2.9
-10.7,-35.8,2.9
PG: RIGHT TAIL
4,0
.6,-33.25,2.9
10.7,-35.8,2.9
10.7,-32.6,2.9
2.,-26.45,2.9
PG: VERT. STABILIZER
4,0
0,-30.,1.5
0,-34.,17.5
0,-30.,17.5
0,-19.7,3.9
CC: FUSELAGE
0.,0.,0.
90.,90.,90.,0.
5
.6,.6,27.8
2.4,2.4,23.3
3.9,3.9,13.3
3.9,3.9,-13.3
.25,.25,-34
XQ:
EN:

```

DRAW [all] [FULL_PAGE , report_size]

It may be abbreviated to D. This command is used for displaying an object. The graphics package used for this purpose is GKS. An example of a DRAW

REPORT SIZE command output appears on Figure E.1.

Parameters:

ALL : May be abbreviated to A. It simultaneously displays the object along all three reference coordinate system axes views, and in the current theta/phi view (X,Y,Z, and theta/phi). If not used, only the theta/phi view is displayed. An example of a DRAW ALL command appears on Figure E.2.

Qualifiers:

FULL PAGE : (default) May be abbreviated to F. It displays the specified theta/phi view of the object in a full page size.

REPORT SIZE : May be abbreviated to R. It displays the specified theta/phi view of the object in a report size.

SHOW origin , scale_factor , device , window , view

It may be abbreviated to SHO. This command displays the requested parameter.

Parameters:

ORIGIN : May be abbreviated to O. Shows the centroid of the object in the Reference Coordinate System.

SCALE_FACTOR : May be abbreviated to S. Shows the current scale factor.

VIEW : May be abbreviated to V. Shows the current values of theta and phi.

DEVICE : May be abbreviated to D. Identifies the current graphics device used.

WINDOW : May be abbreviated to W. Shows the current graphics window extend or width.

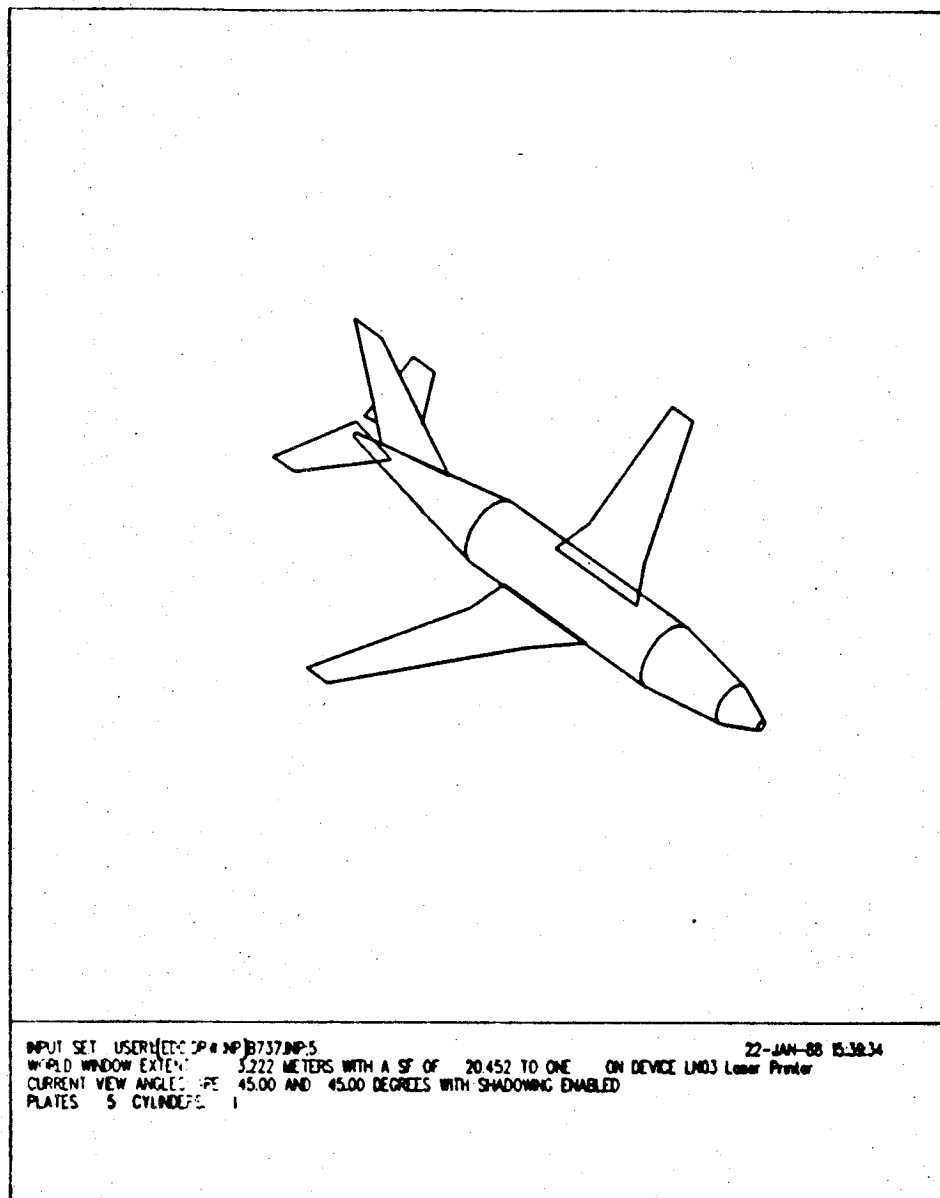
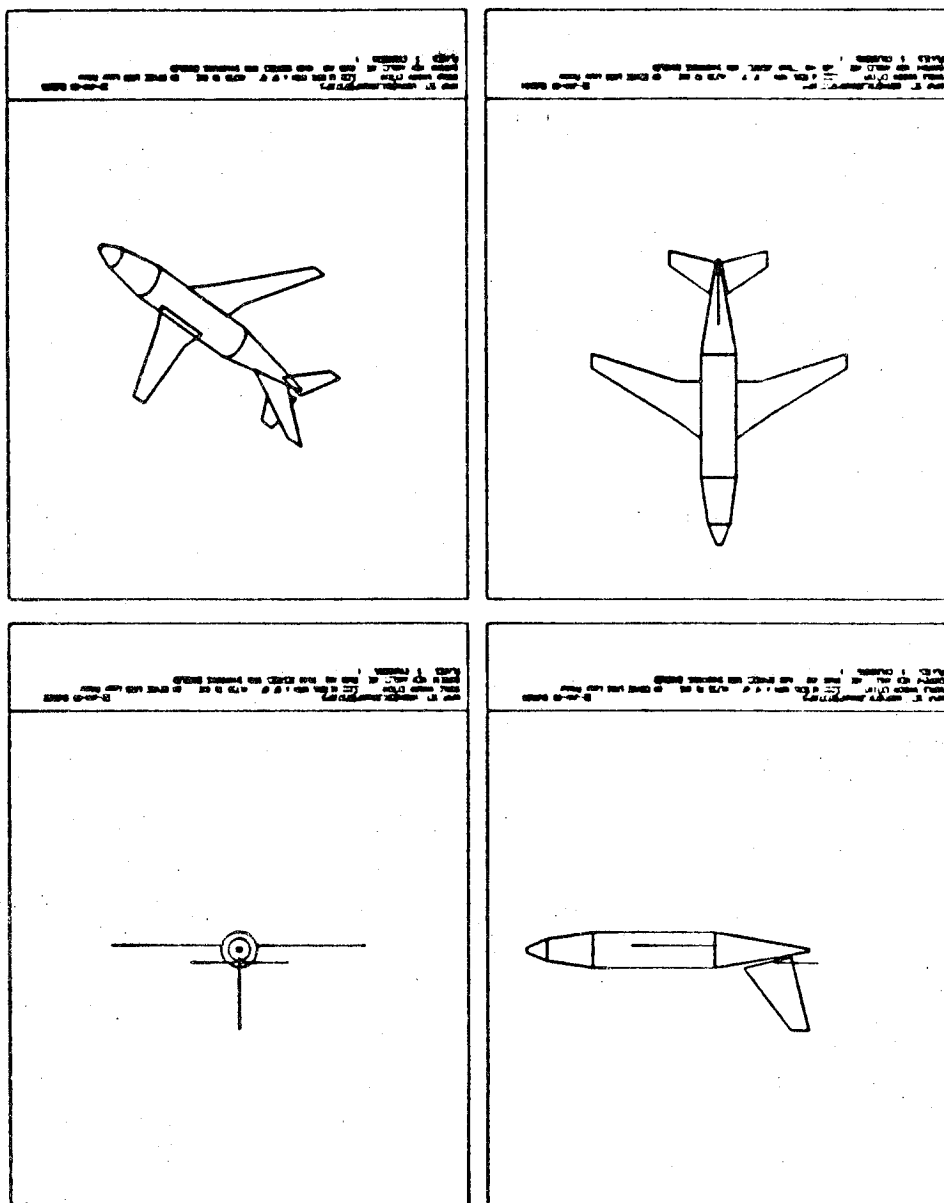


Figure E.1: Output of a DRAW REPORT SIZE command after a SET VIEW 45.,45.is given.

Figure E.2: Output of a DRAW ALL command.



ORIGINAL PAGE IS
OF POOR QUALITY

SET origin , scale factor , device , window , view

It may be abbreviated to SE. This command sets a new value for the specified parameter. If a value is not directly specified in the command, the program is displaying the current value of the parameter and prompts for a new value. After each parameter change, the new value is displayed.

Parameters:

ORIGIN [x,y,z]: Places the centroid of the object at the point (x,y,z) in the Reference Coordinate System. The code defaults to setting the origin at the center of the graphics window.

SCALE FACTOR [value]: Changes the scale factor to the value specified. The code sets the default value of the scale factor in such a way that the geometry about to be drawn fills out the screen. A new value of the scale factor enlarges or reduces the object about the centroid.

DEVICE: Prompts for a new graphics device.

VIEW [theta,phi]: Changes the view according to the new theta and phi.

WINDOW [width]: Changes the window extend to the new width specified.

EXIT

It may be abbreviated to EX. This command terminates execution of the geometry plotting code.

PATTERN CUT

It may be abbreviated to P. This command causes all subsequent angular (theta, phi) specifications to occur with respect to the pattern cut coordinate system. This is the system with respect to which electromagnetic measurements are made, thus views with respect to this coordinate system might be useful for understanding results obtained using the electromagnetics code.

NOPATTERN CUT

It may be abbreviated to NOP. This command causes the theta/phi specifications to occur with respect to the reference coordinate system. A reference system view is the default and can be changed to the pattern cut system view by executing the PATTERN CUT command. Reference coordinate system views might be more useful than the pattern cut views when the user wants to understand the geometry input to the electromagnetics code.

SHADOWING

It may be abbreviated to SHA. This command causes the object to be displayed with hidden parts removed. Shadowing is the default value. Currently, plates and curved surfaces do not shadow one another.

NOSHADOWING

It may be abbreviated to NOS. This command causes the program to display all features, the object is not shadowed.

TEXT_WINDOW

It may be abbreviated to T. This command reenables the appearance of the text window at the bottom of the picture generated by a DRAW command. This is the default when the program is executed unless changed by the NOTEXT_WINDOW command.

NOTEXT_WINDOW

It may be abbreviated to NOT. This command results in no text window appearing at the bottom of the picture. This feature becomes very handy in cases where the user wants to view a plot on a terminal screen quickly, since the generation of the text window is time consuming.

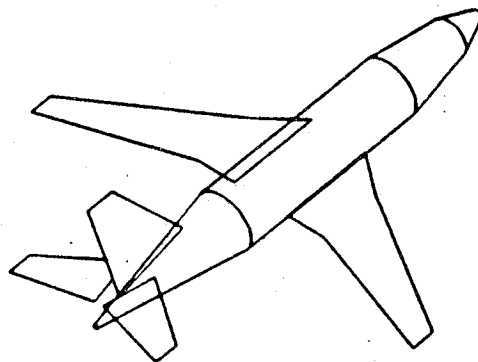


Figure E.3: Output of a DRAW command after a NOTEXT, NOBOX, and SET VIEW 45.,315. is executed.

BOX

It may be abbreviated to B. This command enables a border line to enclose the picture created by a DRAW command. It is the default when the program is executed unless changed by the NOBOX command.

NOBOX

It may be abbreviated to NOB. This command disables the picture border line. It has the reverse effect of the BOX command. It is useful for report writing purposes where it is only desirable to have the geometry plot without the border line or the text window. An example of this feature appears on Figure E.3.

SPAWN

It may be abbreviated to SP. This command allows the user to execute VMS commands without exiting the DRAWS program.

FLUSH

It may be abbreviated to F. This command clears the graphics buffer and sends the plot to the specified plotting device for a hard copy.

HELP [command]

It may be abbreviated to H. This command provides a simple interactive help facility for the user. If a command is not specified, the program lists all commands for which help is available.

Bibliography

- [1] R. J. Marhefka and W. D. Burnside, "Numerical electromagnetic code - basic scattering code (version 2), Part I: user's manual," Technical Report 712242-14, The Ohio State University ElectroScience Laboratory, Department of Electrical Engineering, Dec. 1982. Prepared under Contract No. N00123-79-C-1469 for Naval Regional Contracting Office.
- [2] R. J. Marhefka, "Numerical electromagnetic code - basic scattering code (version 2), Part II: code manual," Technical Report 712242-15, The Ohio State University ElectroScience Laboratory, Department of Electrical Engineering, Dec. 1982. Prepared under Contract No. N00123-79-C-1469 for Naval Regional Contracting Office.
- [3] R. J. Marhefka and L. Takacs, "Manual for obscuration code with space station applications," Technical Report 716199-7, The Ohio State University ElectroScience Laboratory, Department of Electrical Engineering, Dec. 1985. Prepared under Grant No. NSG 1498 for National Aeronautics and Space Administration.
- [4] R. J. Marhefka, "Analysis of aircraft wing-mounted antenna patterns," Report 2902-25, The Ohio State University ElectroScience Laboratory, Department of Electrical Engineering, June 1976. Prepared under Grant No. NGL 36-008-138 for National Aeronautics and Space Administration.
- [5] W. D. Burnside, M. C. Gilreath, R. J. Marhefka, and C. L. Yu, "A study of KC-135 aircraft antenna patterns," *IEEE Trans. Antennas Propagat.*, vol. AP-23, pp. 309-316, May 1975.
- [6] C. L. Yu, W. D. Burnside, and M. C. Gilreath, "Volumetric pattern analysis of airborne antennas," *IEEE Trans. Antennas Propagat.*,

vol. AP-26, pp. 636-641, Sep. 1978.

- [7] W. D. Burnside, J. J. Kim, B. Grandchamp, R. G. Rojas, and P. Law, "Airborne antenna radiation pattern code user's manual," Technical Report 716199-4, The Ohio State University ElectroScience Laboratory, Department of Electrical Engineering, Sep. 1985. Prepared under Grant No. NSG 1498 for National Aeronautics and Space Administration.
- [8] W. D. Burnside and K. W. Burgener, "High frequency scattering by a thin lossless dielectric slab," *IEEE Trans. Antennas Propagat.*, vol. AP-31, pp. 104-110, Jan. 1983.
- [9] R. G. Kouyoumjian and P. H. Pathak, "A uniform geometrical theory of diffraction for an edge in a perfectly-conducting surface," *Proc. IEEE*, vol. 62, pp. 1448-1461, Nov. 1974.
- [10] P. H. Pathak, W. D. Burnside, and R. J. Marhefka, "A uniform GTD analysis of the diffraction of electromagnetic waves by a smooth convex surface," *IEEE Trans. Antennas Propagat.*, vol. AP-28, pp. 631-642, Sep. 1980.
- [11] P. H. Pathak, "Techniques for high-frequency problems," in *Antenna Handbook: Theory, Applications, and Design*, (Y. T. Lo and S. W. Lee, eds.), ch. 4, New York: Van Nostrand Reinhold Co. Inc., 1988.
- [12] W. D. Burnside and R. J. Marhefka, "Antennas on aircraft, ships, or any large, complex environment," in *Antenna Handbook: Theory, Applications, and Design*, (Y. T. Lo and S. W. Lee, eds.), ch. 20, New York: Van Nostrand Reinhold Co. Inc., 1988.
- [13] J. H. Richmond, "Radiation and scattering by thin-wire structures in a homogeneous conducting medium," *IEEE Trans. Antennas Propagat.*, vol. AP-22, p. 365, March 1974.
- [14] G. J. Burke and A. J. Poggio, "Numerical electromagnetic code (NEC) - method of moments," Tech. Rep. NOSC/TD 116, Naval Ocean Systems Center, San Diego, California 92152, July 1977.

- [15] E. H. Newman and R. L. Dilsavor, "A user's manual for the electromagnetic surface patch code: ESP version III," Technical Report 716148-19, The Ohio State University ElectroScience Laboratory, Department of Electrical Engineering, May 1987. Prepared under Grant No. NSG 1613 for National Aeronautics and Space Administration.
- [16] E. L. Pelton, R. J. Marhefka, and W. D. Burnside, "An iterative approach for computing an antenna aperture distribution from given radiation pattern data," Report 784583-6, The Ohio State University ElectroScience Laboratory, Department of Electrical Engineering, June 1978. Prepared under Contract No. N62269-76-C-0554 for Naval Air Development Center.
- [17] R. Backhus, "The determination of the aperture distribution of a linear array through near field measurements," Report 713303-2, The Ohio State University ElectroScience Laboratory, Department of Electrical Engineering, June 1982. Prepared under Contract No. N62269-80-C-0384 for Naval Air Development Center.
- [18] R. C. Rudduck and Y. C. Chang, "Numerical electromagnetic code - reflector antenna code, NEC - REF (version 2), Part I: user's manual," Report 712242-16, The Ohio State University ElectroScience Laboratory, Department of Electrical Engineering, Dec. 1982. Prepared under Contract No. N00123-79-C-1469 for Naval Regional Procurement Office.
- [19] Y. C. Chang and R. C. Rudduck, "Numerical electromagnetic code - reflector antenna code, NEC - REF (version 2), Part II: code manual," Report 712242-17, The Ohio State University ElectroScience Laboratory, Department of Electrical Engineering, Dec. 1982. Prepared under Contract No. N00123-79-C-1469 for Naval Regional Procurement Office.
- [20] C. H. Walter, *Traveling Wave Antennas*, pp. 15-16. New York: Dover Publications Inc., 1979.
- [21] J. D. Kraus, *Antennas*, pp. 464-477. New York: McGraw Hill Book Company, Inc., 1950.

- [22] H. Bach, "Pattern measurements of high frequency satellite - mounted antennas," Tech. Rep. R154, Electromagnetic Institute, Technical University of Denmark, Jan. 1976.
- [23] R. L. Mather, G. V. Vaughn, and J. C. Logan, "Computer techniques for modeling shipboard communications antennas at UHF and above," NELC Technical Note 3313, Naval Ocean Systems Center, San Diego, California 92152, Feb. 1977.
- [24] D. Mensa, "Radar cross section measurements of an idealized aircraft shape," Tech. Rep., Pacific Missile Test Center, Pt. Mugu, California, Apr. 1982.

Index

- Aircraft 298
- Antenna Coupling 237, 247, 250
 - Movement 48
- BF 5, 6, 26, 29, 47, 48, 70, 167, 302, 312
- CC 6, 25, 50, 165, 312
- CE 26, 62
- CF 6, 25, 54, 165, 308
- CG 25, 58, 165
- CM 26, 62
- Comments 62
- Composite Ellipsoid Geometry 54
- Cone Frustum 50
- Corner Reflector 211
- Cylinder - Dipole 259
 - Geometry 58
- Dielectric Plate 218, 222
- Eight Sided Box 214
- Elliptic Cylinder 267
- EN 26, 62
- End Program 62
- Examples (1A) 181
 - (1B) 188
 - (1C) 190
 - (2) 196
 - (3) 200
 - (4) 208
 - (5) 211
 - (6) 214
 - (7) 218
 - (8) 222
 - (9) 225
 - (10) 228
 - (11A) 237
 - (11B) 247
 - (11C) 250
 - (12) 252
 - (13) 259
 - (14) 267
 - (15) 271
 - (16) 279
 - (17) 286
 - (18) 292
 - (19) 298
 - (20A) 302
 - (20B) 308
 - (20C) 312
- Execute Code 154
 - Terms 154
- Far Zone Cut 77
 - Pattern 73
 - Range 101
 - Volumetric Pattern 144
- FM 26, 39, 40, 63, 167, 168, 169, 171, 173, 174, 175
- FR 26, 64, 140

- Frequency 64
 - Sweep 208
- GP 25, 65
- GR 5, 67
- Ground Plane 65
- Interpolated Source 126
 - Receiver 106
- Lossy Dielectric 225
- LP 26, 33, 69, 179, 191
- MOM Receiver Input 110
 - Source Input 131
- NC 26, 51, 56, 59, 70
- Near Zone Cylinder 271
 - Pattern 83
 - Plate 200
 - Scatter 302
 - Using a Cone Frustum 312
 - Using an Ellipsoid 308
- NEC - MM Input 252
- Next Problem 71
 - Next Set of Cylinders 70
 - Plates 70
 - Receivers 70
 - Sources 71
- NG 26, 70
- NM 26, 29, 70, 102
- No Ground Plane 70
 - Antenna Movement 70
- Normalization Factors 91
- NP 26, 70, 81
- NR 26, 70, 99, 104
- NS 26, 71, 119, 122
- NX 26, 51, 56, 59, 71, 81, 99, 104, 119, 122, 286
- OB 6, 26, 72
- Obscuration Option 72
- PD 26, 48, 73, 77, 167
- PF 5, 26, 39, 46, 48, 73, 77, 167
- PG 25, 79
- Plate - Cylinder 286
 - Dipole 181, 188, 190
 - Geometry 79
 - Slot 196
- Plot Data 88
- PN 26, 39, 40, 46, 48, 67, 83, 85, 167, 171, 172, 173, 174, 175
- PP 26, 41, 88, 151, 179, 180, 347, 349
- PR 26, 39, 40, 49, 91, 167, 168, 169, 170, 175, 176
- Printer Output 69
- RA 6, 26, 95, 141, 167
- Radome and Horn 228
- Range Gate 67
- RD 26, 39, 101, 167
- Receiver Array 95
 - Geometry 102
- RG 26, 48, 49, 95, 102, 141, 167
- RI 5, 26, 106
- RM 26, 110, 167
- Rotate-Translate Geometry 112
- RT 25, 45, 46, 112, 113, 157, 158, 161
- SA 5, 6, 25, 115, 120, 141
- Scale Factor 139
- Scattered Fields 47
- SG 5, 48, 49, 115, 120, 141, 252
- Ship Masts 279
 - Yardarm 292


SI 5, 26, 126
SM 5, 25, 131, 252
Source Array 115
 Geometry 120
Swept Frequencies 63

TC 5, 26, 134
Test Cylinder 134
 Output 135
 Plate 138
TO 5, 26, 41, 43, 135, 164, 267
TP 5, 26, 138, 196


UF 25, 139
UN 25, 111, 132, 140
Units of Geometry 140
 of Source 141
US 5, 25, 98, 104, 118, 122, 140,
 141

VD 26, 48, 142, 167
VF 5, 26, 46, 48, 72, 142, 144, 167
VN 5, 26, 46, 48, 67, 147, 167, 171
VP 26, 151
Volumetric Far Zone 142
 Near Zone 147
 Plot Data 151

XQ 5, 26, 47, 154
XT 5, 26, 43, 47, 48, 154, 165, 222



Report Documentation Page

1. Report No. NASA CR-181944		2. Government Accession No.		3. Recipient's Catalog No.	
4. Title and Subtitle Near Zone - Basic Scattering Code User's Manual With Space Station Applications				5. Report Date December 1989	
				6. Performing Organization Code	
7. Author(s) R. J. Marhefka and J. W. Silvestro				8. Performing Organization Report No. 716199-13	
				10. Work Unit No. 482-59-23-15	
9. Performing Organization Name and Address The Ohio State University ElectroScience Laboratory Department of Electrical Engineering 1320 Kinnear Road Columbus, OH 43212				11. Contract or Grant No. NSG-1498	
				13. Type of Report and Period Covered Contractor Report	
12. Sponsoring Agency Name and Address National Aeronautics and Space Administration Langley Research Center Hampton, VA 23665-5225				14. Sponsoring Agency Code	
15. Supplementary Notes Langley Technical Monitor: E. M. Bracalente					
16. Abstract The Numerical Electromagnetic Code - Basic Scattering Code, Version 3, is a user - oriented computer code to analyze near and far zone patterns of antennas in the presence of scattering structures, to provide coupling between antennas in a complex environment, and to determine radiation hazard calculations at UHF and above. The analysis is based on uniform asymptotic techniques formulated in terms of the Uniform Geometrical Theory of Diffraction (UTD). Complicated structures can be simulated by arbitrarily oriented flat plates and an infinite ground plane that can be perfectly conducting or dielectric. Also, perfectly conducting finite elliptic cylinder, elliptic cone frustum sections, and finite composite ellipsoids can be used to model the superstructure of a ship, the body of a truck, an airplane, a satellite, etc. This manual gives special consideration to space station modeling applications. This document is a user manual designed to give an overall view of the operation of the computer code, to instruct a user in how to model structures, and to show the validity of the code by comparing various computed results against measured and alternative calculations such as method of moments whenever available. It also describes in detail the input and output data for the code.					
17. Key Words (Suggested by Author(s)) Numerical Electromagnetic Code Uniform Geometrical Theory of Diffraction Pattern Prediction Code Plate, Elliptic Cylinder, and Cone Frustum Models; Space Station Applications			18. Distribution Statement  Subject Category 32		
19. Security Classif. (of this report) Unclassified		20. Security Classif. (of this page) Unclassified		21. No. of pages 386	
				22. Price	

ORIGINAL PAGE IS
OF POOR QUALITY